

**ANALYSIS OF FIBER LASER MARKING  
CHARACTERISTICS FOR PRODUCING MARKS  
OF VARIOUS GEOMETRICAL SHAPES**

Thesis submitted

by

**MOHIT PANDEY**

**DOCTOR OF PHILOSOPHY (ENGINEERING)**

**DEPARTMENT OF PRODUCTION ENGINEERING  
FACULTY COUNCIL OF ENGINEERING & TECHNOLOGY  
JADAVPUR UNIVERSITY  
KOLKATA-700032  
INDIA**

**2024**

**JADAVPUR UNIVERSITY  
KOLKATA-700032**

**Index No: 253/20/E  
Registration No. 1022016001**

**TITLE OF THE Ph.D. (Engg.) THESIS:**

Analysis of Fiber Laser Marking Characteristics for Producing  
Marks of Various Geometrical Shapes

**NAME, DESIGNATION & INSTITUTION OF THE  
SUPERVISOR:**

  
Prof (Dr.) BISWANATH DOLOI

Professor,  
Department of Production Engineering,  
Jadavpur University,  
Kolkata -700032, India.

**Professor  
Production Engineering Department  
Jadavpur University  
Kolkata - 700 032**

# LIST OF PUBLICATIONS

## International Journal: Published-

- 1) Pandey, M., & Doloi, B. (2024). Analysis of Marking Quality of a Triangular-shaped Inscription Produced on 304 Stainless Steel Using a Low Power Fibre Laser. *Lasers in Engineering* (Old City Publishing), 57, 1-21. **(SCI, Scopus Indexed)**
- 2) Pandey, M., & Doloi, B. (2023). Experimental investigation into fibre laser marking on stainless steel 304. *Advances in Materials and Processing Technologies*, 9(1), 1-14. **(ESCI, Scopus Indexed)**
- 3) Pandey, M., & Doloi, B. (2022). Parametric analysis on fiber laser marking characteristics for generation of square shaped marked surface on stainless steel 304. *Materials Today: Proceedings*, 56, 1908-1913. **(Scopus Indexed)**
- 4) Pandey, M., Doloi, B., & Bhattacharyya, B. (2021). Parametric study on laser marking of circular shape on stainless steel 304. *International Journal of Precision Technology*, 10(1), 3-22.
- 5) Pandey, M., & Doloi, B. (2024). Optimization of Laser Marking on 304 Stainless Steel. *Lasers in Engineering* (Old City Publishing), 58, 213-236. **(SCI, Scopus Indexed)**
- 6) Pandey, M., & Doloi, B. (2024). Analysis on fiber laser marking characteristics of elliptical shaped geometry marked on SS 304. *Advances in Materials and Processing Technologies*, 1-18. **(ESCI, Scopus Indexed)**

## International Journal: Published/Accepted

- (i) Pandey, M., & Doloi, B. (2024) Parametric Analysis of PMMA Laser Marking Using Fiber Laser. Accepted for Publication in *Sadhana Journal* (Springer).

## National Journal: Published

- (ii) Pandey, M., & Doloi, B. (2023). Experimental investigation into fiber laser marking on titanium alloy (Ti6AL4V). *Manufacturing Technology Today*, 22(6), 61-67. **(UGC approved)**

## List of Book Chapters

- i. Pandey, M., & Doloi, B. (2022). Experimental Studies on Laser Marking Characteristics of Stainless Steel 304. In *Advances in Modern Machining Processes: Proceedings of AIMTDR 2021* (pp. 173-184). Singapore: Springer Nature Singapore. **(Scopus Indexed)**
- ii. Pandey, M., Sen, A., Doloi, B., & Bhattacharyya, B. (2023). Modeling and Optimization of Fiber Laser Marking on Stainless Steel 304. In *Optimization*

Methods for Engineering Problems (pp. 325-342). Apple Academic Press.  
(Scopus Indexed)

## **List of Conferences**

1. M. Pandey and B. Doloi “Parametric analysis on fiber laser marking characteristics for generation of square shaped marked surface on Stainless Steel 304” 1st International Conference on Applied Research and Engineering organized by the Department of Mechanical Engineering, Cape Peninsula University of Technology, Cape Town, Western Cape on the 26-28 November 2021
  2. M. Pandey and B. Doloi “Experimental studies on laser marking characteristics of stainless steel 304” 8th International and 29th All India Manufacturing Technology, Design and Research Conference (AIMTDR 2021) Organized by Departments of Mechanical Engineering PSG College of Technology & PSG Institute of Technology and Applied Research Coimbatore during 09 - 11, December 2021
  3. M. Pandey and B. Doloi “Experimental Investigation into Fiber Laser Marking on Titanium Alloy (Ti-6Al-4V)” International Conference on Precision, Micro, Meso and Nano engineering [COPEN 12] held during 8-10 December 2022 at the Indian Institute of Technology Kanpur, Uttar Pradesh, India.
  4. M. Pandey and B. Doloi “Experimental Investigations into Fiber Laser Marking on PMMA” 9th International & 30th All India Manufacturing Technology, Design and Research Conference, Organized by Departments of Mechanical Engineering, IIT BHU, Varanasi during 8th to 10th December 2023.
- ❖ Awarded Best Paper Presentation at 1st International Conference on Applied Research and Engineering ICARAE2021 organized by Department of Mechanical Engineering, Cape Peninsula University of Technology, Cape Town, South Africa

**National Conference: Nil**

**Patents: Nil**



# PROFORMA – 1

## “Statement of Originality”

I, Mohit Pandey registered on 24th February 2020 do hereby declare that this thesis entitled “ANALYSIS OF FIBER LASER MARKING CHARACTERISTICS FOR PRODUCING MARKS OF VARIOUS GEOMETRICAL SHAPES” contains literature survey and original research work done by the undersigned candidate as part of Doctoral studies.

All information in this thesis have been obtained and presented in accordance with existing academic rules and ethical conduct. I declare that, as required by these rules and conduct, I have fully cited and referred all materials and results that are not original to this work.

I also declare that I have checked this thesis as per the “Policy on Anti Plagiarism, Jadavpur University, 2019”, and the level of similarity as checked by iThenticate software is ....6%.....

Signature of Candidate: Mohit Pandey.

Date: 10/07/2024

Certified by Supervisor(s):

(Signature with date, seal)

Broshi  
10/07/2024

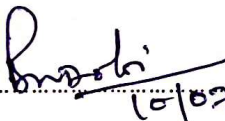
Professor  
Production Engineering Department  
Jadavpur University  
Kolkata - 700 032

# JADAVPUR UNIVERSITY

## FACULTY OF ENGINEERING AND TECHNOLOGY DEPARTMENT OF PRODUCTION ENGINEERING

### CERTIFICATE FROM THE SUPERVISORS

*This is to certify that the thesis entitled "ANALYSIS OF FIBER LASER MARKING CHARACTERISTICS FOR PRODUCING MARKS OF VARIOUS GEOMETRICAL SHAPES" submitted by Mr. Mohit Pandey, who got his name registered on 24<sup>th</sup> February 2020 for the award of Ph.D. (Engg.) degree of Jadavpur University is absolutely based upon his own work under the supervision of Prof. Biswanath Doloi and that neither his thesis nor any part of the thesis has been submitted for any degree/diploma or any other academic award anywhere before.*

  
.....  
10/07/2024  
(Signature of the Supervisor  
with date and official seal)

Professor  
Production Engineering Department  
Jadavpur University  
Kolkata - 700 032



## **ACKNOWLEDGEMENT**

The insight presented in this thesis is undoubtedly a result of the contributions made by numerous outstanding individuals. The author expresses sincere gratitude to the Ph.D. (Engg.) thesis supervisor, Dr. Biswanath Doloi, Professor in the Production Engineering Department at Jadavpur University, Kolkata for his unwavering guidance, helpful suggestions, continuous association, support, encouragement, and valuable advice throughout every stage of this research work. The author recognizes that without Dr. Biswanath Doloi constructive and timely advice, the thesis would not have progressed as smoothly as it did.

The author also extends appreciation for the cooperation and encouragement received from Dr. Bijoy Bhattacharyya, Dr. Biplab Ranjan Sarkar, Dr. Shankar Chakrabarty, and the Head of the Department, Dr. Bijan Sarkar and all the faculty members of the Production Engineering Department at Jadavpur University during the research work. Special thanks go to Mr. Biswanath Das, Mr. Bishwajit Pathak, Mr. P. Bari, and Mr. Subir Sanyal for their consistent support during my research work.

The author expresses gratitude to fellow colleagues, Dr. Santosh Kumar, Mr. Sudip Santra, Mr. Ritesh Hazra, Mr. Naresh Besekar, Mr. Himadri Sekhar Panda, and existing research scholars, Arindam Maity, Kailash Roy and ex-PG students for their constant cooperation, useful assistance, and support during the research work. Special thanks are extended to the FET office and Research section for their cordial assistance and administrative support. The author acknowledges the All-India Council for Technical Education, New Delhi, for introducing the ADF (Engg.) scheme. The author gratefully acknowledges the co-operation and encouragement received from all the faculty members and staff members of Production Engineering Department, Jadavpur University for carrying out research work successfully.

*Mohit Pandey.*  
(Mohit Pandey)

# PREFACE

Laser marking is a thermal process that uses a concentrated laser beam of high intensity to leave a marked surface on a material. This technique can result in significant cost reductions by lowering the cost of manufacturing and tooling, eliminating extra steps and consumables, and reducing inventory and maintenance downtime. Depending on the application and the substance to be marked, a range of laser technologies are available. The material that the laser energy beam is emitted from typically identifies marking lasers. Numerous lasers, such as Nd: YAG, CO<sub>2</sub>, fiber and excimer lasers are available for marking operations on a wide range of materials. Different laser light wavelengths produced by various laser mediums have an impact on their acceptability and effectiveness for marking on various engineering materials. There are numerous other variations among the lasers in terms of thermal efficiency, heat transfer, minimum and maximum power output etc., and each of these features has an impact on the materials. Although CO<sub>2</sub> lasers can mark a variety of materials, including plastic, wood, glass, paper, leather, stone, etc., they often have limited marking capabilities on highly conductive materials, especially bare metals.

The pulsed Nd:YAG lasers are effective for marking a wide range of materials including metals and ceramics due to their wavelength (1.064 microns) which is precisely 10 times smaller than that of CO<sub>2</sub> lasers. It may be concentrated to a very small area in the micron range with a higher power density that aids in producing fine marking. They result in less thermal distortion and a smaller heat impacted zone. A fibre optic connection can also be used to transmit Nd: YAG laser energy, giving factories more flexibility. The Nd: YAG laser when used in pulsed mode have the capacity to brand metal by ablating it or changing its colour through carbonization and annealing. A laser source and CNC system are two of the many mechanical, electrical, and optical parts that make up a laser marking system. The work piece's surface is altered by the concentrated laser light's absorption, which results in the desired marking effect. The surface temperature rises when the laser light is absorbed by the target material which causes the substance to change colour.

Because of its adaptability and distinctive features, laser marking has become one of the most recent methods for permanently marking materials. In essence, laser marking methods involves either material removal or material surface alteration as revealed by literature studies. The number of laser variables involved in the laser marking process is the main cause for concern for producing good quality laser marked surface on

engineering materials. A variety of engineering applications can now be supported by laser marking because to improvements in laser technology and a greater knowledge of how lasers interact with matter. Due to its superior characteristics, such as contact and wear-less machining, improved flexibility, and the potential for a high degree of automation, speed, durability etc., laser marking has currently emerged as one of the best ways to mark a variety of technical materials. As a result, laser marking is frequently used to brand numerous important components in order to prevent product theft and unauthorized reproduction.

In the last ten years, fiber lasers have become the most adaptable and quickly developing laser systems, successfully challenging the dominance of other forms of laser in a variety of manufacturing, medical, meteorological, and military applications due to its flexibility and lower maintenance cost.

It is clear from a review of earlier literature that researchers concentrated on the analysis of line marking but that none of them paid attention to the image quality characteristics of surface marking on engineering materials which is helpful for the generation of specific logo of any organization or institutional as a part of its authenticity. The present research objective focus on fiber laser surface marking procedures and to investigate the potential for marking on various engineering materials such stainless steel 304, Ti6Al4V, and PMMA. Different combinations of process variables such as laser irradiation, pulse rate, duty cycle, and scan rate were utilized in order to produce feasible good quality geometric shapes laser marking characteristics. Based on feasibility, the goals of the current research activity have been merged in accordance with the resources available, as follows:

- i. To carry out basic experiments on fiber laser marking operation for selecting the range of process variables to mark various geometrical shapes on different engineering materials.
- ii. To investigate the influences of laser marking process variables such as laser irradiation, pulse rate, assist gas, scan rate on marking characteristics such as mark intensity, width of laser marked surface and geometrical features on different engineering materials.

- iii. To produce various geometrical shapes such as circular, triangular, rectangular, elliptical, pentagonal and hexagonal on different engineering materials by laser marking process.
- iv. To mark various geometrical shapes on engineering materials such as SS 304, Ti6Al4V, and PMMA at minimum possible time with better marking characteristics.
- v. To carryout optimal analysis of fiber laser marking characteristics for producing marks of various geometrical shapes.

The complete research work is prepared in a well-organized manner into different chapters numbering from one to seven. A brief summary of each chapter is provided as follows:

Chapter 1 outlines an overview of laser marking processes, material removal mechanism, present needs, and applications. The selection of different engineering materials, along with their applications, is also discussed in this chapter. Literature reviews of previous works are incorporated and studied for finding out the existing knowledge gap to outline the research objectives.

Chapter 2 provides the details of fiber laser marking set up along with the description of the various parts that have been used for experimental purpose. It also shows the marking strategy and the methods employed for generation of complex geometrical shapes such as square, triangle, circle, ellipse, hexagon, pentagon or a combination of these geometrical shapes.

Chapter 3 presents process parameter selection and experimentation for fiber laser marking on stainless steel 304. Basic study were conducted in order to analyze the influences of process variables on the responses of fiber laser marking on stainless steel 304. Then fiber laser marking of square shaped geometric surface on stainless steel 304 has been done based on minimum laser power. Afterwards, experimental investigation into fiber laser marking on elliptical shaped geometry at focused and defocused position has been done for the generation of better quality laser marked surface. The studies include additional process variables such as defocused distance which also plays an important role in the change in marking contrast. Next, marking of equilateral triangular shaped laser marked surface has also been carried out based on minimum laser irradiation and time requirement using one factor at a time (OFAT) method. The process variables

set that has been obtained using one factor at a time method were further utilized for the marking of other complex geometrical shapes such as pentagon, hexagon and a combination of this geometrical shapes.

Chapter 4 highlights the mathematical modelling based on response surface methodology. Development of Empirical formula and ANOVA test for the responses have been conducted. Influences of process variables on marking characteristics of equilateral triangle shaped laser marked surfaces and the surface and contour plots have also been generated in order to analyze the range of process variables for achieving better marking characteristics. Apart from that, the single objectives as well as multi objective optimization of responses have been performed to find the optimal set of process variables for achieving optimum value of the responses.

Chapter 5 provides the study of marking quality characteristics on Ti6Al4V with the aid of the fiber laser system. The chapter provides the influences of process variables on line and surface marking which is responsible for the change in marking characteristics. The comparative studies not only helpful in the generation of better quality line marked surface but also helpful in the generation of better quality geometric shapes on the surface of Ti6Al4V.

Chapter 6 focus on the studies of influences of process variables on laser part marking on black, red and white PMMA materials which had a wide range of applications in engineering fields. The effects of different process variables on the responses provide a set of process variables for a particular types of PMMA that has been undertaken for experimentation. Besides, an effort has also been made in order to analyze the surface roughness and UV-VIS-NIR spectroscopy of different types of PMMA as additional quality characteristics of fiber laser line marking.

Chapter 7 contains the general conclusions based upon various experimental results and discussions which have been summarized in brief. Apart from that, the chapter also contains the future scope of work which can be carried out by other researchers in order to extend the work in the areas of laser marking.

## VITA

The author, Mr. Mohit Pandey, son of Mr. Ram Pravesh Pandey and Mrs. Anju Devi was born on 13<sup>th</sup> June 1993 in Kolkata, West Bengal. He studied in Andhra Association School and passed the Secondary Examination of WBBSE in the year 2009 and Higher Secondary Examination of WBCHSE from National High School in the year 2011 respectively with 1<sup>st</sup> class.

The author was graduated with Mechanical Engineering degree in the year 2015 from Seacom Engineering College, Howrah, West Bengal affiliated to West Bengal University of Technology with First class. The author qualified GATE (Graduate Aptitude Test in Engineering) and received AICTE approved post graduate fellowship for a period of two years i.e. 2017-2019. The author completed his M.E. in Production Engineering in the year 2019 from Production Engineering Department, Jadavpur University, Kolkata. The author acknowledge the support from ADF (AICTE Doctoral Fellowship) for 2 years as JRF (August, 2019 –July, 2021) and another two years as SRF (August, 2021 – July, 2023) during the tenure of research for Ph.D work. The author has published five research papers in international journals, one in national journal, two book chapters as well as presented eight research papers in reputed international conferences related to advance machining process during his tenure of research in Production Engineering Department, Jadavpur University.



DEDICATED TO MY PARENTS, TEACHERS ,GUIDE

.....

MY PILLAR OF STRENGTH AND SOURCE OF  
INSPIRATION

FOR THEIR ENDLESS SUPPORT, LOVE AND  
ENCOURAGEMENT

# TABLE OF CONTENTS

	<b>Page No.</b>
<b>TITLE SHEET</b>	
<b>UNIVERSITY SUBMISSION FORM</b>	i
<b>LIST OF PUBLICATIONS OUT OF THE RESEARCH WORK</b>	ii-iii
<b>STATEMENT OF ORIGINALITY</b>	iv
<b>CERTIFICATE FROM THE SUPERVISORS</b>	v
<b>ACKNOWLEDGEMENT</b>	vi
<b>PREFACE</b>	vii-x
<b>VITA</b>	xi
<b>DEDICATION</b>	xii
<b>TABLE OF CONTENTS</b>	xiii- xviii

## **CHAPTER 1. INTRODUCTION**

1.1 Need of Laser Marking	3-5
1.2 Advantages of Fiber Laser Marking	5-6
1.2.1 Applications of Fiber Laser Marking	6-8
1.3 Basic Mechanism of Laser Marking	9-18
1.3.1 Marking by Material Removal from the Surface	9-13
1.3.1.1 Etching	9-10
1.3.1.2 Surface Melting	10-11
1.3.1.3 Ablation	11-12
1.3.1.4 Engraving	12-13
1.3.2 Marking by Surface Modification	14-18
1.3.2.1 Foaming	14-15
1.3.2.2 Carbonization	14-15
1.3.2.3 Annealing	15-16
1.3.2.4 Coloring	16-18

1.4 Various Laser Marking Techniques	18-24
1.4.1 Beam Steering Technique	18-19
1.4.2 Mask Projection Technique	20-21
1.4.3 Polygon Scanner Technique	21-23
1.4.4 Scanning Technique by Movement of Work Piece	23-24
1.5 Fiber Laser in Marking	24-29
1.5.1 Brief History of Fiber Laser	25
1.5.2 Present Status of Fiber Laser	25-27
1.5.3 Classification of Fiber Laser	28
1.5.4 Comparison between Fiber Laser and Other Lasers for Marking	28-29
1.6 Basic Principle of Fiber Laser Generation Process	29-31
1.7 Principle of Fiber Laser Marking Process	31-32
1.8 Literature Review of Fiber Laser Marking Processes	32-56
1.8.1 Laser Marking Using Different Lasers	33-35
1.8.2 Fundamentals of Various Laser Marking Techniques	35-40
1.8.3 Laser Marking on Different Materials	40-48
1.8.4 Laser Marking Systems	49-51
1.8.5 Basic Parametric Influences of Laser Marking	51-53
1.8.6 Optimization and Modelling of Laser Marking	53-56
1.9 Research Gap	57
1.10 Objectives and Scope of the Present Research Work	57-58

## **CHAPTER 2. MATERIALS AND METHODS**

2.1 Experimentation	59
2.2 Materials used as workpiece for Laser Marking	59-62
2.2.1 Stainless Steel 304	59-60
2.2.2 Titanium Alloy (Ti6Al4V)	60-61
2.2.3 Polymethyl Methacrylate (PMMA)	61-62
2.3 Details of Diode Pumped Fiber Laser Marking System	62-70
2.3.1 Fiber Laser Generation Unit	63- 67
2.3.1.1 Optical Fiber	64
2.3.1.2 Silicate Glass	65

2.3.1.3 Rare Earth Doped Elements	65
2.3.1.4 Fiber Bragg Gratings (FBGs)	65-66
2.3.1.5 Laser Diodes	66
2.3.1.6 Fiber Couplers	66
2.3.1.7 Fiber Laser Isolators	66
2.3.1.8 Fiber Coupled Acousto-Optic Modulator	66-67
2.3.2 Fiber Laser Delivery System	67- 69
2.3.2.1 Collimator	67
2.3.2.2 Beam Bender	67
2.3.2.3 Beam Delivery Unit and Focusing Lens	67-69
2.3.3 Assist Air Supply Unit	69
2.3.4 CNC Controller for X–Y–Z Movement	70
2.4 Strategy for Laser marking	70-73
2.5 Fundamental Working Principles of CNC Pulsed Fiber Laser Marking Techniques Process	74-75
2.6 Advancement of CNC pulsed diode fiber laser marking techniques in comparison to simple laser marking process	75

### **CHAPTER 3. EXPERIMENTAL INVESTIGATION INTO FIBER LASER MARKING ON STAINLESS STEEL 304**

3.1 Experimental Planning for the analysis of marking characteristics of surface marking	76-77
3.2 Results and Discussion on Laser Marking of Rectangular Shaped Surface	78- 86
3.2.1 Influences of Laser irradiation on marking characteristics on Stainless steel 304	78-79
3.2.2 Influences of Assist gas pressure on Marking characteristics on Stainless steel 304	79-81
3.2.3 Influences of Transverse feed on Marking characteristics on Stainless steel 304	81-86
3.3 Results and Discussion on Laser Marking of Square Shaped Surface	87-92
3.3.1 Influences of Laser Irradiation on Marking Characteristics of Square shaped Laser Marked Surface	87-88

3.3.2 Influences of Pulse rate on Marking Characteristics of Square shaped Laser Marked Surface	89-90
3.3.3 Influences of Scan rate on Marking Characteristics of Square shaped Laser Marked Surface	90-92
3.4 Results and Discussion on Laser Marking of Elliptical Shaped Surface	93- 106
3.4.1 Influences of Laser irradiation on Marking Characteristics of Elliptical Shaped Laser Marked Surface	96-97
3.4.2 Influences of Pulse rate on Marking Characteristics of Elliptical Shaped Laser Marked Surface	97-99
3.4.3 Influences of Scan rate on Marking Characteristics of Elliptical Shaped Laser Marked Surface	99-100
3.4.4 Influences of Defocusing Distance on Marking Characteristics on Stainless steel 304	100-102
3.4.5 Studies based on Scanning Electron Microscope (SEM) images on Elliptical Laser Marked Surface	102-106
3.5 Results and Discussion on Laser Marking of Equilateral Triangle Shaped Surface	107- 121
3.5.1 Parametric Influences of Laser Irradiation and Pulse Rate on Marking Characteristics of Equilateral Triangle Shaped Laser Marked Surface	110-112
3.5.2 Parametric Influences of Scan Rate on Marking Characteristics of Equilateral Triangle Shaped Laser Marked Surface	112-114
3.5.3 Parametric Influences of Duty Cycle on Marking Characteristics of Equilateral Triangle Shaped Laser Marked Surface	114-115
3.5.4 Some studies based on scanning electron microscope (SEM) on marking characteristics of Equilateral Triangle Shaped Laser Marked Surface	115-121
3.6 Results and Discussion on Laser Marking of Circular Shaped Surface	122- 129
3.6.1 Influences of Laser irradiation on Marking Characteristics of Circular Shaped Laser Marked Surface	123-125
3.6.2 Influences of Pulse rate on Marking Characteristics of Circular Shaped Laser Marked Surface	125-126
3.6.3 Influences of Duty cycle on Marking Characteristics of Circular	126-128

Shaped Laser Marked Surface	
3.6.4 Influences of Scan rate on Marking Characteristics of Circular	128-129
Shaped Laser Marked Surface	
3.7 Outcomes of the Present Research Work	129-131

## **CHAPTER 4. MODELLING AND ANALYSIS OF FIBER LASER MARKING OF STAINLESS STEEL 304 BASED ON RESPONSE SURFACE METHODOLOGY**

4.1 Modeling and Analysis of Fiber Laser marking of SS 304	132-148
4.1.1 Experimental Planning	134-135
4.1.2 Development of Empirical Modeling based on RSM	135-136
4.1.3 ANOVA Test Results of the Developed Models	136-139
4.1.4 Analysis of Fiber Laser Process Variables on Marking Quality	139-148
Characteristics of Stainless Steel 304	
4.1.4.1 Parametric Influences on Mark Intensity of SS 304	140-142
4.1.4.2 Parametric Influences on Angle deviation of SS 304	143-145
4.1.4.3 Parametric Influences on Area Deviation of SS 304	146-148
4.2 Parametric Optimization of Fiber Laser Marking on SS 304	149-155
4.2.1 Single Objective Optimization of the Responses	149-150
4.2.2 Multi-Objective Optimization of the Responses	151-154
4.3 Outcomes of the Present Research Work	154-155

## **CHAPTER 5. EXPERIMENTAL INVESTIGATION INTO FIBER LASER MARKING ON Ti6Al4V**

5.1 Selection of the Process Variables and Responses	156
5.2 Results and Discussion on Marking Characteristics of Ti6Al4V	157- 169
5.2.1 Influences of Transverse feed on Marking Characteristics of	157-159
Ti6Al4V	
5.2.2 Effects of Laser irradiation on Line and Surface Marking	159-160
Characteristics of Ti6Al4V	

5.2.3 Effects of Pulse rate on Line and Surface Marking Characteristics of Ti6Al4V	161-162
5.2.4 Effects of Scan rate on Line and Surface Marking Characteristics of Ti6Al4V	162-164
5.2.5 Effects of Duty cycle on Line and Surface Marking Characteristics of Ti6Al4V	164-168
5.3 Outcomes of the Present Research	168-169

## **CHAPTER 6. EXPERIMENTAL INVESTIGATION INTO FIBER LASER MARKING ON PMMA**

6.1 Introduction to Fiber Laser Marking on PMMA	170
6.2 Results and Discussion on Laser Marking of Black PMMA	170-174
6.2.1 Effects of Laser irradiation on Marking Characteristics of B-PMMA	170-171
6.2.2 Effects of Pulse rate on Marking Characteristics of B- PMMA	171-172
6.2.3 Effects of Scan rate on Marking Characteristics of B-PMMA	172-174
6.3 Results and Discussion on Laser Marking of Red PMMA (R-PMMA) and White PMMA (W-PMMA)	174-185
6.3.1 Spectrum analysis of red and white PMMA	174-178
6.3.2 Effects of Laser irradiation on Marking Characteristics of red and white PMMA	178-180
6.3.3 Effects of Pulse rate on Marking Characteristics of red and white PMMA	180-182
6.3.4 Effects of Scan rate on Marking Characteristics of red and white PMMA	182-185
6.4 Outcomes of the Present Research	186

## **CHAPTER 7. GENERAL CONCLUSIONS AND FUTURE SCOPE OF RESEARCH**

7.1 General Conclusions	187-189
7.2 Future Scope of the Present Work	189-192

## **BIBLIOGRAPHY**

## LIST OF FIGURES

No.	Title of the figures	Page No.
1.1	Types of Industrial Lasers and their Categorization	2
1.2	Different applications in the field of laser marking	2
1.3	Laser Marking by Etching	10
1.4	Laser Marking by Surface Melting	10
1.5	Marking by Laser Ablation	13
1.6	Marking by Laser Engraving	13
1.7	Marking by Laser Foaming	15
1.8	Marking by Laser Carbonising	15
1.9	Marking by Laser Annealing	17
1.10	Laser Colour Marking	17
1.11	Beam Steering Technique	19
1.12	Mask Projection Technique	20
1.13 (a)	Polygon Scanner Method	23
1.13 (b)	Pre-objective and Post-objective System in Polygon Scanner Method	23
1.14	Scanning Technique by movement of workpiece	23
1.15	Schematic diagram of a pulsed fiber laser system	27
1.16	Schematic representation of a mode-locked fiber laser with acousto optic modulator	27
1.17	Schematic diagram of a master oscillator power amplifier (MOPA) design of fiber laser	27
1.18	Acceptance angle of fiber with quantities related to the numerical aperture	31
2.1	EDX analysis of Stainless steel 304	60
2.2	Schematic view of diode pumped fiber laser marking system	63
2.3	Photographic view of fiber laser generation unit	64
2.4	Photographic view of the collimator	68



2.5	Photographic view of beam bender	68
2.6	Photographic view of beam delivery unit and working table	68
2.7	Photographic view of an air compressor with moisture separator	69
2.8	Line diagram for the generation of complex geometrical shapes	72
2.9	Schematic diagram of the working process of laser marking	75
3.1	Schematic representation of laser marked and unmarked surface for the calculation of gray value	76
3.2	Schematic representation of associated terms and laser scanning direction related to laser marking	77
3.3	Influence of laser irradiation on mark intensity of surface marking of width 0.48mm	79
3.4	Microscopic view of laser marked surface at variant laser irradiation (a) 50 W (b) 30 W (c) 20 W	79
3.5	Variation of (a) mark intensity (b) marked width with laser irradiation with and without the application of assists gas pressure of surface marking of width 0.48mm	80
3.6	Visual perspective of marked surface with the supply of assist gas pressure of surface marking of width 0.48mm	80
3.7	Variation of marking characteristics (a) mark intensity and time requirement (b) width of mark with change of scan rate at transverse feed of 8 $\mu$ m/laser stroke of surface marking of width 0.48mm	82
3.8	Microscopic view of laser scanned surface with change of scan rate at transverse feed of 8 $\mu$ m/laser stroke (a) 35 mm/s (b) 21 mm/s (c) 7 mm/s	82
3.9	Variation of marking characteristics (a) mark intensity and time requirement (b) width of mark with change of scan rate at transverse feed of 6 $\mu$ m/laser stroke of surface marking of width 0.48mm	83
3.10	Microscopic view of laser scanned surface with change of scan rate at transverse feed of 6 $\mu$ m/laser stroke (a) 35 mm/s (b) 21 mm/s (c) 7 mm/s	83

3.11	Variation of marking characteristics (a) mark intensity and time requirement (b) width of mark with change of scan rate at transverse feed of 4 $\mu$ m/laser stroke of surface marking of width 0.48mm	84
3.12	Microscopic view of laser scanned surface with change of scan rate at transverse feed of 4 $\mu$ m/laser stroke (a) 35 mm/s (b) 21 mm/s (c) 7 mm/s	84
3.13	Variation of marking characteristics (a) mark intensity and time requirement (b) width of mark with change of scan rate at transverse feed of 2 $\mu$ m/laser stroke of surface marking of width 0.48mm	85
3.14	Microscopic view of laser scanned surface with change of scan rate at transverse feed of 2 $\mu$ m/laser stroke (a) 35 mm/s (b) 21 mm/s (c) 7 mm/s	85
3.15	Photographic view of alphabet and number marked using fiber laser	86
3.16	Variation of Marking Characteristics with respect to laser irradiation in marking of square shaped laser marked surface	88
3.17	Surface texture of laser marked surface at different laser irradiation (a) 7.5 W, (b) 10.5 W, (c) 12.5 W, (d) 15 W when other process variables such pulse rate of 50 kHz, duty cycle of 99 % and scan rate of 35 mm/s were kept constant in marking of square shaped laser marked surface.	88
3.18	Variation of Marking Characteristics with respect to Pulse rate in marking of square shaped laser marked surface	89
3.19	Surface texture of laser marked surface at different pulse rate (a) 52.5 W, (b) 55 kHz, (c) 57.5, (d) 60 kHz when other process variables such laser irradiation of 15 W, duty cycle of 99 % and scan rate of 35 mm/s were kept constant in marking of square shaped laser marked surface.	89
3.20	Variation of marking characteristics (a) mark intensity (b) angle and time with change of scan rate in marking of square shaped laser marked surface	91

3.21	Plot of time requirement to mark the surface with respect to side of square	91
3.22	Photographic view of square shaped laser marked surface	91
3.23	Microscopic view of elliptical shaped laser marked surface (a) region selection for mark intensity calculation (b) Measurement of major and minor axis of elliptical shaped image. (c) Direction of laser travel for ellipse generation.	93
3.24	Pictorial representation for the calculation of mark intensity value of laser marked surface using MATLAB software	94
3.25	Surface roughness measurement through MITUTOYO Surf test SJ 410	95
3.26	Variation of marking characteristics (a) mark intensity and area deviation (b) surface roughness with change of laser irradiation in case of ellipse	97
3.27	Variation of marking characteristics (a) mark intensity and area deviation (b) surface roughness with change of pulse rate in case of ellipse	98
3.28	Variation of marking characteristics (a) mark intensity and area deviation (b) surface roughness with change of scan rate in case of ellipse	99
3.29	Variation of marking characteristics (a) mark intensity, (b) area deviation (c & d) surface roughness with change of defocusing distance in case of ellipse	100
3.30	Microscopic view of laser marked surface at defocussed condition in case of ellipse	100
3.31	SEM images of laser marked surface at defocussed condition of 2 mm in positive direction (a) Full laser marked surface (b) Enlarged view of inner laser marked surface in case of ellipse	103
3.32	SEM images of marked surface with the EDX analysis of inner marked surfaces at focussed condition (a) Full laser marked surface, (b) Enlarged view of inner laser marked surface, (c) EDX analysis of spot of inner laser marked surface in case of ellipse	103

3.33	SEM images of laser marked surface at defocussed condition of 2 mm in negative direction (a) Full laser marked surface, (b) Enlarged view of inner laser marked surface, (c) EDX analysis of spot of inner laser marked surface in case of ellipse	104
3.34	SEM images of laser marked surface at defocussed condition of 4 mm in negative direction (a) Full laser marked surface (b) Enlarged view of inner laser marked surface in case of ellipse	104
3.35	Surfaces marked with laser at defocusing distance of 2 mm in negative direction	106
3.36	Area selection for evaluating mark intensity in case of equilateral triangle	107
3.37	Schematic diagram of marked laser surface and associated terms related to the process of laser marking	109
3.38	Microscopic view of marked laser surface with measurement in marking equilateral triangle shaped laser marked surface	109
3.39	Marking characteristics variation with change of laser irradiation and pulse rate in marking equilateral triangle shaped laser marked surface	110
3.40	Microscopic view of images at different laser irradiation and pulse rate in marking equilateral triangle shaped laser marked surface	112
3.41	Marking characteristics variation (a) mark intensity, (b) Angle,(c) Area deviation with change of scan rate in marking equilateral triangle shaped laser marked surface	113
3.42	Microscopic view of marked laser surface with change of scan rate (a) 28 mm/s (b) 21 mm/s (c) 14 mm/s (d) 7 mm/s in marking equilateral triangle shaped laser marked surface	113
3.43	Marking characteristics variation (a) mark intensity (b) Angle (c) Area deviation with the change of duty cycle in marking equilateral triangle shaped laser marked surface	115
3.44	SEM images of triangular marked laser surface at different location	116

3.45	SEM images of marked laser surface at different scan rate (a) 7 mm/s and (b) 35 mm/s	116
3.46	EDX analysis of triangle marked laser surface as shown in Fig. 3.44 (c) site no.2	117
3.47	SEM images of the surface at defocused position in marking equilateral triangle shaped laser marked surface	117
3.48	EDX analysis of the spot as shown in Fig. 3.47 in marking equilateral triangle shaped laser marked surface	117
3.49	Requirement of time to mark the different triangular sized surface	119
3.50	Different geometric marked laser surface for setting the scan rate (a) at 7 mm/s (b) at 21 mm/s (c) at 35 mm/s (d) at 7mm/s	119
3.51	Laser marked surface of pentagon at better obtained process variables	121
3.52	Laser marked surface of hexagon at better obtained process variables	121
3.53	Deviation of Mark intensity with Transverse feed in marking circular shaped laser marked surfaces	122
3.54	Microscopic view of laser marked surface at variable transverse feed per laser stroke (a) 4 $\mu\text{m}$ /laser stroke (b) 8 $\mu\text{m}$ /laser stroke (c) 12 $\mu\text{m}$ /laser stroke in marking circular shaped laser marked surfaces	122
3.55	Variation of marking characteristics with change of laser irradiation in marking circular shaped laser marked surfaces	124
3.56	Microscopic view of laser marked surface at variant laser irradiation (a) 7.5 W, (b) 12.5 W, (c) 17.5 W	124
3.57	Variation of marking characteristics with change of pulse rate in marking circular shaped laser marked surfaces	125
3.58	Microscopic view of laser marked surface at variant pulse rate (a) 50 kHz (b) 55 kHz (c) 60 kHz	125
3.59	Deviation of mark intensity with duty cycle in marking circular shaped laser marked surfaces	127
3.60	Microscopic view of laser marked surface at variant duty cycle (a) 20% (b) 30% (c) 40%	127

3.61	Variation of marking characteristics with change of scan rate in marking circular shaped laser marked surfaces	129
3.62	Microscopic view of laser marked surface at variant scan rate (a) 5 mm/s (b) 15 mm/s (c) 25 mm/s	129
4.1	Schematic view of laser travel for the generation of equilateral shaped laser marked surface along with measurement of responses	133
4.2	Contour plot of Mark Intensity with respect to Pulse rate and Laser irradiation in marking equilateral triangle shaped laser marked surface	141
4.3	Surface plot of Mark Intensity with respect to Pulse rate and Laser irradiation in marking equilateral triangle shaped laser marked surface	141
4.4	Contour plot of Mark Intensity with respect to Duty cycle and Scan rate in marking equilateral triangle shaped laser marked surface	142
4.5	Surface plot of Mark Intensity with respect to Duty cycle and Scan rate in marking equilateral triangle shaped laser marked surface	142
4.6	Contour plot of Angle deviation with respect to Pulse rate and Laser irradiation in marking equilateral triangle shaped laser marked surface	144
4.7	Surface plot of Angle deviation with respect to Pulse rate and Laser irradiation in marking equilateral triangle shaped laser marked surface	144
4.8	Contour plot of Angle deviation with respect to Duty cycle and Scan rate in marking equilateral triangle shaped laser marked surface	145
4.9	Surface plot of Angle deviation with respect to Duty cycle and Scan rate in marking equilateral triangle shaped laser marked surface	145

4.10	Contour plot of Area Deviation with respect to Pulse rate and Laser irradiation in marking equilateral triangle shaped laser marked surface	147
4.11	Surface plot of Area Deviation with respect to Pulse rate and Laser irradiation	147
4.12	Contour plot of Area Deviation with respect to Duty cycle and Scan rate in marking equilateral triangle shaped laser marked surface	148
4.13	Surface plot of Area Deviation with respect to Duty cycle and Scan rate in marking equilateral triangle shaped laser marked surface	148
4.14	Optimization plot for mark intensity in marking equilateral triangle shaped laser marked surface	150
4.15	Optimization plot for Angle Deviation in marking equilateral triangle shaped laser marked surface	150
4.16	Optimization plot for Area Deviation in marking equilateral triangle shaped laser marked surface	150
4.17	Optimization plot for multi objective optimization in marking equilateral triangle shaped laser marked surface	151
4.18	Image of a laser-marked surface taken at its ideal parametric setting	152
4.19	SEM images of different sites of marked surface at optimal process variables settings	152
4.20	3D and 2D Surface profile of laser marked surface at optimal parametric settings in marking equilateral triangle shaped laser marked surface	153
4.21	Photographic view of other geometric shape marked at optimal parametric setting	153
5.1	Microscopic view of (a) line and (b) surface laser marking on Ti6Al4V	156
5.2	Variation of mark characteristics with change of transverse feed on Ti6Al4V	158

5.3	Microscopic images of laser marked surface at variant transverse feed on Ti6Al4V	158
5.4	Influence of laser irradiation on line and surface marking on Ti6Al4V	160
5.5	Microscopic view of line and surface marked surface with respect to laser irradiation on Ti6Al4V	160
5.6	Influence of pulse rate on line and surface marking on Ti6Al4V	161
5.7	Microscopic view of line and surface marked surface with respect to pulse rate on Ti6Al4V	161
5.8	Influence of scan rate on line and surface marking on Ti6Al4V	163
5.9	Microscopic view of line and surface marked surface with respect to scan rate on Ti6Al4V	163
5.10	Influence of duty cycle on line and surface marking on Ti6Al4V	165
5.11	Microscopic view of line and surface marking with respect to duty cycle on Ti6Al4V	165
5.12	Laser marked surface of pentagon at better obtained process variables	167
5.13	Laser marked surface of hexagon at better obtained process variables	167
5.14	Laser marked surface of square at better obtained process variables	167
5.15	Laser marked surface of circle at better obtained process variables	167
6.1	Influence of laser irradiation on marking characteristics of B-PMMA	171
6.2	Influence of pulse rate on marking characteristics of B-PMMA	172
6.3	Influence of scan rate on marking characteristics of B-PMMA	173
6.4	Character marked at better obtained process variables	173
6.5	Symbol and Character marked at laser irradiation of 15% of 50 W, pulse rate of 120 kHz, and scan rate of 35 mm/s on B-PMMA	174
6.6	Spectroscopy test results of B-PMMA before and after laser marking operation (a, b) Reflectance, (c, d) Absorbance, (e,f) Transmittance	175



6.7	Spectroscopy test results of R-PMMA before and after laser marking operation on (a, b) Reflectance, (c, d) Absorbance, (e,f) Transmittance	176
6.8	Spectroscopy test results of W-PMMA before and after laser marking operation (a, b) Reflectance (c, d) Absorbance (e,f) Transmittance	177
6.9	Influence of laser irradiation on marking characteristics of R-PMMA and W-PMMA	179
6.10	Laser surface marked on W-PMMA and R-PMMA at 100 % laser irradiation	179
6.11	Influence of pulse rate on marking characteristics of R-PMMA and W-PMMA	181
6.12	Influence of scan rate on marking characteristics of R-PMMA and W-PMMA	183
6.13	Microscopic view of marked laser surface on red PMMA (a) 35 mm/s, (b) 21 mm/s and (c) 7 mm/s	183
6.14	3D Surface Profile of W-PMMA at variant scan rate (a) 35mm/s and (b) 7 mm/s	184
6.15	3D surface view of laser surface marked at scan rate of 7 mm/s on R-PMMA	184
6.16	Photographic view of some character marked on W-PMMA at laser irradiation of 100 % of 50 W, pulse rate of 85 kHz, and scan rate of 35 mm/s.	185
6.17	Photographic view of some character marked on R-PMMA at laser irradiation of 100 % of 50 W, pulse rate of 85 kHz, and scan rate of 35 mm/s.	185

## LIST OF TABLES

No.	Title of the Tables	Page No.
1.1	Comparison of laser with other forms of marking systems	4
1.2	Ablation depth and fluence of different material	12
2.1	Composition of Stainless Steel 304	60
2.2	Chemical compositions of Ti6Al4V	61
2.3	Properties of Ti6Al4V	61
2.4	Properties of PMMA	62
2.5	Specification of Laser Marking Machine	63
2.6	Advancement of CNC Pulsed Diode Fiber Laser Marking Techniques in Comparison to Simple Laser Marking Process	75
3.1	Process variables and their levels in case of ellipse	96
3.2	Selection of process variables and their range in case of equilateral triangle	107
4.1	Process Parameter and their levels in marking equilateral triangle shaped laser marked surface	134
4.2	Response values based on experimental plan using CCRD in marking equilateral triangle shaped laser marked surface	135
4.3	ANOVA for Mark Intensity in marking equilateral triangle shaped laser marked surface	137
4.4	ANOVA for Angle Deviation in marking equilateral triangle shaped laser marked surface	138
4.5	ANOVA for Area Deviation in marking equilateral triangle shaped laser marked surface	139
5.3	Comparison of Theoretical and Actual mark intensity of obtained colours on marked surface on Ti6Al4V	166

## 1. INTRODUCTION

In order to mark or print bar codes, matrix codes, universal product codes (UPCs), serial numbers, etc., industries often use laser marking which is a flexible, programmable, and environmentally friendly process that uses a thermal process of high intensity laser beam to create a contrasting mark on the material surface. The primary use of laser marking is for the traceability and identification of products. The method of marking can be broadly classified into two categories: material removal or surface modification. With high-energy lasers, the former can be accomplished by melting and vaporisation, or ablation. In contrast, in the latter, material is not removed. Instead, the laser light changes the composition of the material to produce a high contrast mark. The advantages of laser marking over conventional marking methods like inkjet, hot stamping, or mechanical scribing are flexibility, speed, indestructibility, reliability, the lack of consumables, and high levels of cleanliness. Applications for fiber laser marking include jewellery, medical implants, surgical tools, automotive items, and a wide range of other products. Although CO<sub>2</sub> lasers are frequently used to mark painted and anodized metals, plastics, wood, and glass, they are not appropriate for marking polished metals due to the high reflectivity of most metals at a wavelength of 10.6 microns. On ceramics and semiconductor materials, pulsed CO<sub>2</sub> and Nd: YAG lasers can both produce effective marking results [1]. However, higher resolution is achieved by Fiber or Nd: YAG lasers as its line width is shorter than that of CO<sub>2</sub> lasers. When it comes to marking very transparent materials, second and third harmonic Nd: YAG lasers operating at 532 and 355 nm, as well as ultraviolet excimer lasers, are sometimes the best option. The numerous laser types utilised in various industries and their classification are shown in Fig. 1.1. For smaller components that require fine marking with little effects on workpiece surface in organisation like electronic, medical, aerospace, and other industries are pushing the limitations of work in the micron range. The use of laser technology is useful in keeping up the industry needs for smaller geometries and ever-tighter standards. In addition, the cost inefficiency and longer marking times have created a foundation for considering enhanced alternative marking technologies that can address the outstanding issues related to conventional marking procedures [2].

Fig.1.2 highlights different applications in the field of laser marking employed by organisation in modern world.

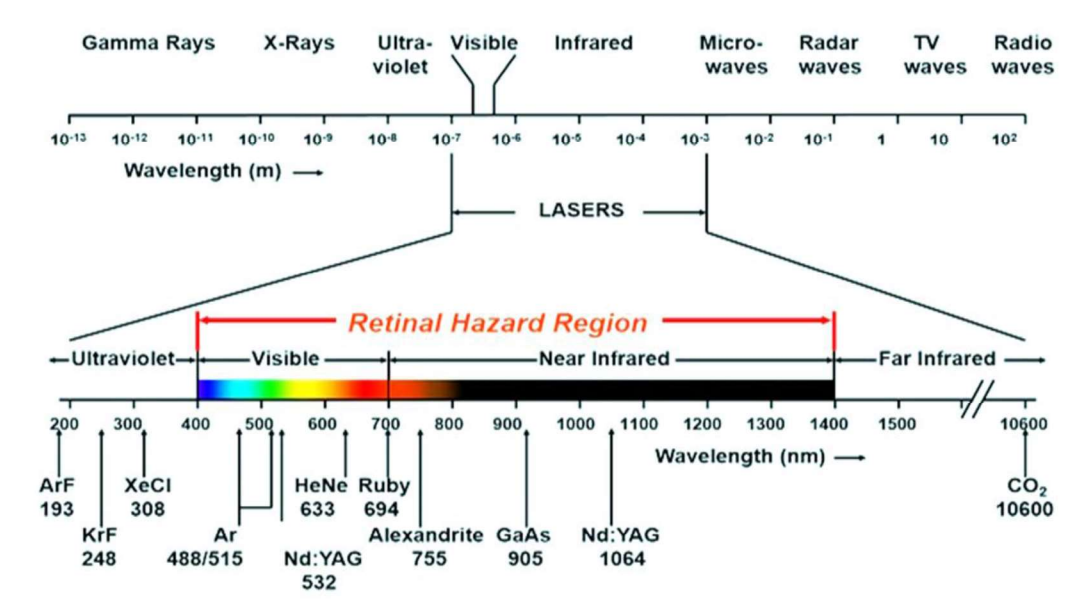


Fig.1.1 Types of Industrial Lasers and their Categorization

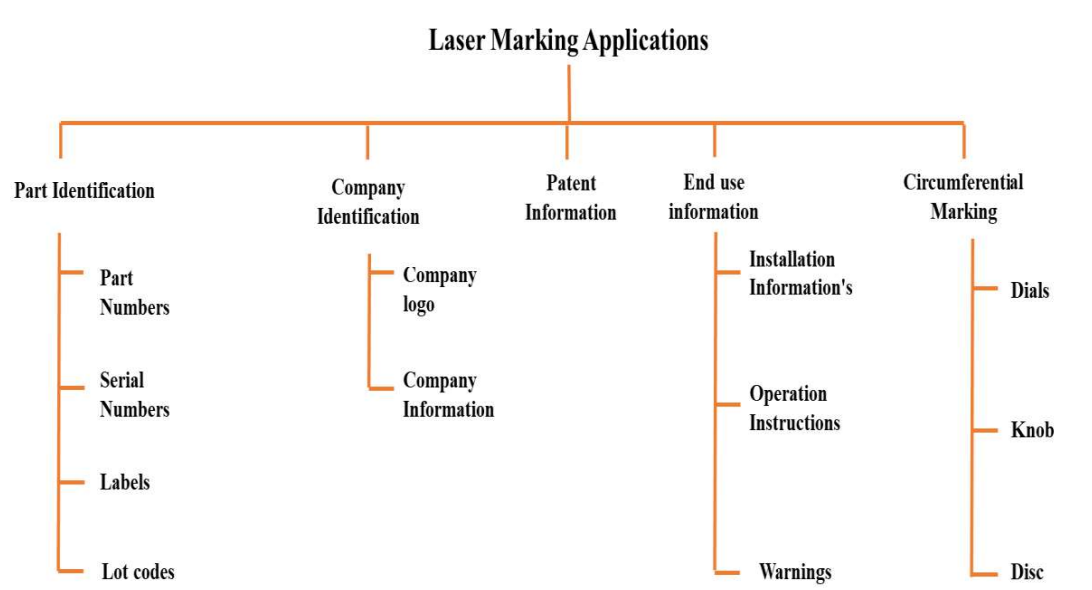


Fig.1.2 Different applications in the field of laser marking

As a result, non-traditional marking strategies for manufacturing smaller forms and sizes become an instant success for both academics and business people. At the same time, the

standards for the marking process are being raised in terms of quality, adaptability, speed, and manufacturing costs. Researchers found that Nd:YAG laser of 1064 nm wavelength is suitable for carrying out enormous operation such as cutting, drilling, grooving, marking etc. but due to its high maintenance cost it has been replaced with fiber laser which has little or no maintenance cost. Moreover, the machined surface achieved through fiber laser has better characteristics as compared to Nd: YAG laser. In the present study, three distinct materials such as Stainless Steel 304, Ti6Al4V, and PMMA are chosen for the generation of good quality laser marking characteristics which has wide applications in the areas of orthopaedic implants, electronics, refractory applications, seals, and pump impellers parts etc.

## **1.1 Need of Laser Marking**

The laser marking of a specific geometrical shape such as square, ellipse, circle, hexagon, pentagon and equilateral triangle can be used by any organisation as a part of product identification and protection against counterfeiting in several fiercely competitive industries. The marking procedure differs based on the products that need to be tagged. There are numerous ways to brand items directly. Choosing the most appropriate approach for the application is essential to its success. Before choosing the best approach, it is crucial to consider and try out as many as strategy which has pros and cons of its own. Table 1.1 presents a comparative analysis of several marking techniques. Many traditional marking techniques are used before laser marking became popular. A low voltage current is used in the electrochemical etching process to mark the object's surface. This is frequently employed for product runs with limited volume. With an ink jet marking technique, tiny dots are sprayed straight onto the surface. An ink jet creates marks with a high contrast. One does not consider ink jet to be a permanent marking technique. Dot peen is a percussion marking technique that makes marks by creating depth. For applications where the symbol must endure the full life cycle, dot peen is advised. But there are certain materials where conventional markings are unsuitable such as data matrices that require machine reading because they are devoid of contrast and resolution, making them challenging to view from a distance. Additionally, they should not be used in any delicate application where it is forbidden to damage the substrate such as in the case of medical devices, chrome-plated bathroom fixtures, cutlery, aerospace, automotive, etc. Although ink markings can result in extremely readable and long-lasting inscriptions, the process is labour-intensive and takes

a lot of processes. Furthermore, there are difficulties in maintaining the equipment and managing print quality [3]. However, laser marking is a clean, energy-efficient, non-contact method that doesn't require any consumables. Additionally, because it doesn't require any chemicals or inks like other marking methods like chemical etching or inkjet and it is an environmentally friendly technique. The exponential rise in the usage of direct marking of part information facilitate the user for tracking information of parts manufactured. Laser marking plays a pivotal role in marking of medical devices to automotive and aerospace parts as it creates contrast marks with minimal harm to the performance of parts. Marking the symbols and bar codes used for process control during manufacturing in factories is one of the main uses of laser marking. Bar codes are useful for providing information needed for further processing during a product's manufacturing process. The component information could be represented by barcodes, data-matrix codes, or human-readable alphanumeric characters.

**Table1.1** Comparison of laser with other forms of marking systems [4]

<b>Parameter</b>	<b>Laser</b>	<b>Ink Jet</b>	<b>Dot Peen</b>	<b>Chemical Etching</b>
Best for	Most applications	High speed moving parts	Large/thick metal parts	Thin metals, repeated marks
Mark quality	Excellent	Average	Poor	Excellent
Materials	Most materials	Most materials	Metals	Metals only
Mark Permanence	Permanent	Marking can be rubbed off in time	Permanent	Permanent
Speed	Fast	Fast	Slow	Slow
Integration	Highly flexible system for production line and also programming and remote operation	Basic mark control	Basic mark control	NA
Maintenance	Maintenance free	Daily maintenance needed to ensure inks are flowing properly and the machine is free from any residual built-up during marking	Daily maintenance needed to ensure stylus pens are working well	Daily maintenance needed to ensure masks are working well
Capital cost	More	Less	Less	Less
Running cost	Less	More	More	More

The advantages of laser marking technology also include reduced cost of ownership, enhanced environmental profile, simple and adaptable automation. This automated solution will lower the amount of defects and increase production. In order to maintain quality control, it is also used to indicate a product's lot and serial numbers, which provide information on the product's manufacturing date and location. Marking helps manufacturers to reduce the number of products that are recalled from the market for identification of the production lot, which protects them against a significant consumer complaint. In this sense, food quality assurance dates are identified by laser marking, which enables manufacturers to prominently display the duration of their liability for the product and enables customers to make purchases without concern by simply figuring out how old a product is. Most 90% laser marking applications nowadays are "non-aesthetic" that include bar codes, expiration dates, identifying numbers, and specifications, especially for parts that carry a high probability of failure. The remaining 10% are aesthetic applications, primarily in the form of product distinctiveness and business logos [5].

## **1.2 Advantages of Laser Marking**

The last several years have seen a notable increase in the applications for fiber lasers. This is mostly because of a few features of laser marking and the benefits they provide over photo etching or other traditional marking techniques. Setup time can be significantly decreased, and CAD programs make it simple to generate laser mark layouts for the productive manufacture of new designs. Compared to other marking techniques, fiber laser marking has many advantages and some of the advantages of laser marking are listed below [6]:

### **(i) Precise and High-Quality Markings**

A wide range of products can benefit greatly from this technology because laser systems generate images that are clear and long-lasting. Reproducible high-resolution characters and images are produced by this intrinsically correct technology. In contrast to printed marks, which are on the material's surface, laser marks are really implanted in the material, enhancing the image's endurance and resistance to wear. Therefore, under typical operating conditions, regular cleaning is less likely to cause harm to laser markings.

### **(ii) Greater Design Flexibility**

When it comes to flexible design, laser marking surpasses other techniques. The laser equipment can make images on geometrically complicated uneven surface or other

inaccessible surfaces because there is no direct contact with the surface to be marked. CNC software has a provision to change several images quickly and even more design flexibility is possible with a typing speed of 200 letters per second, or 2000 mm/s, can be written with a computer-controlled laser mark. The time to mark can be significantly shortened by producing prototypes in small batches more readily.

#### **(iii) Low operating cost**

Modern manufacturers can save a significant amount of money by employing laser marking technology instead of photo etching or other marking techniques. As painting processes have advanced to provide coatings of higher quality, laser marking has grown in popularity as a viable substitute for traditional methods. By integrating creative designs in a shorter amount of time, laser marking provides panel manufacturers with the competitive edge they need in the highly competitive world of just-in-time manufacturing.

#### **iv) Non-contact and automated process**

Since laser marking is a noncontact procedure, there is no wear on the tools. Additionally, it does not cause the product to become overheated, distort physically, or undergo any chemical changes. Small indentation areas that are inaccessible with traditional marking techniques can be readily marked with a laser. It requires no extra handling because it is simple to incorporate into automated production lines. Products with a variety of shapes can be marked using lasers, which can be optimally computer controlled. Computers can swiftly alter marks without the need for retooling. The laser marking equipment may be safely integrated into the production line because of the low rejection rates.

### **1.2.1 Applications of Laser Marking**

Laser marking is incredibly useful for marking a wide variety of materials. Fig. 1.2 presents a different applications in the area of laser marking. When producing an indelible, high-quality mark requires a clean, quick, non-contact marking method, laser marking offers an attractive answer [7]. The following are the examples of laser marking applications:

#### **(i) Metals**

Laser marking is a very precise and hygienic method of working with metal. Products and component parts can be marked with codes, logos, and serial numbers at the highest resolution possible. The metal surface is not harmed during contact-free metal marking



with the laser. Laser marking of metals is commonly used in tool manufacture, medical technologies, and product labelling and coding in the electronics industry. An exceptionally useful technique for burr-free, delicate marking on materials is the annealing method.

#### **(ii) Plastics**

When it comes to permanently and impenetrably marking data, codes, and other information on items, laser marking techniques for plastics are becoming more and more popular. Technically speaking, light and dark markings are currently achievable, but the design and packaging industries are continuously requesting coloured markings and greater design possibilities using laser technology. With the laser, a wide variety of widely used polymers can be accurately and long-lastingly inscribed or engraved. Cost-effective labelling is possible even for small batch sizes because of high flexibility and quick setup times. Fiber lasers are commonly used to mark codes, logos, data matrices, and clear texts. Acrylonitrile butadiene, polycarbonates, polyamides, polybutylene terephthalate, and polyolefins (polyethylene, polypropylene) are materials that are particularly well suited for this procedure.

#### **(iii) Human implants**

Making a lasting trace on the material's surface to enable reading and recognition is the goal of laser marking. Prior to usage, the surfaces of surgical instruments and implants placed in human bodies must be thoroughly cleaned and sterilised. Under these circumstances, the materials' lifetime and dependability are known to be severely limited by corrosion deterioration and surface property changes. In particular, if traditional marking (dot peen, chemical etching, etc.) is used, the anticorrosion properties of different stainless steels are often changed.

#### **(iv) Stones**

Granite, marble, slate, and other polished, possibly dark natural stones are excellent candidates for laser branding. The stone's surface dissolves when marking with a laser. It affects the substance directly. Therefore, there's no need to make a stencil. The better the outcomes of stone marking, the more uniform and finely grained the stone is. In reality, tombstones, paperweights, and decorations are common uses of laser marking on stone. It is also feasible to create unique stone tiles that are laser-markable.

#### **(iv) Wood**

When it comes to marking wood and timber, lasers perform best on toys, décor pieces, artistic crafts, mementos, Christmas decorations, gifts, architectural models, and wood inlays. Personalisation and individualization are frequently crucial when using a laser to mark wood. For example, picture frames can have text or lines added to them to boost its value, and the laser can mark photos or even logos in incredibly detailed ways. With a laser, the user can refine wood to an extremely high grade and with great versatility. Given that wood is a natural material, the laser operator must take into account a number of factors when dealing with it, including its density and resin content. Balsa wood and other soft wood varieties mark more quickly and with less laser irradiation. Hard wood, on the other hand requires a higher laser irradiation to mark.

#### **(v) Glass**

On a variety of glasses, including pressed glass, float glass, crystal glass, and mirror glass, glass marking provides amazing design possibilities. Mirrors, bottles, glasses are the most intricate object to directly laser marked photos and graphics. With the use of laser, any pattern that can be printed and also can be etched on to glass.

#### **(vi) Product Recognition and Identification for various applications**

Product liability and environmental concerns have led to a growing importance of product recognition and identification. Now the important applications for laser marking have been determined, and more research and development are undergoing. Automotive applications such bumpers, headlamps, body panels, underbonnet parts, and structural elements are among them. There is also a great deal of promise in electrical and electronic applications, such as switches, plugs, connections, capacitor housings, and bobbins. Consequently, the relevance of labelling industrial components and semi-finished goods is increasing quickly. Simultaneously, the marking process is subject to progressively more demanding specifications for quality, flexibility, speed, and manufacturing cost. The preferred method for tracking, personalisation, and permanent product identification is laser marking. The following is a list of the wide range of applications in the field of product identification and recognition such as marking text and graphics on plastic computer peripherals, identifying components by adding text, images, and part numbers to gears of automotive products, putting text and pictures on epoxy-packed integrated circuits of electrical ,electronic components and promotional products and giftware.

## **1.3 Basic Mechanism of Laser Marking**

A considerable quantity of energy is produced in a narrow, defined area using lasers. This concentrated energy when falls heats, melts, or vaporises and simultaneously oxidised the material in specific regions to cause laser marking operation. By melting, annealing, or vaporising materials, lasers can produce striking contrasts that are all distinctly permanent. The idea behind laser marking is that a laser beam can change a surface's optical characteristics when it strikes it. This can happen in a number of different methods. Marking mechanisms can be broadly classified into two categories:

**(a) Marking by material removal from the surface.**

**(b) Marking by surface modification.**

### **1.3.1 Marking by Material Removal from the Surface**

This process involves either melting, vaporising, or photochemically breaking down the material, or ablation and engraving it to leave a visible mark. There is a discernible high contrast mark as a result of the surface morphology. Hereafter, the specifics of these mechanisms are examined [8].

#### **1.3.1.1 Etching**

The technique of laser etching involves raising the surface temperature to a point where substrate surface melting occurs. A material's surface is heated by the laser beam, and as it cools, the material changes in texture. Small quantities of material are actually removed from the metal object during the etching process in order to form a mark. The actual etching process begins when a solid in contact with a gas or liquid, a gas in contact with a solid, or both a solid and a gas at the same time absorb laser light. The solid and gas or liquid will react as a result of the stimulation. Absorption causes electronic excitation, which can melt, heat, or cause instantaneous direct heating, depending on the wavelength of light employed. Photochemical refers to the former and photothermal to the latter. When it is desirable to minimise the thermal burden on a material, etching is preferred over ablation due to its relatively low input energy need.

Industrial applications for etching include marking tools or parts with barcodes, logos, and serial numbers. It works exclusively with specific metals, some polymers, and surfaces coated in metal. The necessity of laser marking an IC package is growing as a result of the

current advancements in the miniaturisation of micro-electronic components. In some situations, deep laser etching on an IC package may damage the IC itself, therefore marking at several micrometre depth is necessary. The photographic view of laser etching marked sample is shown in Fig. 1.3. This method's benefit over laser colouring is its rapid marking speed because it requires less depth than colouring metallic substrates. Substantial outcomes are consistently achievable at penetration depths of less than 25  $\mu\text{m}$ . On some metals, however, this approach should not be applied because fissures formed in the molten metal during cooling can spread into the underlying surface material, where material integrity is crucial to the part. In the event that the part is under stress or has frequent temperature cycling, these cracks may widen downward. Part failures and metal fatigue have been caused by these situations. It is not advised to use laser etching on items thinner than 1.5 mm.

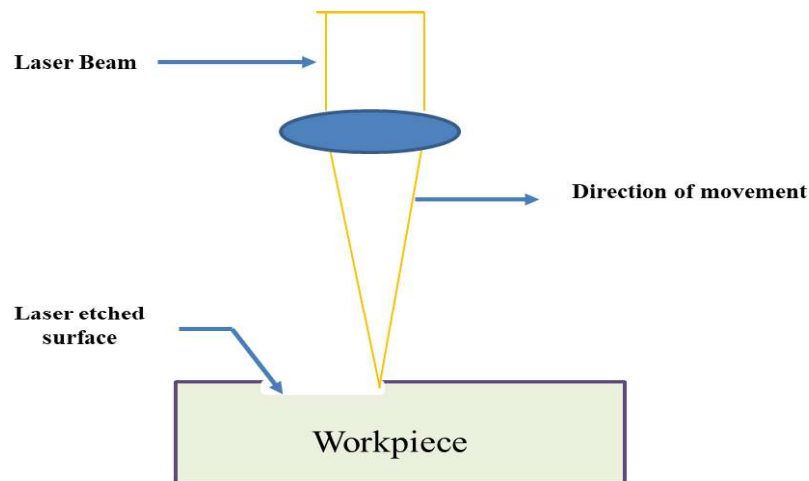


Fig.1.3 Laser Marking by Etching

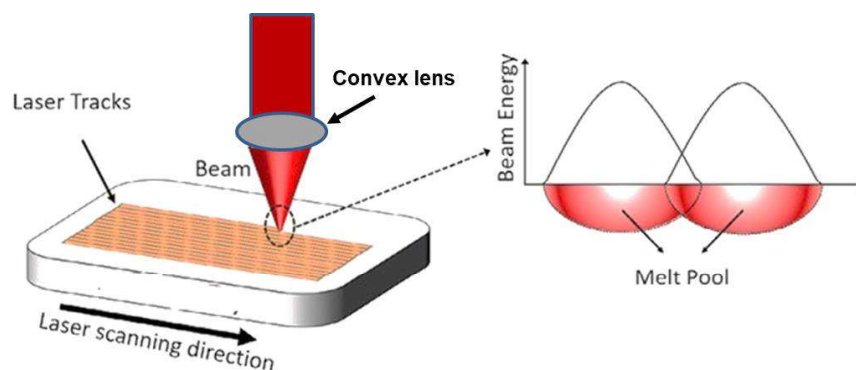


Fig.1.4 Laser Marking by Surface Melting

### **1.3.1.2 Surface Melting**

Melting can result in the substance becoming molten in condition. A coating, such as paint, anodization, chrome, black oxide, etc., is removed by the laser beam to expose the underlying material. Because of the stark contrast between the coating and the base material, this technique produces extremely detailed and crisp characters and designs. With metallics, this method is rarely employed because it provides no discernible benefits. A large range of commercial plastics produce marking pictures with outstanding quality and colour contrast. It is common to achieve excellent results at penetration depths of less than 25  $\mu\text{m}$ . Fig.1.4 depicts photographic view of marked surface by melting. This type of laser marking was initially created to remove opaque layers off from transparent objects. Laser marking of anodized aluminium and labels composed of unique multiple-layer foils are usually done by the same procedure. The labels are cut off without causing any damage to the carrier foil after marking.

### **1.3.1.3 Ablation**

Ablation is the ejection of material caused only by the interaction of a high-intensity laser pulse with the material. It is typically explained in terms of physical processes as vaporisation, ionisation, or exfoliation. The most common environments for ablation are vacuum or air. The substance absorbs some of the incident light energy and converts it to heat. The ablation schematic image is depicted in Fig. 1.5. The temperature of the bulk material increases with material conductivity and thermal capacity. A particular threshold temperature is reached at which melting and vaporisation occur. Vapour-caused melt ejection and vaporisation are the methods utilised to remove portions of the heated material from such high temperatures zone. It forms a circular crater whose diameter is roughly equal to the focus beam diameter. Condensed vapour is deposited as debris on the surface surrounding of the contact region, and solidified melt forms a recast layer on the crater wall. Proper selection of processing variables can reduced debris and recast layer to the least amount which is helpful for the visibility of the laser mark. Shorter pulses are generally more effective and result in fewer undesired depositions close to the processing area. Furthermore, material removal threshold values are reachable because, for a given beam energy  $E$ , the peak beam intensity (power / area) is larger for short beam area.

The material is heated and melted to the vaporisation temperature by the absorbed energy which resulted in material removal, heat-affected zone, a recast layer, microcracks,

shockwave-induced surface damage, and material debris. Furthermore, from the leading edge of the pulse, the vaporised material produces hot plasma, which is maintained throughout the duration of the pulse. Owing to the shielding effects of plasma, which defocuses and absorbs pulse energy, greater penetration necessitates a larger fluence or irradiance [9]. Table 1.2 shows the ablation depth and associated fluence range.

Table 1.2 shows ablation depth and fluence of different material [10]

<b>Material</b>	<b>Ablation depth (<math>\mu\text{m}</math>)</b>	<b>Fluence (<math>\text{J}/\text{cm}^2</math>)</b>
Polymer	0.3 – 1.0	1 2
Metal	0.1 – 0.3	5 10
Ceramic	0.1 – 0.3	3 10

Material is taken out of the work piece, which frequently leaves the hue mostly unchanged. Because of the great laser energy absorption and heat creation, this kind of interaction is frequently observed when carbon black is employed for coloration. When the method is applied to homogeneous materials, the contrast between the ablated regions and the substrate causes the mark to appear. As an alternative, it can be used on layered substrates, where the ablated area reveals a highly contrasted underlying region. This is a widely used method for marking polymers. Partially removed coating layers from the base material that are color-marked are removed using ablation.

#### **1.3.1.4 Engraving**

The material in the laser path is removed by melting displacement and/or evaporation when the laser beam penetrates the surface. Substrate material is removed during laser engraving, which uses more heat than laser etching. Melting is the result of a localised rise in temperature above the material's melting point. A mark is created as a result of the material's altered surface structure once it has solidified again. A photographic view of laser engraving technique is shown in Fig. 1.6. Similar to a deep electro-chemical etch marking, this method creates a deep light marking. Since the material vaporises and is expelled during the marking process, laser engraving cannot produce the great contrast achieved by laser colouring or etching. Since most materials' structural strength is found in the integrity of their surfaces, this method seems to be the most appropriate for laser marking; however, it generally causes less damage to the substrate than laser etching, and it can cause micro cracking in certain materials. Similar to laser etching, power microscope (10X)

magnification makes direct laser engraving easy determinable. It is not advised to use laser engraving on items thinner than 2.5 mm. Colour oxides can be created if needed to highlight the marking even more.

Only intense grinding will be able to erase the incredibly strong markings left by laser engraving. For product branding that is resistant to forgeries, laser engraving is utilised. Thermoplastic materials are frequently marked with CO<sub>2</sub> lasers using this method. Direct vector engraving or beam rastering are two methods for creating marks. When an abrasion-resistant mark is needed, engraving is preferable.

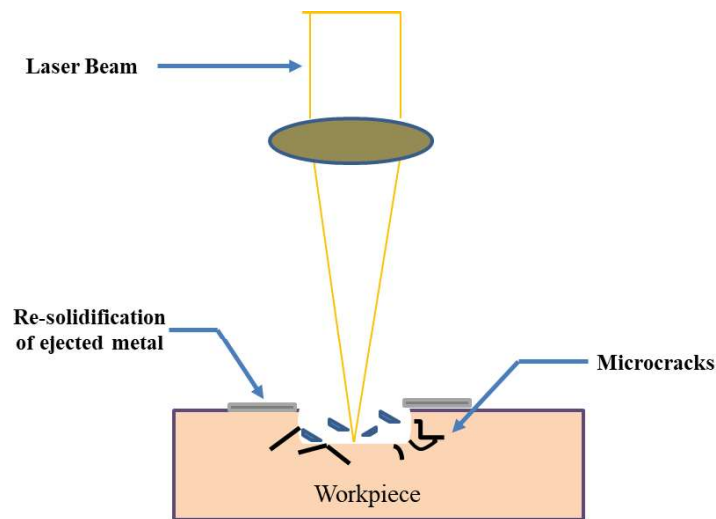


Fig.1.5 Marking by Laser Ablation

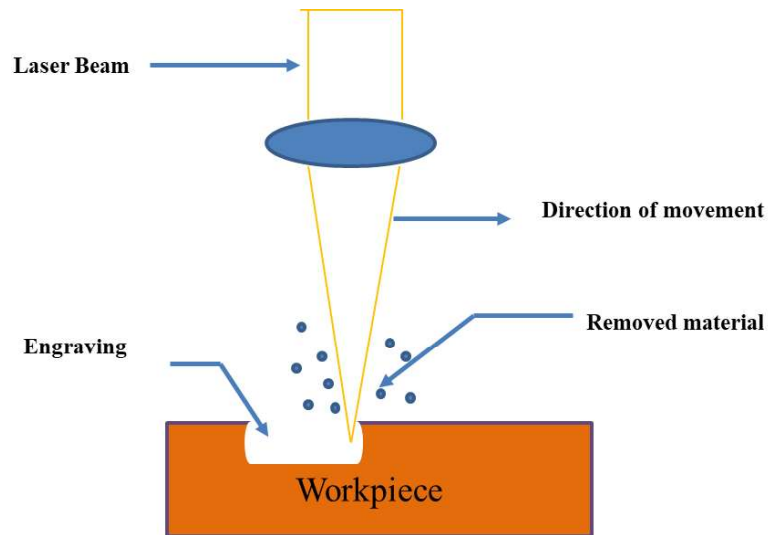


Fig.1.6 Marking by Laser Engraving

### **1.3.2 Marking by Surface Modification**

In this technique, without removing any material, the laser radiation modifies the composition of the substance to produce a high contrast mark. It might melt the substance locally, which would lead to oxidation or chemical changes that would leave an obvious mark. The following lists the specifics of the mechanisms.

#### **1.3.2.1 Foaming**

When the local temperature around the absorption site of polymer material is high enough to cause burning or evaporation to produce gases, the foaming process takes place. Molten polymer which surrounds the heated gases, cause them to expand and generate bubbles. Controlling the laser's energy can cause foaming, which produces bubbles that scatter light and create a white or light-on-dark marking contrast. High pulse frequencies from the laser must be used to achieve this kind of effects, which will cause the compound to transmit heat at a high rate. Foaming produces very strong contrasts and can be used to create white coloured marks on dark surfaces. Fig.1.7 shows photographic view of foaming process. Tiny gas bubbles form in the molten material, giving the material a type of plastic foam and increasing its volume. Because of this, the treated portions seem significantly brighter than the surrounding content. The marking protrudes from the surface in certain instances. This kind of marking is called a foamed marking. Gas pockets occur when a plastic material is heated by a laser beam, causing the material to froth and leave a foamed light mark. The foam penetrates the polymer surface to a depth of roughly 60 microns, rising to a height of about 40 microns from the surface. The marking's wear resistance may be significantly diminished because it is somewhat raised on the surface.

#### **1.3.2.2 Carbonisation**

On a light surface, laser heating resulted in localised carbonisation of the polymer matrix that can produce a dark or black marking. A photographic view of the carbonisation process is shown in Fig. 1.8. The process starts when the material around the adsorption site experiences a local temperature increase from the absorbed energy that is high enough to initiate thermal breakdown of the polymer. Only the material's surface is turned black by the laser, leaving the surface smooth and devoid of cuts. Lubricating parts are covered by this marking. Additionally, it works well with materials like silicon wafer, stainless steel,



and iron group metals where visibility is a key concern. On fabrics with bright colours, the effects is most noticeable. Excessive local heating and carbonisation may alter the matrix's physical characteristics which may occasionally result in dark brownish marks.

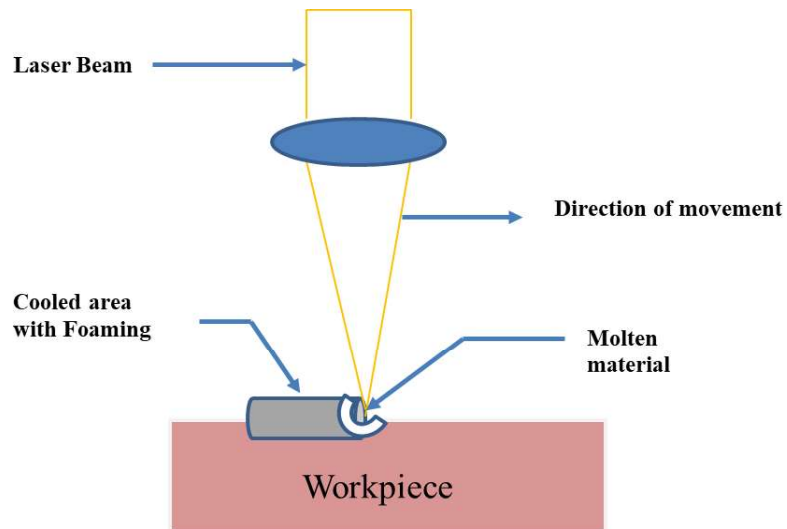


Fig.1.7 Marking by Laser Foaming

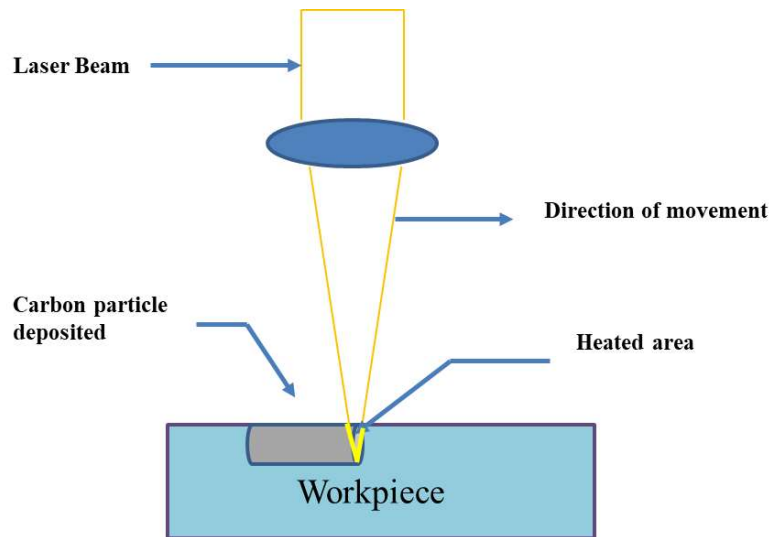


Fig.1.8 Marking by Laser Carbonising

### 1.3.2.3 Annealing

Metal is heated with a laser to almost melting temperatures, changing the colour of the material's top layer. The heat from the laser beam causes annealing, which leaves a permanent, dark mark free of burrs and with no discernible surface penetration. Heat and

oxygen produce an irreversible mark during laser annealing that leaves no trace of material ablation. All metals, particularly stainless steel, that change colour when exposed to heat and oxygen can be treated using laser annealing. Annealing frequently results in a dark, iridescent appearance, and the text or graphic may occasionally display a subtle rainbow of pink, blue, and green hues. The colour is significantly Influenced by the heat source's temperature. Fig.1.9 shows the photographic view of annealing laser marked surface. Annealing usually yields the darkest results and it leaves no cuts or shallow marking. This method is frequently applied to medical equipment that are utilised inside the human body because it leaves the metal unaltered. Annealing usually results in the darkest mark of all three techniques and leaves no cuts or shallow engravings like those found in marking and etching. Annealing has several benefits over burr-filled methods when marking surfaces that have previously been completed. The annealing process is slower than laser engraving because it only uses heat effects. Metallics can have their surfaces annealed at relatively low temperatures. With very little material penetration, the marking beam will create a distinct, contrasting line to the surrounding material. One benefit of marking by annealing is that it preserves the surface, which is crucial for some medical applications, particularly those involving implanted devices. The process's drawback is that the beam velocity needs to be maintained somewhat slowly since heat must pass through the material [11].

#### **1.3.2.4 Colouring**

Certain metallic substrate materials can be coloured by laser colouring without being burned, melted, or evaporated. This is accomplished by slowly moving a relatively low intensity laser beam across the surface to discolour the mark's region. This laser marking technique leaves a high-quality, non-disruptive marking with excellent contrast. The photographic view of coloured marked surface is depicted in Fig. 1.10. Unfortunately, not all materials may be treated with this method. The materials that have already been heat treatment may not respond well to it, and certain stainless steel alloys may lose some of their resistance to corrosion. Laser compositions cannot be harmful or have a negative impact on the look, feel, or functionality of the product. Additives can aid in enhancing the qualities of absorption. Fiber lasers, Nd: YAG, and Nd: Vanadate-type lasers are suitable laser sources for laser colouring.

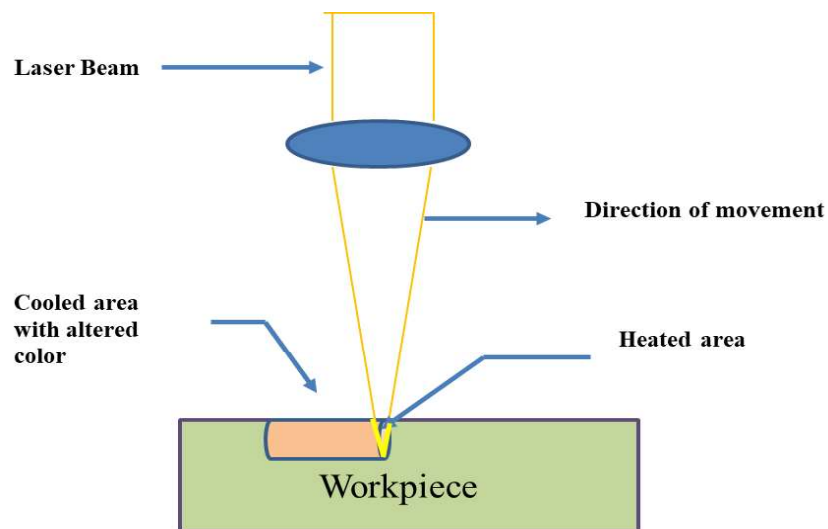


Fig.1.9 Marking by Laser Annealing

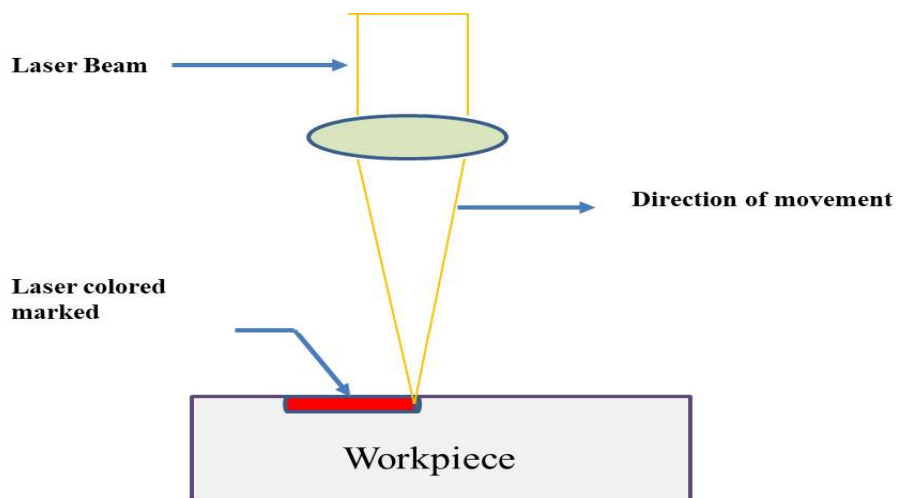


Fig.1.10 Laser Colour Marking

**Table 1.3** List of colour and corresponding colorant [11]

Inorganic		Organic	
Color	Colorant	Color	Colorant
White	TiO <sub>2</sub>	Yellow	Di-chlorobenzidine derivatives
Yellow	Iron oxide Fe <sub>2</sub> O <sub>3</sub> .H <sub>2</sub> O		
Black	Iron oxide Fe <sub>3</sub> O <sub>4</sub>		
Green	Chromium oxide Cr <sub>2</sub> O <sub>3</sub> and Cr <sub>2</sub> O <sub>3</sub> .2H <sub>2</sub> O	Orange	Dianisidine derivatives
Chrome orange	(PbCrO <sub>4</sub> ) x. (PbO) y		
Cadmium yellow	Mixed CdS/ZnS	Red	Toulidine reds

Furthermore, bleaching and photo reduction procedures can make advantage of the harmonic wavelengths of 355 nm (UV) and 532 nm (green). Since there is no discernible heating of the material, UV-induced photo reduction is frequently referred to as "cold marking." This is the most widely used technique for marking polymers, including ABS and polycarbonate. When examined under low (10X) magnification. The laser colouring process is not recommended for parts thinner than 2.5 mm. It is used when the surface must remain flat. Table 1.3 gives the various colorants that can be used for laser marking.

## **1.4 Various Laser Marking Techniques**

Laser marking follows four techniques namely; beam-steering technique, mask projection technique, polygon scanner technique and the scanning technique by movement of work piece. These techniques are discussed here-in-after.

### **1.4.1 Beam Steering Technique**

The substrate surface is the focus of the laser beam in the beam steering technique. Beam steered laser markers guide the laser beam across the surface to be marked using mirrors installed at top fast, computer-controlled galvanometers. Either the substrate is translated with regard to the fixed laser beam, or the laser beam is scanned with respect to the stationary substrate, to mark the desired pattern. Within the marking field, each galvanometer—one on the Y-axis and another on the X-axis—provides the beam motion. To lessen divergence, the beam is first widened and pointed in the direction of the galvanometer mirrors. After going through a lens, it is directed towards the workpiece. When employing mirrors in a laser beam scanning system, it's critical to preserve the focus conditions at different beam deflection angles. To attain a high-power density on the substrate surface, the laser light is focused using a flat field lens assembly. The working distance, depth of focus, and focus size are crucial variables in the beam steering approach. The diffraction phenomenon places a limit on the lowest spot size. It's a straightforward method with several benefits, like easy CAD file interface and straightforward, low-cost optics. With the right programming, it is possible to create any desired image.

Getting the desired pattern produced in a single scanning step is one of the main challenges with the beam steering technique for big area processing. Frequently, it is necessary to do several scans that are near to each other or overlap, which means that the beam must be repositioned after each scan. As a result, the beam steering technique process is frequently referred to as the "step-and-scan" process since it requires moving the sample between two

laser scans and turning off the laser. The overall marking time could significantly rise as a result of this irregular laser scanning. Moving the part has the drawbacks of requiring clamping for the part and also it requires a larger, heavier motion system. The moving beam's other drawback is that it could cause alignment issues and focal point size changes due to changes in beam route. Sync scan is a recently discovered technology where the sample moves constantly as the scanning mirrors scan the substrate's beam. The scan field is updated continually as the sample is moved, enabling the pattern to be written continuously [12]. F-theta flat field lenses are commonly used in contemporary laser scanning systems because they guarantee a constant laser focus plane across the work area, enabling extremely uniform marking over the substrate. In some instances, the lens will furthermore be telecentric, ensuring that the laser beam always stays perpendicular to the substrate's surface in addition to maintaining a level focus plane. Fig. 1.11 is a simple configuration for beam steering laser marking. This allows for the marking of extremely delicate patterns with great picture clarity (resolution > 600 dpi). As a result, the laser is moved quickly in relation to the work piece, and a high-quality mark can be produced by adjusting the laser's variables.

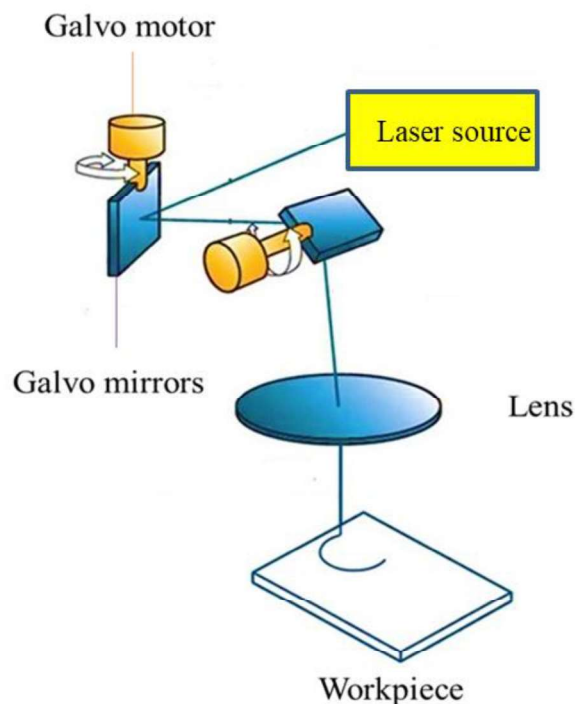


Fig.1.11 Beam Steering Technique

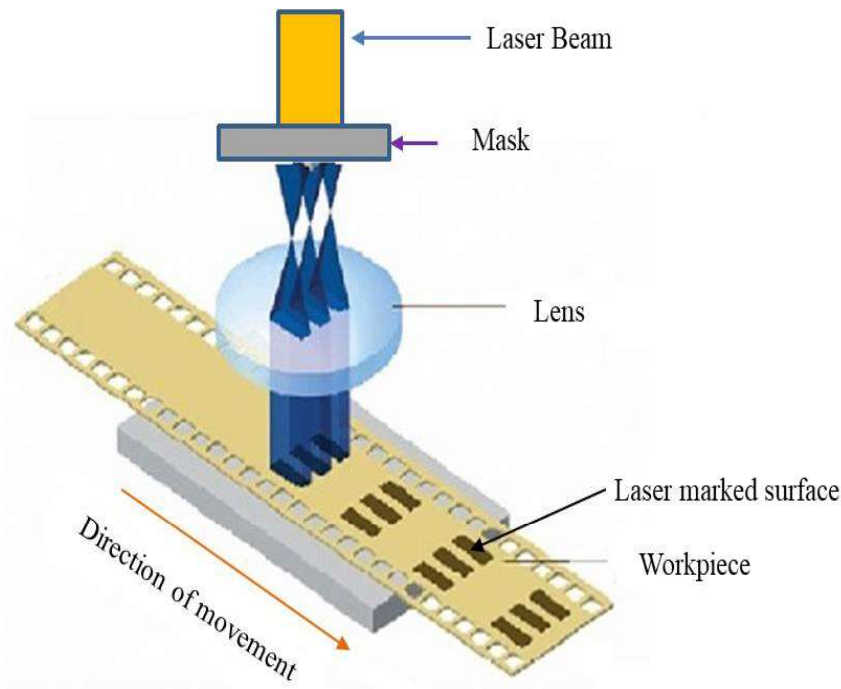


Fig.1.12 Mask Projection Technique

#### 1.4.2 Mask Projection Technique

In the mask projection process, laser light is used to illuminate a mask that represents the pattern that is to be generated on the substrate. A mask's primary use is to shield an object's unmarked areas. It can be placed in close proximity to the work piece, or a lens can be used to concentrate the transmitted pattern on the object to the required size. If the mask does not need to be altered, mask marking happens quickly. It is possible to install various masks on a rotating wheel and arrange them appropriately, however doing so lowers the marking rate. It takes fairly high power lasers to make the mark because only a portion of the beam is delivered. Masks are also convenient when using materials that are sensitive to heat.

The material is shielded from heat and/or smoke damage by the mask, which also absorbs excess heat. Typically, a thin layer of chrome metal covers a quartz substrate that is used to make the masks. The mask could be made of glass substrates coated with dielectrics or a metal stencil with connecting strips. Water-based latex products are known as liquid masking materials. They are sprayed in liquid form, which dries into a rubbery, flexible coating. The material of this mask is polyester film. Like single-sided tape, the film masking material is twisted into a roll. Just cover the material with the film and smooth out

any bubbles present in it. Paper masking material is available in several tack grade levels and has a self-adhesive backing. The more aggressive adhesive is recommended for unfinished wood.

The laser beam is homogenised and tailored to create a consistent distribution of intensity throughout the exposed mask area. A projection lens is then used to project and reduce the pattern on the mask to the substrate. With just one or more laser pulses, a sizable pattern can be created on the surface using the projection patterning technique. The depth of structures machined on the substrate surface depends on the number of shots [13]. The mask projection approach is shown in Fig. 1.12. The consistent feature depth is one of the key attributes generated by the basic mask projection approach. The cost of the masks can be high, particularly for intricate models. High manufacturing rates are possible with this technology, although it is not very flexible. The synchronised overlay scanning method is one such advancement. This method synchronises the velocity of the substrate and the mask. The most crucial step in obtaining the depth profiles on the substrate is to position an appropriately shaped aperture above the mask. To get desired features, different combinations of masks and apertures can be employed.

#### **1.4.3 Polygon Scanner Technique**

A polygon scanner is a type of scanner that has three or more reflecting surfaces on its rotating optical element. In many situations, the preferred approach is polygonal laser scanning. Fig. 1.13(a) illustrates the polygon scanning technique. It is applicable to laser marking. One direction is the laser beam's deflection due to a revolving polygon mirror. The number of scanning points along a line is the first parameter that needs to be specified when configuring a scanning system. The number of scanning points, spot size, and permissible fluctuation in spot size all play a major role in determining whether the system is post-objective or pre-objective. For this reason, polygon scanners are not very effective. The less expensive option, post-objective scanning, should be considered first to see if its disadvantages can be tolerated. When there is a significant depth of field and a relatively narrow scan angle, or when the target plane is curved, post objective scanning is employed. As can be seen in fig. 1.13(b), the last focusing element in post-objective scanning is situated before the polygon. At this stage, the beam is on axis, therefore a relatively basic lens can serve as the final focusing element. A top-notch f-Theta scan lens or mirror system is utilised in pre-objective scanning to create a flat field and linear scan velocity on the

target. After specifying the number of resolvable points  $N$ , the next step is to choose an active scan angle  $\theta$ , also known as the angular resolution. One can provide an angular resolution or scan angle in the case of a post-objective system.

The scan lens determines the active scan angle if the system is pre-objective and a scan lens has been chosen as a system constraint. The lens can be costly and typically has two to five elements. The bulk of applications use this technique since post-objective scanning presents some limitations. In system design, there is a trade-off between polygon speed and the number of facets. A specific line rate can be produced by a variety of facet count and polygon speed combinations. Even though polygons can be produced with a wide variety of facet counts, less facets translate into cheaper production costs. In addition, having more facets generally drives up polygon size, which can have a serious impact on the bearing selection and cost.

In order to write patterns, the laser energy must be regulated by a mask. Additionally, a second movement is needed to enable a two-dimensional scan. Typically, the best component of a polygon scanner is a metal mirror. Other scanners, such as a pentaprism, cube beam splitter, or monogon, may be include as one facet in addition to the polygonal scanner. Applications needing large apertures, large scan angles, high throughput, high scan rates, or unidirectional scans works well with polygon scanners. It is necessary to consider the optical properties of the scan mirror when defining a polygonal scanner. The polygonal mirror requires an improvement or protective coating, such as a more expensive multilayer dielectric coating, protected gold, or inexpensive aluminium with a silicon monoxide topcoat. Whether an application calls for visible, mid-infrared, or deep ultraviolet radiation, coatings can be customised to meet its needs. In the majority of applications, Polygon scanners are used in conjunction with another method to generate an additional axis through beam steering or object motion. In doing so, the polygon scanner generates the quick scan axis of motion and produces a raster image.



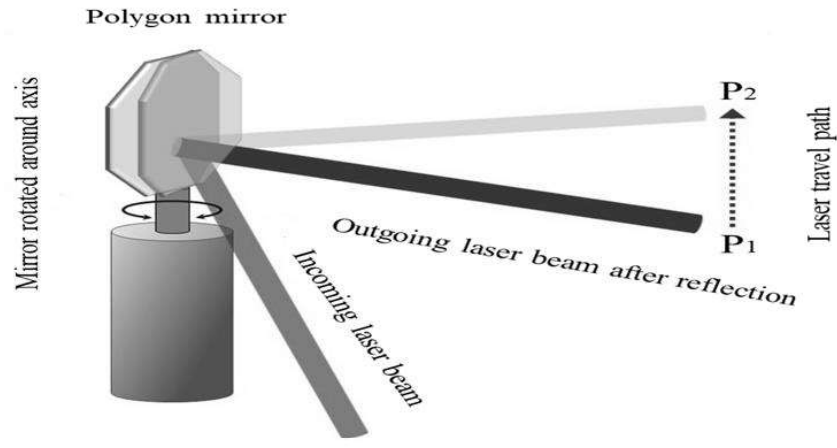


Fig.1.13 (a) Polygon Scanner Method

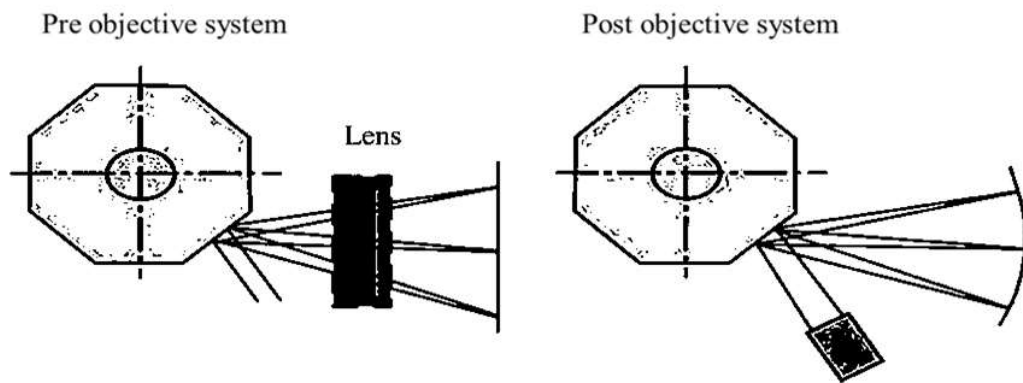


Fig.1.13 (b) Pre-objective and Post-objective System in Polygon Scanner Method

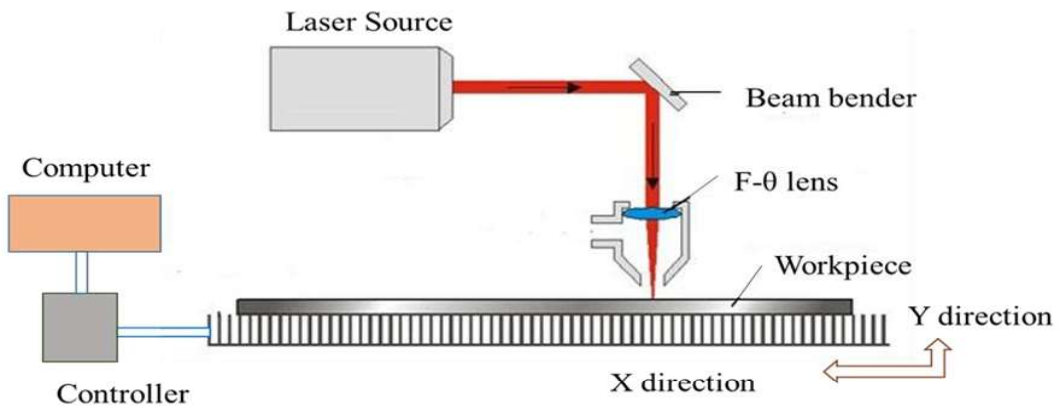


Fig. 1.14 Schematic View of Scanning Technique by Movement of Work Piece

#### **1.4.4 Scanning Technique by Movement of Work Piece**

Laser marking can be achieved by moving the work piece while maintaining a stationary laser, or by moving the laser in accordance with the profile that needs to be generated. In this work, the work piece is marked using the former technique. Fig. 1.14 displays a schematic illustration of the marking technique. The laser beam is directed from the laser head through a beam bender, which bends it 90 degrees so that a lens can concentrate it on the work item. The X-Y table under CNC control has the work piece put on it. After the laser beam has been properly focused by means of a focusing lens, the work piece movement along the X-Y axis and the focusing lens movement along the Z axis are CNC controlled and can be operated via a computer for marking. A nozzle directs the laser beam onto the work piece, providing air—the primary gas—to the surface of the object to facilitate material removal and inhibit resolidification. One can achieve a high peak power laser beam by utilising a Q-switched Nd: YAG laser. This makes it possible to mark various materials with high quality. Furthermore, the focusing lens's alignment is crucial because if the beam's centre is not coaxial with the lens's centre, the beam that follows the lens won't be straight, which will significantly reduce marking efficiency. Therefore, extra care must be taken to ensure that the focusing lens is properly oriented. Plotting software such as AutoCAD or Corel Draw can be used to create unique figures, logos, and characters. These plots can then be transferred to laser marking software to create CNC programmes. With the use of CNC drive systems, it is possible to mark with a variety of typefaces, desired sizes and orientations by directing the work piece's motion according to a CNC programme.

### **1.5 Fiber Laser in Marking**

Over the last ten years, fiber lasers have emerged as the most versatile and rapidly growing type of laser systems. Applications in industry, medicine, meteorology, and the military that were previously dominated by traditional solid state and gas lasers have seen success with their employment. Sales of fiber lasers for metal cutting have reached 1.1 billion dollars worldwide and are increasing at a rate of three to four percent per year. Additionally, fiber lasers have been gradually replacing CO<sub>2</sub> and Nd-YAG lasers in a variety of production sectors due to their higher efficiency, better beam quality, lower maintenance requirements, and ability to handle highly reflective materials.

### 1.5.1 Brief History of Fiber Laser

Fiber lasers with an average laser irradiation of 10 W to 50 W have a significant market share in the field of delicate and precise marking, grooving, cutting. The technique of combining optical fiber with laser systems began when Snitzer in 1961 discovered the advantages of placing a rare earth element in single mode optical fiber cavity to create a stable single spatial mode as laser output. Snitzer and Koester demonstrated flash lamp pumped neodymium doped multimode optical fiber lasers after the initial study. Furthermore, in the mid-1980s, practical work on single-mode optical fiber lasers started following the initial developments in rare earth doping methods that made use of modern vapour-phase deposition optical fiber fabrication operations. However, the development of single high-power mode optical fiber lasers proved to be inconsequential in commercial and industrial applications because the majority of single-mode fiber lasers have low average powers. In the end, the telecom boom of 2001 gave high-power optical fiber laser technology the push it needed to advance. A significant amount of concentrated research and development work produced multimode diodes that are far more powerful and durable at a much lower cost for the creation of the fiber laser. Moreover, the military-funded initiatives made a significant contribution to the advancement of related technologies and the development of higher power fiber lasers [14].

### 1.5.2 Present Status of Fiber Laser

The fundamental wavelength of a fiber laser can vary between 1 and 2  $\mu\text{m}$ , depending on the host material and dopant used. Shortwave and midwave infrared wavelength bands are being covered by high-power fiber lasers. The active gain medium of a fiber laser is an optical fiber doped with rare earth elements such as neodymium ( $\text{Nd}^{3+}$ ), ytterbium ( $\text{Yb}^{3+}$ ), or erbium ( $\text{Er}^{3+}$ ). Near-infrared (NIR) wavelengths are used by high-power fiber lasers.  $\text{Yb}^{3+}$  ions are the most commonly employed rare earth ions due to their energy level structure and minor quantum defect. However for marking applications, fiber lasers with an output of less than 50W perform better than high power lasers. Fiber lasers can also be Q-switched to produce high peak power pulses at pulse repetition rates of tens or hundreds of kilohertz. Furthermore, the fundamental wavelength of the fiber laser can be used to machine a vast array of metals and ceramics. The applications that requires high power laser sources in a variety of areas includes pulsed oscillators and spectral modulation to favour fiber lasers. Fiber lasers is a type of guided-wave laser system that has an advantage

over ordinary laser systems since the modes are firmly determined by the laser cavity. These days, ultrafast fiber lasers have a place in both industry and science. They are based on fiber oscillators that are passively mode-locked. The amplification that occurred across the several stages of the ultrafast fiber laser generation and beam delivery system allowed them to reach the necessary output pulse energies. Additionally, effective heat dissipation is made possible by the fiber shape's large surface area to volume ratio. Fiber lasers are more compact than other standard laser systems because they don't require a cooling unit and have a longer runtime. In the last few decades, alternative fiber laser host glasses for the shortwave to midwave infrared spectrum have been created. The alternate glasses' energy must be less than the transition energy of the rare earth doping element in order to have a high luminescence efficiency. In shortwave and midwave infrared fiber lasers, glasses like chalcogenide, tellurite, germanate, and fluoride oxide have been used. ZBLAN is the most sophisticated fluoride glass available for short to midwave infrared fiber lasers. Fluoride glasses are currently by far the most efficient host material for the longer emission wavelengths when compared to a silicate glass host. Numerous fiber components are reliant on the complete fiber systems rather than just the beam delivery system. The chirped pulse amplification (CPA) technique for ultrafast fiber laser systems is an ongoing design concept for the prevention of nonlinear processes in the fiber amplifiers for increased utilisation in various micro-marking applications [15]. With fiber lasers, IPG Photonics has so far achieved the highest single mode power of 10 kW and the highest multimode power of 50 kW. Fig. 1.15 displays a schematic representation of a pulsed fiber laser system. In the ytterbium fiber laser head, fiber laser generation is achieved through the power source. After that, the beam goes to the collimator. Then laser beam travels through a bending mirror and ends up at an F- $\theta$  lens. The workpiece is processed by the camera assembly unit using CCDTV regardless of whether it is centred on a focal point. The individual components of the fiber laser system are discussed in chapter 2.

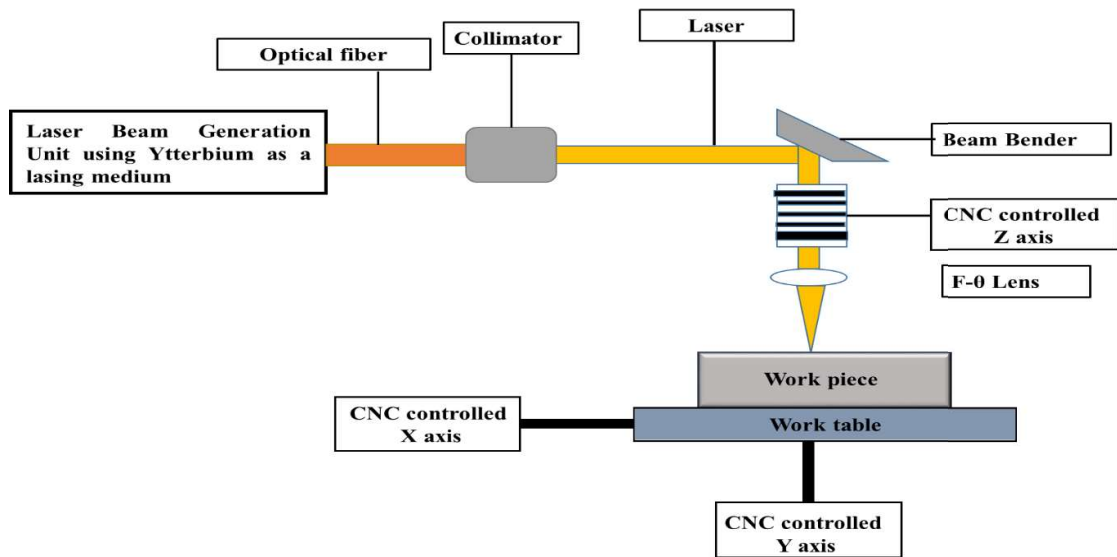


Fig. 1.15 Schematic diagram of a pulsed fiber laser system

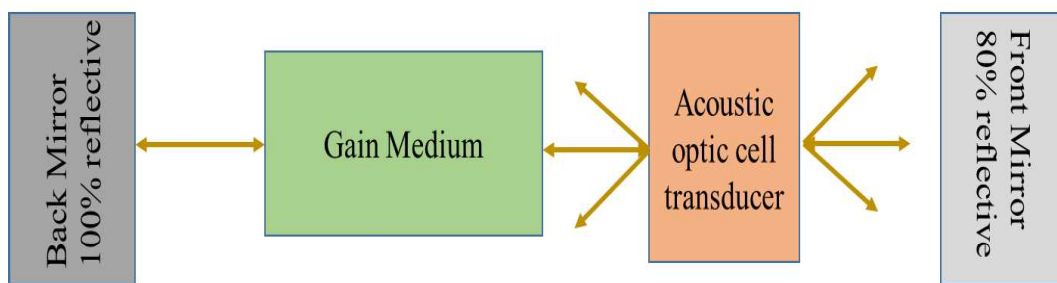


Fig. 1.16 Schematic representation of a mode-locked fiber laser with acousto optic modulator

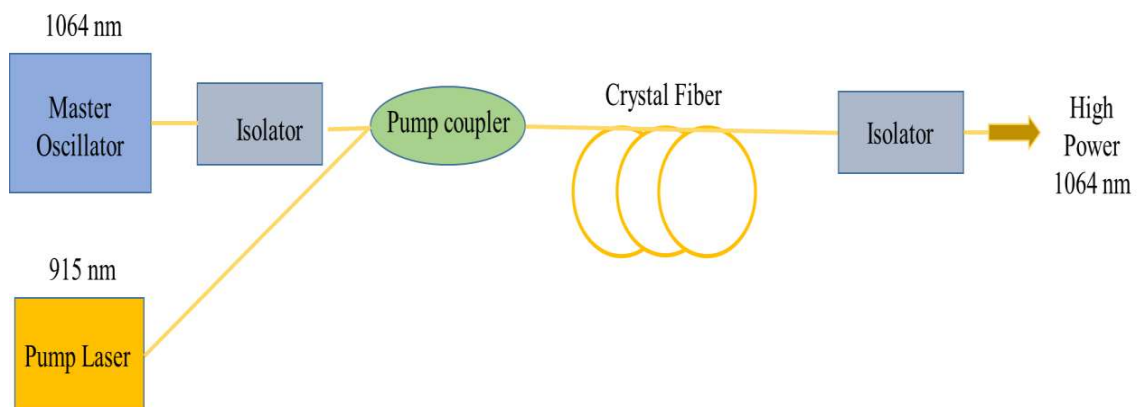


Fig. 1.17 Schematic diagram of a master oscillator power amplifier (MOPA) design of fiber laser

### 1.5.3 Classification of Fiber Laser

In general, there are two kinds of fiber lasers: pulsed fiber lasers (b) and continuous fiber lasers (a). Furthermore, three categories of fiber lasers are identified: single frequency, Q-switched, and mode-locked. A continuous fiber laser is composed of an output coupler (OC), fiber Bragg gratings, and a high reflector (HR). Continuous wave fiber lasers can have single or multiple transverse modes. A single mode continuous fiber laser can generate a high-quality beam for material processing, even if multimode industrial lasers can output more power.

When operating in pulsed mode, a single frequency fiber laser is pumped by a single mode pump diode, yielding an output power that can vary from several tens to hundreds of milliwatts. Q switching is possible for pulse lengths ranging from low nanoseconds to microseconds using fiber lasers. Longer pulses can be generated with Q switched fiber lasers because their fibers are longer than typical. On the other hand, if the pulse length is longer than the round-trip cavity time, pulse breakup may occur.

Conversely, the mode-locked fiber laser (Fig. 1.16) uses the fundamental cavity mode structure in an optical fiber oscillator to its fullest potential in order to produce a short pulse. The front mirror reflects just 20% of the photons that are needed to create the laser light, whereas the rear mirror reflects 100% of them. An acousto-optical modulator (AOM) used as a pulse selector is shown in Fig. 1.16. In recent years, end-to-end all fusion fiber master oscillator power amplifier (MOPA) systems have also been implemented using fiber-coupled semiconductor lasers (Fig. 1.17). In MOPA, the pulsed operation is accomplished through the use of an external electronically controlled modulator. A pulsed fiber-based MOPA serves as the master oscillator in a bulk solid-state laser. Fig. 1.17 shows a high core diameter, single transverse mode ytterbium doped fiber laser. By using the preamplifier to boost the signal pulse energy, the photonic crystal fiber (PCF) may achieve high pulse energies. While a pulsed mode of the fiber laser is usually employed to generate a high peak intensity laser beam in order to accomplish high aspect ratio micro-channels, micro-holes, etc., and continuous mode of the fiber laser is better suited for cutting thick materials. Fiber lasers can alternatively be referred to as nanosecond, picosecond, or femtosecond pulsed fiber laser systems, depending on the regime of the pulse width [16].

### **1.5.4 Comparison between Fiber Laser and Other Lasers for Marking**

Shorter wavelengths combined with high focus ability, increased system flexibility, high component yield and uptime, enhanced reliability, high repeatability, high aspect ratios with the highest precision, extensive material coverage, fully automated, economical processes seem to be advantageous for fiber lasers used in micro-marking of thin sheet metal. Apart from marking it can also be used for machining purpose. Olsen et al. found that fiber laser cutting is more effective than CO<sub>2</sub> laser cutting. The outcomes of their tests also demonstrated that burr-free cuts in AISI 304 stainless steel, which has a thickness of 1 and 2 mm, could be produced at a variety of cutting rates using a fiber laser micro-machining system. Further studies on the fiber laser micro-machining technique further showed that fiber lasers are more effective than CO<sub>2</sub> and Nd-YAG lasers in machining a variety of materials. In addition, 4 kW fiber lasers have superseded 4 kW CO<sub>2</sub> lasers in terms of the amount of components and goods that can be produced. As a result, maintenance and electricity costs have dramatically dropped. In addition to it, 2 kW fiber laser can cut thick plates up to 1 inch or even thicker with the same edge quality at speeds similar to a 4 kW CO<sub>2</sub> laser [17].

Fiber lasers have replaced Nd-YAG lasers in a number of micro-machining applications, such as marking, drilling, micro-cutting of stents and thin sheets of ferrous and non-metal materials, because of their improved cut edge quality, faster cutting speeds, smaller heat affected zones (HAZ), smoother surfaces, and lower propensity to form micro cracks [18]. Marking on polycrystalline silicon is another important application in which fiber lasers can perform better than Nd-YAG lasers (silicon wafer). The number of research projects using fiber laser machining of difficult-to-machine materials has dramatically increased in the last few years.

## **1.6 Basic Principle of Fiber Laser Generation Process**

By raising a material (a rare earth element) in the active medium from its ground state to an excited state and causing a population inversion in that medium, the fundamental idea of a fiber laser can be realised. Atoms in the active medium typically exist in their ground states; in order to bring these atoms to an excited state, energy from outside the system must be provided. In fiber laser, there are several choice for elevating pump light to high power. Launching straight into the pump cladding at one or both fiber ends is the easiest. To pump light inside the fiber, fiber linked pump diodes are often used. Multiple diode

lasers are used to create a population in the active medium, a process known as pumping. The application of the fiber laser and the necessary output power determine the precise number of diode lasers. The plane of propagation of light in pulsed mode optical fiber does not vary since pulsed mode fiber has a conditional property. When the light polarisation plane is coupling into the fiber, it must be oriented at a specific angle to the direction of the fiber stress gradient. There are five factors that determine the entry of light in fiber which are named as (a) fiber type, (b) fiber size, (c) numerical aperture, (d) refractive index and (e) doping of the fiber. The protective covering is integrated with one core, one cladding, and fiber. While the pumped beam propagates across the outer layer cladding, the lasing mode propagates within the core. The Helmholtz Eigen value equation is derived from Maxwell's equations and can be used to determine the guided modes of a waveguide. At every boundary, the equations guarantee all pertinent field continuities. A guided mode propagates at  $\beta$  (propagation constant) and keeps a constant wave front since it is a robust basic spatial distribution. Equation 1.1 illustrates it as follows:

$$E(r, \theta, z) = E_0(r, \theta) e^{-ibz} \quad \dots \text{Eq.1.1}$$

Where,  $E_0$  is transverse mode distribution,  $r$  and  $\theta$  are the polar coordinates in the marked region, and  $z$  is the propagation distance. The whole set of waveguide's mode variables can be ascertained once the normalised frequency is known. The outer layer cladding's main purpose is to contain the pump light, enabling the core to be pumped using a high-power beam. After combining all of the distinct diode laser outputs into a single beam, the beam is then injected into the fiber laser's inner cladding at an angle that guarantees complete internal reflection at the interface between the inner and outer claddings. This can happen only if two requirements are satisfied. One need is that, as the light beam moves towards the medium, its index of refraction must be greater than the medium's index of refraction. As the pump beam moves from the inner cladding to the outside cladding, this need is satisfied. The second requirement is that, as seen in Fig. 1.18, the angle of incidence of the laser beam ( $\theta_a$ ) on the inner/outer cladding contact must be larger than the critical angle ( $\theta_c$ ).



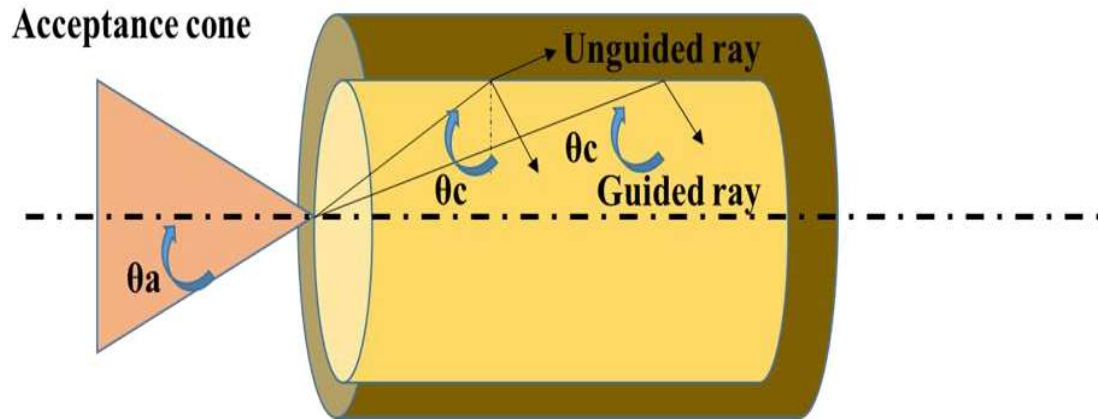


Fig. 1.18 Acceptance angle of fiber with quantities related to the numerical aperture

A small amount of light escapes the inner core and enters the outer core following complete internal reflection. Consequently, the energy present in the pump light is absorbed by the rare earth doping atoms as they achieve excited states. The pump light enters the fiber laser core after the incidence of complete internal reflection at the interface between the inner and outer cladding. Additionally, the majority (>90%) will interact with the rare earth doping atoms in the core, resulting in a population inversion. In order to lower energy through fluorescence production within the core photons, a fraction of these energised atoms rapidly decays. The energy difference between the excited and lower energy states of the rare earth atoms will then be reflected in the photons. At that time, these photons pass through the core and, with the help of stimulated emission, cause other earth photons to decrease in energy to their lowest possible levels. As this process continues, increasingly coherent, collimated photons with comparable wavelengths eventually fill the core to saturation which resulted in the generation of laser light. The light interacts with mirrors or fiber Bragg gratings (FBG) as it travels towards the end of the core. Here, two occurrences take place: some light partially reflects into the core and the light is totally reflected into the core. More stimulated emission is the result of the second phenomena, whereas light transmission is the outcome of the first.

## 1.7 Principle of Fiber Laser Marking Process

The near-infrared (NIR) or infrared (IR) regions make up the fiber laser's operational range. The foundation of the fiber laser micro-machining process is the way the laser light interacts with the working material's top surface to remove a tiny quantity of material. It is commonly

known that the photon energy and the laser working wavelength are inversely related, meaning that the higher the photon energy, the shorter the wavelength. When the fiber laser's operating wavelength of 1064 nm is shortened to either the first order harmonic wavelength of 532 nm or the second order harmonic wavelength of 264 nm, the thermal process transforms into a chemical process. Consequently, rather of melting and vaporising, the work piece material's bonds break. Consequently, the process of fiber laser micro-marking can be divided into two unique aspects: the photo-thermal process and the photo-chemical process. The majority of photo-thermal reactions are found in metals, ceramics, alloys, etc. Rapid thermal cycling, heating, melting, and partial evaporation of the heated volume of the material are the characteristics of photo-thermal processes. For different technical materials, fiber laser micro marking can be done at nanosecond or femtosecond time intervals.

The laser-material contact time affects the marking quality. Three processes can be identified based on the temporal regime of the laser-material interaction. All three processes begin with the photon being absorbed by an electron, and the next physical stages are then modified based on the time regime. The workpiece is heated to both the melting and vaporisation temperatures during the nanosecond ablation of the metals by the absorbed laser energy. Heat conduction into the solid substance is responsible for the energy loss throughout the contact duration. The adverse heat affected zone (HAZ), which can be partially addressed by picosecond ablation, is connected with nanosecond pulse ablation. When energy is transferred from the electrons to the lattice in picosecond ablation, the pulse length remains constant. But there is also a significant quantity of evaporation and the creation of a melted zone inside the material that affects the picosecond ablation. Since there is no time for heat transfer to the lattice during this sequence of procedures in femtosecond ablation, this linked issue can be resolved. Consequently, femtosecond ablation exhibits precision marking features with a low or non-existent heat impacted zone [16].

## **1.8 Literature Review of Fiber Laser Marking Processes**

Over 50 years have passed since the invention of laser technology, and for the last 25 years, lasers have been employed in real-world applications. Lasers are widely employed in practically every sector and advancement since Theodore Maiman created the first one in 1960. The (optical) laser was not created until after the maser (microwave amplification by

stimulated emission of radiation) was created in 1954 by Charles Townes and Arthur Schawlow utilising ammonia gas and microwave radiation. The field of lasers has experienced fast expansion due to extensive research. At Bell Laboratories, Joseph E. Geusic and Richard G. Smith created the Nd: YAG (neodymium-doped YAG) laser in 1964. Among the most important inventions of the 20th century has to be the laser. Since its discovery, the Nd: YAG laser has been applied in a wide range of fields. It began its foray into the realm of laser marking in the late 1980s. In the beginning, the food items and commodities were marked with details via marking. Gradually, the versatility and uses of laser marking in diverse domains prompted scholars to do research in this area. As a result, a thorough analysis of the basic and applied research on the laser marking process has been conducted and is presented in the section that follows. This section also highlights the most recent advancements in the research activities related to laser marking, which are divided into a number of sections, including:

- (a) Laser marking using different lasers**
- (b) Various laser marking techniques**
- (c) Laser marking on different materials**
- (d) Laser marking systems**
- (e) Parametric influences on laser marking**
- (f) Optimization and modelling of laser marking**

### **1.8.1 Laser Marking Using Different Lasers**

Distinct types of lasers can be used for marking because they have distinct features and beam wavelengths. Researchers used excimer, CO<sub>2</sub>, UV, femtosecond, and nanosecond lasers for marking purposes and investigated how well each type of laser performed on various materials. The information regarding the study conducted by different researchers is covered in the part that follows.

Ricciardi et al. [19] performed marking on computer keyboard using an excimer laser. The goal was to mark keyboards quickly and easily on the production line without using harmful printing solutions. The marking procedure was processed by examining the contrast and depth of colour change in relation to laser variables and polymer composition. A blend of polycarbonate (PC) and acrylonitrile butadiene styrene (ABS) was selected in order to get

the best possible mark quality on its surface. The process of foaming the polymer surface under laser radiation was also examined, and the key elements involved were identified. It was demonstrated that the mark contrast was diminished by foaming effects, and that the issue could be resolved by maintaining low concentrations of titanium dioxide. The utilisation of carbon black which was used to colour plastic products also produces a significant contribution to marking. Because the mark contrast was dictated by backdrop reflectivity, the grade of surface preparation also had an impact on marking quality. Analysis revealed that laser-printed symbols for computer keyboard passed the standards tests on different polymeric materials such as PC, ABS, and polystyrene.

Plinski et al. [20] carried out novel approach to marking based on the spectrum characteristics of CO<sub>2</sub> laser radiation. The two primary marking techniques such as multi-dot and continuous were taken into consideration. The marking techniques that were taken into consideration required intricate mechanical systems of shutters or galvanometric mirrors which was omitted by using the diffraction marker. A piezo ceramic transducer and a diffraction grating were the only executive components of the marker. The most promising design for application to the diffraction marker was demonstrated to be the slab waveguide configuration of the RF stimulated CO<sub>2</sub> laser fitted with an unstable resonator. It also displayed a well-ordered signature, which made programming the PZT controlling system easier, functioned with a reasonably high output power which produces great spectral purity on marking.

Valette et al. [21] looked into the potential of femtosecond laser therapies in order to prevent corrosion processes and also to increase the longevity at the indicated location of austenitic 316 L and martensitic Z30C13 stainless steels. The passive condition, rate of corrosion, and susceptibility to localised corrosion of the samples were ascertained by electrochemical studies. The corrosion potential of the marked surfaces in comparison to the untreated ones was determined by potentiodynamic tests. In order to assess the engraved parts' natural long-term deterioration, more extended immersion tests were conducted. Then, using surface characterizations as a foundation, the electrochemical behaviour was elucidated. To ascertain the impacts of femtosecond laser marking, metallurgical analysis based on EDX and X-ray diffraction data were also investigated. The indicated samples have not changed chemically, according to EDX analysis. For the marked parts, only the presence of oxygen has been found; this is linked to the production of a very thin oxide layer on the surface that allows markings to be read, and it has no negative effects on the

electrochemical properties. Furthermore, the chemical makeup remained unaltered, maintaining and even improving the passive properties of both stainless steels in light of their vulnerability to localised corrosion.

Penide et.al [22] carried out experimental study on the process of marking alumina by three different lasers working in two wavelengths: 1064 nm (Near-infrared) and 532 nm (visible, green radiation) and colorimetric analysis had also been carried out in order to compare the resulting marks and its contrast. It has been observed that treatment areas in argon and in air do not show much difference in the marking shade. However, they do show difference in the amount of removal material. The one made in argon has removed more quantity of material (both aluminium and oxygen atoms) than the other one, so ablation is higher under inert atmosphere by green laser treatment. Therefore, by carrying out laser treatments in argon, marks are notably darker than in air can be resulted with higher contrast. It concluded that the atmosphere is the key parameter, being the inert one the best choice to produce the darkest marks.

Peter et. al [23] carried out analysis of laser marking with Nd:YAG laser using process parameter like pulse rate ,lamp current, laser scan rate on varies laser marking characteristics like mark width, mark depth and marking intensity on alumina ceramics. It has been observed that mark width, mark depth and mark intensity depends on interaction process of laser beam and material which further relies on process parameter .High pulse rate leads to low peak power which reflects in achieving minimum mark width and depth but improves the mark intensity .Increase in lamp current causes more material vaporization and thus both mark width and depth are increased. Scan rate plays a major role in overlapping the laser beam spot. Lower the scan rate increases the overlapping of laser beam spot which results in better quality mark and maximum mark depth.

### **1.8.2 Various Laser Marking Techniques**

Various marking techniques were applied to various materials, including etching, ablation, colouring, surface nitriding, and surface oxidation. Many scholars have also examined marking using other methods like writing, scribing, and engraving. The following provides specifics regarding the research work's findings:

Noor et al. [24] executed several techniques and procedures of Nd: YAG laser marking of plastic and ceramic integrated circuit packages. The review covered the impact of the laser variables on material qualities and mark legibility features. The primary forms of marking

on plastic packaging were peeling or ablation of a coating layer, ablation of matrix components, melting or foaming of the surface, and colour change. It was discovered that Nd: YAG laser marking system produces good quality marks requiring little to no rework and enabling the laser marking of ceramic packaging extremely adaptable.

Qi et al. [25] performed laser-marking on stainless steel using a Q-switched Nd: YAG laser. The impact of the laser beam's pulse rate on the depth, width, and contrast of the mark was examined. Utilising an optical microscope, scanning electron microscopy, and surface profiling tool, the impact of pulse rate on the mark's width and depth was assessed. Mark contrast was measured using an image-analysis system that included a charged couple device (CCD) and a frame-grabber card. It was discovered that the interaction process between the laser beam and the material greatly influences mark depth, width, and contrast. The mark quality was also significantly impacted by the laser's pulse rate. Maximum mark depth was reached at a pulse rate of 3 kHz, but mark width remained nearly constant at varying pulse frequencies. The improvement in mark contrast was caused by a decrease in material evaporation and increase in oxidation. Analysis revealed that maximum mark contrast was achieved at pulse rate of 8 kHz.

Stewart et al. [26] examined the effects of laser ablation on multi-layered coloured inks printed on regular white paper. The goal was to investigate the possibility to create a fully tactile three-colored image by carefully removing ink layers. White/cyan/white/black layers made up the four layered ink samples that were subjected to laser ablation using Q-switched Nd:YAG laser. At the ideal laser variables, the heat effects on the paper were not considerable; however, charring of the underlying paper occurred when the energy density was over  $3 \text{ Jcm}^{-3}$ . The outcomes shown that, despite charring with deeper ablation, it was able to remove the inks selectively to reveal both the top white and cyan layers. A decomposition/evaporation mechanism was also put forth to explain the ink ablation process.

Zheng et al. [27] investigated to produce high contrast and tunable colours on a stainless steel surface using a KrF excimer laser beam. On the sample surface, the laser beam aided in the production of semi-transparent oxide layers with a range of thicknesses and morphologies. In order to comprehend the colours produced by the laser, ellipsometry and atomic force microscopy were utilised to examine the thickness and surface morphology of the oxide coatings. It was discovered that the thickness of the oxide layer affects the colours

produced by the laser whereas granular structures in the laser-treated sections impacted light scattering and oxide development.

Dumont et al. [28] conducted pulse experiments on glass used for pharmaceutical purposes, which were needed to be labelled to enable tracing and controlling along the distribution line by the production company. Two types of glass such as FIOLAX-amber and FIOLAX clear were used for the exposure to two distinct irradiation wavelengths (266 and 355 nm), each with a different pulse number and fluency. By creating a single pixel from many markings, it was possible to alter the encoded text and visibility, as well as the overall matrix's optical appearance with considerable flexibility, excellent reproducibility, and low failure rate.

Gao et al. [29] investigated the laser color marking of Titanium alloy (TC4) substrate material by surface oxidation. Exploration of thermal field helps in controlling color of TC4 surface. It was observed that by varying thermal field different colors can be obtained by changing only one variable within the suitable range. The process parameter involved were scan rate of 70-800mm/s, laser irradiation of 15 w, pulse rate of 125 kHz and scanning interval of 40µm. The surface morphology and microstructure of the specimens were examined by optical microscopy(OM) and scanning electron microscopy(SEM) respectively.

Ma et.al [30] carried out stability analysis on coloring surface of stainless steel using nano second pulsed laser under varying process variables such as defocusing distance, scan rate, scanning interval, pulse repetition frequency and release on time color marking. It was observed that for a particular set of process of process parameter a certain specific color was obtained. After conducting the same experiment for five times color stability analysis was used to evaluate the difference between the standard and other obtained color marking using international chromatic color difference formula  $\Delta E^*_{ab} \leq 7$  for holding stability. The experiments proved that all obtained color difference(such as green, orange, blue, yellow and purple except grey) satisfy the color difference formula and are acceptable in nature. Furthermore, it was also observed that marking position and defocusing distance, scanning interval and scan rate has a significant impact on color stability of stainless steel whereas pulse rate and release time are fixed for each determined colors.

Chen et al. [31] used laser direct writing on the indium tin oxide (ITO) glass. The ITO films of glass substrate was ablated using the Nd:YAG UV laser with different repetition rate of

laser and feeding speed of XY table. Results showed that the line width of the patterns would be affected by the feeding speed and the repetition rate of the laser and the small line width was obtained with a repetition rate of 6 kHz and the feeding speed of 50 mm/s.

Kathuria [32] carried out surface nitriding of yttria ( $\text{Y}_2\text{O}_3$ ) stabilised tetragonal zirconia (t-ZrO<sub>2</sub>) under nitrogen environment using pulsed Nd-YAG laser irradiation. As per the results, the original tetragonal zirconia and the modified one have different crystallographic structures. The development of nitrides (ZrN) was observed, revealing the relationship between surface morphology, crystallographic structure, and laser spot overlap degree to attain high surface hardness and good surface quality. The ZrN surface nitriding was successfully accomplished with a yellow-gold hue. Atoms of nitrogen replace oxygen in the network as they enter the zirconia. The nitrided surface's X-ray diffraction revealed changes in its peaks' shift and d-spacing, or lattice parameter. The surface's Raman spectra demonstrate an effective transformation of the t-ZrO<sub>2</sub>, exhibiting the characteristic yellow-gold colour of ZrN with high wear resistance. The hardness was very high measuring upto 1409 HV. Nitriding was achieved by partial transformation of t-ZrO<sub>2</sub> into cubic zirconia (c-ZrO<sub>2</sub>) deep in the bulk due to nitrogen concentration gradient and the development of a few micron thick gradient layer of ZrN structure on top. Ultimately, it was demonstrated that it worked well for decorative marking.

Fernandez-Pradas et al. [33] employed Nd: YAG laser beam operating in continuous wave mode as a tool to print coloured enamel patterns on tile surfaces. The tiles were positioned on a lift table so that their surface would be in line with the laser scan head's focus, which has a beam spot with a diameter of roughly 300  $\mu\text{m}$ . Samples were exposed to radiation by scanning at speeds ranging from 5 to 1000 mm/s in a series of 5 mm long lines using laser beam strengths of 12, 20, 25, and 30 W. The combination of beam strength and scan speed defined the cumulative energy density of the laser beam, which in turn determined the properties of the lines. For the lines to adhere, the glazed substrate had to melt at a minimum cumulative energy density. The lines showed a glassy centre area where the melted glazed substrate was combined with enamel material, and darker edges where a layer of enamel was adhered to the glazed substrate. It doesn't take much more material to generate the lines once the collected energy density hits 500 J/cm<sup>2</sup>. Analysis revealed that the lines breadth and depth grew as linear function of square root of the accumulated energy density.



Chen et al. [34] designed a scribing laser marking system based on a digital signal processor (DSP) in the galvanometric marking approach. A 10.6  $\mu\text{m}$  CO<sub>2</sub> laser marking system was used, and it performed well with marking materials like glass, plastic, paper, wooden goods, and coated materials. Power supply, laser source, delivery optics, control system, and cooling system were all common components of a laser marking system. The study used Borland C++ Builder software to create a laser marking human-machine interface (HMI). It could process the documents, change object documents, define marking variables, load text and graphics from .bmp and .dxf files, and interact with DSP. The successful D/A combined converter of the DSP with the HMI allowed for more precise control over the rotating angle of the galvanometric scanning mirrors. As a result, the DSP-based scribing laser marking system has higher resolution than standard ones, and the entire marking system is both affordable and compact. In order to mark various materials, the developed laser marking system also used the vector scan method with circle times of 2 second to mark 5x7 characters at 57 word per second with a spot size less than 300  $\mu\text{m}$ . The positioning reaction time of the scanning actuator was the primary determinant of the marking speed. However, laser irradiation, pulse repetition rate, pulse duration, and control delay must be set properly for the best quality.

Hana et al. [35] utilised laser controlled oxide formation on Ti-6Al-4V alloy under ambient circumstances as an artistic tool. It is very effective tool for creating controlled and even areas of colour and designs that appeared spontaneously on the surface of commercial purity titanium alloy plate at moderate power 60 W of pulsed CO<sub>2</sub> laser that was directed via an X-Y beam positioning system within an integrated system and interfaced with commercial graphics software. At CO<sub>2</sub> laser line energies over a threshold of 0.4–1.1 W/mm, the parent titanium alloy surface morphology was dramatically changed, resulting in a more even surface; nevertheless, at line energies above 0.75 W/mm, there were also indications of surface cracking. The X-ray diffraction (XRD) study revealed the presence of TiO and Ti<sub>2</sub>O titanium oxides on the surface in addition to rutile titanium dioxide (TiO<sub>2</sub>), which was previously thought to form an outer surface layer and be in charge of interference hues. The findings supported the idea of a graded surface layer that progresses from an outward layer of TiO<sub>2</sub> to lower layers of oxides that are richer in titanium.

Leone et al. [36] employed a Q-switched diode-pumped Nd:YAG green laser to deeply etch several types of wood without causing surface carbonisation. It was discovered that not all types of wood could be engraved; this depended on the structure of the wood as well as the

existence of substantial variations in density. Deep engraving and the carbonisation phenomenon were easily achieved on all types of wood at all tested frequencies at a relatively low speed of 10mm/s. The etched depth was quite shallow at speeds more than 40 mm/s, and deep engraving needed repeated laser scans. The mean power, the pulse rate, the beam speed, and the number of repetitions all had a significant impact on the etched depth. Elevating the speed led to the achievement of engraving with a narrower frequency range surrounding the maximum output power value. There existed a linear relationship between the mean power and the maximum speed required to achieve engraving. For the purpose of predicting the etched depth, a straightforward linear model based on energy consideration was put out and confirmed. A relationship between the model coefficients and the density of the wood was discovered by taking into account the laser mean power, the beam speed, and the number of repetitions.

Li et al. [37] conducted research on comprehensive understanding of the oxide formation process that occurs when stainless steel is in air and is exposed to a Q-switched third-harmonic Nd:YVO<sub>4</sub> laser beam with a wavelength of 355 nm. It was discovered that the colours created by laser irradiation were very responsive to laser energy density. Important processing variables that impacted the colours were the scanning direction, speed, laser irradiation, and focus plane offset. Subsequent research revealed that the laser scan rate had an impact on the first oxidation reaction. Optical microscopy, scanning electron microscopy (SEM), and a time-of-flight secondary ion mass spectrometer (TOF-SIMS) were used to examine the oxide layer. When the laser beam scanned at a 500 mm/s speed, Cr was selectively oxidised at the Cr-rich surface. A duplex oxide structure comprising an exterior layer of Fe oxide solution and an interior layer of Cr oxide solution was created when the laser beam was scanned at a 400 mm/s speed. During several laser scanning runs, Fe diffused to the surface, increasing the thickness of the oxide layer. After every laser pass, the duplex layer's composition varies. After six laser passes, the amount of Cr in the outer layer steadily decreases and purer Fe oxide is created. At the oxide/base metal interface, microcracks were seen, and the frequency of these cracks grew with the number of laser scan passes. Because Fe diffusion in the oxide layer is constrained by a longer diffusion distance across the thicker oxide layer and microcracks at the oxide/base metal interface, the oxide growth rate reduced as the number of laser passes increased and their thickness tended to stabilise.

### 1.8.3 Laser Marking on Different Materials

To investigate the impact of lasers on various materials, including leather, paper, wood, and other materials such as ceramics, glass, plastics, denim fabric, steel of various grades, and egg shells, marking was done. The findings are shown below.

Alexander et al. [38] employed palladium (II) acetate and various orasol dyes for the first time to create permanent markings of varied colours on ceramic and plastic surfaces. An argon ion laser with a wavelength of 514 nm was used to create the markings by photothermal deposition procedure. Two methods of laser marking were applied using palladium (II) acetate and orasol dyes. The first was the method of mask marking and real-time motion marking was the second. The product surface was left intact, and high contrast and well-defined colour markings were created in addition to a metallic silver finish. The categorization of the marking mechanism as a photo thermal process was contingent upon the specific type of substrate. Both qualitative and quantitative descriptions of the relationship between the various marking variables such as power, line width, and speed/exposure duration were provided. The marking process was found to be dependent on the chemical and physical properties of the film as well as its concentration.

Dascalu et al. [39] conducted research in removing indigo dye from denim support effectively by the laser fading technique. To find the ideal wavelength, they ran tests at three distinct laser wavelengths: CO<sub>2</sub> (10.6  $\mu$ m), YAG (1064 nm and its second harmonic, 532 nm), and YAG (1064 nm). The right laser irradiation density and fluency were also utilised. Power density was shown to be the most significant factor. The optimal option was determined to be the Nd:YAG laser operating at 532 nm. The investigation demonstrated that the CO<sub>2</sub> laser beam had an impact on the fiber structure of the textile, even though the denim and CO<sub>2</sub> laser interaction process was the strongest. The phenomena of heating and vaporisation was the primary cause. The high power density of the Q-switched Nd:YAG laser caused fading as a result of shock wave and plasma production.

Feng et al. [40] used 532 nm Nd: YAG laser to label compounds including carbon black (CB) and polypropylene (PP). Laser processing of typical polymers was discovered to involve cooperative thermophysical and photochemical processes. The highly loaded CB/PP compounds' widely dispersed CB particles prevent incoming photons from penetrating much deeper into the bulk material. This limited the laser-CB interactions to a very thin layer below the surface, creating a pit that was comparatively shallow. The

polymer caused the ablated region to appear white as the excited CB particles burst away from the surface, standing out dramatically against the original surface's black backdrop. The CB concentration and the physical characteristics of the laser, such as its fluence, wavelength, and repetition rate, were linked to the marking clarity (MC). Thus, it was determined that a CB level of less than 3.0% may yield a good MC. It was clear that at 0.1% CB/PP, more fluence resulted in more definite marking, but for 10.0% CB/PP, there was hazy marking.

Chitu et al. [41] employed CO<sub>2</sub> laser scanning to mark both organic and inorganic materials. The continuous wave mode of a sealed-off CO<sub>2</sub> laser was employed in the tests, and the laser beam was projected onto the target using a galvanometric scanner. By adjusting the laser's output power, the object's location in the focal plane, the scanning modes, and a number of scanning variables from the software—mark speed, jump speed, mark-jump-polygon delay, laser-off delay, laser-on delay, gain (scaling), and mirror—laser marking on materials was investigated. This application's developed software was employed in executing the operation. The maximal laser irradiation of 15 W was adequate to produce pictograms using three different scanning modes (vectorial, raster, and step-and-hold) on a variety of materials. A maximum pulse rate of 200 Hz and 2 kHz, respectively, were employed for the two power supply. The amount of time that heat could permeate the surrounding material was shortened by the brief pulse duration. Short pulse length pulsed laser marking was found to produce better quality, more contrast, and improved uniformity. By reducing the area of the heat-affected zone (HAZ), a pulsed CO<sub>2</sub> laser was able to produce markings of higher quality. To produce high-quality marks on materials, the irradiation circumstances and laser settings were further optimised.

Kim et al. [42] assessed the laser patterning system's viability for making light guiding panels using a laser branding procedure. A continuous wave 50W CO<sub>2</sub> laser was used to create a number of light guide patterns in order to understand the effects of laser irradiation and scan rate on groove geometry. As laser irradiation increased and scan rate decreased, the manufactured grooves grew wider and deeper. Scanning electron microscope (SEM) photography was utilised to evaluate the surface geometry, and a Topcon-BM7 was employed to quantify brightness. Compared to a printing-type LGP (1787 cd/cm<sup>2</sup>), a laser-machined LGP offered a higher luminance (8000 cd/cm<sup>2</sup>). However, the laser-machined LGP's homogeneity was worse. The laser-marked grooves' underdesigned pattern intervals may be the cause of the low uniformity, however if better pattern design was done, it might

be improved. Consequently, 5W and 0.4 m/s were proposed as the laser patterning marking conditions.

Dusser et al. [43] studied the process of deep marking of various materials using a Ti:Sa laser system that produced 150 fs pulses at a 5 kHz repetition rate. The idea was to create a third data storage axis by using the depth of a marked surface. The goal was to transform a depth that was done into a grey level throughout the reading process. Transparent polymers appear to be a good option for the fundamental materials used in 3D laser marking, with deep marking obtained by specialised processing. Roughness has been shown to affect light transmission as well. By using back light for reading, it was determined that laser deep marking can be useful for 3D coding, but only on certain transparent materials.

Witaya et al. [44] used 532 nm Nd: YAG laser to create data matrix symbols on carbon steel substrates. The ISO/IEC 16022 bar code technology specification for data matrix was then used to assess the laser marked data matrix symbol's quality. To investigate the impact of various variables on the quality of the laser direct-part marked symbols, several experiments were carried out. It was discovered that a number of variables had a major impact on the quality of the data matrix symbols that the laser produced, including the kind of carbon steel, the percentage of laser tool path overlap, profile speed, average power, and frequency. The examination of the data revealed that factors that prevented the laser-marked data matrix symbols from receiving a better final grade were contrast and print growth.

Chen et al. [45] created laser marking on eggshells using pulsed CO<sub>2</sub> laser. Using a scanning electron microscope, the diameters of the indicated holes on the fragile eggshell were estimated. The findings showed that the size of indicated holes was influenced by an increasing number of shots. The depths of the holes bored with varying numbers of shots were roughly equal to one-fourth of the eggshell. The eggshell's bottom was unharmed by the pulsed CO<sub>2</sub> laser branding method. A thin coating of eggshell could be removed by high-energy beams, and in the process, a contrasting mark that was both tamper-proof and easy to read was produced. The heat affect zone (HAZ) had no effects on the egg theca, and the laser coding approach did not harm the eggshell's underside either as per the experimental findings. The date coding on the eggshell might be accomplished with laser

marking instead of ink printing. The outcomes demonstrated that it could be feasible to laser code a freshness date and a traceability code on each egg.

Leone et al. [46] executed laser marking on AISI 304 steel using a Q-switched diode pumped Nd:YAG laser. Using digital photographs of the marks, the contrast index was used to analyse the mark contrast. The breadth and roughness of the mark were measured and studied using energy dispersive X-ray technology in conjunction with optical and scanning electron microscopy to characterise its properties. According to the experimental findings, contrast improved up to a characteristic value. Surface roughness and oxidation both increased as a function of frequency. Furthermore, there was a positive correlation between reduced scan rates and current intensities and the maximum visibility value. The optimal processing settings for maximum mark visibility were determined by building an empirical model and taking into consideration the operational limitations of the laser equipment in use.

Leone et al. [47] carried out laser marking of Inconel to find out the relation between process variables and mark characteristics i.e. mark geometry and readability. A 30 W Q-switched Yb:YAG laser was used to mark the surface of Inconel 718 sheets at different process variables such as average laser irradiation, pulse rate and scan rate. The mark geometry was acquired by 3D surface profiling system whereas mark readability was determined in terms of Weber contrast. Experimental results revealed that average power and linear energy has a crucial role in mark geometry formation, whereas pulse rate has a significant weight in image formation. Furthermore master response optimisation was adopted to achieve the optimal setting of process variables for better value of marking characteristics, keeping mark contrast and width to be in maximised condition and height to be in minimized condition. Composite desirability function were also performed to simultaneously optimize the mark characteristics. It was observed that optimum contrast and width achieved was 0.55 and 145.37  $\mu\text{m}$  and minimum depth achieved were 8.09 respectively.

Shivakoti et al. [48] carried out experimental analysis on laser marking of gallium nitride material using diode pumped Nd:YAG laser. The process parameter such as lamp current pulse rate and scan rate etc. were utilized to study their impact on laser marking characteristics i.e. mark width, mark depth and mark intensity. Furthermore, RSM based experimental design was adopted to study the in-depth influences of process variables and

the optimised value of process variables were determined using desirability function analysis. Experimental results revealed that optimized multi-objective parametric combination based on RSM methodology were current of 19A, pulse rate of 4780Hz and scan rate of 5mm/s. However, sensitivity analysis revealed that current and pulse rate have most significant contribution for varying the mark width, mark depth and mark intensity.

Sun et al. [49] carried out work on the fabrication of nano-ripples on titanium work piece using femtosecond laser induced periodic surface oxidation. The nano-ripples were formed at different pulse energies and scan rate. Experimental results revealed the consistency of spectral changes in the reflection and transmission mode, equivalent to the principle of diffraction grating. Moreover, the obtained colours were sensitive to angles. Ripples orientation strongly affect the colour intensity while viewing angles and incident angles effects the type of colours. However, the used method of pattern segmentation for encryption and decryption of information without affecting the overall pattern of marked surface, provides a new concept of colour display, information security and anti-counterfeiting.

Liu et al. [50] investigate the effects in surface properties of polymer caused due to the change of laser process variables of Nd: YAG laser. The process variables involved were laser irradiation, scan rate and pulse rate which were utilised for the modification of surface properties i.e. surface morphology, carbonisation and wettability. The morphological change in the PI film was analysed using 3D optical microscope whereas carbonization characteristics analyzation was performed using grey scale extraction tool in the Photoshop software. Experimental results revealed that within the range of studied process variables pulse rate and laser irradiation have greater contribution towards carbonization area rate of marked surface and wettability than scan rate.

Lecka et al. [51] carried out analysis work regarding the impact of oxide layers, caused as a result of laser radiation in normal ambient condition on titanium grade 2. The setting of different process variables in and out the focal plane has a contribution to both improvement and deterioration of surface quality. After performing microscopic examination roughness such as calorimetry, adhesion, wettability, electrochemical test etc. Results revealed that samples manufactured in the focal plane exerts a high corrosive resistance, adhesion and lower roughness compared to those samples whose experiments were performed out of focal plane. However, Raman analysis does not show the precise determination of chemical

composition but highlighted the appearance of several peaks in the spectrum. Laser treatment resulted in the formation of oxide layers such as  $\text{TiO}_2$ , and  $\text{Ti}_2\text{O}_3$  oxides in both anatase and rutile phase, a factor responsible for effective protection barrier for laser induced surface.

Odintsova et al. [52] investigate the possibility of laser colour marking on titanium Grade 2 for industrial application. The factors such as repeatability, marking stability and productivity under aggressive condition were of prime concern. The laser marking operation was performed by Mini Marker 2 based on ytterbium fiber laser IPG photonics of wavelength 1064 micrometre. The paper focussed on increasing the performance of laser colour marking with minimal effects on the work piece surface. The stability of marked area was analysed in terms of chemical and environmental resistance. Experimental results revealed that laser colour marks on titanium showed very high susceptibility to various chemicals such as salts and acids and also has the ability to withstand high and low temperature at high humidity levels.

Jwad et al. [53] carried out work to erase the selective portion of oxide-based colours on titanium material using nanosecond fiber laser source of 1064 nm manufactured from SPI Laser. Experiments were performed on reconfigurable laser micro processing platform with 3D scanner and 100 mm telecentric F- $\theta$  lens. The maximum pulse rate used was 1 MHz which was spitted with 25 pulse duration from 15 to 220 nanosecond. The marked portion of material is reprocessed in a low oxygen environment in order to reduce the possibility of forming metal oxide on the surface of metal. A specially designed chamber was employed to achieve low oxygen atmosphere by purging the air out and replace with argon, whose flow rate and pressure were maintained at 25 L/min and 5 bar respectively.

Astarita et al. [54] carried out laser marking process on titanium cold sprayed coating on aluminium substrate. The varied process parameter which involved in marking test of titanium rolled sheets of grade 2 were laser irradiation, scan speed etc. The marked portion were observed by optical microscope and SEM for finding out maximum penetration depth, width of marks and internal damages which were introduced by the processes. It was observed that the heat input rules the marking process, in particular three different conditions were observed: (i) irregular groove due to a too high energy released for unit length; (ii) regular mark with hidden damages; (iii) regular and effective mark; (iv) regular but inadequate groove due to a low heat input. Moreover, a higher mark penetration on Ti



coating was observed compared to the Ti sheet. The results also highlighted possibility to introduce severe and hidden damages in both materials if the process variables were not properly set.

Penide et al. [55] carried out experimental study on the process of marking alumina by lasers working in two wavelengths: 1064 nm (Near-infrared) and 532 nm (visible, green radiation) and colorimetric analysis had also been carried out in order to compare the resulting marks and its contrast. Experimental results showed that marking carried out in argon had more quantity of material (both aluminium and oxygen atoms) removed than the other one which carried out in air. Furthermore, laser marking carried out in argon atmosphere produced darker marks than air as demonstrated by colorimetric analysis. Therefore, it may be concluded that the atmosphere is the key parameter, being the inert one the best choice to produce the darkest marks.

Cheng et al. [56] carried out work on enhancing the laser marking characteristics of propylene using antimony doped tin oxide @ polyamide (ATO@PI). The use of ATO possess high photo- thermal conversion efficiency and PI shell has carbonization rate, The SEM and TEM results revealed that PI was tightly coated around ATO surface and structure of laser sensitive composite were approximately spherical. Experimental results revealed that after laser irradiation of 1064 nm, the carbonization of ATO@PI was much higher than pure ATO giving higher value of marking characteristics of polymer work piece.

Kibria et al. [57] conducted experimentation analysis in laser surface texturing process on pure titanium material employing a pulsed Nd:YAG laser system. Response surface methodology (RSM) based design of experiments was implemented to conduct the experiments and the result so obtained was further analysed to improve its performance. The four process variables were average power (W) , Pulse rate(kHz), scan rate (mm/s) and transverse feed(mm), each has five levels, based on which experiments were conducted to minimise the surface roughness (Ra and Rz) . Optimized response values of lateral surface roughness (Ra) was 2.93  $\mu\text{m}$ , transverse surface roughness (Ra) was 3.32  $\mu\text{m}$ , lateral surface roughness (Rz) was 19.48  $\mu\text{m}$  and transverse surface roughness (Rz) was 18.89  $\mu\text{m}$  at parametric combination of average power at 9 W, pulse rate at 1400 Hz, laser beam scan rate at 2 mm/s and transverse feed at 0.02 mm.

Cui et al. [58] investigated the phenomena of surface oxidation on AISI 304 stainless steel. Results revealed that different morphologies and phase composition associated with one

laser spot varies from centre to edge after Nd:YAG laser pulsed oxidation. XRD analysis revealed the presence of various oxides such as gamma iron,  $\text{Cr}_2\text{O}_3$ ,  $\text{Fe}_2\text{O}_3$  and  $\text{MnO}_2$  which were obtained after oxidation of element. The laser spot extremities had high chromium and less iron element content with opposite trend at laser spot centre. Moreover, oxidation behaviour and mechanism of its generation on stainless steel by Nd:YAG pulsed laser were discussed based on the analysis of thermo-kinetic and experimental results.

Adams et al. [59] carried out work on creation of oxide coating on surface of stainless steel 304 by nanosecond pulsed laser. Experimental results revealed that continuous metal oxide were grown with increase of laser fluence when laser beam is focussed on work piece in ambient condition. However, for large fluence with excess of 600-800J/cm<sup>2</sup> resulted in the decrease of coating thickness due to the effects in oxide growth. Experimental results revealed that the oxide growth obtained by pulsed laser irradiation modified the composition of stainless steel by affecting the chromium and manganese content within the melt zone. The spectral reflectance and chromaticity of oxide coating were determined using spectrophotometry. The coating exhibited low diffuse reflectance in the visible part of spectrum and their chromaticity varied between 0.29 to 0.38 with change in oxide thickness.

Lawrence et al. [60] studied the electromechanical and chemical behaviour of oxide coating which were grown on stainless steel 304 by nanosecond pulsed laser. The variation in oxide thickness produces characteristics colour and its control relied on process variables. The mechanical properties of developed oxide depends on thickness. The elastic modulus of material is insensitive of layer processing whereas hardness showed a decrease in its value as film thickness decreases below 100 nm. Experiment revealed that on application of indentation thickness oxide fracture circumferentially whereas thin oxide undergo radial cracking. The behaviour of metal were due to differences in film thickness and toughness of oxides. Thick oxide had duplex layer consisting of  $\text{MnCr}_2\text{O}_4$  and  $\text{Fe}_3\text{O}_4$  and thin oxide layer lack  $\text{Fe}_3\text{O}_4$ .

Adams et al. [61] carried out work on the mechanism, of oxide growth aimed its effects on titanium caused by nanosecond pulsed laser radiation. Experiment revealed that oxide formation has three zones  $\text{TiO}_2$ ,  $\text{TiO}$  and  $\text{TiO}_x\text{N}_{1-x}$ . The combined thickness vary in the range of 10 to 120 nm with the increase of laser fluence. The developed oxide coating

possess different colours which vary with oxide thickness, interference of incident white light. The depth achieved in the process was 25  $\mu\text{m}$  for highest fluence value.

Huiling Hui et al. [62] studied the effects of Nd: YAG pulsed laser on surface properties of polyamide films. The modification and formation of surface properties of PI films depend on process variables such as laser irradiation, scan rate and pulse rate. The responses under consideration were surface morphologies, carbonization characteristics and wettability. Experimental results revealed that within the range of processing variables, laser irradiation and pulse rate had a greater contribution towards carbonization rate and wettability than scan rate.

Raillard et al. [63] studied the chemical and topographic effects of femtosecond laser irradiation on steel surface. The centre portion of laser irradiation had cavities with conical spikes and outer ring zone with ripples. Experimental curve revealed that 1 micrometre depth cavities was best load carrying capacities and good lubrication properties whereas elemental depth profile revealed the increase of oxide layer thickness by a factor of 1.7 as compared to carbide layer. The distribution of carbon depends on laser intensity and number of laser pulse which lead to amorphization of irradiated zones according to melt quenching phenomena.

Senegacnik et al. [64] studied the influences of process variables such as laser pulse fluence, number of laser pulse and pre-existing defect on samples of steel and titanium surface by pulsed laser. LIPSS formation was caused by interaction between laser and surface which were used to improve or change the surface structure. Experimental results revealed that fluence lower than single pulse fluence, which served the threshold for ablation, lead to LIPSS formation with period 100-500 nm whereas higher pulse fluence resulted in larger spatial period between 800-1100 nm. The paper also highlighted that change of process variables lead to different topographical and chemical characteristics of top layer surface of sample which were used for experimentation.

Moura et al. [65] investigated the characteristics of surface texturing in terms of morphology and chemical means of titanium alloy (Ti6Al4V) produced by Nd:YAG laser. Experimental results revealed that oxide layer formed on the titanium surface had components of  $\alpha$  Ti, Ti<sub>6</sub>O and Ti<sub>2</sub>O on textured surface. The titanium oxide thickness obtained had good electrical insulation value of about 90% efficient which may be suitable for smart implants.

Lehr et al. [66] observed that gas environment such as nitrogen , argon, and oxygen had significant impact on the laser machined surface. The attainment of different surface topographies and morphologies corresponding to different gas environment has different marking characteristics which provides uniqueness in the area of laser marking.

#### **1.8.4 Laser Marking Systems**

There are numerous commercially available marking machines, and in order to obtain high-quality markings, the system must be improved. An overview of the numerous improvements made to the laser marking machine, such as integrating 3D laser measurements into the laser systems and giving the system feedback, is provided in the section that follows.

Amara et al. [67] carried out experimental approach with the aim to bring a contribution to the comprehension of the occurring phenomena during fiber laser color marking of steels. A home-made marking device using a pulsed fiber laser has been used to treat steel samples under different laser beam operating variables, for different compositions of the processed steel, and at normal atmospheric conditions. The treated samples were analyzed either by optical and scanning electronic microscopy, as well as by energy dispersion spectroscopy. Different colors have been obtained on the treated stainless steels by varying the laser variables or by varying the chemical composition of the substrates. The characterization of the obtained layers by pulsed laser irradiation, allowed us to conclude that an oxidation phenomenon responsible of the surface modification leads to a colored surface observation. It can be concluded also that the different colors, obtained on the same sample, are due to a difference in the thicknesses of the oxidized layers resulting from different operating variables.

Flury et al. [68] employed a low-cost diffractive optical element (DOE) Nd: YAG laser to mark intricate shapes, such industrial logos, with a high enough quality. There are many uses of (DOE) in the field of laser marking using pulsed Nd:YAG lasers. The holographic media, which is actually a silica substrate with modulated resin, is used in the manufacturing of the DOE. The approach described made use of contact photolithography and a commercial resin that was extremely reasonably priced. The elements are binary and were created using contact photolithography and commercial resin, however they offer helpful reconstruction for a variety of uses. Lastly, using a marking test on sensitised paper, the effects of the pulse duration on the reconstruction shape were assessed and shown.

Chen et al. [69] presented a technique for reducing the field distortion error in a CO<sub>2</sub> laser marking system. For a laser marking equipment, minimising the field distortion in a scanned image was crucial. Therefore, in order to correct the field-distortion error in galvanometric scanning systems, a compensation mechanism has to be found. In order to determine the function of the galvos' correction control commands, which can correct for distortion errors in galvanometric scanning systems, the compensation methodology was applied in the surface curve fitting method. The method successfully lower the field distortion errors in the laser marking machine, according to experimental data. As a result, the method could be widely used to improve the accuracy of the majority of two-dimensional machine systems, including XY tables, and could successfully reduce the field distortion error of the galvanometric scanning system.

Diaci et al. [70] presented a unique technique for quickly and flexibly laser marking of slanted, curved, and freeform work-piece surfaces. The technique relied on combining a three-dimensional (3D) laser marking system with a three-dimensional (3D) laser measurement system. A digital camera was coupled with 3D laser marking system for the measurement of the workpiece surface's 3D shape right before processing. The 3D shape of a work-piece surface was measured using a low power continuous wave laser regime, and processing was done using a high peak power pulsed laser regime. Usually, the measurement process took less than ten seconds. A special piece of software was created to enable process control, laser mark placement on to the measured surface, and 3D surface measuring. The locus of 3D trajectory of the processing beam resulted in the formation of 3D surface data. As long as the processed surface is inside the 3D laser processing system's operating range, neither the 3D shape nor the orientation of the work piece was known beforehand. This significantly increases processing flexibility by doing away with the requirement for precise work-piece positioning prior to processing of laser marking.

Lin et al. [71] used a delta motor driving module and a high-speed, high-resolution line scan CCD for positioning feedback in laser marking system. A unique 1-D calibration model of the line scan CCD was created and the system was calibrated using a template. The calibration algorithm was used to determine each IC's pertinent location in the tray. In this autonomous optical inspection system, sub-pixel calculations, gain and offset calibrations, and normalised tests were carried out. The process was stable as process capability index reaching over 1.2, positioning accuracy of 9  $\mu\text{m}$ , and total processing time was roughly 2-2.5 s for laser correction marking, scanning, and identification.

Wang et al. [72] devised a technique for preventing distortions in the laser marking system. Inherent and random mistakes were the primary cause of the distortions. The galvanometer scanning produced the pillow-shaped distortion, but the various focal lengths and magnifications at the various focal lens heights would result in the barrel-shaped distortion. A straightforward technique known as linear compensation was proposed. For testing, over ten sets of laser marking machines were selected in order to validate the suggested method. Initially, all of the laser machines marked a conventional square. Following an examination of the marking findings, three representative machines with noticeable distortions were selected for additional testing. It was seen that the marking quality had increased, demonstrating the algorithm's efficacy and demonstrating its flexibility and ease of use.

### **1.8.5 Basic Parametric Influences on Laser Marking**

The quality of the marking on the material is influenced by laser marking variables. Following an analysis on a variety of materials, the impact and influences of several variables, including pulse rate, speed, air pressure, laser beam power, and pulse width, on the marking quality features, such as mark width and mark intensity, are explored.

Ng et al. [73] examined laser marking on four distinct types of sample plates: (a) anodized aluminium; (b) stainless steel; (c) poly-butylene tetraphthalate (PBT); and (d) phenol formaldehyde using Nd: YAG laser with a 1.5 W output. For a normal power setting, there was a clear correlation between the laser marking speed and the laser marking time. The three illumination modes—tungsten, fluorescent, and daylight—as well as the variable marking speeds for the various materials were taken into consideration when calculating and plotting the CIE colour difference values. For stainless steel, a growing colour difference with marking speed trend was found for both daylight and fluorescent illumination. There seemed to be a slight decrease in colour difference at marking speeds of about 5 m/s while using tungsten illumination. Marking stainless steel at a pace of about 5 m/s seemed to be standard practice, regardless of the kind of lighting. In the case of PBT, colour difference values seemed to rise with marking speed under tungsten and fluorescent light and a plateau was reached at marking speeds of about 200 m/s. The daylight curve appeared to follow a similar pattern, although a higher marking speed of about 320 m/s was required to obtain a comparable plateau value. Hence, with the exception of marking speeds exceeding 300 m/s, colour difference was more distinct when viewed under the artificial illuminants of tungsten and fluorescent.

Ng et al. [74] studied the quantitative evaluation of four different surface types utilising spectrophotometers and a Nd:YAG laser. For the unmarked surfaces, the reflectance values demonstrated a declining tendency in the following order: PBT, anodized aluminium, stainless steel, and phenol formaldehyde. The marked and unmarked anodized aluminium surfaces had nearly identical reflectance traces. On the other hand, it was distinct and wavy for stainless steel. In PBT and phenol formaldehyde, the reflectance spectra for both marked and unmarked surfaces were comparatively flat. Lower marking rates were chosen for PBT in order to raise the average reflectivity. Gradually lowering the marking speed led to an increase in average reflectance for phenol formaldehyde.

Velotti et al. [75] carried out laser marking of titanium coating with an aim to characterize the laser marking process on Cold Spray Deposition (CSD) Ti coating, in order to study the influences of the laser marking process variables (pulse power and scan rate), on the groove geometry of the marking. The experimental marking tests were carried out through a 30 W MOPA Q-Switched Yb: YAG fiber laser under different process conditions. The groove geometry was measured through a HIROX HK9700 optical microscope. The results showed the effectiveness of the laser process to produce high quality marks on the titanium layer and also highlighted that the importance of the penetration depth which increased after coating application, as index for the evaluation of the mark geometry

Park et al. [76] carried out laser marking on a silicon wafer in order to increase the productivity of the finished product. The laser marking width estimation model was developed using a process monitoring system. A photodiode was used to measure the plasma light emitted during laser marking in order to monitor the process. Because of the rapid marking process, the photodiode on a coaxial line was able to precisely record light emission. An optical sensor was used to measure the plasma created by the laser's interaction with the wafer. With an increase in laser irradiation came an increase in line width due to increase in the interaction between the laser and the wafer. The relationship between the signal obtained from the optical sensor and the subsequent line width was examined for every laser irradiation setting. Four statistical regression models were created using the experimental data to determine the line width that best reflected the marking quality. The line width was estimated using multiple linear regression, multiple nonlinear regression, neural network, and second order polynomial regression models. To compare the accuracy of each model quantitatively, the coefficient of determination and average error rate were computed for each model. It was demonstrated that when it came to the

average error rate and coefficient of determination in the estimation performance, the neural network model outperformed all other models.

Antonzak et al. [77] used industrial Yb:glass fiber laser of 1062 nm with an output power of 20 W for laser marking AISI 304 stainless steel. The evaluation of colour change was conducted using the CIE colour difference formula. If the colour difference parameter value was less than seven, the colours were deemed similar. No appreciable variations were seen for a few process variables, including the thickness and starting temperature of the samples and the size of the designated region. The main factors affecting the reproducibility of the colour acquired were the laser irradiation value, the metal plate's scan speed, and the marked surface's location in relation to the system's focal plane. Changes in power density, or energy density, on the designated surface was also a factor affecting reproducibility of the colour. The process variables for each colour were determined by keeping in mind that the length, frequency, and spacing between pulses. Stability was needed for all those characteristics that impact colour, ranging from 1% to 2%, depending on the colour. It suggested that in order to simplify and automate the process of laser marking, changes needed to be made to the current systems. Utilising an active feedback loop in an industrial setting needed process variables to be stable at a certain degree. This might be achieved, for instance, by continuously measuring the laser's output power and the distance between the lens and the marked object.

#### **1.8.6 Optimization and Modelling of Laser Marking**

Modelling techniques are useful tools for determining how different laser marking variables affect the mark on different types of materials. A few modelling tools, including the response surface methodology (RSM), artificial neural networks (ANN), Taguchi method, and finite element analysis based on ANSYS, were used to investigate the changes in marking variables and attributes. The specifics are provided below.

Chen et al. [78] used the Taguchi technique of experimental design for the optimisation of process variables for Q-switched Nd:YAG laser micro-engraving of iron oxide coated glass. Five important process variables have been investigated and found to have a considerable impact on line width: beam expansion ratio, focal length, average laser irradiation, pulse repetition rate, and engraving speed. The engraving line width was the main reaction that was being examined. The tests were planned using an  $L_{16}$  orthogonal array. Based on the investigation, it was shown that a minimum line width of 18  $\mu\text{m}$  could



be achieved by using a 5X beam expansion ratio, 50 mm focal length, 0.4 W laser average power, 5 kHz pulse repetition rate, and 5000 mm/min engraving speed.

Peligrad et al. [79] performed laser marking of clay tiles using a high-power diode laser. The output response melt pool width was measured with a quick CCD recording system and examined using image-processing software whereas traverse speed and laser irradiation were the input quantities that were undertaken. It was possible to get reasonable agreements between the designed model outputs and the measured data. Apart from that, errors less than 1.3µm of the melt pool width were discovered. With a laser irradiation of about 60 W and a beam velocity of about 6–10 mm/s, a smooth, well-defined mark was produced on materials.

Peligrad et al. [80] created multi-input and multi-output dynamic model for laser marking of ceramic materials in order to understand the behaviour of the process. Melt pool temperature and shape were determined using a pyrometer and a fast charge coupled device camera were used for the observable signals. The traverse speed and laser irradiation were the input quantities that were examined. For  $f = 100$  Hz, a smooth, well-defined mark with errors of less than 1% was obtained at a beam velocity of 10 mm/s and laser irradiation of about 70 W.

Jangsombatsiri [81] used an artificial neural network model to laser direct the part marking operation of data matrix symbols on carbon steel substrates using a 532-nm Nd: YAG laser. The objective was to assess the direct-part marked data matrix symbols' quality in accordance with ISO/IEC 16022. Data sets for training, validating, and testing artificial neural network models were created using the outcomes of the experiment on identifying essential laser variables. Subsequently, for validation, the comparable multiple linear regression models were compared with the single output artificial neural network models. When it came to laser direct-part marking of data matrix symbols on carbon steel substrates, the single-output artificial neural network models outperformed the multiple linear regression models in terms of prediction accuracy.

Chen et al. [82] examined the temperature model of the marking characters created on the eggshell using the finite element analysis programme ANSYS. The ANSYS parameter design language was used to set the variables, generate the meshing model, and simulate the action of a gaussian dispersed laser beam on the eggshell surface. The temperature distribution field is shown by the simulation results. Additionally, in order to determine

whether laser beams damaged the eggshell's interior, characters were marked on the fragile eggshell and found safe inside. The mark's depth and width were determined by SEM. One-fourth of the eggshell's overall thickness is accounted for the heat-affected area, which prevents the inner layer from deteriorating. The heat-affected region by laser marking is similar to that of the simulation, according to the findings of the comparison between the ANSYS simulation and the laser marking experiment. There was no comparable uncertainty in adopting the laser, but stamping the characters in ink might cause the ink to seep through. It takes only a fraction of a second to mark the date on an egg using a laser, compared to covering it with ink. However, the items' quality and people's health are considerably more assured in laser marking.

Lehmuskero et al. [83] demonstrated that the colours marked on stainless steel were created by multiple contiguous chromium oxide layers of varying thicknesses. On the stainless steel surface, the colour creation energy ranged from 0.5 to 13  $\mu\text{J}$ , which is equivalent to the oxide layer thickness of 1 to 350 nm. Improved control over the laser marking process of stainless steel was made possible by the combination of the colour model, energy and oxide thickness correlation, and a stronger physical understanding of the process. Future research may look into the application of colour pixeling, particularly the creation of flat top intensity. Current techniques combine map transforming and gray-level patterning techniques with reflecting and refractive elements or diffractive elements could result in the flat top with an antireflection coating positioned between the sample and the laser beam so that higher intensities are reflected from the coating and lower intensities are transmitted.

Kang et al. [84] investigated novel production method to create light guide panels through laser marking technique. Effective variables were investigated for producing LGP by laser and DOE for achieving higher levels for the factors. Power, scan rate, line-to-gap ratio, and number of lines were the four main factors that were chosen in order to create a light guide panel with high brightness and uniformity. A web-based design tool was created to create light guide panel designs across a network, and it helped the designer to create a number of prototype patterns. Each specimen's brightness was measured using Topcon-BM7 on an area measuring 100 mm by 100 mm. The highest uniformity and brightness were obtained at 40 W, 30 mm/s with a 100:50 ratio. The most significant influences on brightness and uniformity were the number of lines and the ratio of line gap. The laser machined BLU produced a luminance of 3523  $\text{cd}/\text{cm}^2$  with uniformity of 92% after the Taguchi method was used to determine the optimal amounts of each parameter.

## 1.9 Research Gap

Fiber laser marking is a well-established and widely used technology in various industries due to its precision, efficiency, and versatility. However, like any technology, it continues to evolve, and there are several research gaps and opportunities for improvement. These gaps may vary depending on the specific application or industry focus. Below are some key research gaps in fiber laser marking:

- i. Research is needed to improve marking quality on challenging materials like composites, ceramics, and emerging alloys used in aerospace and electronics.
- ii. Investigations into how to effectively mark or code multi-layered materials without damaging underlying layers.
- iii. Optimizing laser systems to achieve higher marking quality with reduced power consumption.
- iv. Minimizing HAZ to prevent material degradation, especially in sensitive applications like medical implants or electronics.
- v. Enhancing the ability to mark on 3D or curved surfaces without distortion.
- vi. Ensuring marks maintain integrity in harsh environments (e.g., marine or industrial settings).
- vii. Improving the ability to mark high-contrast, readable codes on very small surfaces for micro and nanotechnologies.
- viii. Research into embedding QR codes or barcodes with improved scan ability and integration with IoT systems.
- ix. Enhancing fiber laser marking systems to be seamlessly integrated into robotic arms or automated assembly lines for high-speed manufacturing.
- x. Exploring how laser marking can be tailored for sensitive applications like marking biodegradable implants or creating micro-patterns for drug delivery systems.
- xi. Investigating the potential health impacts of fumes or debris generated and to search for remedial action during the marking process, particularly for high-power lasers.

## 1.10 Objectives and Scope of the Present Research Work

Fiber laser marking involves using a fiber-optic laser source to mark workpiece surface. It is widely employed in various industries for its high precision, speed, and versatility etc. Prior scholars have conducted some investigations on the line marking characteristics of

various materials using various laser types and the change of process factors on materials such as metals, ceramics etc. But they have not focussed on analysis of image quality with lower possible time to mark the surface. Infact, there hasn't been enough research done on surface and line laser marking of engineering materials like PMMA, Ti6Al4V and Stainless steel 304. The current study projects the analysis of line as well as surface laser marked image quality characteristic using fiber laser. The influences of accompanied process variables on marking characteristics were also further optimised for optimum value of responses undertaken for marking engineering materials. Within the constraints of the available resources and feasibility, the current research work's aims have been divided into the following modules:

- i. To carry out basic experiments on fiber laser marking operation for selecting the range of process variables to mark various geometrical shapes on different engineering materials.
- ii. To investigate the influences of laser marking process variables such as laser irradiation, pulse rate, assist gas, scan rate on marking characteristics such as mark intensity, width of laser marked surface and geometrical features on different engineering materials.
- iii. To produce various geometrical shapes such as circular, triangular, rectangular, elliptical, pentagonal and hexagonal on different engineering materials by laser marking process.
- iv. To mark various geometrical shapes on engineering materials such as SS 304, Ti6Al4V, and PMMA at minimum possible time with better marking characteristics.
- v. To carryout optimal analysis of fiber laser marking characteristics for producing marks of various geometrical shapes.

In order to get better quality marking characteristics, the current research work comprises a thorough examination using pulsed fiber laser marking on diverse engineering materials. Also, the current study will explore potential future research topics with additional surface features as well as new research areas in the field of laser marking on advanced engineering materials.

## **2. MATERIALS AND METHODS**

The section deals with selection of materials and the methods employed in executing laser marking operation on engineering materials. The solid-state CNC pulsed diode pump fiber which is utilised for laser marking purposes has tremendous potential for performing different operations on different material. The detailed of which is shown in the following sub section

### **2.1 Experimentation**

The analysis has been carried out for the generation of complex geometrical shapes such as circle, ellipse, triangle, square, hexagonal and pentagonal using fiber laser and their quality characteristics were analysed for the generation of better-quality laser marked surface. The work executed had a promising role in organisation as a part of product branding and also the work is innovative as any logos, figures, alphabets can be marked with better marked features.

### **2.2 Materials used as work piece for Laser Marking**

In the present study three materials such as PMMA, Ti6Al4V, and SS 304 were used for executing laser marking operation for the generation of better-quality laser marked surfaces. The materials have wide application in engineering and biomedical fields and executing good quality laser marking operation may find application in an organisation for product branding. A brief discussion about materials is discussed below:

#### **2.2.1 Stainless steel 304**

Stainless steel 304 falls under the category of high alloys steel which is comprised of high chromium austenitic stainless steels. The addition of chromium improves general corrosion and pitting resistance. It also offers good mechanical properties at elevated temperature. SS 304 resists atmospheric corrosion, as well as, moderately oxidizing and reducing

environments. The alloy also has excellent resistance to intergranular corrosion along with high strength and toughness at cryogenic temperatures. It is also used for biomedical applications due to its mechanical properties, biocompatibility, and corrosion resistance.

Table 2.1 Composition of Stainless Steel 304

Element	Weight %	Atomic %
Mg	2.26	4.91
Si	2.11	3.96
Cr	17.33	17.57
Fe	70.03	66.13
Ni	8.27	7.43

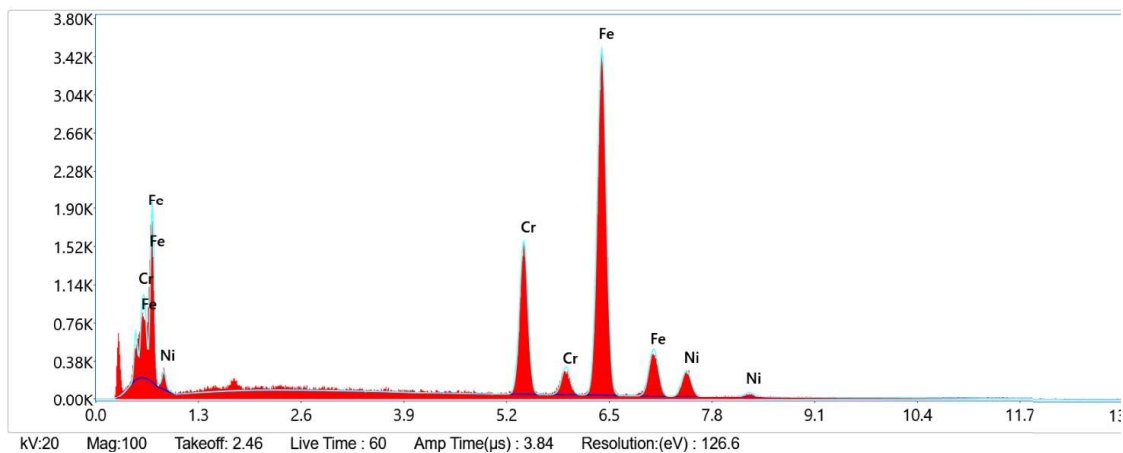


Fig.2.1 EDX analysis of Stainless steel 304

### 2.2.2 Titanium Alloy-Ti-6Al-4V

Ti6Al4V and Ti5Al2.5Sn are the two primary titanium alloys that are commonly utilised in a variety of manufacturing and biomedical industries. But Ti6Al4V alloy holds a larger share of the titanium market. The titanium industry is expanding quickly, due to metal's high specific strength and resistance to corrosion. Titanium alloys, which have a density of roughly 55% of steel, are frequently utilised for heavily loaded aerospace components that operate at low to moderately raised temperatures such as airframe and jet engine components. There are two crystallographic types of titanium. The alpha ( $\alpha$ ) phase is the crystal structure of hexagonal close-packed (hcp) titanium, which is economically pure and unalloyed at room temperature. This structure changes into the beta ( $\beta$ ) phase, a body-centered cubic (BCC) structure, around 883 °C. The compositions of alpha and beta alloys allow for a mixing of  $\alpha$  and  $\beta$  phases, with between 10% and 50% of the  $\beta$  phase present at

ambient temperature. The most common form of  $\alpha + \beta$  alloy is Ti-6Al-4V which have good formability and mainly employed in aerospace, automotive and bio-medical industries.

Table 2.2 Chemical compositions of Ti6Al4V

Elements	Al	V	Ti	Alloying element
Composition	5.55%	3.95 %	89%	Rest

Table 2.3 Properties of Ti6Al4V

Properties	Values
Density	4.43 g/cc
Tensile Strength (UTS)	895–930 MPa
Yield Strength	825–869 MPa
Young's Modulus	110–114 GPa
Elongation	6-10 %
Thermal Conductivity	6.7 W/m-K
Melting Point	1604 - 1660 °C

### 2.2.3 Polymethyl Methacrylate (PMMA)

PMMA is a rigid thermoplastic which comprises of a chemical combination of a vast number of monomer molecules and possessed superior mechanical, chemical, and electrical properties. At present, with the advancement of a host of polymer materials with their superior properties and cost-effectiveness, the entire micro-fluidic marketplace has shifted towards the micro-fabrication of polymer materials instead of glass as well as silicon. Among the various polymer materials, thermoplastic polymers have gained popularity in the domain of microfluidic devices due to robust elasticity and melting by thermal energy over other polymers and plastics. PMMA is biocompatible since it provides excellent resistance to temperatures, chemical reactions, and human tissue, etc. Due to which, it is used in many other applications such as windows, dentures, bone implants, aquariums, and ice hockey rinks etc.

The various applications of PMMA include:

- (a) Biomedical applications, especially for drug delivery and cranioplasty.
- (b) It is also utilized in a composite for the construction of pneumatic actuators for micro-pumps.
- (c) It is also an excellent choice of material for the fabrication of chemical sensors.

Table 2.4 Properties of PMMA

Properties	Values
Density	1.17-1.20 g/cm <sup>3</sup>
Melting Point	160°C (320° F).
Specific Heat	1466 J/Kg K
Thermal Conductivity	0.167-0.25 W/m-k
Elongation	2-10 %
Thermal Expansion	72-162 ×10 <sup>-6</sup> /K

## 2.3 Details of CNC Pulsed Diode Pumped Fiber Laser Marking System

Laser marking is the most efficient and flexible process to mark on any material. From the details of the past literature, it is understood that organisation often use laser marking as a part of its identification. As fiber laser produces near infrared light at a wavelength of 1064 nm, it is more easily absorbed by a vast range of materials. The line width produced by fiber lasers is narrower due to which fine markings can be performed on the engineering materials. Pulsed fiber laser has the potential to mark text, logo and various geometric shapes on PMMA, SS304, and Ti6Al4V alloy. Apart from that, it produces high peak power which can be employed in performing various operation such as drilling, cutting, grooving etc. Besides, fiber lasers have widespread applications in vast areas of automotive, aerospace, high power applications, etc.

Multi diodes pumped CNC based Ytterbium (Yb<sup>3+</sup>) doped 50W fiber laser having a wavelength of 1064 nm with a TEM<sub>00</sub> mode of operation, made by M/S Sahajanand Laser Technology Limited (Model: SCRIBO SLF 175) is utilized for laser marking operations. The schematic view of the fiber laser system is shown in Fig. 2.2.

The fiber laser system consists of (a) laser generation unit; (b) fiber laser delivery system; and (c) assist air supply unit. The laser generation unit further consists of (i) optical fiber; (ii) silicate glass; (c) rare earth doped elements; (iv) fiber Bragg gratings; (v) laser diodes; (vi) fiber couplers; (vii) isolators; and (viii) fiber coupled acousto-optic modulator (AOM). Under fiber laser delivery system, (i) collimator; (ii) beam bender; and (iii) beam delivery unit are the subsystems. Besides, assist air supply unit, as well as a CNC controller unit for



X-Y-Z axis, are also integral parts of the fiber laser system. The working table transverses in the X-Y direction for the present system. The maximum attainable speed is limited to 35 mm/sec. The specifications of the CNC pulsed fiber laser beam machining system are given in table 2.5.

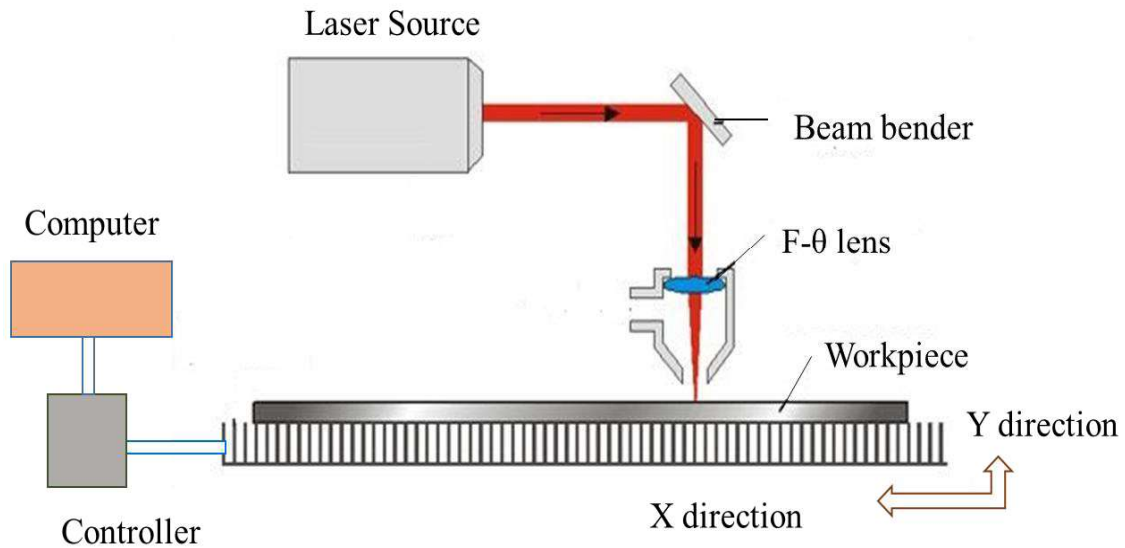


Fig.2.2 Schematic view of diode pumped fiber laser marking system

**Table 2.5** Specification of Laser Marking Machine

Laser type	Diode Pumped Pulsed Fiber Laser
Mean Power	50 W
Max. Apex Power	7.5 kW (approx.)
Pulse rate	50-120 kHz
Wavelength	1064 nm
Operation mode	Pulsed mode
Laser pulse width	120 ns
Focused spot Diameter	21μm

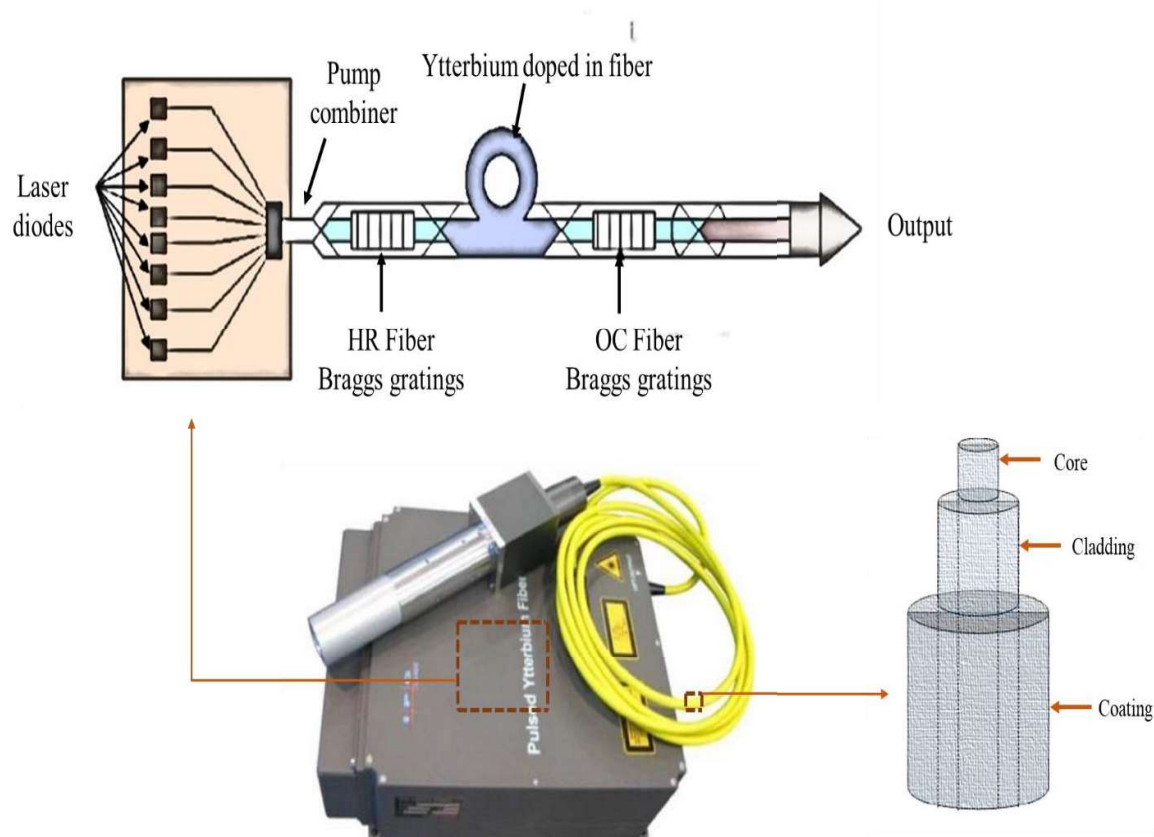
### 2.3.1 PULSED Nd: YAG LASER GENERATION UNIT

The fiber laser generation unit consists of a total of eight elements, i.e., (i) optical fiber; (ii) silicate glass; (c) rare earth doped elements; (iv) fiber Bragg gratings; (v) laser diodes; (vi) fiber couplers; (vii) isolators; and (viii) fiber coupled acousto-optic modulator. A

photographic view of a fiber laser generation unit is shown in Fig. 2.3. The details description is given hereunder.

### 2.3.1.1 Optical Fiber

The primary constituent of a fiber laser is an optical fiber. An optical fiber made of silicate glass is shown in Fig. 2.3. The core of the fiber, as well as the cladding, is made of with silicate glass. The detail of silicate glass is discussed in the next sub topic. Doping in the core of the fiber is essential to raise the core's refractive index. Germanium is added for doping of the fiber core. On the contrary, if fluorine and boron are used as dopants, the refractive index of silicate glass decreases. As the present fiber laser system operates in 1064 nm wavelength, the intrinsic loss within the fiber (dB/km) is high. The fiber laser is elongated to a few meters long to reduce the loss. In the present system, the length of the optical fiber is 3 meters. For protecting the glass surface, a layer of acrylic coating with a higher refractive index is used. The coating used in fiber further prohibits the propagation of unwanted light in the cladding glass.



2.3 Photographic view of fiber laser generation unit

### 2.3.1.2 Silicate Glass

Silicate glass is the most widely used as optical fiber in several low powers to high power fiber laser applications. Unlike crystals, glass molecules are disordered but are rigidly bound. The structure of the glass is bonded with several matrix molecules such as silicate ( $\text{SiO}_4$ )<sup>4-</sup> or phosphate ( $\text{PO}_4$ )<sup>3-</sup> glasses respectively. In addition to this, a wide range of optical transparency, allows the silicate glass to achieve the lowest loss of optical communication. Silicate glass is mechanically robust, demonstrating remarkable tolerance to bending. Silicate glass also demonstrates a high degree of chemical resistance.

### 2.3.1.3 Rare Earth Doped Elements

Fiber amplifiers are doped with laser-active rare earth ions in the fiber core to absorb the light. These doped earth elements amplify the light via stimulated emission. Some of the examples of rare earth ions are ytterbium ( $\text{Yb}^{3+}$ ), erbium ( $\text{Er}^{3+}$ ), thulium ( $\text{Tm}^{3+}$ ), and neodymium ( $\text{Nd}^{3+}$ ). Incorporation of rare earth ions inside the fiber core requires disruption of the regular glass network. Some of the critical factors leading to the characterization of rare earth doped fibers are: (a) passive optical fiber; (b) active mode area; (c) numerical aperture; (d) cut off length; (e) bend losses; (f) rare earth doping concentration; (g) wavelength-dependent effective absorption and emission cross sections and (h) the speed of the energy transfer. In the present system, fiber laser boosts of ytterbium-doped rare earth ions in the multimode regime of the fiber.  $\text{Yb}^{3+}$  ions have recently become the dopant of choice for high-power fiber lasers. As a laser-active ion in solids, such as crystals and glasses,  $\text{Yb}^{3+}$  offers several advantages compared with commonly used  $\text{Nd}^{3+}$  ions [70]. These advantages include:

- (i) A longer upper-state lifetime.
- (ii)  $\text{Yb}^{3+}$  doped laser-active glasses have broad and robust absorption bands near 915 and 976 nm.
- (iii) A small quantum defect which results in lower thermal load per unit of pump power.
- (iv) An absence of the excited state absorption and up-conversion losses.
- (v) Room-temperature excited state lifetime is approximately 1 ms.

### 2.3.1.4 Fiber Bragg Gratings (FBGs)

Fiber Bragg gratings (FBGs) are critical elements in enabling the development and commercial success of fiber lasers. Most fiber Bragg gratings are mainly used in single-mode fibers, and the physical modelling of FBGs are often relatively simple. The working principle of FBGs

same as dielectric mirrors. At each periodic refraction of FBGs, a small amount of light is reflected. FBGs are found to be highly stable at room temperature. For utilizing FBGs in fiber lasers, the wavelength and bandwidth required are in the region of 0.1–1 nm and centre wavelength control  $\pm 0.5$  nm, respectively.

#### **2.3.1.5 Laser Diodes**

Laser diodes are utilized in fiber lasers for pumping of the photons. In the present system, to generate 50W of average laser irradiation, eight numbers of diodes are utilized for optical pumping. Optical pump sources based on single-emitters are typically coupled into a 105/125 fiber, i.e., 105 $\mu$ m of diameter core along with a 125  $\mu$ m diameter of silica glass cladding. Depending on the number of diodes, the average laser irradiation of the laser is varied, i.e., the higher number of diodes, higher the average power. Typical commercially available multi-emitter pumps consist of 3, 5, 7, or more laser diodes combined into a single 105/125 delivery fiber and delivering 60–140 W laser output.

#### **2.3.1.6 Fiber Couplers**

Fiber couplers are the essential elements of a fiber laser. The delivery fibers are limited due to the industry standard fibers have either 105 $\mu$ m or 200 $\mu$ m of core diameters in most of the cases. Fiber couplers combine one or more input fibers and also several output fibers depending on power distribution within the fiber laser.

#### **2.3.1.7 Fiber Laser Isolators**

Inter-stage optical isolation is required during multiple stages of amplification with the aid of a fiber amplifier. Fiber-coupled isolators are the cost-effective components which prevent back reflections by only allowing light to travel in one direction. Fiber to free space isolators, for output from a master oscillator power amplifier (MOPA) system, is commercially available at 50 W. Currently, the limit for commercially available high-power isolators occurs around 50 W in the case of fiber laser and are commonly utilized in the nanosecond pulsed fiber laser.

#### **2.3.1.8 Fiber Coupled Acousto-Optic Modulator**

Pulsed fiber lasers with nanosecond pulse durations and mill joule pulse energy have many applications in materials processing. Q-switching is generally used to generate optical pulses in an oscillator, which are then amplified in MOPA arrangement to boost their power further. The Q switch function is typically implemented by an acoustic-optic modulator (AOM), which can turn off a beam by deflecting it in a different direction. The beam is deflected by a traveling

acoustic wave, which is controlled electrically by radio frequency (RF) signal typically at the few tens to few hundreds of MHz. AOM takes to turn a beam on or off is typically 5 to 100 ns, roughly limited by the transit time of the acoustic wave across the beam. When faster control is necessary, electro-optic modulators (EOMs) are generally used. Typically, a commercially available fiber coupled AOM Q-switch is limited to 1 W of average power handling and peak power handling of 30 kW.

### **2.3.2 Fiber Laser Delivery System**

The fiber laser delivery system consists of a collimator, beam bender, beam delivery unit, and focusing lens. The details of each aforesaid unit are discussed in the following subsections.

#### **2.3.2.1 Collimator**

The light output from an optical fibre is converted into a free-space collimated beam using a collimator, where the fibre end is securely placed at a distance from the lens that is roughly equal to the focal length. Because different fibre optic collimators produce varying collimated beam sizes, the focal length can vary as well. For example, larger collimated beams require larger diameters as well as longer lengths. For multimode fiber laser systems, the collimated beam size depends on the launch conditions as well as bending of the fiber. The photographic view of the collimators is shown in Fig. 2.4. In the present set up, the beam diameter at the collimator end is 9 mm.

#### **2.3.2.2 Beam Bender**

In order to ensure that the laser is perpendicular to the focus lens, a beam bender with 100% reflectivity is positioned after the collimator at a 45° angle with the horizontal plane. A charge coupled device camera (CCD), which is additionally connected to a CCTV, is positioned at the top of the beam bender. In Fig. 2.5, the photographic view of a beam bender is shown.

#### **2.3.2.3 Beam Delivery Unit and Focusing Lens**

The focusing lens, which has a 71 mm diameter F- $\theta$  lens shielded from dust and other contaminants by a nozzle, is where the laser ultimately propagates. The F- $\theta$  lens is commonly used in laser marking, engraving, and cutting systems. The fibre laser beam has a spot diameter of 21  $\mu\text{m}$ . Precise and proper alignment of the laser beam falling on the focusing lens's surface is required. The laser beam will have less energy and poorer

micromachining efficiency if the lens's centre and the beam's centre do not line up. This is because the beam that passes through the lens will not be linear. There are two units that are employed for focusing: CCD and CCTV cameras.

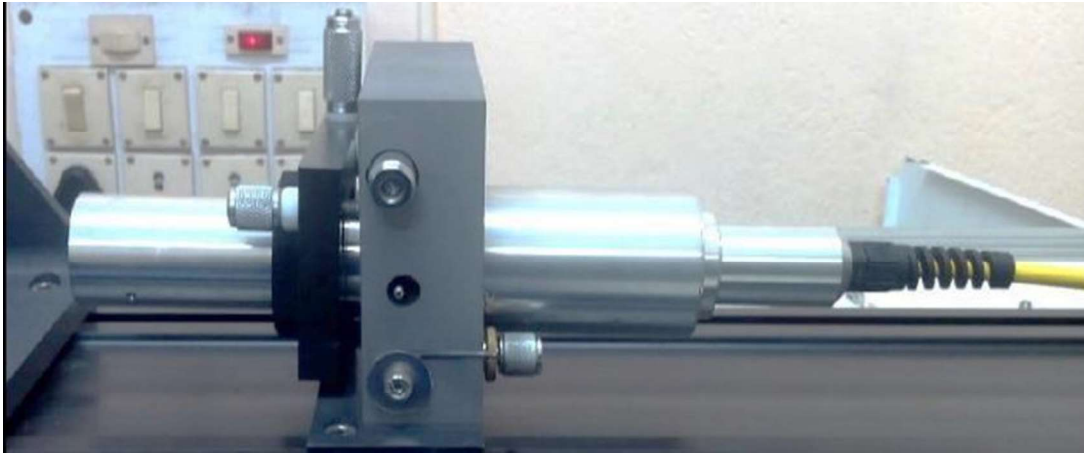


Fig.2.4 Photographic view of the collimator

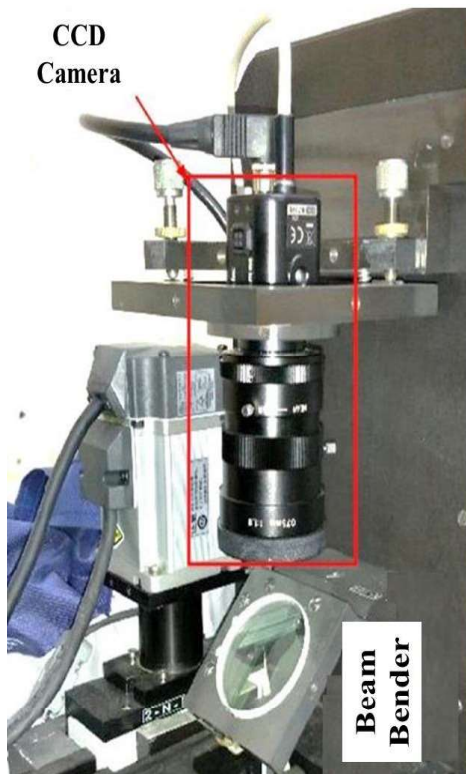


Fig.2.5 Photographic view of beam bender

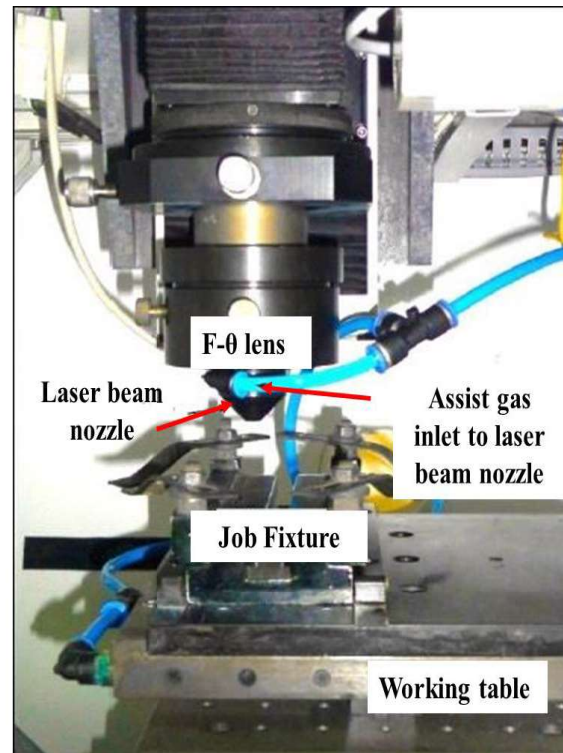


Fig.2.6 Photographic view of beam delivery unit and working table

The CCD camera is positioned at the top of the laser head to take pictures while the laser micro-machining is being done. In addition, the beam needs to be directed towards the surface in order to achieve the best results for micro-machining. The concentrated beam's location on the workpiece is adjusted by the CCTV. This apparatus is linked to the CCD camera in order to acquire a precise laser beam focusing state. The laser beam is appropriately focused for the proper utilization of the energy of the laser beam on the workpiece surface. Therefore, the laser beam's focal point position needs to be appropriately adjusted. In the experimental setup, a CNC controlled arrangement is offered to efficiently modify the focal point of the lens position through the Z axis. Fig. 2.6 represents the photographic view of the F- $\theta$  lens.

### 2.3.3 Assist Air Supply Unit

Depending on the micro-machining process and material selection, a co-axial nozzle coupled to the beam delivery system can supply inert gases like nitrogen, argon, helium, etc. in addition to compressed air. To partially counteract the re-solidification of the molten material from the micro-machining zone, the accompanying gas jet flow helps remove the molten material from the ablated surface. The supply line needs to go via a moisture separator and be connected to a pressure regulating valve if dry compressed air flow is needed into the laser micro-machining zone. A vacuum job fixture in the lab setup can support a workpiece up to 1 mm thick when the compressed gas pressure is 6 kgf/cm<sup>2</sup>. The air compressor is additionally equipped with a moisture separation machine to eliminate any moisture from the gas. Fig. 2.7 shows the photographic view of an air compressor with a moisture separator.

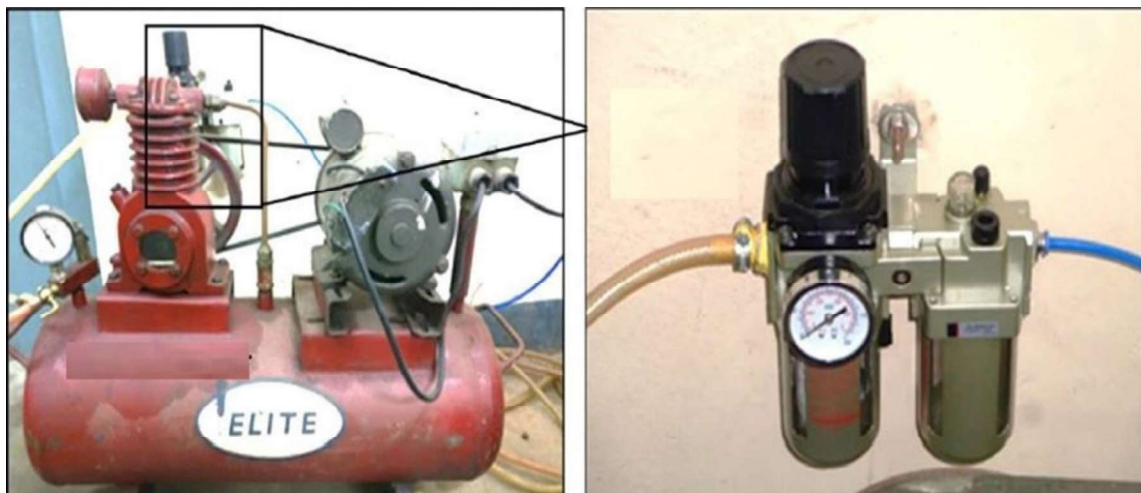


Figure 2.7 Photographic view of an air compressor with moisture separator.

### **2.3.4 CNC Controller for X–Y–Z Movement**

The movement of the laser nozzle along the Z axis and the worktable along the X-Y axis are both managed by a CNC controller unit. Each axis has a servo motor attached to it, which is also connected to the servo interfacing unit. The computer system (interface software: I mark plus) that controls the X-Y worktable's axis motions is coupled to this servo controller. In the event that the X, Y, or Z axes need to move, the computer system instructs the servo interfacing unit, which then transmits the command for the corresponding servo motor movement in the needed directions. Depending on the uses of the fibre laser systems, the axis of the system can be controlled by a galvanometer-type motor system or a CNC-based motor system. It is best to use a galvanometer-type system for marking and scribing applications. A CNC-based system is widely known for its ability to perform cutting, drilling, and other micro-machining tasks, in contrast to the system previously mentioned. The software interfaced with CNC laser system has provisions to coordinate the operation of the laser beam supply, motion control of workstation, etc. In the present system, I mark, gyro and Q Saw software are utilized for various micro-machining operations, i.e., micro-cutting, microdrilling, marking, surface texturing, etc. I mark software is mainly utilized for CNC programming, whereas the other two software described above is for setting the depth of cut and cutting angle.

## **2.4 Strategy for Laser marking**

The section deals with the methods and laser set up process variables which have been employed for generating complex geometrical shapes such as square, triangle, ellipse, hexagon and pentagon, circle. The detailed of which are listed below:

The process of laser marking operation needs the application of either AUTOCAD or the development of CNC codes for the specific movement of the laser beam in the desired direction. The CNC-controlled fiber laser system is managed by I-mark software (version 8.4.1). The generated CNC code or the image drawn with the help of AUTOCAD when feed to the software developed the image on the work screen of the software. The fault code, if any, in the CNC code will be displayed by the red mark which makes the user understand the defect code in the developed CNC code and can be altered or changed accordingly for correction.



The movement of work table displayed on the CCTV (closed circuit television) help to understand the correctness of the code generated. In general, laser marking operation performed on the material surface is of two ways of i.e. by material removal or modification of surface. The marked image obtained by laser marking operation were captured in optical microscope using lens of 5 X magnification factor operated by LEICA software or OLYMPUS STM 6 for measuring the image width and then processed by the MATLAB software for image quality analysis using the formula given in equation 2.1 [23].

$$\text{Mark Intensity} = \frac{g_{\text{unmarked}} - g_{\text{marked}}}{g_{\text{white}} - g_{\text{black}}} \dots\dots\dots \text{Eq.2.1}$$

where c is marked intensity value,  $g_{\text{unmarked}}$  is the calculated gray value of unmarked surface,  $g_{\text{marked}}$  is the calculated gray value of marked surface,  $g_{\text{white}}$  is the gray value of white surface taken as 255 ( standard),  $g_{\text{black}}$  is the gray value of black surface taken as 0 (standard).

Mark intensity is the measure of illumination of marked surface and unmarked surface when exposed to light. It is computed in terms of grey value of marked and unmarked portion of marked surface. Grey value means greyscale image value which denotes the value of each pixel depending on the light intensity information. Such images typically display from the black (marked portion) to the brightest white (unmarked portion). It was computed for lased marked and unmarked region through analysis using MATLAB software whereas the standard grey value of white and black surface is computed as 255 and 0 respectively. The value thus obtained were computed in equation 2.1 for the valuation of mark intensity of laser marked surface

The software MATLAB is useful to analyse the image quality in terms of pixel value of certain portion of selected image. Engineers and scientists can use the programming environment MATLAB to analyse data, develop algorithms, and build models for use in the workplace and in the classroom. Deep learning and machine learning, communications and signal processing, image and video processing, test and measurement, control systems, computational finance, and computational biology are just a few of its applications. The image quality analysis through MATLAB displays image data in terms of array generally  $m * n$  grid of pixels where m is the number of rows and n is the number of columns. The individual pixel value was culminated into grey value of laser marked surface for the

analysis of mark intensity value of the region of laser marked surface. Higher the value of mark intensity, better will be the quality of image.

Following are the line diagram of some geometrical shapes which had been marked and their line diagram are shown below:

The generation of any geometric laser marked surface in CNC pulsed diode pumped fiber laser consists of multiple laser spot which resulted in the overlap of laser spot in both horizontal and vertical direction which had a considerable effects on the marking characteristics. The transverse feed selected also represents the region overlap by laser spot in performing the laser marking operation.

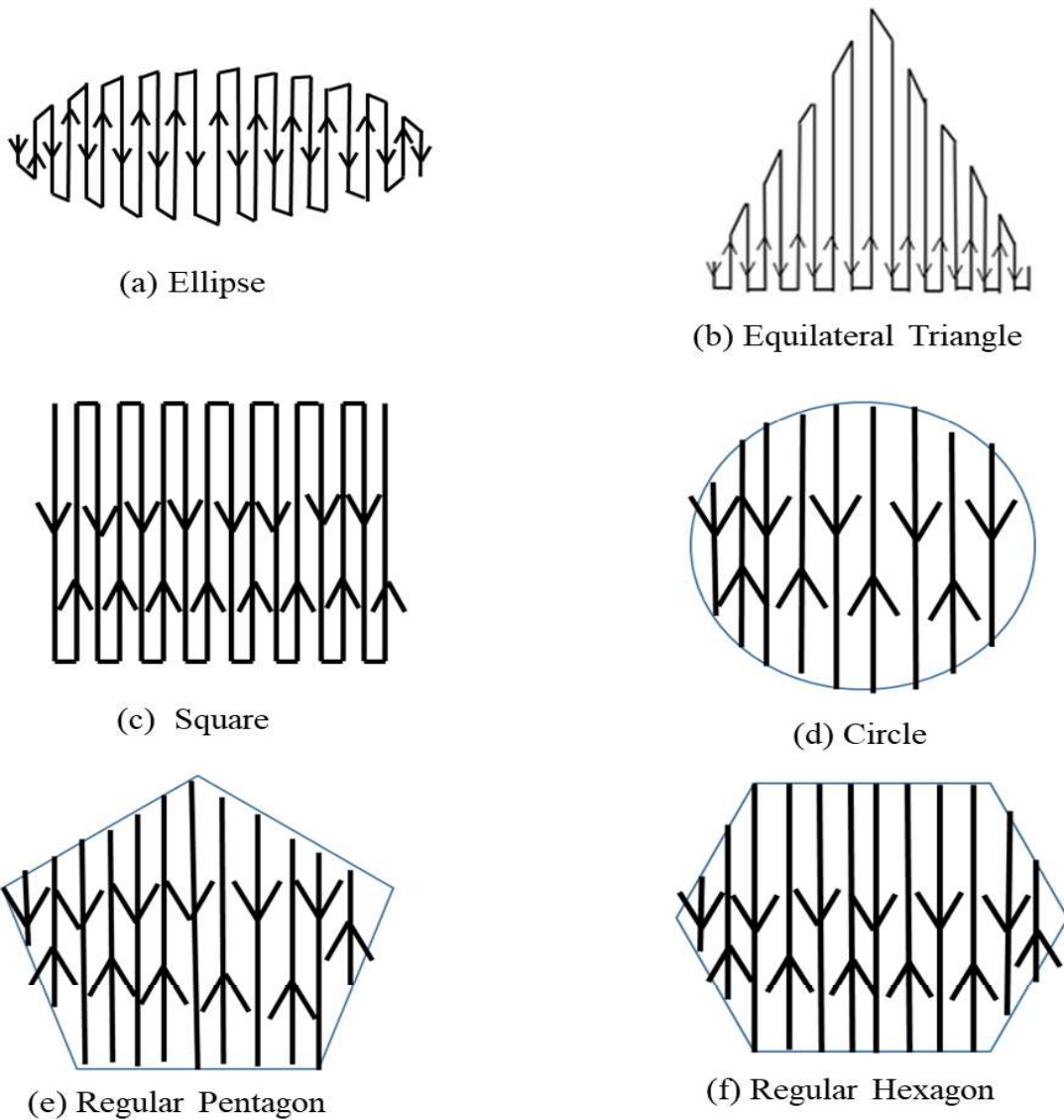


Fig.2.8 Line diagram for the generation of complex geometrical shapes

The overlap of laser spot obtained are generally of two types i.e. transverse overlap and lateral overlap which were calculated by the formula as follows [48] :

$$\text{Transverse overlap} = 1 - \frac{D_t}{D} \quad \dots \text{Eqn.2.2}$$

$$\text{Lateral overlap} = 1 - \frac{v}{f \times D} \quad \dots \text{Eqn.2.3}$$

Where D and  $D_t$  were the laser beam diameter and transverse feed of laser beam, v represent scan rate and f represents pulse rate.

Generally to generate any specific geometric shape, various process variables such as laser irradiation, duty cycle, pulse rate, number of passes, and scan rate are used. They were allowed to vary in specific interval in order to generate good quality laser marked surface. The detail of each process variables are given below:

(i) **Laser Irradiation:** Laser irradiation indicates the instantaneous power that is irradiated on a given workpiece for melting and evaporation of the molten material. It is usually the average power of the system expressed in watt (W).

(ii) **Duty Cycle:** The time duration of the laser pulse is combined with both the rise and fall. The pulse length is generally described as the width of the curve at half height. Duty cycle is considered as the percentage of the cycle time.

(iii) **Pulse Rate:** Pulse rate is the number of pulses of laser per second. Higher the pulse rate lower is the peak power of laser beam. It is expressed in kilohertz (kHz).

(iv) **Number of Passes:** The number of passes is a unit less parameter which defines how many times the laser beam will move to and fro in a specific length for a specific geometrical feature.

(v) **Scan Rate:** Scan rate is defined by the speed at which working table transverses at X and Y directions. The unit is given at mm/sec. Scan Speed is controlled by a CNC controller system for each of the axis.

The detailed analysis regarding the influences of process variables on laser marked surface are discussed in consequent chapters.

## 2.5 Fundamental Working Principles of CNC Pulsed Fiber Laser Marking Techniques Process

The fundamental working principles of CNC pulsed fiber laser marking involve the precise application of high-energy laser pulses to modify the surface of a material. This process combines laser technology with computer numerical control (CNC) for accurate and programmable marking. The process can be broken down into the following steps:

i. **Design Creation:**

- A marking design (text, patterns, barcodes, etc.) is created using CAD software.
- The design is converted into a G-code, which the CNC system uses to control the laser movement.

ii. **Material Placement:**

- The workpiece is securely mounted on the marking platform.

iii. **Beam Generation:**

- The fiber laser source generates high-intensity laser pulses.
- The pulsed nature of the laser ensures controlled energy delivery, avoiding overheating.

iv. **Beam Focusing and Steering:**

- The laser beam is aligned by collimators, directed by galvanometer mirrors, and focused into a precise spot by focusing optics.
- The focused laser spot has an extremely high energy density.

v. **Material Interaction:** The laser beam interacts with the surface of the material based on the energy intensity and pulse duration:

- **Vaporization/Engraving:** High energy evaporates material, creating deep marks.
- **Melting:** Heat melts the material, forming shallow marks.
- **Oxidation/Annealing:** Heat causes surface oxidation, resulting in a color change without material removal.

A schematic diagram also shown regarding the process of laser marking operation in Fig.2.9

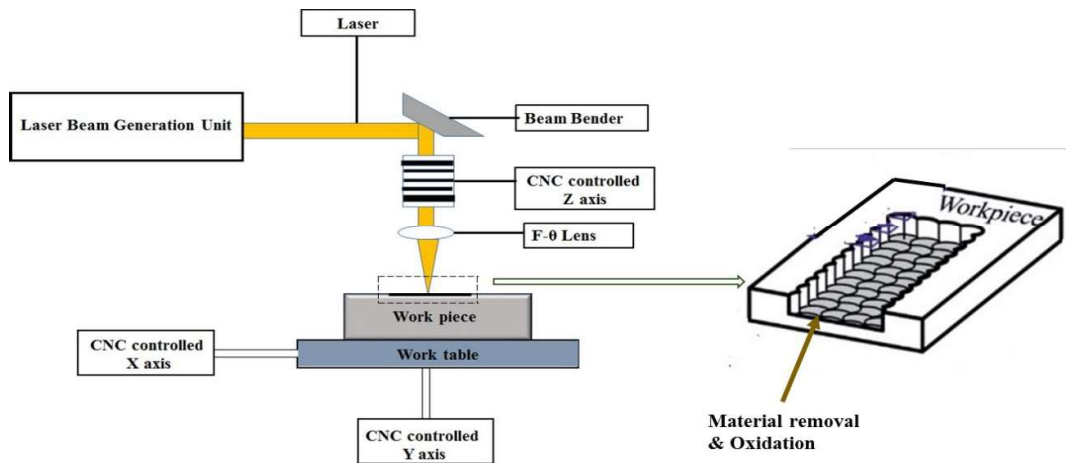


Fig.2.9 Schematic diagram of the working process of laser marking

## 2.6 Advancement of CNC Pulsed Diode Fiber Laser Marking Techniques in Comparison to Simple Laser Marking Process

The advancement of CNC pulsed diode fiber laser marking techniques compared to simple laser marking processes stems from innovations in precision, efficiency, material compatibility, and operational flexibility. Below is a comparison highlighting key advancements:

Sl. No.	Simple Laser Marking:	CNC Pulsed Diode Fiber Laser Marking
1.	It can lack precision, as they emit a continuous stream of energy, making it challenging to control depth and heat-affected zones	Utilizes advanced fiber laser technology with pulsed diode pumping which delivers short, high-energy bursts, enabling precise control over material interaction.
2.	Limited control over the laser's energy delivery, leading to inconsistent depth and potential thermal damage to surrounding areas	High precision achieved through CNC integration, allowing micron-level accuracy in marking patterns. Pulsed operation minimizes thermal effects, reducing deformation and discoloration in sensitive materials.
3.	Typically limited to specific materials.	Wide material compatibility, including metals, ceramics, polymers, and composites.
4.	Often manual or semi-automated, leading to slower processing speeds and less repeatability.	Faster marking speeds due to higher repetition rates and optimized energy delivery.

# Chapter 3

## 3. EXPERIMENTAL INVESTIGATION INTO FIBER LASER MARKING ON STAINLESS STEEL 304

Laser Marking on stainless steel 304 employed in biomedical applications to provide uniqueness of the product manufactured by the organisation. It is permanent and durable marking without undergoing thermal or chemical stress. The generation of good quality geometric shapes such as square, circle, ellipse, polygon and hexagon or a combination of the two or more geometric shapes resembles the generation of any logos as a part of product identity.

### 3.1 Experimental Planning for the analysis of marking characteristics of surface marking

The laser marking operation was carried out by using program of length 2 mm and width of 0.48 mm with transverse feed of  $8\mu\text{m}/\text{laser stroke}$  and then processed to I-Mark software for laser marking operation. The mark intensity calculated based on the transverse feed value of  $8\mu\text{m}/\text{laser stroke}$  and by varying the process variables was again recalculated by varying the transverse feed i.e. from  $8\mu\text{m}$  to  $2\mu\text{m}/\text{laser stroke}$  along with the change of process variables for the analysis of marking characteristics.

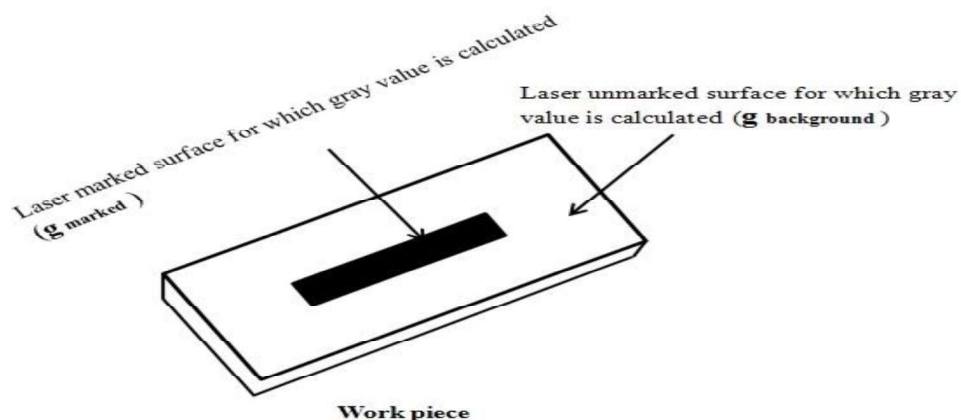


Fig.3.1 Schematic representation of laser marked and unmarked surface for the calculation of gray value

Fig.3.1 shows the schematic diagram of laser marked and unmarked surface. The area of which were used for the calculation of gray value which then placed in equation 2.1 for analysis of mark intensity (c) value.

Thus from equation 2.2 it is evident that transverse feed plays a significant role in case of transverse overlap. Decrease of transverse feed ( $D_t$ ) resulted in the increase of transverse overlap and vice versa. On the other hand from equation 2.3, it becomes evident that scan rate and pulse rate plays a significant role in lateral overlap. Increase of scan rate and decrease of pulse rate resulted in the decrease of lateral overlap factor and vice versa whereas laser beam diameter ( $D$ ) was fixed in both cases which is  $21\mu\text{m}$ . Upon analysis transverse feed in the range of  $2\text{--}14\ \mu\text{m/laser stroke}$ , transverse feed of  $8\ \mu\text{m/laser stroke}$  provides better result in terms of better marking characteristics and time. The transverse overlap yields a value of  $61.9\%$  at a transverse feed of  $8\ \mu\text{m/laser stroke}$ . The detailed analysis was discussed in section 3.3.

A schematic diagram has been shown in Fig.3.2 which comprises of transverse and lateral overlap region of laser spot along with the direction of laser scanning which was used for the generation of laser marked surface for better understanding of the process.

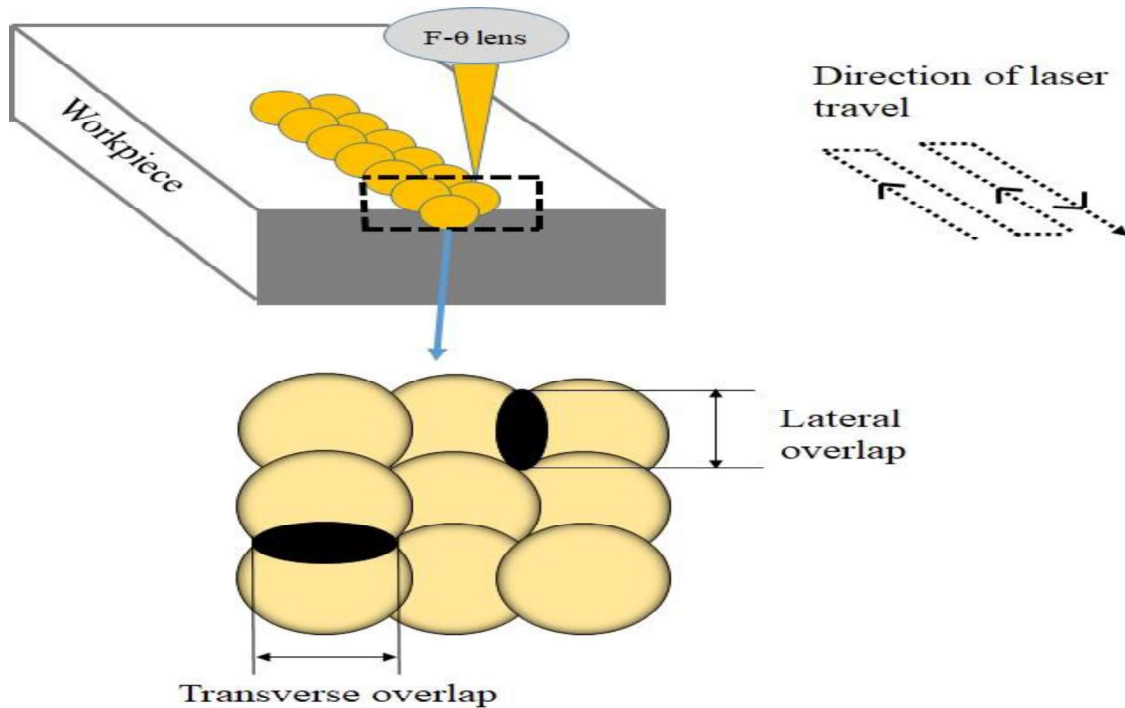


Fig.3.2 Schematic representation of associated terms and laser scanning direction related to laser marking

### **3.2 Results and Discussion on Laser Marking of Rectangular Shaped Surface**

The discussions include the impact of process variables such as laser irradiation, assist gas pressure, scan rate, transverse feed, and pulse rate on marked qualities such as mark intensity and marked width. The marked portion resulted by changing the variables each in turn gives an idea of process variables settings in order to get the better value of responses.

#### **3.2.1 Influences of Laser irradiation on Marking Characteristics on Stainless steel**

**304**

Fig.3.3 shows the variation of mark intensity with the variation of laser irradiation when process variables such as transverse feed (TF) of 8 $\mu$ m/laser stroke, scan rate (SS) of 35 mm/s, pulse rate (PF) of 120 kHz, duty cycle (DC) of 99 % were kept constant. Increased laser irradiation increases the oxidation phenomenon of the surface at the ambient condition with an increase of spattering of a pulsed laser. Due to this, the adjacent areas received heat and resulting in the change of colour from white to yellow. It was seen that better marking was seen at lower value of power especially at a power of 20 W with 1.18 minute duration of time when other process variables were held constant. Apart from that, the optical and visual appearance of laser marked surface at such high power seems to be inappropriate for further application in terms of quality as shown in Fig. 3.4.

Fig. 3.4 (a), (b), and (c) are the microscopic view of the laser marked surface at a laser irradiation of 50 W, 30 W, and 20 W using LEICA optical microscope with lens of 5 X magnification. Due to high laser energy at 50 W the adjoining areas gets heat which resulted in the increase of width and oxidation. The decrease of laser energy points to the decrease of the width of the laser-marked surface as shown in Fig. 3.4.(b) and (c). It was observed that the lower the laser irradiation, the lower will be the width and oxidation of the marked surface. Experimental studies suggest that laser irradiation of 20 W can be used for marking purposes since its width is closer to the width set via CNC software. The mark intensity value at a laser irradiation of 20 W is 0.80 which can be further investigated to improve its quality. Thereafter, the scan rate is allowed to vary from 35 mm/s to 7 mm/s which also shows a significant change in marking characteristics.



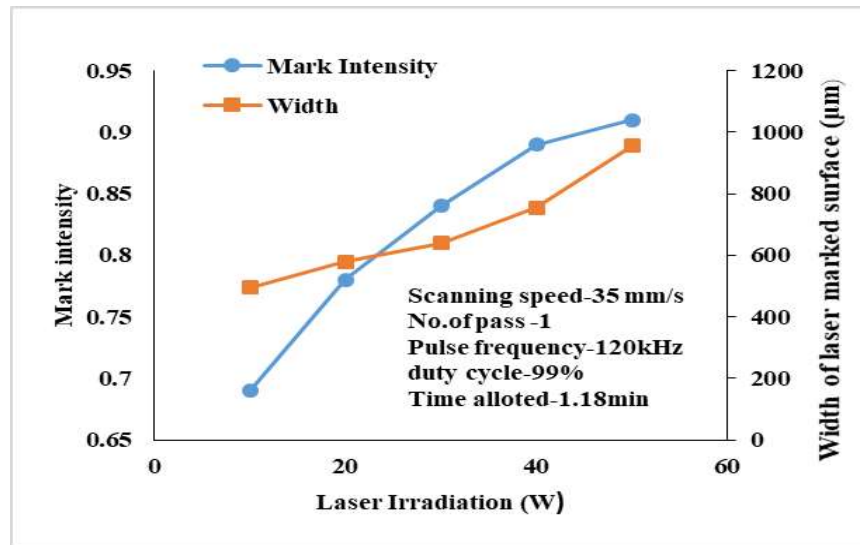


Fig.3.3 Influences of laser irradiation on Mark intensity

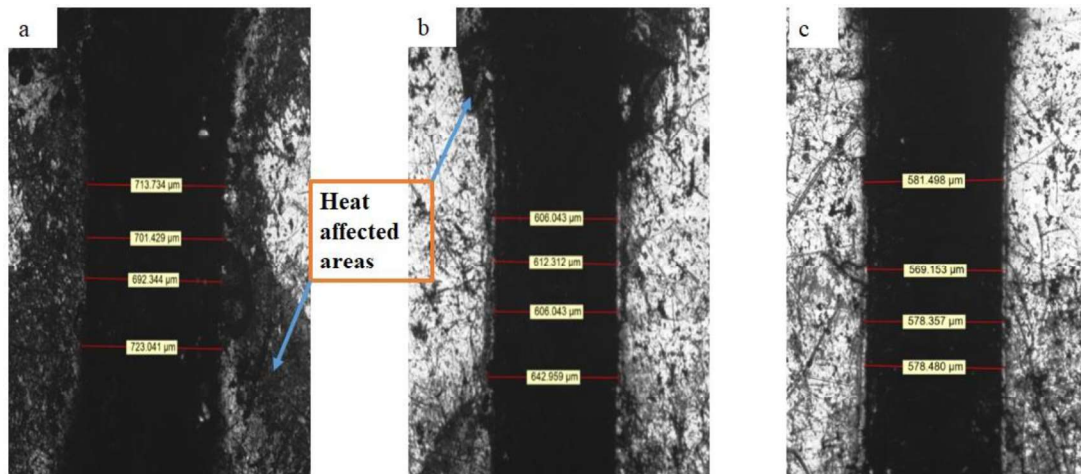


Fig.3.4 Microscopic view of laser marked surface at variant laser irradiation (a) 50 W (b) 30 W (c) 20 W

### 3.2.2 Influences of Assist gas pressure on Marking Characteristics on Stainless steel 304

Fig. 3.5 illustrates the change of laser mark intensity and width with laser irradiation with and without the application of assist gas pressure during laser marking operation when variables such as transverse feed (TF) of 8 μm/laser stroke, scan rate of 35mm/s, duty cycle of 99%, pulse rate of 120 kHz were kept constant. Experimental results showed that supply of assist gas at high pressure resulted in the increase of unwanted marking characteristics i.e., increase of mark width at assist gas pressure of 2.5 bar and 1.5 bar with simultaneous

decrease of gray value of laser marked surface when compared to laser marked surface without the supply of assist gas. Such distribution of heat is lowered when the assist gas pressure of 1 bar was applied which resulted in the decrease of mark width but on the other hand, it decreases the gray value of marked surface.

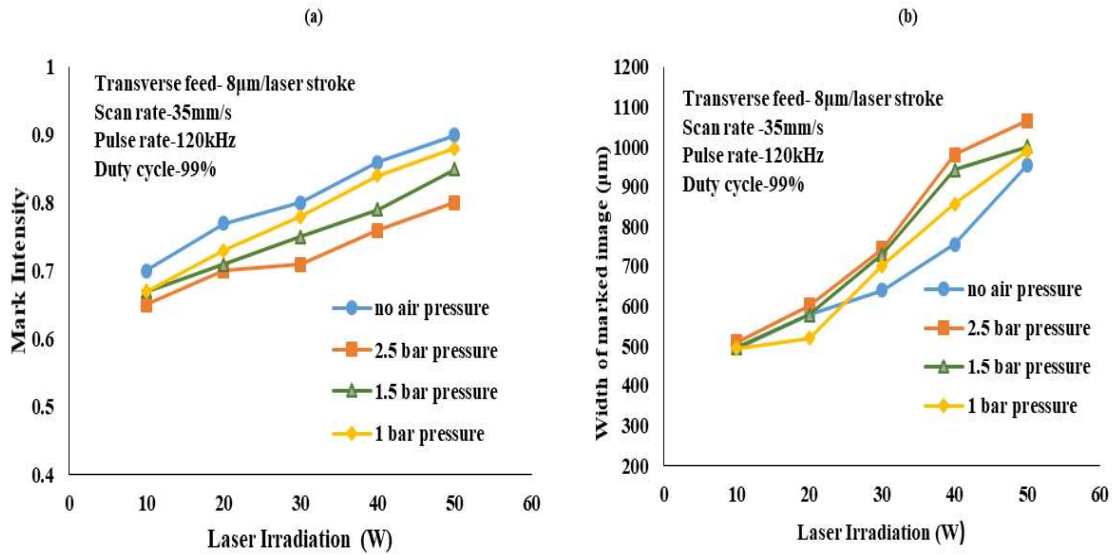


Fig. 3.5 Variation of (a) mark intensity (b) marked width with laser irradiation with and without the application of assists gas pressure

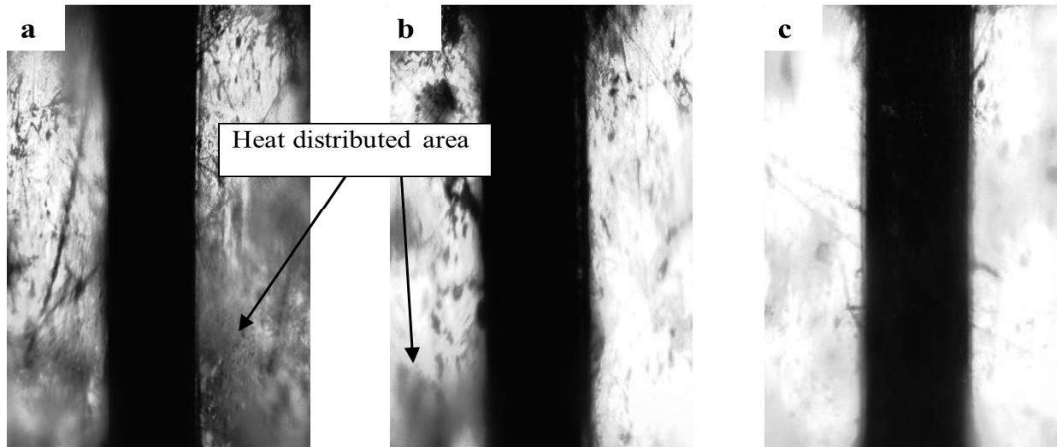


Fig. 3.6 Visual perspective of marked surface with the supply of assist gas pressure

Fig. 3.6 showed the visual perspective of marked surface when the assist gas was supplied and process variables such as transverse feed of 8 µm/laser stroke, pulse rate of 120 kHz, duty cycle of 99 % and scan rate of 35 mm/s were kept constant. Fig.(a), Fig.(b) and Fig.(c) of Fig. 3.6 are the photographic view of laser marked surface at 20 W laser irradiation and

at a pressure of 2.5 bar, 1.5 bar and 1 bar respectively. The supply of assist gas pressure marks the distribution of heat from the focused area. It resulted in the increase of width and poor surface finish as observed from Fig. 3.6.

After analysing the quality of laser marked surface laser irradiation of 20 W was kept fixed. Thereafter, attempts were made to identify the variety of marking characteristics with scan rate change without assist gas pressure supply.

### **3.2.3 Influences of Transverse feed on Marking Characteristics on Stainless steel 304**

Fig. 3.7 shows the variation of marking characteristics with the change of scan rate when process variables such as transverse feed of 8  $\mu\text{m}$ /laser stroke, laser irradiation of 20 W, pulse rate of 120 kHz, and duty cycle of 99% were kept constant. It was observed that the decreased scan rate resulted in the increase of mark intensity and width of laser marked surface. It is due to more time of heat interaction with the work piece surface which causes oxidation. Lower scan rate also increases the time of laser interaction for the same size of the surface to be marked. Studies revealed that better value of marking characteristics was observed at a scan rate of 21 mm/s both in terms of quality of marked surface and time duration of marking.

Fig. 3.8.(a), (b) and (c) are the microscopic view of laser scanned surface at a transverse feed of 8  $\mu\text{m}$ /laser stroke, laser irradiation of 20 W, pulse rate of 120 kHz and duty cycle of 99%. Lowered value of scan rate has a projection towards increase of unwanted marking width which happens due to the distribution of heat in the side areas as can be observed from Fig. 3.8. (b) and (c). Further studies were carried out at transverse feed of 6  $\mu\text{m}$ /laser stroke which can be observed in Fig. 3.9.

Fig. 3.9 shows the variation of marking characteristics with the change of scan rate when process variables such as transverse feed of 6  $\mu\text{m}$ / laser stroke, laser irradiation of 20 W, pulse rate of 120 kHz, and duty cycle of 99% were kept constant. It is observed that a decrease of transverse feed from 8 to 6  $\mu\text{m}$ / laser stroke increases the time duration from 1.18 minute to 1.44 minute upon using scan rate of 35 mm/s. In addition to, it also increases the mark intensity and width of laser marked image due to greater overlap of laser spot which provides better oxidation within and outside the desired marked area. Studies revealed that better value of marking characteristics was observed at a scan rate of 30 mm/s both in terms of quality of image and time requirement of marking of desired surface.

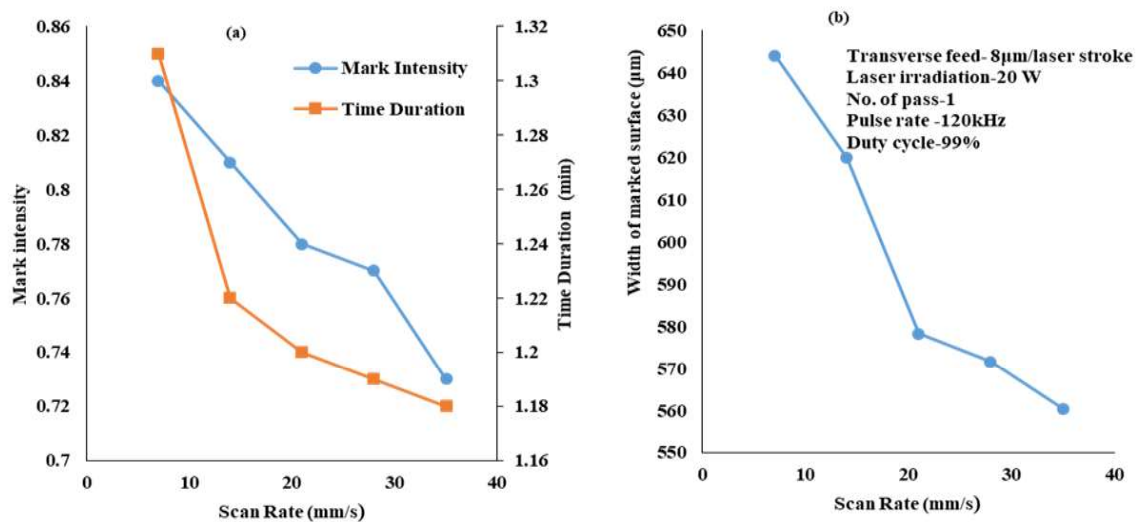


Fig. 3.7 Variation of marking characteristics (a) mark intensity and time requirement (b) width of mark with change of scan rate at transverse feed of 8 $\mu\text{m}$ /laser stroke

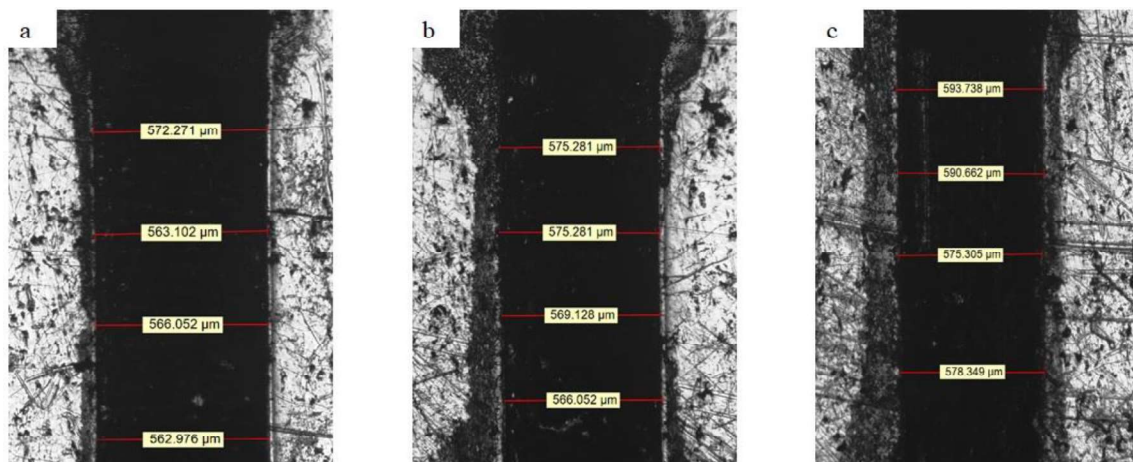


Fig. 3.8 Microscopic view of laser scanned surface with change of scan rate at transverse feed of 8 $\mu\text{m}$ /laser stroke (a) 35 mm/s (b) 21 mm/s (c) 7 mm/s

Fig. 3.10.(a), (b), and (c) are the microscopic view of the laser-scanned surface at a transverse feed of 6 $\mu\text{m}$ /laser stroke, laser irradiation of 20 W, pulse rate of 120 kHz, and duty cycle of 99%. The analysis revealed that a better mark intensity value achieved was at a scan rate of 7 mm/s as shown in Fig.3.10.(c). But from the point of view of less time requirement, scan rate of 35 mm/s holds good which also had a good value of marking

characteristics. Thus further studies were carried out in order to analyse the larger possible attainment of marking intensity value with lesser possible mark width which was done by decreasing the transverse feed to 4  $\mu\text{m}/\text{laser stroke}$ .

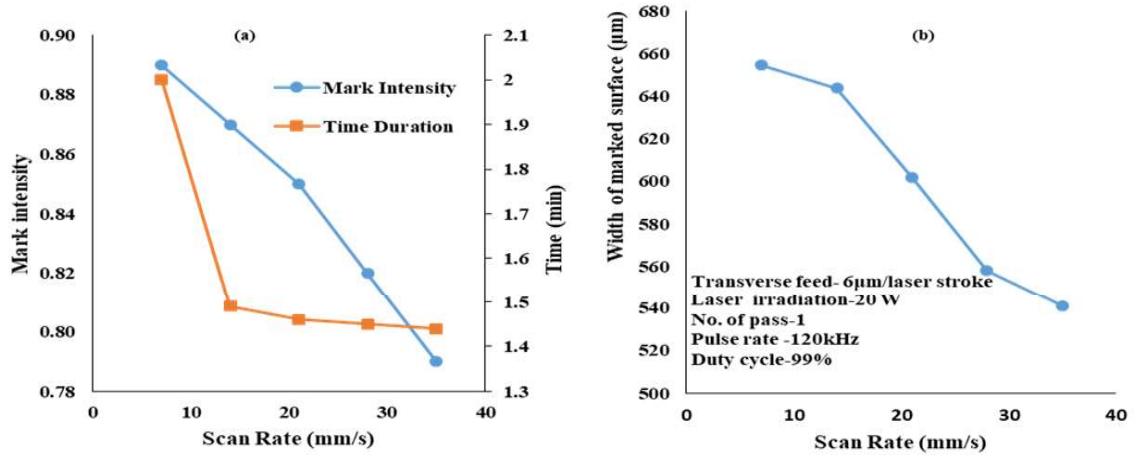


Fig. 3.9 Variation of marking characteristics (a) mark intensity and time requirement (b) width of mark with change of scan rate at transverse feed of 6  $\mu\text{m}/\text{laser stroke}$

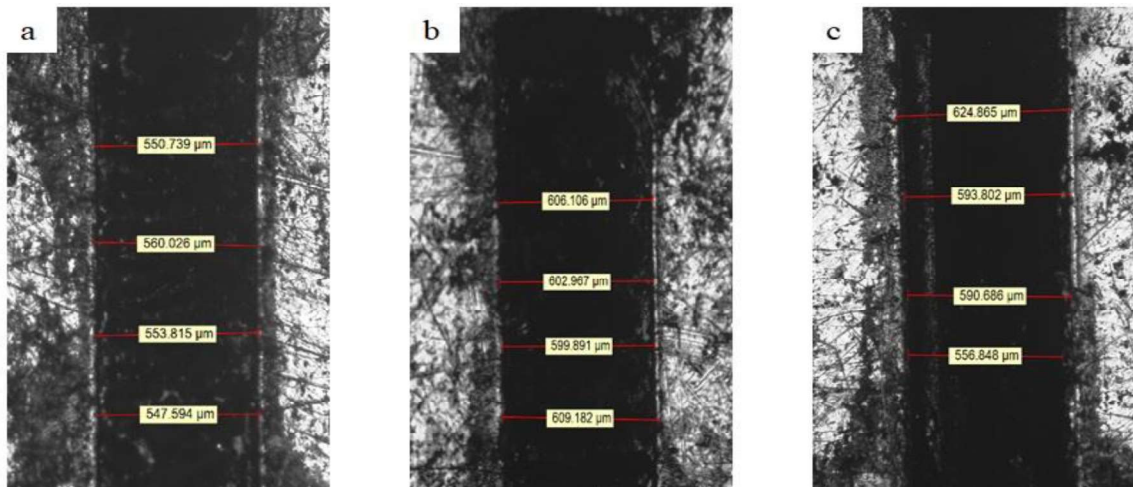


Fig. 3.10 Microscopic view of laser scanned surface with change of scan rate at transverse feed of 6  $\mu\text{m}/\text{laser stroke}$  (a) 35 mm/s (b) 21 mm/s (c) 7 mm/s

Fig. 3.11 shows the variation of marking characteristics with the change of scan rate when process variables such as transverse feed of 4  $\mu\text{m}/\text{laser stroke}$ , laser irradiation of 20 W, pulse rate of 120 kHz and duty cycle of 99% were kept constant. The time required to mark the image was 2.34 minutes at scan rate of 35 mm/s with a further increase of marking characteristics. As the transverse feed value decreases laser overlap region increases which



increases the oxidation phenomena and laser marked width. Studies revealed that a better value of marking characteristics was observed at a scan rate of 35 mm/s both in terms of quality of mark and time requirement of marking.

Fig. 3.12. (a), (b), and (c) are the microscopic view of the laser-scanned surface at a transverse feed of 4 $\mu$ m/laser stroke, laser irradiation of 20 W, pulse rate of 120 kHz, and duty cycle of 99%. Fig.3.12. (c) has large average width with a better mark intensity value as compared to Fig.3.12. (a) and (b) as revealed by measurement. Further studies were carried out to further increase the mark intensity value by decreasing the transverse feed to 2  $\mu$ m/laser stroke and varying the scan rate which can be observed in Fig.3.13.

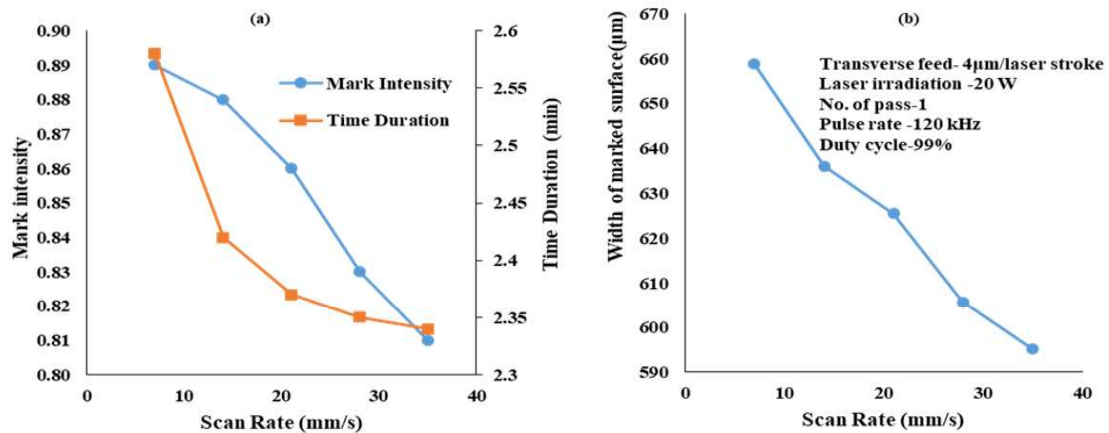


Fig. 3.11 Variation of marking characteristics (a) mark intensity and time requirement (b) width of mark with change of scan rate at transverse feed of 4 $\mu$ m/laser stroke

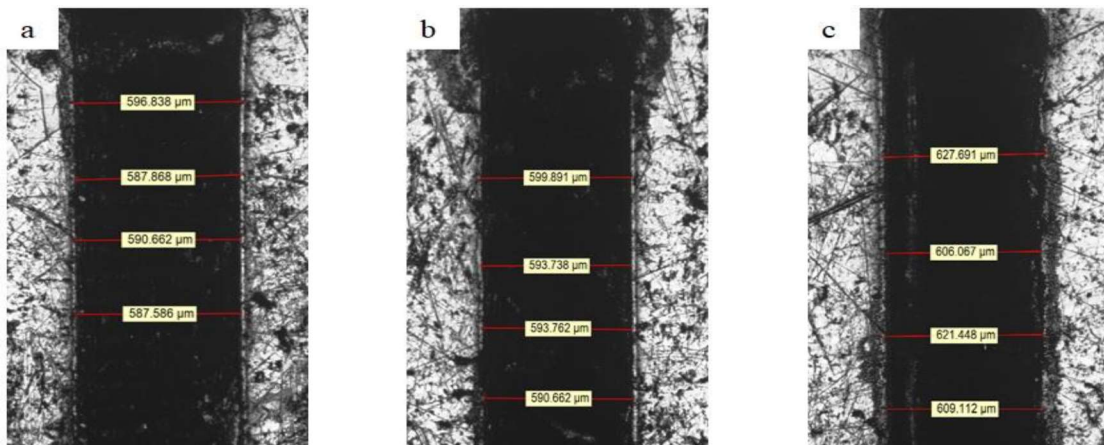


Fig. 3.12 Microscopic view of laser scanned surface with change of scan rate at transverse feed of 4 $\mu$ m/laser stroke (a) 35 mm/s (b) 21 mm/s (c) 7 mm/s

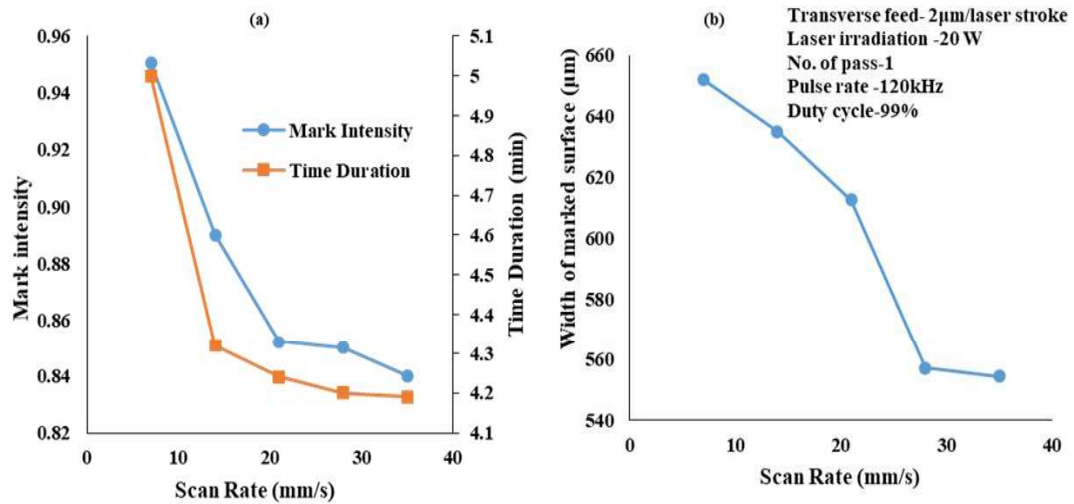


Fig. 3.13 Variation of marking characteristics (a) mark intensity and time requirement (b) width of mark with change of scan rate at transverse feed of 2μm/laser stroke

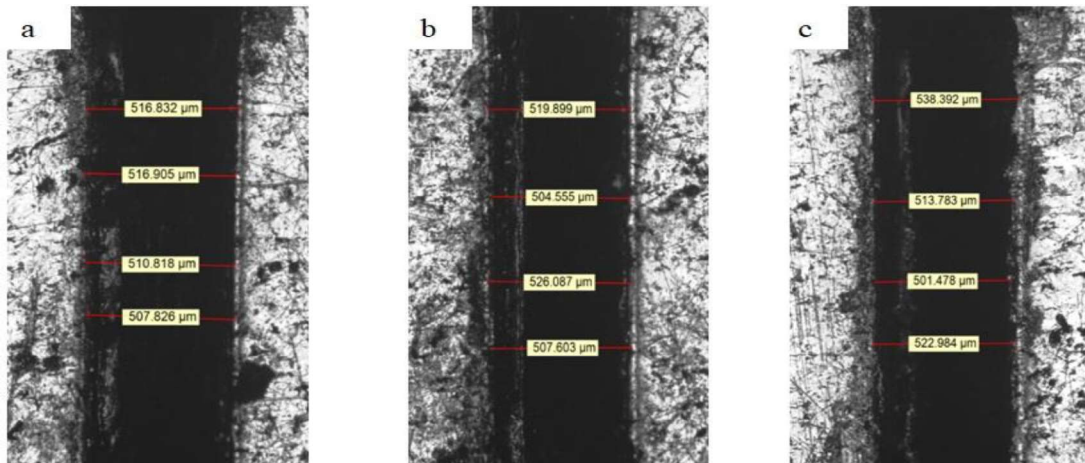


Fig. 3.14 Microscopic view of laser scanned surface with change of scan rate at transverse feed of 2μm/laser stroke (a) 35 mm/s (b) 21 mm/s (c) 7 mm/s

Fig. 3.13 shows the variation of marking characteristics with scan rate change when process variables such as transverse feed of 2μm/laser stroke, laser irradiation of 20 W, pulse rate of 120 kHz, and duty cycle of 99% were kept constant. Decrease of scan rate from 35 mm/s to 7 mm/s increases the time of heat interaction with the workpiece surface. Due to this, a better oxidation phenomenon occurs which led to the increase of the gray value of marked surface and thereby mark intensity value. As per Fig. 3.13, larger value of mark intensity achieved was about 0.94 at a scan rate of 7 mm/s whereas mark width achieved was about 650 μm. The increase of width at lower transverse feed and lowered scan rate causes the

side areas of desired marked surface to get heat-affected which increases unwanted mark width.

Fig. 3.14. (a), (b) and (c) are the microscopic view of laser scanned surface at different scan rate marked at a transverse feed of  $2\mu\text{m}/\text{laser stroke}$ , laser irradiation of 20 W, pulse rate of 120 kHz and duty cycle of 99% respectively. Experimental results revealed that higher value of mark intensity observed at lower value of transverse feed i.e.,  $2\mu\text{m}/\text{laser stroke}$  and scan rate (SS) of 7 mm/s but it requires more time to mark the surface as compared to transverse feed of  $8\mu\text{m}/\text{laser stroke}$ ,  $6\mu\text{m}/\text{laser stroke}$  and  $4\mu\text{m}/\text{laser stroke}$ . Thus, depending on the better marking characteristics or less time duration, higher transverse feed should be set.

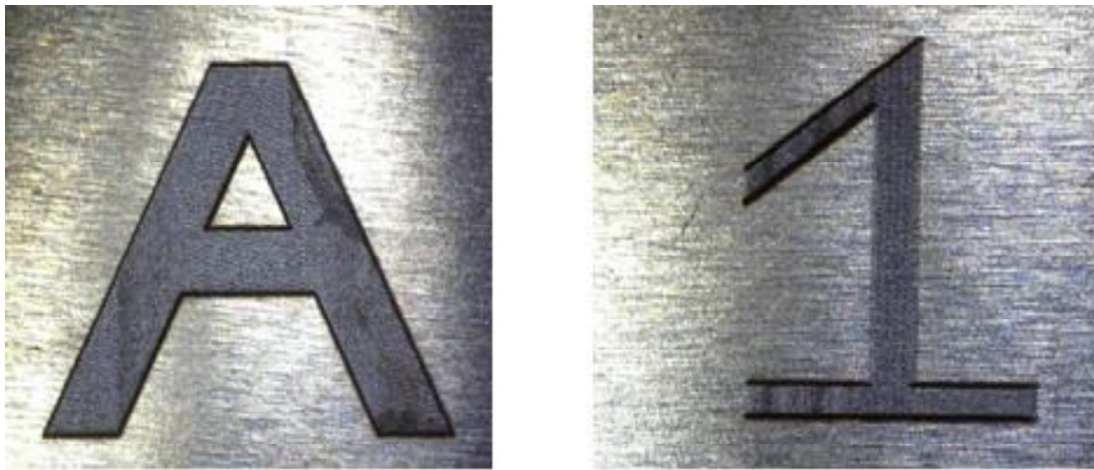


Fig. 3.15 Photographic view of alphabet and number marked using fiber laser

The studies mentioned above were carried out at normal ambient condition but further improvement can be possible by applying any other assist gas such as Nitrogen ( $\text{N}_2$ ) or Helium (He). As researchers revealed that gas environment also had a significant impact on the machined surface. Thus, to keep the mark intensity high with lower increase of width, lower value of transverse feed should be set but for lower time to mark the surface with lower increase in width, higher value of transverse feed should be set but the transverse feed value should not exceed more than  $21\mu\text{m}/\text{laser stroke}$  as it resulted in line marking instead of surface marking. Fig.3.15 shows the photographic view of alphabet (A) and number (1) marked using at a transverse feed of  $8\mu\text{m}/\text{laser stroke}$ , laser irradiation of 20 W, pulse rate of 120 kHz, duty cycle of 99% and scan rate of 35 mm/s. The surface is marked based on better marking characteristics to mark the surface which could be helpful in the development of any other geometric shape.



### **3.3 Results and Discussion on Laser Marking of Square Shaped Surface**

The section discussed with the influences of process variables such as laser irradiation, scan rate and pulse rate on marking characteristics of square shaped marked surface such as mark intensity and angle attainment by the sides of square. The marked portion obtained on variation of the process variables one at a time provides a brief idea of the setting of process variables to get the desired output responses. In addition to, the marked portion consists of multiple parallel laser lines at a transverse feed of 8  $\mu\text{m}$ /laser stroke which also changes the longitudinal and transverse overlap on change of process variables. Attempt was made to mark the surface using lower laser power. The discussions of which were listed in subsequent sub section.

#### **3.3.1 Influences of Laser Irradiation on Marking Characteristics of Square shaped Laser Marked Surface**

Fig.3.16 highlighted the variation of laser irradiation on laser marked surface when process variables such as scan rate of 35 mm/s, pulse rate of 50 kHz, duty cycle of 99 % were kept constant. The increase of laser irradiation causes better oxidation layer at the surface at ambient condition which improves the gray value of marked surface when laser irradiation varies between 12.5 W and 15 W but with further enhancement of power cause laser spattering. Due to which, the adjacent areas gets heat affected which resulted in the change of colour from polished white to light yellow. Furthermore, it was observed that average angle attainment at the side's increases on increase of laser irradiation. Apart from that, the transverse feed value of 8  $\mu\text{m}$ /laser stroke provided at the extremities for the generation of square shaped geometrical surfaces is also responsible for the increase of angle at the extremities of square.

Fig. 3.17 are the microscopic view of square shaped laser marked surface captured with the use of OLYMPUS STM 5X. Fig.3.17. (a-d) are the marked surfaces corresponding to the laser irradiation of 7.5 W, 10 W, 12.5 W and 15 W respectively. The marked surfaces shown possess containment of angle at the sides of square whose average has been calculated and depicted in the Fig.3.17. Apart from that, the photographs also revealed the transition of marked surface from light yellow to deep black on enhancement of laser irradiation from 7.5 W to 15 W. Such marked surfaces generally occurs due to the improvement of surface oxidation and increase in calculated gray value of square shaped marked surface.

Apart from laser irradiation, other process variables such as pulse rate and scan rate were also varied in order to analyse its influences on laser marking characteristics as discussed in subsequent subsection.

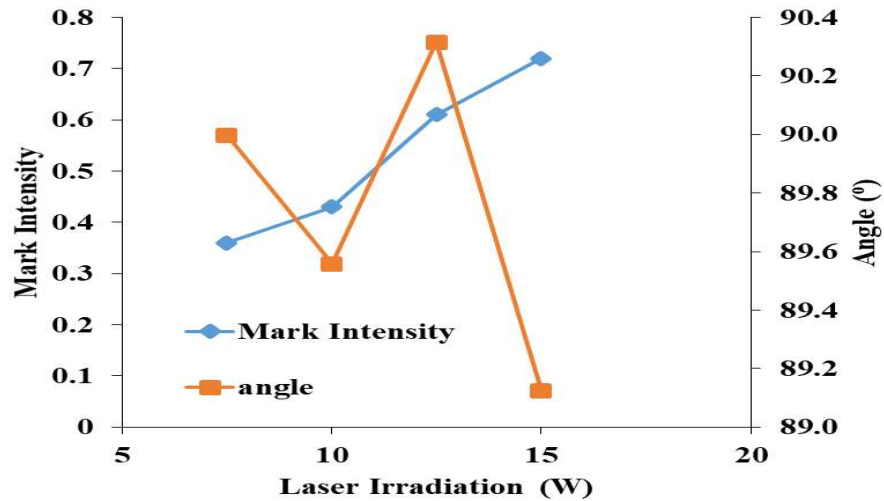


Fig. 3.16 Variation of Marking Characteristics with respect to laser irradiation

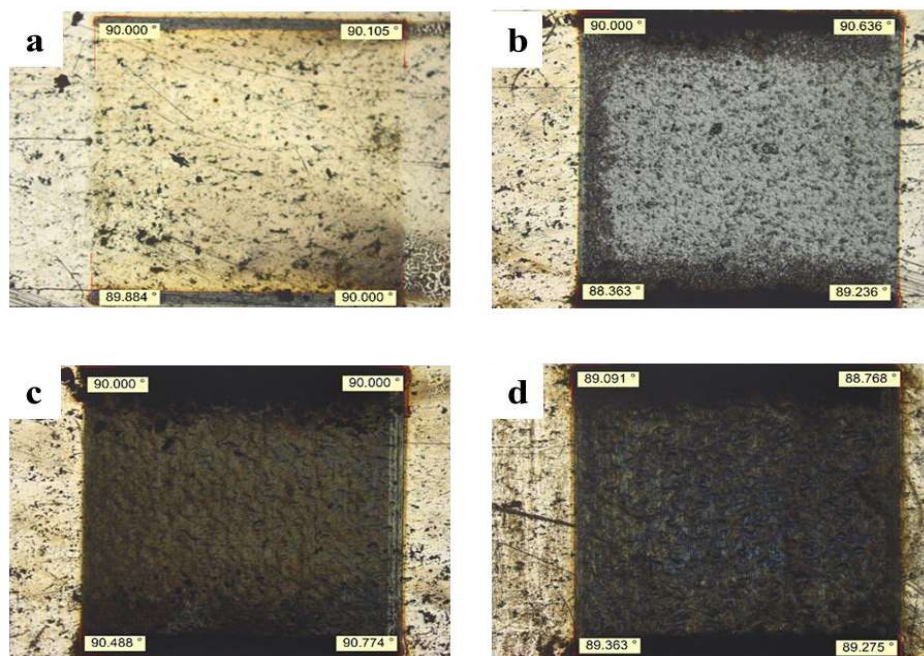


Fig. 3.17 Surface texture of laser marked surface at different laser irradiation (a) 7.5 W, (b) 10.5 W, (c) 12.5 W, (d) 15 W when other process variables such pulse rate of 50 kHz, duty cycle of 99 % and scan rate of 35 mm/s were kept constant.

### 3.3.2 Influences of Pulse rate on Marking Characteristics of Square shaped Laser Marked Surface

Fig.3.18 highlighted the variation of pulse rate on laser marked surface when process variables such as scan rate of 35 mm/s, laser irradiation of 15 W, duty cycle of 99 % were kept constant.

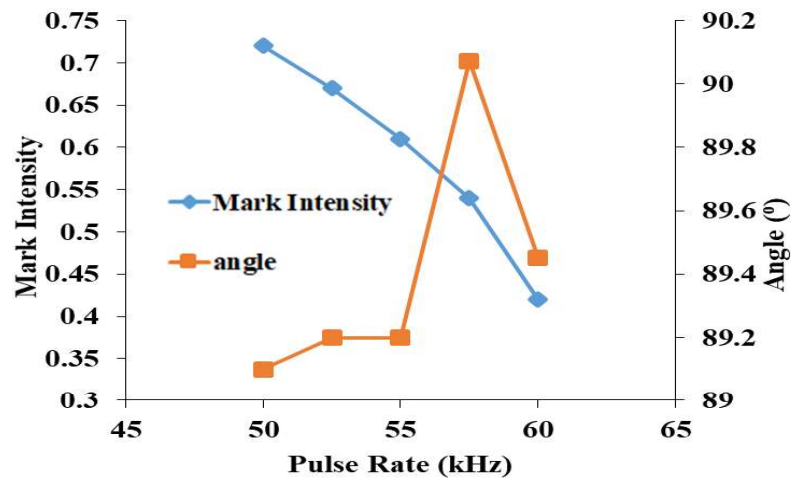


Fig. 3.18 Variation of Marking Characteristics with respect to Pulse rate

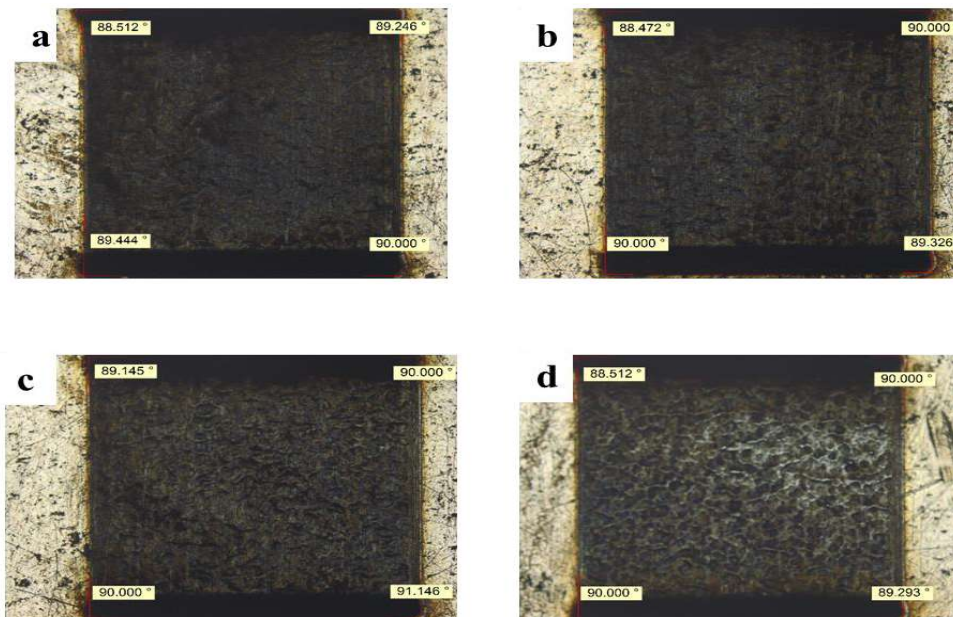


Fig. 3.19 Surface texture of laser marked surface at different pulse rate (a) 52.5 W, (b) 55 kHz, (c) 57.5, (d) 60 kHz when other process variables such laser irradiation of 15 W, duty cycle of 99 % and scan rate of 35 mm/s were kept constant

It was observed that increase of pulse rate from 50 kHz to 60 kHz resulted in the decrease of mark intensity value. Higher pulse rate reduces the energy content of laser beam when all other process variables were kept constant. Due to which, less oxidation occurs at the surface which cause decrease in the grey value of marked surface but the other hand, it makes the angle held by the sides of square close to 90°. Experimental studies revealed that lower value of pulse rate i.e., 50 kHz should be preferred for good mark intensity value but from the point of view of accuracy of angle containment at the sides of square, pulse rate of 57.5 kHz should be preferred.

Fig. 3.19 are the microscopic view of square shaped laser marked surface at varying pulse rate captured with the use of OLYMPUS STM 5X. Fig. 3.19.(a-d) are the marked surfaces corresponding to the pulse rate of 52.5 kHz, 55 kHz, 57.5 kHz and 60 kHz respectively. Experimental studies revealed that the calculated gray value of square shaped marked surface is better at pulse rate of 50 kHz i.e., Fig. 3.19 (a) in terms of mark intensity value. But from angle point of view, Fig. 3.19 (c) should be preferred.

Since laser irradiation of 15 W and pulse rate of 50 kHz provides better marking characteristics so they were held constant and further analysis on marking characteristics was made by varying the scan rate as discussed in section 3.3.3.

### **3.3.3 Influences of Scan rate on Marking Characteristics of Square shaped Laser Marked Surface**

Fig. 3.20 highlighted the variation of scan rate on laser marked surface when process variables such as laser irradiation of 15 W, pulse rate of 50 kHz, duty cycle of 99 % were kept constant. It was observed that decreased of scan rate from 35 mm/s to 7 mm/s resulted in deep laser marking at the workpiece surface which occurs due to increase of time of heat interaction at lower scan rate that provides better oxidization with the material surface which in turn increases the gray value of laser marked surface. It was observed that better value of mark intensity was observed at lower value of scan rate i.e. 7 mm/s as seen in Fig. 3.20.(a). On the other hand, decrease of scan rate resulted in the increase of time requirement to mark the surface for a particular dimension. Apart from that, increase of angle held by the sides of square was also noticed which approaches above 90° as seen in Fig. 3.20.(b). Considering minimum time to mark the surface with better mark intensity, scan rate of 35 mm/s should be preferred.

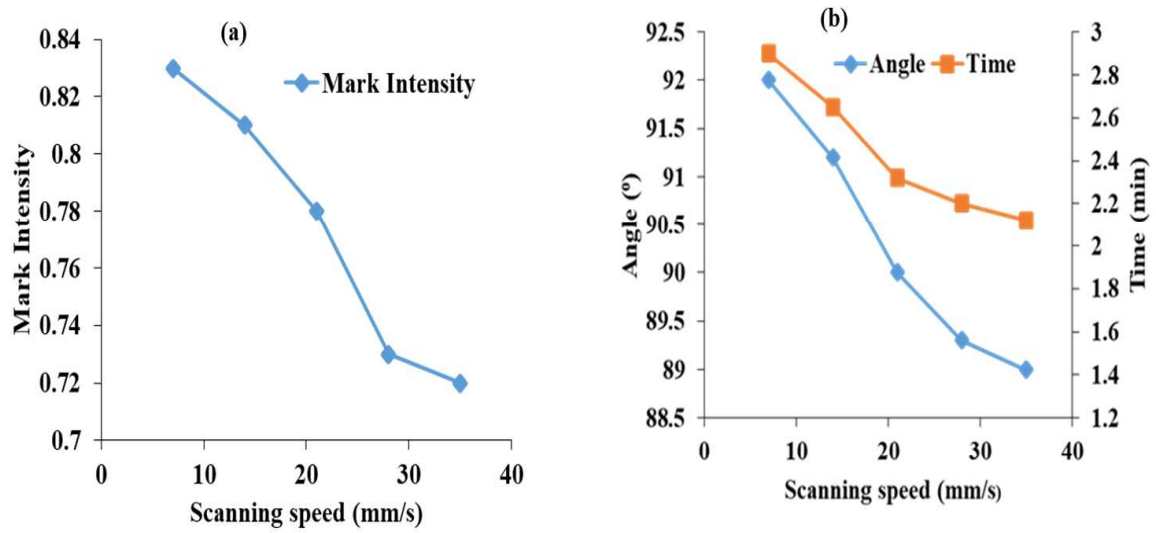


Fig. 3.20 Variation of marking characteristics (a) mark intensity (b) angle and time with change of scan rate

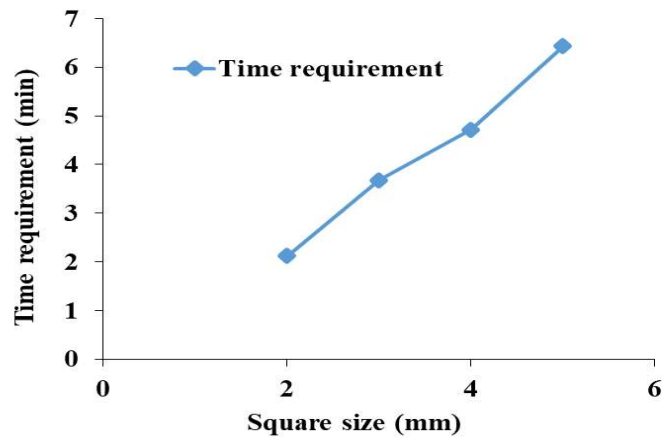


Fig. 3.21 Plot of time requirement to mark the surface with respect to side of square

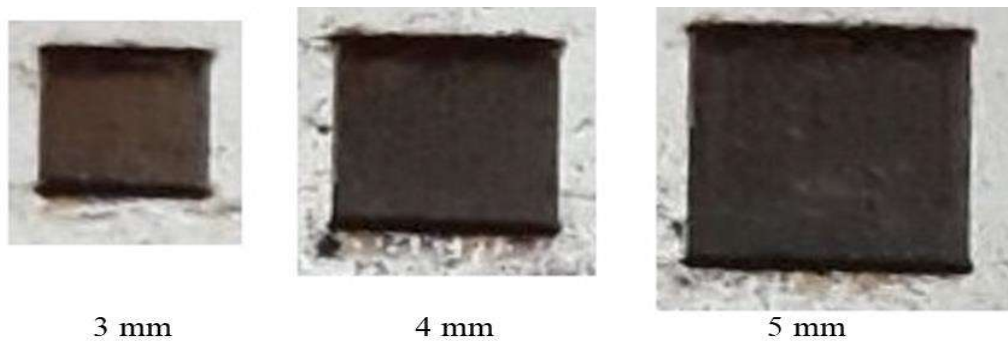


Fig. 3.22 Photographic view of square shaped laser marked surface.

Based on the study, it was observed that better value of marking characteristics was achieved at a laser irradiation of 15 W, pulse rate of 50 kHz and scan rate of 35 mm/s. Thus, further studies were laid down to focus on the duration of time required to mark the surface of side 2 mm, 3mm, 4mm and 5 mm as shown in Fig.3.21. The photographic views of square shaped marked surface of different sides are shown in Fig.3.22

Upon marking square shaped laser marked at better obtained process variables, it was observed that the average value of angle held by the sides of square is 89.3°. The percentage error was calculated using the formula given in equation 4.4 and the value of error obtained was 0.77%.

### 3.4 Results and Discussion on Laser Marking of Elliptical Shaped Surface

The section deals with the detailed analysis of the responses which were undertaken for the evaluation of marking characteristics such as mark intensity, area deviation, and surface roughness. A program of ellipse with transverse feed of  $8\text{ }\mu\text{m}$ /laser stroke and having major axis of  $4000\text{ }\mu\text{m}$  and minor axis of  $2000\text{ }\mu\text{m}$  had been generated for carrying out operation using diode pumped fiber laser in order. The study were made to observe the effects of defocussing distance on laser marking characteristics. The detailed discussion were shown below.

Fig. 3.23 shows the region selection for evaluating mark intensity along with the measurement of major and minor axis of elliptical shaped laser marked surface. The image is captured using LEICA optical microscope and then processed to the MATLAB software for evaluating mark intensity. The responses such as mark intensity, area deviation and surface roughness of laser marked surface are significant as it reveals how precise and good quality marked surface has been achieved through fiber laser with high value of mark intensity, lower area deviation and surface roughness.

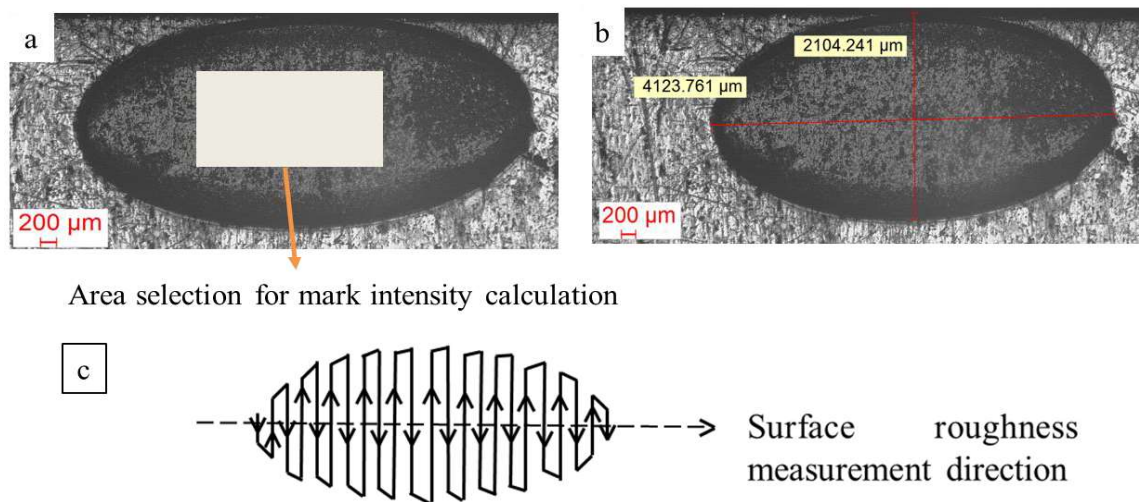
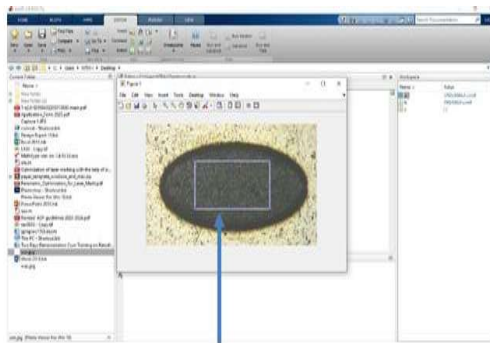
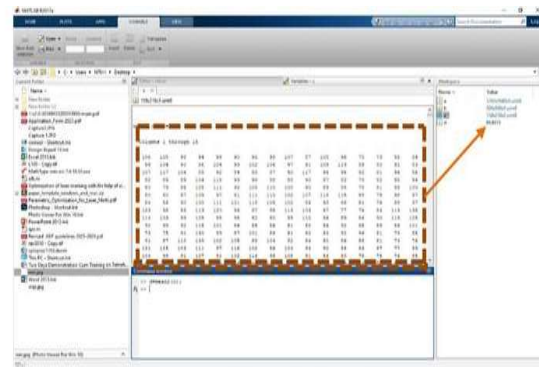


Fig. 3.23 Microscopic view of elliptical shaped laser marked surface (a) region selection for mark intensity calculation (b) Measurement of major and minor axis of elliptical shaped image. (c) Direction of laser travel for ellipse generation.



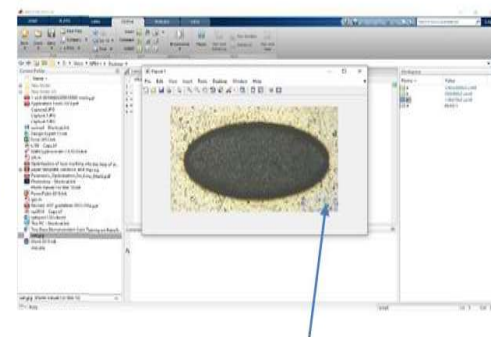
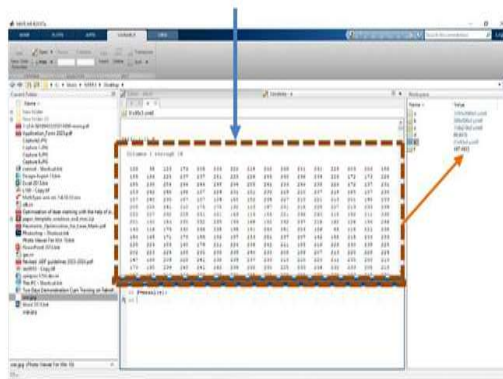


Region selection for calculating grey value of laser marked surface



Pixel value of selected marked surface is displayed as shown in dotted line which then culminated to form grey value as shown by orange arrow

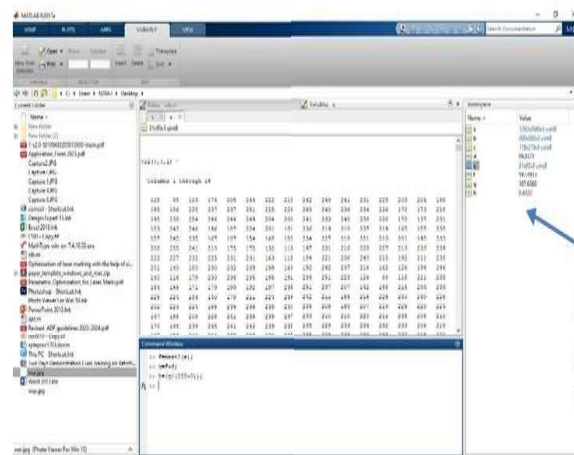
Pixel value of selected unmarked surface is displayed as shown in dotted line which then culminated to form grey value as shown by orange arrow



Region selection for calculating grey value of unmarked region

The average pixel value of laser marked surface and unmarked surface is then subtracted and stored in variable g

The difference thus obtained is then divided by difference between gray value of white surface (equivalent to 255) and black surface (equivalent to 0) to obtain mark intensity value



Final computed mark intensity value

Fig. 3.24 Pictorial representation for the calculation of mark intensity value of laser marked surface using MATLAB software



The measurement of area deviation is computed by analysing the difference between actual and predicted value of the elliptical shaped laser marked surface and the obtained value is then computed in equation 3.1 for the calculation of area deviation.

$$\text{Marked Area Deviation} = |\text{Actual Marked Area} - \text{Theoretical Marked Area}| \dots \text{Equation 3.1}$$

Predicted value and actual value of an area can be calculated using the formula

$$\text{Area of Ellipse} = \pi \times a \times b \dots \dots \dots \text{Equation 3.2}$$

Where ‘a’ is the major axis and ‘b’ is the minor axis of ellipse. Actual area of laser marked surface is achieved by measurement of major and minor axis of elliptical shaped marked surface using LEICA optical microscope of resolution 1 nm whereas theoretical major and minor axis were fixed to 4000  $\mu\text{m}$  and 2000  $\mu\text{m}$  respectively.

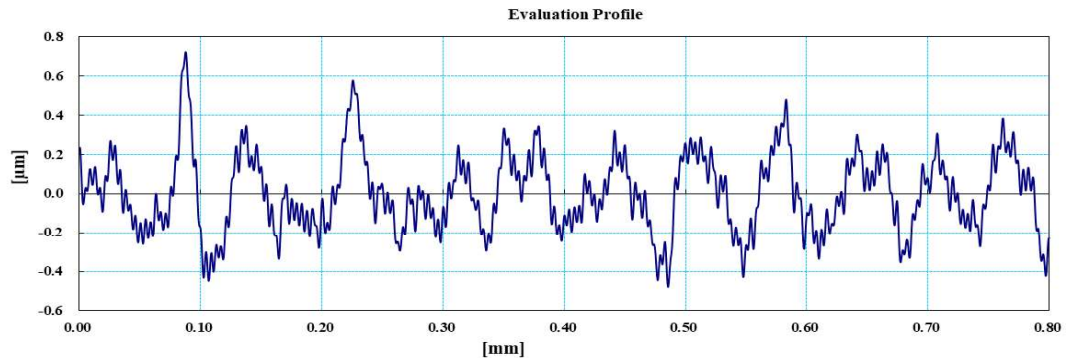


Fig. 3.25 Surface roughness measurement through MITUTOYO Surftest SJ 410

Fig. 3.25 shows the surface roughness measurement of marked surface which was measured using an MITUTOYO (SJ 410) surface roughness tester. It is a contact type which has a resolution of 1nm. The cut off length employed was 0.8 mm. The direction of movement of stylus on laser marked surface is shown in Fig. 3.23.

The work is carried out with an assumption that the laser spot overlap in both longitudinal and transverse direction is above 60% over the entire surface of elliptical shaped laser marked surface. Its limitation include that the analysis of laser marking operation cannot be performed below pulse rate of 50 kHz, and scan rate of above 35 mm/s as it does not lies within the specified limit of laser marking machine.

In order to determine the better process parameter combinations for producing high-quality laser marked surfaces, a series of trial experiments were conducted by varying the process

variables within the suitable range for the development of better quality laser marked surface. Initially attempt were made to mark the surface at minimum power and minimum time. But the results revealed that laser irradiation below 5 W cause insignificant marking when other process variables were held constant. Table 3.1 provides range of process variables which had been used for analysis of better quality elliptical laser marked surface.

**Table 3.1 Process variables and their levels**

Process variables	Value Range				
Laser Irradiation (W)	7.5	10	12.5	15	17.5
Pulse Rate (kHz)	50	67.5	85	102.5	120
Scan Rate (mm/s)	35	28	21	14	7
Defocusing Distance (mm)	-2	-1	0	1	2

In order to analyse the influences of process variables for achieving better marking characteristics in terms of high mark intensity, low area deviation and low surface roughness. The process variables were allowed to vary one at a time (OFAT) in order to have detailed analysis as discussed in the following subsection.

### **3.4.1 Influences of Laser irradiation on Marking Characteristics of Elliptical Shaped Laser Marked Surface**

Fig. 3.26 shows the impact of laser irradiation on the characteristics of laser marking when process variables like pulse rate of 50 kHz, scan rate of 35 mm/s and duty cycle of 99 % were held constant. It has been observed from Fig.3.26. (a) that with the increase of laser irradiation from 7.5 to 17.5 W, the work piece yields higher oxidation which resulted in the increase of marking characteristics in terms of mark intensity. It was observed that higher value value of mark intensity achieved was 0.70 at laser irradiation of 17.5 W whereas lower value of 0.45 was achieved at a laser irradiation of 7.5 W.

High laser irradiation increases the material removal at the periphery and inner portion of laser marked surface due to which it resulted in the increase of area deviation and surface roughness. It was observed from Fig.3.26.(a) that lower area deviation of  $1530000 \mu\text{m}^2$  and minimum surface roughness Ra of  $0.189 \mu\text{m}$ , Rq of  $0.214 \mu\text{m}$ , and Rz of  $2.016 \mu\text{m}$  from Fig.3.28.(b) were achieved at a laser irradiation of 7.5 W but lower mark intensity value points the use of laser irradiation to a higher value. However, it was also observed that the increase of laser irradiation above 12.5 W causes laser spattering which is responsible for

the increase of surface roughness and area deviation. The analysis of laser marked surface can also be done in terms of surface roughness since the graph provides the value of mark intensity and surface roughness upon variation of laser irradiation when other process variables were held constant. So the roughness variables which lies within the desired range is also an indication of better marking characteristics.

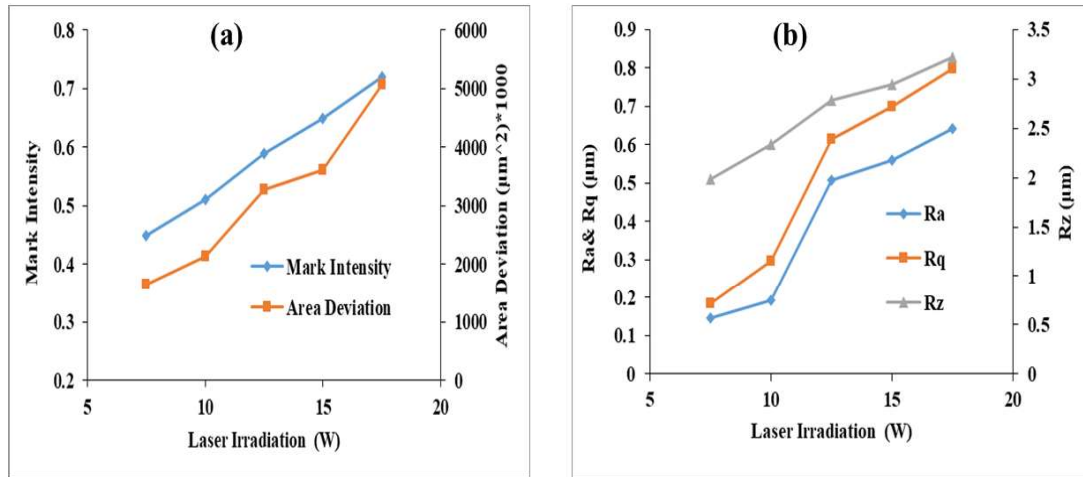


Fig. 3.26 Variation of marking characteristics (a) mark intensity and area deviation (b) surface roughness with change of laser irradiation

Upon all the marking characteristics taken into consideration, laser irradiation of 12.5 W provide average results of marking characteristics in terms of mark intensity, area deviation and surface roughness. Thus laser irradiation of 12.5 W was made fixed and then further studies were made by changing other process variables like pulse rate, scan rate, and defocusing distance for higher mark intensity value and lower area deviation and surface roughness value of marked surface through laser.

### 3.4.2 Influences of Pulse rate on Marking Characteristics of Elliptical Shaped Laser Marked Surface

Fig. 3.27 illustrates the impact of pulse rate on the marking characteristics of marked surface when other process factors like laser irradiation, duty cycle, and scan rate were held constant at 12.5 W, 99%, and 35 mm/s, respectively. It was observed from Fig. 3.27. (a) that with the increase of pulse rate from 50 kHz to 120 kHz resulted in the decrease of mark intensity from 0.60 to 0.45 and area deviation from  $3400000 \mu\text{m}^2$  to  $2500000 \mu\text{m}^2$  respectively. Increase of pulse rate produces shorter pulse length which possess lower peak power. This causes mild thermal effects at the work piece surface due to which the value of mark intensity, surface roughness and area deviation decrease. Equation 3.3 provides the

relation between peak power, pulse rate, laser irradiation and pulse duration of pulsed mode laser. In the present system pulse duration of 120 nanosecond (ns) was system constant and when a particular average power were held constant, peak power totally depends on pulse rate. So on increasing pulse rate, peak power of laser decrease and vice versa.

$$\text{Peak power} = \frac{\text{Average laser irradiation}}{\text{Pulse rate} \times \text{Pulse duration}} \dots\dots\dots \text{Equation 3.3}$$

The marked surface also consists of multiple of laser spots so changes in pulse rate also changes the lateral and longitudinal spot overlap. Higher pulse rate decrease the overlap of laser spot in both lateral and longitudinal direction due to which surface roughness decreases and reaches to a value Ra of 0.25 $\mu\text{m}$ , Rq of 0.325  $\mu\text{m}$ , and Rz of 1.42  $\mu\text{m}$  as seen in Fig. 3.27.(b).

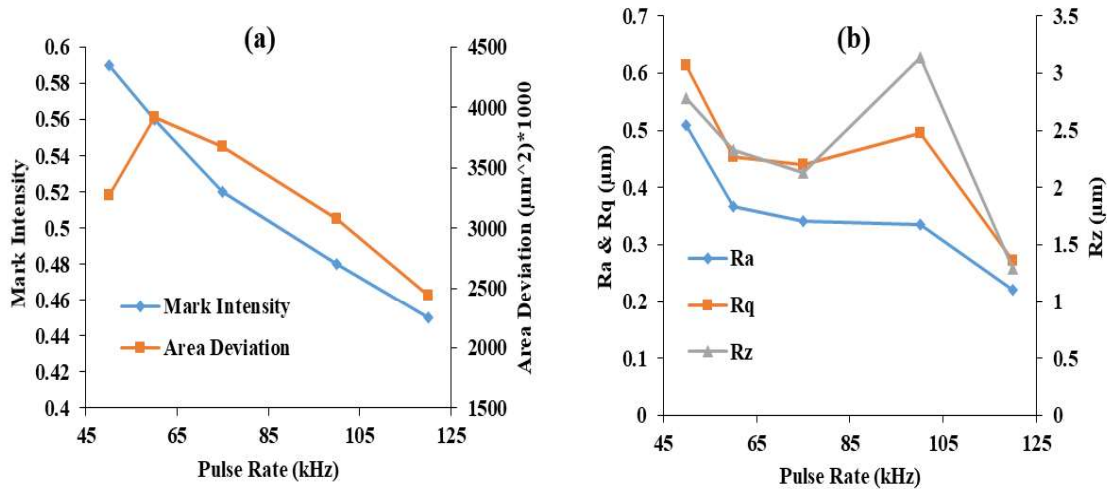


Figure 3.27 Variation of marking characteristics (a) mark intensity and area deviation (b) surface roughness with change of pulse rate

Thus, in order to have minimum area deviation and surface roughness, pulse rate of 120 kHz provides better results when other process variables were held constant but fall in mark intensity restricts its use. Considering average better marking characteristics, pulse rate of 85 kHz yields better results in the range of 50 to 120 kHz.

Thus further studies were made by fixing laser irradiation to 12.5 W and pulse rate to 85 kHz and varying other process variables like scan rate, and defocusing distance. The pulse rate variation within the proper range also indicates the change in colour of the work piece's surface because of the overall impacts of the material and thermal properties.

### 3.4.3 Influences of Scan rate on Marking Characteristics of Elliptical Shaped Laser Marked Surface

Fig. 3.28 illustrates the change of scan rate with marking features when other process variables like laser irradiation, pulse rate, and duty cycle were fixed at 12.5 W, 85 kHz, and 99%, respectively. Lower scan rate increases the amount of time that heat interacts with the workpiece which increases the amount of energy absorbed by the laser scan region. As a result, there was high surface oxidation present on the work piece's surface which resulted in the higher possible mark intensity value, area deviation and surface roughness of marked region. Apart from that the extremities of laser marked region are high susceptible to material removal due to prolonged heat interaction at lower value of scan rate on or below 7 mm/s. This prohibits the further study upon use of lower value of scan rate lower than 7 mm/s and also to mark the surface by minimum possible time, lower value of scan rate should be eliminated.

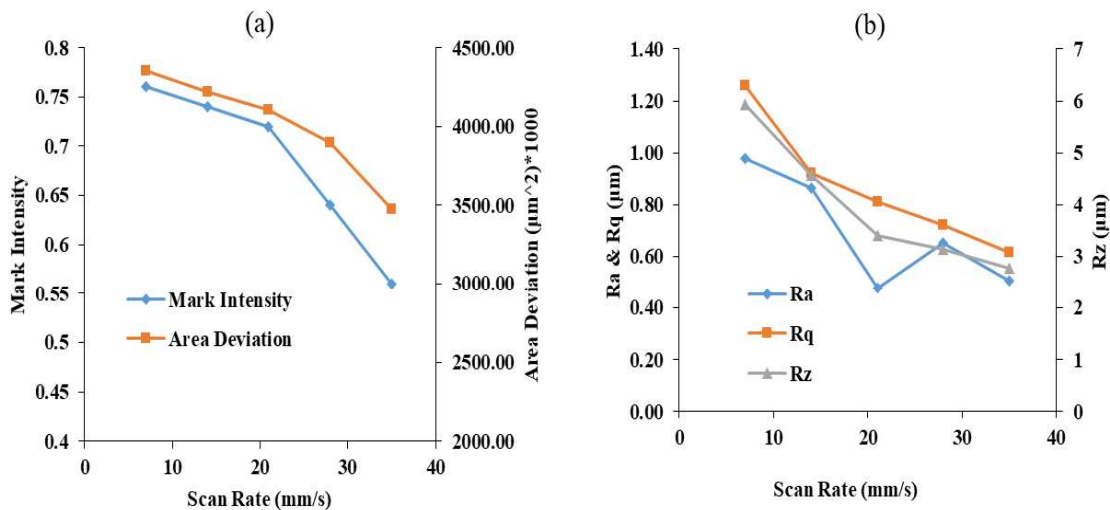


Fig. 3.28 Variation of marking characteristics (a) mark intensity and area deviation (b) surface roughness with change of scan rate

It was seen from Fig. 3.28. (a) that with the decrease of scan rate from 35 mm/s to 7 mm/s yields mark intensity value of 0.76 and area deviation of  $4320000 \mu\text{m}^2$  whereas surface roughness Ra of  $0.96 \mu\text{m}$ , Rq of  $1.35 \mu\text{m}$  and Rz of  $6 \mu\text{m}$  were obtained at lower value of scan rate of 7 mm/s as can be seen in Fig. 3.28(b) respectively. Apart from that, prolonged heat interaction at lower scan rate causes adjoining areas to be heat affected. Thus from the point of view of better marking characteristics, scan rate of 21 mm/s yields better results. Upon analysis at a scan rate of 21 mm/s, it was revealed from Fig. 3.28. (a) that the value

of mark intensity achieved was 0.73 and area deviation is  $4000000 \mu\text{m}^2$  and from Fig. 3.30.(b) the value of surface roughness (Ra, Rq and Rz) were found to be  $0.50 \mu\text{m}$ ,  $0.60 \mu\text{m}$ , and  $3.5 \mu\text{m}$  when other process variables were held constant. Further studies were also made by varying distance of z axis in both positive and negative direction in order to observe the variation in marking characteristics as discussed in next section.

### **3.4.4 Effects of defocusing distance on the characteristics of laser marking**

Fig. 3.29.(a),(b),(c-d) shows the variation of mark intensity, area deviation, and surface roughness with change in defocusing distance when other process variables such as laser irradiation, pulse rate, scan rate and duty cycle were fixed at 12.5 W, 85 kHz, 21 mm/s and 99 % respectively. The defocusing distance is allowed to vary by 1 mm and 2 mm in both positive and negative z direction from the focussed point to observe its influences on marking characteristics. Experimental results revealed that the defocusing distance by 2 mm in negative z direction had tremendous influences on marking characteristics. The mark intensity value reaches a value of 0.80, area deviation increases to  $4412000 \mu\text{m}^2$  and surface roughness Ra, Rq and Rz increase to  $3.056 \mu\text{m}$ ,  $4.320 \mu\text{m}$ , and  $20 \mu\text{m}$  respectively. The decreases of defocusing distance by further 1 mm in negative z direction resulted in the increase of decrease in mark intensity, area deviation and surface roughness with non-uniform laser marking. As the laser beam distribution is Gaussian, its maximum energy lies at the centre of laser spot. The movement of z axis by progressive 1 mm in negative z axis moves the workpiece in defocus condition due to which diameter of laser beam increases with decreased energy impinges at the workpiece surface. Greater area exposure to laser beam provides higher oxidation due to which mark intensity, area deviation and surface roughness increases at 2 mm defocusing distance in negative direction. The movement of z axis by further 1 mm in negative direction, further increase the diameter of laser beam which makes the surface non luminous with increased area deviation. Furthermore, the movement of z axis by 1 mm in positive direction from focussed point decreases the marking characteristics and forms light marking. Higher movement of z axis diverges the laser beam due to which it's effective energy decreases and forms light marking. The laser marking on the workpiece surface becomes further lighter and forms no marking at all at defocusing distance of 4 mm in positive direction.

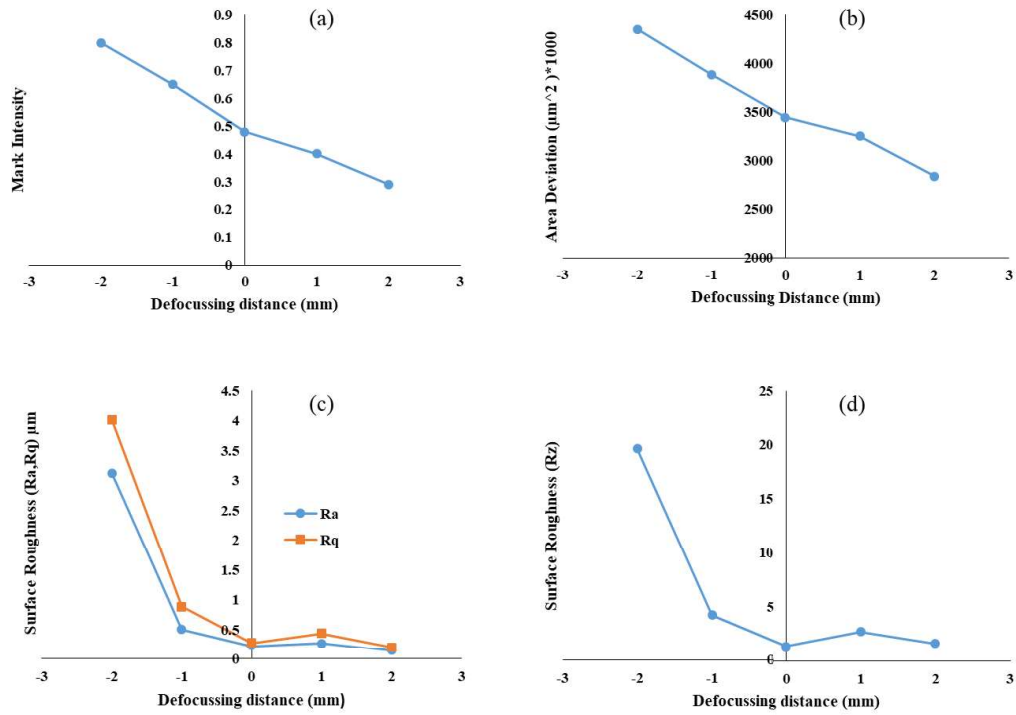


Fig. 3.29 Variation of marking characteristics (a) mark intensity, (b) area deviation (c & d) surface roughness with change of defocusing distance

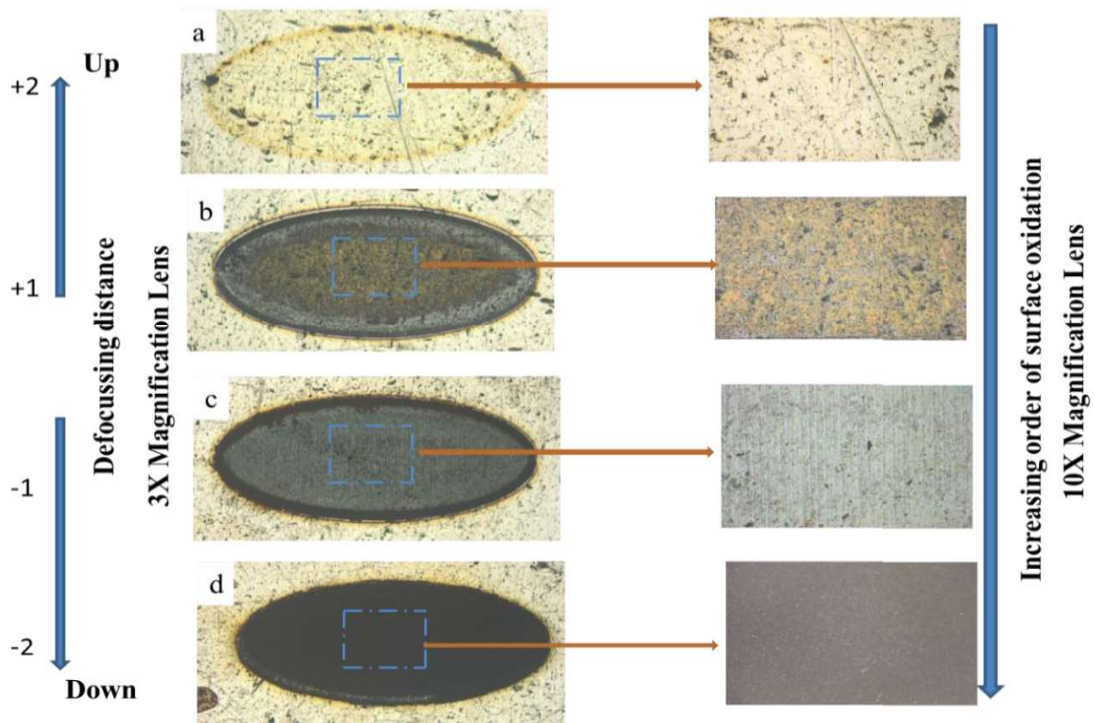


Fig. 3.30 Microscopic view of laser marked surface at defocussed condition

Fig. 3.30 shows the microscopic view of laser marked surface at defocusing distance of 1mm and 2 mm in both positive and negative direction from focused position. The minimum value of surface roughness and area deviation were observed at defocusing distance of 2 mm in positive z direction which would further decrease on increasing the defocusing distance in positive z direction. But since the laser marking is lighter, further use of defocusing distance in positive direction makes the marking so lighter that it becomes difficult to analyse.

The defocusing distance by 1 mm and 2 mm in negative direction increases the luminous intensity due to higher oxidation but decreases after using defocusing distance beyond 2 mm in negative direction due to increase area of laser spot with decrease energy content. The studies thus revealed that better value of marking characteristics could be achieved if laser irradiation, pulse rate, scan rate and defocusing distance were fixed at 12.5 W, 85 kHz, 21 mm/s and 2 mm in negative z direction respectively.

Apart from that, some studies were also been made based on SEM images in order to observe the effects of process variables on laser marking characteristics. The detailed of which is discussed in section 3.4.5.

#### **3.4.5 Studies based on Scanning Electron Microscope (SEM) images on Elliptical Laser Marked Surface**

The surface structural analysis has been conducted on the surface obtained by carrying out experiment at both focussed and defocussed position at an interval of 2 mm in both positive and negative axis for better observation. It was observed that at defocussed condition of 4 mm in positive direction, no laser marking was observed at the sample surface neither through SEM images because at defocus at 4 mm in positive direction, laser beam diverges due to which its effective energy decreases which resulted in the formation of insignificant marking. Fig. 3.31 shows the SEM images at laser irradiation of 12.5 W, pulse rate of 85 kHz, scan rate of 21 mm/s with defocussed distance of 2 mm in positive z direction. It was observed that less material was removed around the periphery of laser marked surface with less oxidation at inner marked surface. In fact, uniform oxidation does not prevail everywhere inside the laser marked region due to which it less luminous as compared to laser marked surface at focussed position. The surface roughness value  $R_a$ ,  $R_q$ , and  $R_z$  were found to be 0.128  $\mu\text{m}$ , 0.165  $\mu\text{m}$ , and 0.777  $\mu\text{m}$  respectively.



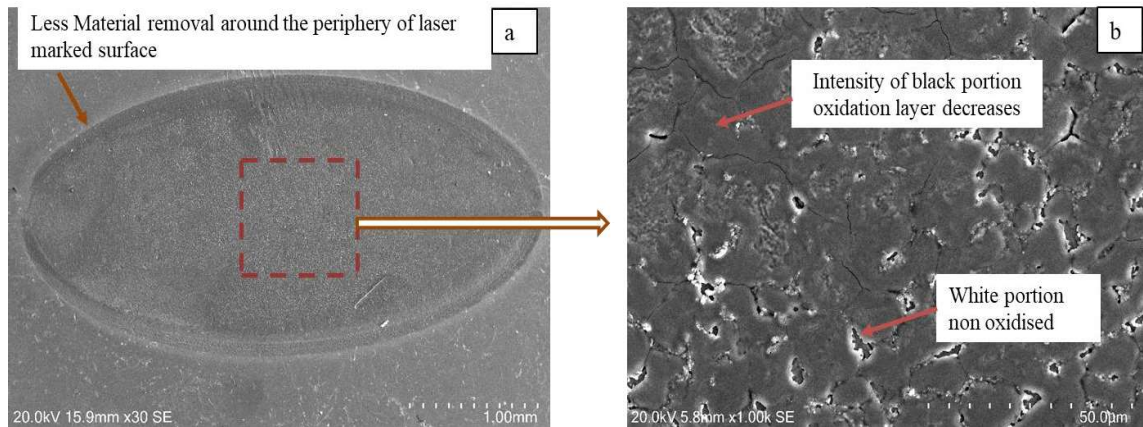


Fig. 3.31 SEM images of laser marked surface at defocussed condition of 2 mm in positive direction (a) Full laser marked surface (b) Enlarged view of inner laser marked surface

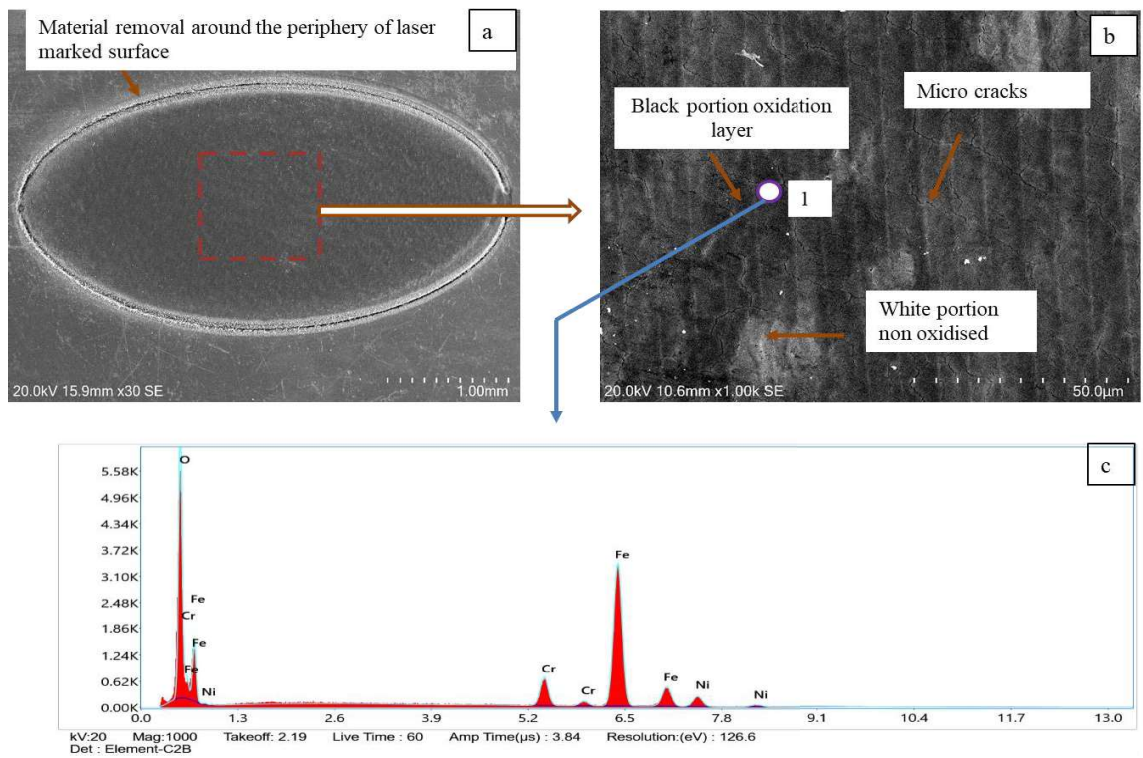


Fig. 3.32 SEM images of marked surface with the EDX analysis of inner marked surfaces at focussed condition (a) Full laser marked surface, (b) Enlarged view of inner laser marked surface, (c) EDX analysis of spot of inner laser marked surface

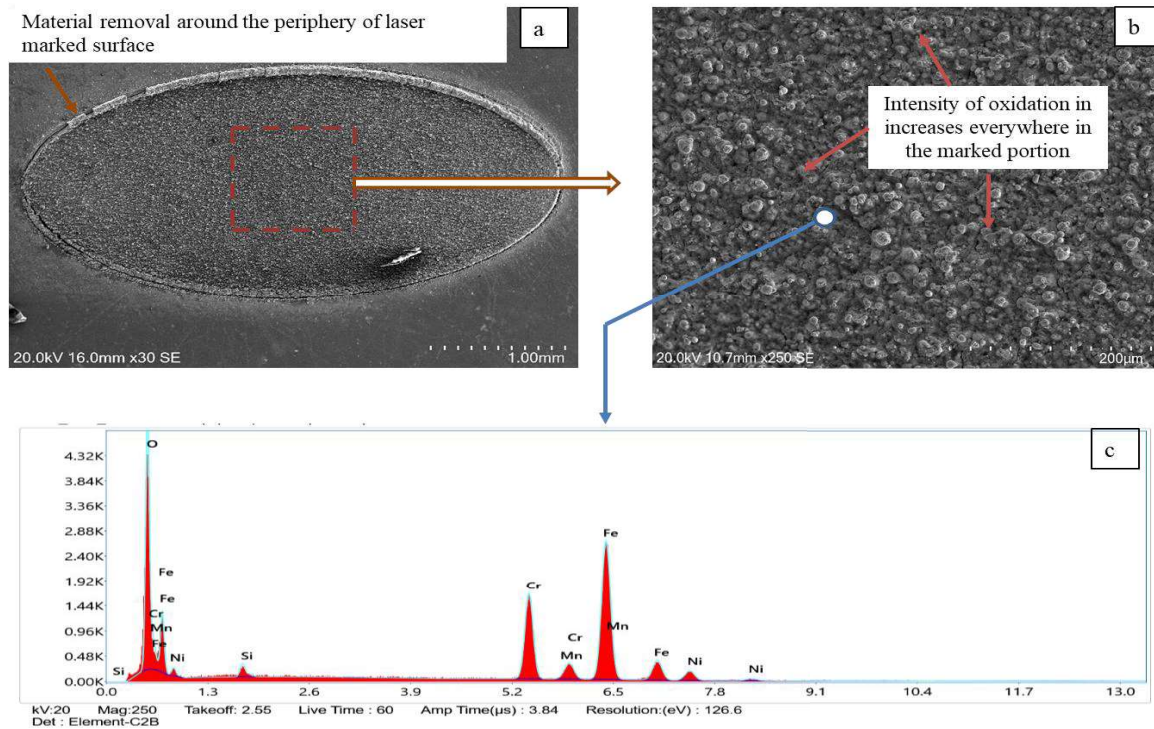


Fig. 3.33 SEM images of laser marked surface at defocussed condition of 2 mm in negative direction (a) Full laser marked surface, (b) Enlarged view of inner laser marked surface, (c) EDX analysis of spot of inner laser marked surface

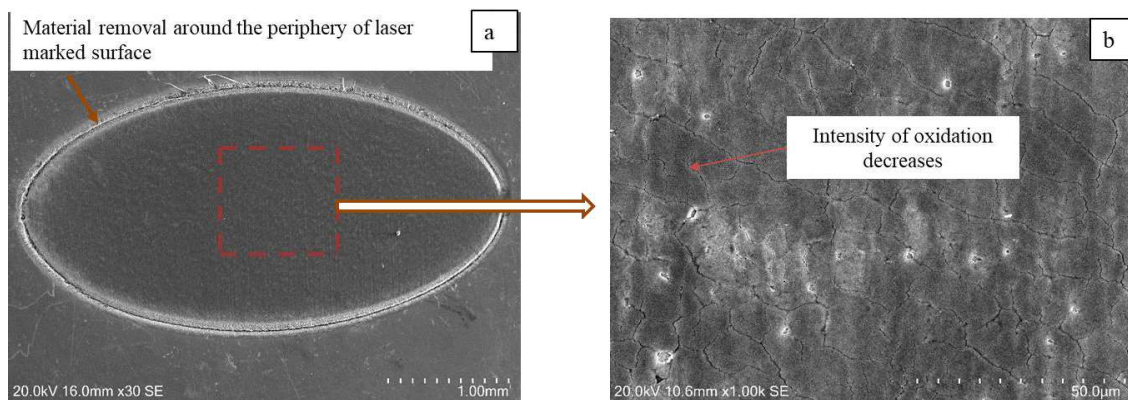


Fig. 3.34 SEM images of laser marked surface at defocussed condition of 4 mm in negative direction (a) Full laser marked surface (b) Enlarged view of inner laser marked surface

Fig. 3.32 shows the SEM images at laser irradiation of 12.5 W, pulse rate of 85 kHz, scan rate of 21 mm/s at focussed position. The black portion possess high oxidation whereas white portion remains non-oxidised. In fact, uniform oxidation does not prevail throughout the inner laser marked surface. Due to which it appears to be less attractive. The EDX analysis revealed that amount of oxygen present at the black oxidised region was 45.28 %

by weight whereas no oxidation prevailed at white region of inner laser marked surface. The surface roughness value Ra, Rq, and Rz were found to be 0.159  $\mu\text{m}$ , 0.191  $\mu\text{m}$ , and 0.761  $\mu\text{m}$  respectively. Further study on laser marking was done by defocusing the z axis by 2 mm in negative direction in order to observe its influences on laser marking characteristics which is shown in Fig. 3.33.

Fig. 3.33 shows the SEM images at laser irradiation of 12.5 W, pulse rate of 85 kHz, scan rate of 21 mm/s with defocussed position of 2 mm in negative direction. It was observed uniform oxidation in the form of nodules prevailed throughout the laser marked region with more oxidation at black region and less oxidation at the nodules. Due to oxidation of surface everywhere within the laser marked surface it appears to be more luminous as compared to laser marked surface at focussed position. Moreover, material has also been removed from the periphery of marked surface. The EDX analysis revealed that amount of oxygen present at the spot was 37.67 % by weight. Thus by analysis, it becomes evident that oxygen plays a vital role in the generation of marking contrast and it appears to be much more attractive if oxidation of surface prevailed throughout the laser marked surface. The surface roughness value Ra, Rq, and Rz were found to be 1.438  $\mu\text{m}$ , 1.744  $\mu\text{m}$ , and 6.443  $\mu\text{m}$  respectively. Attempt were also made to further study the influences of defocus distance by 2 mm in negative direction i.e. 4 mm in negative direction of z axis from the focussed point.

Fig. 3.34 shows the SEM images at laser irradiation of 12.5 W, pulse rate of 85 kHz, scan rate of 21 mm/s with defocussed position of 4 mm in negative direction. It was observed that less material was removed around the periphery of laser marked surface with less oxidation at inner marked surface. In fact, uniform oxidation does not prevail everywhere inside the laser marked region due to which it less luminous as compared to laser marked surface at defocussed position of 2 mm in negative direction. The EDX analysis revealed that amount of oxygen present at the spot of black marked oxidation inside region was 44.29 % by weight but no oxidation prevailed at other spot of inside region. The surface roughness value Ra, Rq, and Rz were found to be 0.123  $\mu\text{m}$ , 0.151  $\mu\text{m}$ , and 0.650  $\mu\text{m}$  respectively. Since uniform oxidation does not prevailed at defocus distance of 4 mm in negative direction no further study was made in negative direction.

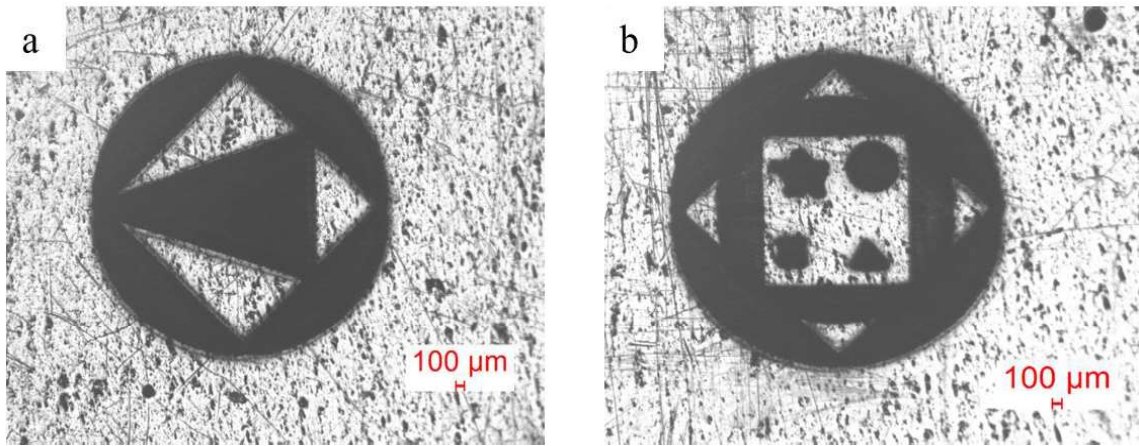


Fig. 3.35 Surfaces marked with laser at defocusing distance of 2 mm in negative direction

Fig. 3.35. (a) and (b) represent some arbitrary shaped surfaces marked with laser upon application of process variables such as laser irradiation of 12.5 W, pulse rate of 85 kHz, scan rate of 21 mm/s and duty cycle of 99 % with defocusing distance of 2 mm in negative direction. It was observed that apart from large size geometric surface as shown in Fig.3.35. (a) , very small size surface such as triangle, circle, star and rectangle can be made on the surface of workpiece at defocussed position of 2 mm in negative direction as shown in Fig. 3.35.(b).



### 3.5 Results and Discussion on Laser Marking of Equilateral Triangle Shaped Surface

The laser marking procedure necessitates the creation of a software code to carry out the procedure. An equilateral triangle shaped program with sides 3 mm and transverse feed of 8  $\mu\text{m}$ /laser stroke were fed to the CNC-controlled fiber laser system. Attempt were made to mark the surface using low laser irradiation and minimum possible time. Apart from that, some SEM images studies were also made to observe the effects of process variables on laser marked surface. Table 3.2 list the process variables lower and higher value which has been used for experimentation.

**Table 3.2 Selection of process variables and their range**

Process variables	Units	Minimum value	Maximum value
Laser irradiation	W	7.5	20
Pulse rate	kHz	50	60
Duty Cycle	%	10	90
Scan rate	mm/s	7	35

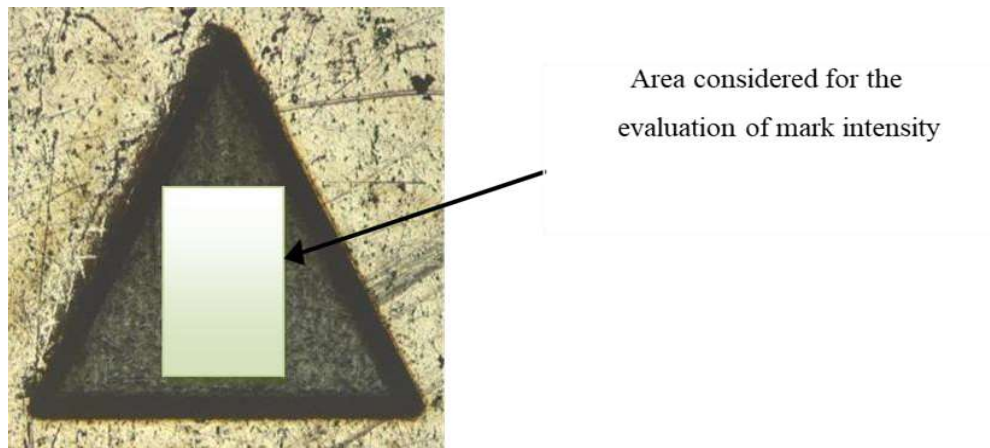


**Fig. 3.36 Area selection for evaluating mark intensity**

Fig. 3.36 display the region selection of mark quality calculation formed by the combination of vertical and transverse overlap utilized for generation of marked laser surface of equilateral triangular shaped marked laser surface.

Moreover, the average angle of equilateral triangle shaped marked laser surface was calculated using the formula given in Equation 3.4.

$$\text{Average Angle} = \left[ \frac{\text{Angle}_1 + \text{Angle}_2 + \text{Angle}_3}{3} \right] \quad \dots \text{Eq.3.4}$$

Where Angle<sub>1</sub>, Angle<sub>2</sub>, and Angle<sub>3</sub> were the angles hold by the sides of triangular-shaped marked laser surface. The average angle value gets changed due to the change of heat interaction with the work piece surface which resulted from the alteration of process variables like laser irradiation, scan rate, duty cycle, and pulse rate. The process variables change also resulted in the deviation of the marked image between the actual and predicted values. Such deviations were calculated as per Equation 3.1.

Fig. 3.37 shows the schematic diagram of marked laser surface and associated terms related to the process of laser marking for the generation of equilateral shaped laser marked surface. Fig. 3.38 exhibits a microscopic view with measurement of responses of marked laser surface based on which analysis was carried out.

The angle which is shown in Fig. 3.38 were utilized to calculate the average value using the Eq.3.4 which differs for a different set of process variables whereas the base and height of marked laser surface were utilized to find the predicted area.

The calculation of area deviation was done with the difference between the actual and predicted marked laser surfaces. The actual marked area denotes the area marked by the laser after performing the marking operation. The height and base of the triangle is measured using an optical measuring microscope in a scale of microns.

The height and base of marked laser surface were put forward to calculate the area using the formula

$$\text{Actual Marked Area} = 0.5 * \text{Base} * \text{Height} \quad \dots \text{Eq.3.5}$$

Whereas the theoretical height of an equilateral triangle is given by  $\frac{\sqrt{3}}{2} * a$

where 'a' represent the measurement of sides of an equilateral triangle which was **3 mm** which yields a predicted area value of **3897114  $\mu\text{m}^2$** .

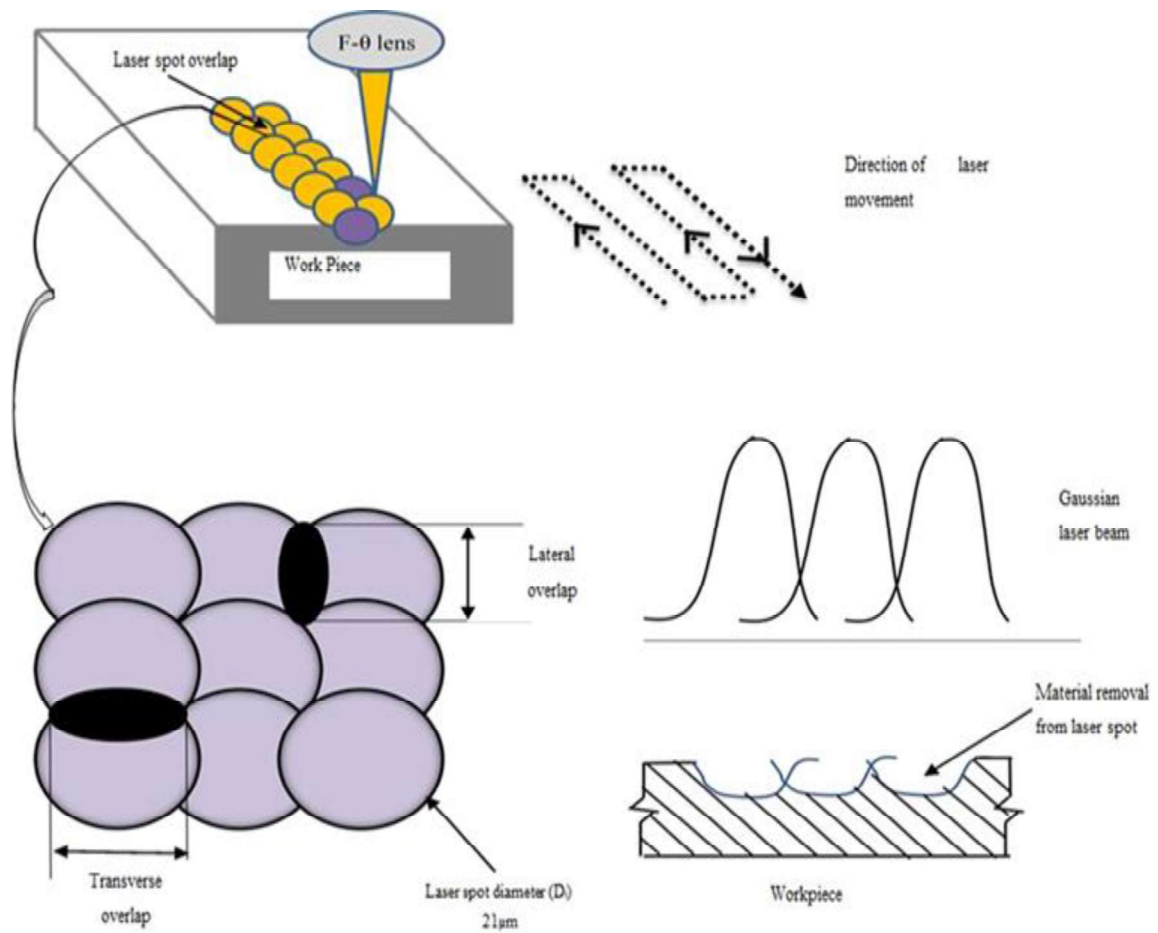


Fig. 3.37 Schematic diagram of marked laser surface and associated terms related to the process of laser marking.

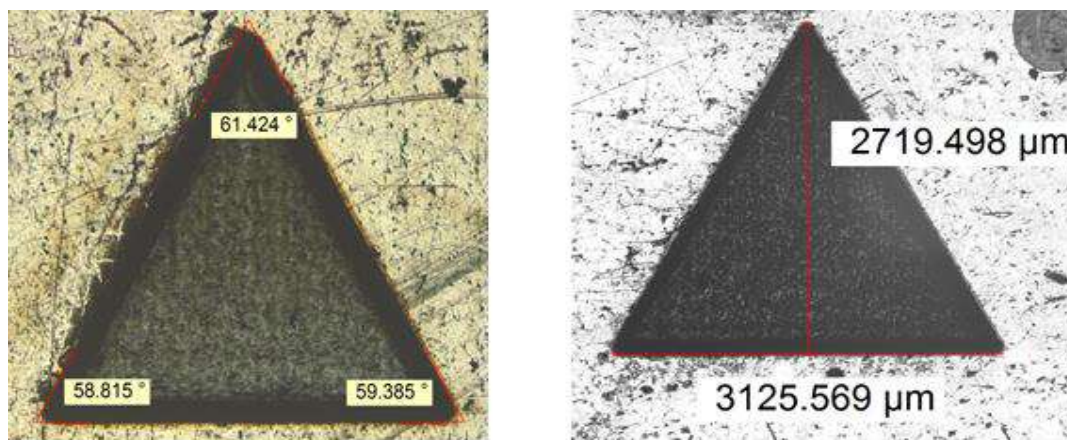


Fig. 3.38 Microscopic view of marked laser surface with measurement

### 3.5.1 Parametric Influences of Laser Irradiation and Pulse Rate on Marking Characteristics of Equilateral Triangle Shaped Laser Marked Surface

Fig. 3.39 displays the alteration of marking quality with the change of laser irradiation and pulse rate. The range of laser was allowed to vary from 7.5 W to 20 W along with the simultaneous change of pulse rate when variables like scan rate and duty cycle were fixed to 35 mm/s and 99 % respectively.

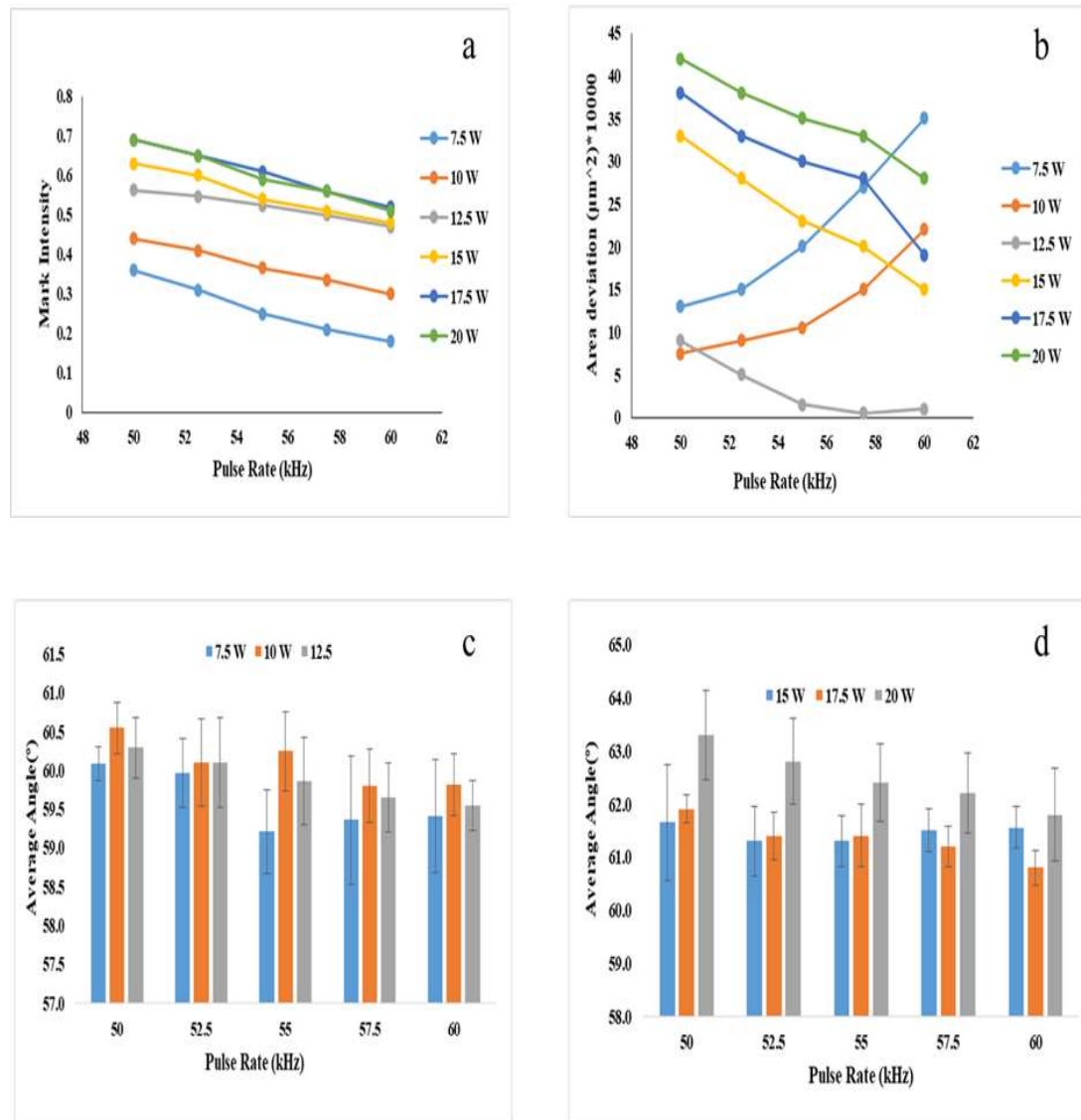


Fig. 3.39 Marking characteristics variation with change of laser irradiation and pulse rate

Studies revealed that the application of laser irradiation of 7.5 W possesses less significant marking on the surface compared to high laser irradiation of 20 W. High laser irradiation



encounters higher oxidation at ambient conditions due to which a high gray scale value is observed at the marking surface. But the use of high laser irradiation causes excessive spattering at the work piece surface which in turn increases the heat-affected in the adjoining areas with the poor outlook of the surface. High laser irradiation with a high scan rate resulted in high area deviation with angle deviation of the marked laser surface. Fig. 3.39. (a) shows that the higher mark intensity value attained was at laser irradiation of 20 W i.e. 0.70 whereas a lower mark intensity value was attained at 7.5 W laser irradiation which was 0.38. Thus from grayscale value point of view, laser irradiation seems to be a dominating factor that has a potential to higher oxidation value. The surface were also marked using a lower laser irradiation of 5 W, pulse rate of 50 kHz, scan speed of 35 mm/s, and duty cycle of 99%, but the results were quite similar to the laser unstained surface which provides limitation to the study for further research.

Fig. 3.39.(b) shows that maximum value of deviation of marked area achieved was  $440000 \mu\text{m}^2$  at a laser irradiation of 20 W, pulse rate of 50 kHz, scan rate of 35 mm/s and duty cycle of 99 % whereas minimum area deviation achieved was  $80000 \mu\text{m}^2$  at a laser irradiation of 10 W. The second lowest area deviation of marked laser surface can be seen at a laser irradiation of 12.5 W but its mark quality value was good as compared to laser irradiation of 10 W. Fig. 3.39.(c & d) display the alteration of average angle and its deviation with the change of laser irradiation and pulse rate when variables like duty cycle of 99% and scan rate of 35 mm/s remain unchanged. The largest angle deviation was recorded at 20 W laser irradiation, whereas the least angle deviation was obtained at 7.5 W laser irradiation. High power resulted in laser spattering which apart from increasing mark quality and area deviation also increases the average angle beyond  $60^\circ$ . Among all the laser irradiation taken into consideration, it was observed that laser irradiation of 12.5 W and pulse rate of 50 kHz is good in terms of the average value of marking characteristics.

Fig. 3.40 shows a microscopic image of a marked laser surface under different laser irradiation and pulse rate conditions. It was observed that laser irradiation of 7.5 W had less impact on the surface of the work piece whereas laser irradiation of 20 W had a high gray scale value of marked laser surface due to better oxidation. It also resulted in the distribution of heat in the adjoining areas which increase the unnecessary marking characteristics. The laser-stained surface at laser irradiation of 12.5 W provides better marking characteristics as compared to 7.5 W and 20 W laser marked surface. Increased

pulse rate above 60 kHz resulted in a decrease in mark quality value, as well as a reduction in angular and area deviation. Higher pulse rate resulted in the lower peak power of the laser pulsed beam. Such low peak power pulsed beam marks surface leaner with minimal increase of area and angular deviation.

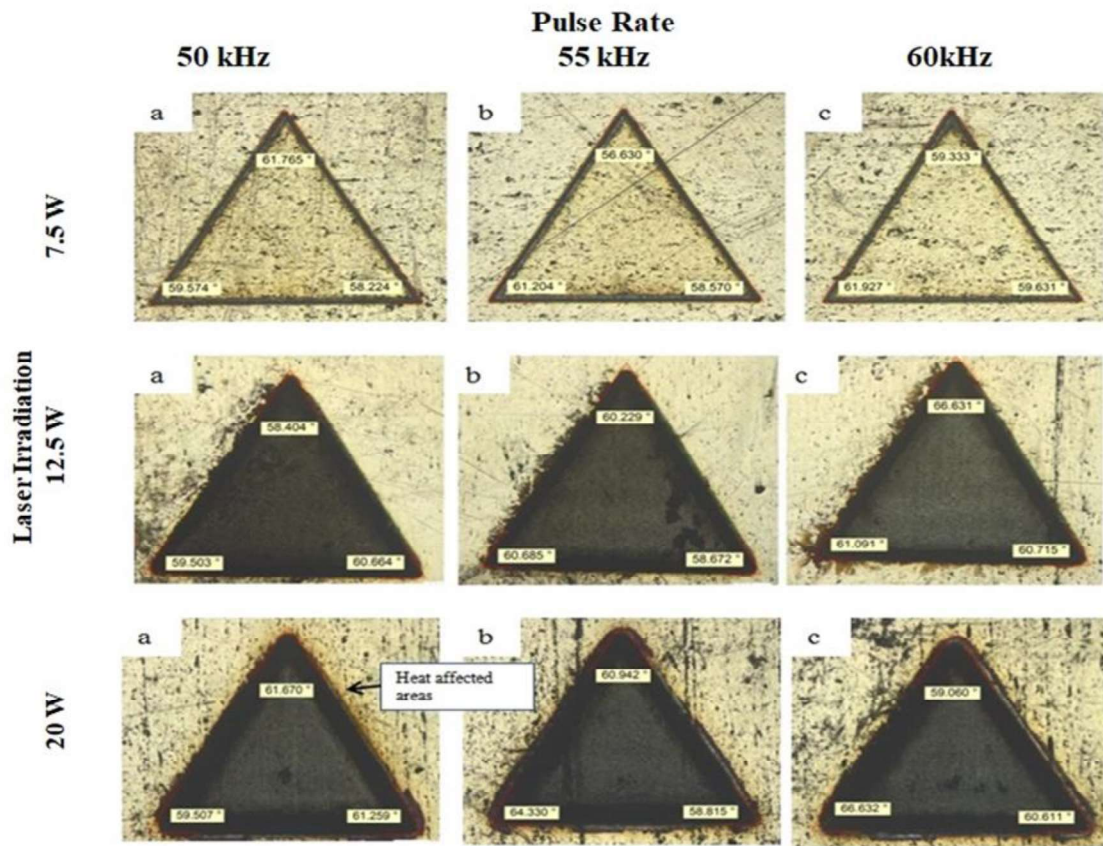


Fig. 3.40 Microscopic view of images at different laser irradiation and pulse rate

It is evident from Fig. 3.40 that laser irradiation of 7.5 W marks surface leaner and laser irradiation of 20 W cause heat affected to the surroundings of scanned area. The surface marked at 12.5 W laser irradiation, 50 kHz pulse rate, 99 % duty cycle, and 35 mm/s scan rate yielded good marking characteristics values. Apart from laser irradiation and pulse rate, efforts were also given to investigate the impact of scan rate on marking properties. The detailed analysis were shown in section 3.5.2.

### 3.5.2 Parametric Influences of Scan Rate on Marking Characteristics of Equilateral Triangle Shaped Laser Marked Surface

Fig. 3.41 exhibits the marking quality differences with the change of scan rate when laser irradiation of 12.5 W, pulse rate of 50 kHz, and duty cycle of 99 % remains unchanged.

Due to increased duration of heat interaction with the work piece surface upon implementing of scan rate from 28 mm/s to 7 mm/s, superior mark quality image appeared on the surface of stainless steel. Apart from that, it also increases the amount of time to mark the surface from 2.19 min to 2.44 min for the same size the triangular surface.

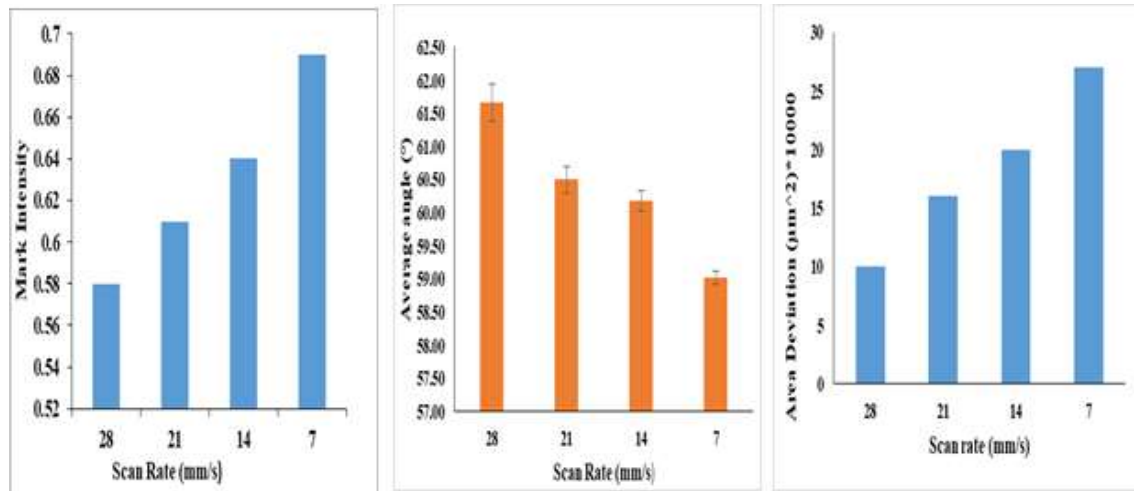


Fig. 3.41 Marking characteristics variation (a) mark intensity, (b) Angle, (c) Area deviation with change of scan rate

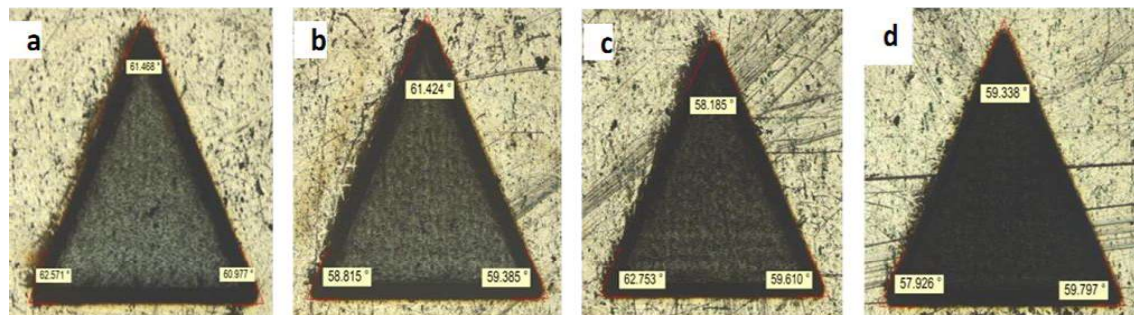


Fig. 3.42 Microscopic view of marked laser surface with change of scan rate (a) 28 mm/s (b) 21 mm/s (c) 14 mm/s (d) 7 mm/s

Experimental studies revealed that the high mark intensity value achieved was 0.70 at a scan rate of 7 mm/s whereas the average angle achieved was 61.66°. Moreover, a decrease of scan rate from 28 mm/s to 14 mm/s points an angle close to 60° which is quite an acceptable value for an equilateral triangle marked laser surface. Further, a decrease of scan rate increases more heat interaction with the work piece surface which appears to be much more precise as compared to other scan rate. But, a decrease of scan rate projected an increase in the area deviation up to 250000  $\mu m^2$  on the use of a scan rate of 7 mm/s. Moreover, the setting of a lower scan rate also increases the time required to mark the

surface. The time requirement also increases if the marked surface is larger than a 3 mm equilateral angle triangle. Thus from the marking quality point of view, a lower value of scan rate holds good but for the lesser time requirement to mark the surface, higher value of scan rate holds good.

Fig. 3.42 revealed the microscopic image of marked laser surface at a variant scan rate in order to observe the change in marking quality obtained by laser marking operation. Fig. 3.42. (a-d) were the microscopic images of marked laser surfaces corresponding to the scan rate of 28 mm/s, 21 mm/s, 14 mm/s, and 7 mm/s when other variables like laser irradiation of 12.5 W, pulse rate of 50 kHz, and duty cycle of 99 % were held constant. When the scan rate is reduced from 28 mm/s to 7 mm/s, the internal surface of a triangular-shaped marked laser surface changes from light black to deep black. As a result, grayscale value of the marked laser surface increases which provide an increase in the mark intensity value.

The present research work focused to create good quality marked laser surfaces at lesser laser irradiation and less time requirement. The studies mentioned above becomes evident that the process variables like laser irradiation of 12.5 W, 50 kHz pulse rate, 99% duty cycle, and 35 mm/s scan rate should be selected for the less possible time to mark the surface but from a marking intensity point of view, scan rate of 7 mm/s should be preferred. In addition to that, efforts were also laid to analyze the effects of the duty cycle on marking quality which are discussed in section 3.5.3.

### **3.5.3 Parametric Influences of Duty Cycle on Marking Characteristics of Equilateral Triangle Shaped Laser Marked Surface**

Fig. 3.43 displays the alteration of marking quality with the change of duty cycle when laser irradiation of 12.5 W, pulse rate of 50 kHz, and a scan rate of 35 mm/s remain unchanged. It was noticed that the decrease of a duty cycle from 99 % to 10 % resulted in the decrease of the grayscale value of marked laser surface which happens due to a decrease in on-time heat interaction with the work piece surface. As a result, there is less oxidation at the work piece surface, resulting in the drop of mark quality value of the equilateral triangle marked laser surface. On the other hand, it points to the average angle close to 60° due to lower heat interaction and as such it does not aid in the increment of length of marked laser surface. Results revealed that the deviation of laser-stained surface varies from 90000

$\mu\text{m}^2$  to 120000  $\mu\text{m}^2$  on the decrease of a duty cycle from 90 % to 10% respectively. Experimental results revealed that lower area deviation was observed at a duty cycle of 50 % but a lower grayscale value of marked laser surface restricts its use.

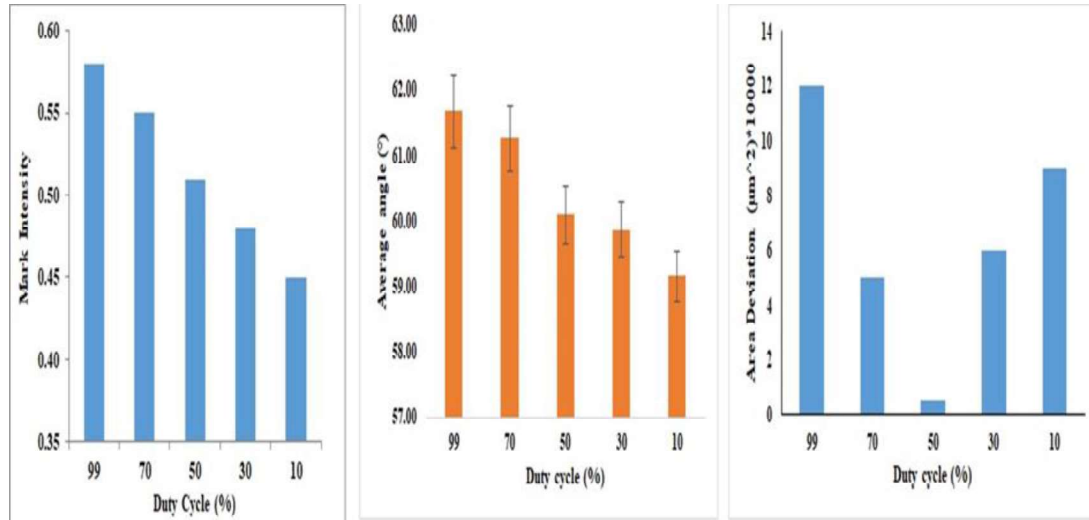


Fig. 3.43 Marking characteristics variation (a) mark intensity (b) Angle (c) Area deviation with the change of duty cycle

Based on the overall studies obtained by varying the process variables one factor at a time it can be revealed that 12.5 W laser irradiation, pulse rate of 50 kHz, scan rate of 35 mm/s, and duty cycle of 99 %, provide marking quality with good value based on less time requirement to mark the surface on grade 304 stainless steel by laser marking operation.

### 3.5.4 Some studies based on scanning electron microscope (SEM) images on marking characteristics

Fig. 3.44 showed the SEM images captured using scanning electron microscope (SU 3800) with a supply voltage of 20 kV. The top, sides and middle portion of marked laser surface at laser irradiation of 12.5 W, pulse rate of 50 kHz, duty cycle of 99 % and a scan rate of 35 mm/s were utilized to analyze the laser beam effects on marked laser surface. The EDX analysis of SEM images revealed the fact that the oxidation phenomenon has a vital role in the change of marking contrast. The area adjacent to the marked laser surface is less prone to oxidation as compared to the internal marked laser surface. Apart from material removal from the periphery of desired marked laser surface, some oxide formation has also been noticed close to the periphery as shown in Fig. 3.44. (b & d). The internal marked laser



surface as shown in Fig. 3.44.(c) which has been utilized for the analysis was subjected to many small microcracks which have zero oxidation value as revealed from EDX analysis. The area apart from micro-cracks has some oxidation which helps in the generation of the required grayscale value of marked laser surface. When the scan rate is reduced from 35 to 7 mm/s, the interior surface texture changes abruptly, and the development of different oxides raises the grayscale value of the marked laser surface

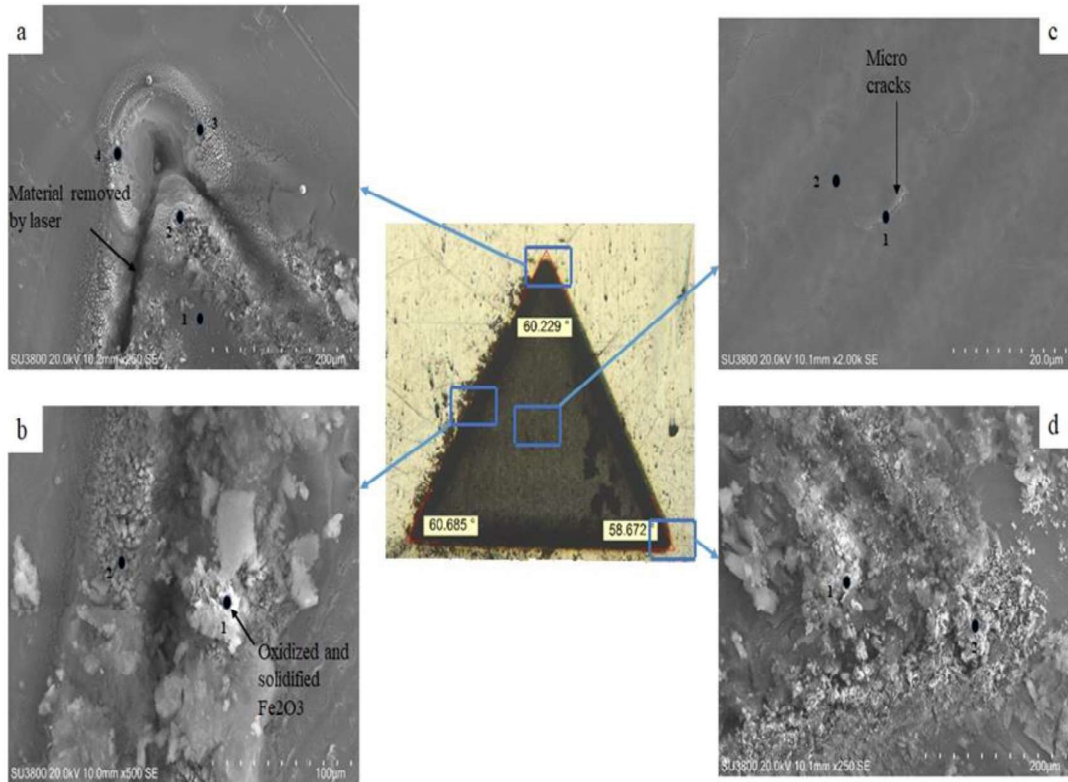


Fig. 3.44 SEM images of triangular marked laser surface at different location

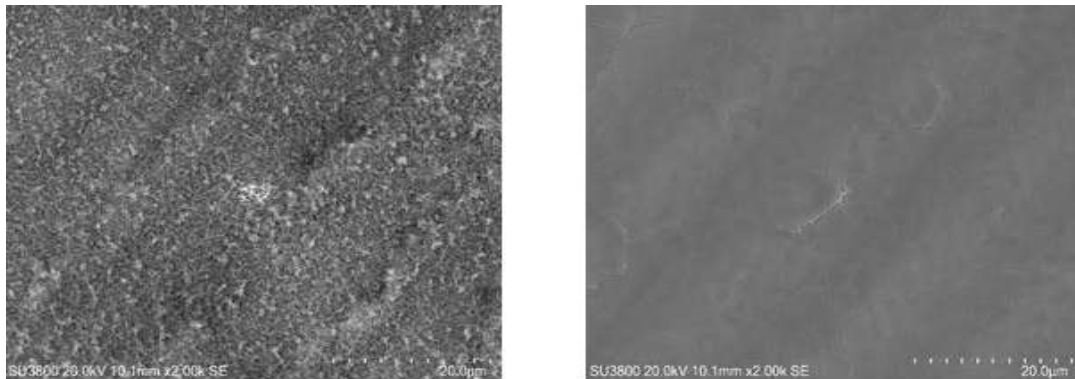


Fig. 3.45 SEM images of marked laser surface at different scan rate (a) 7 mm/s and (b) 35 mm/s

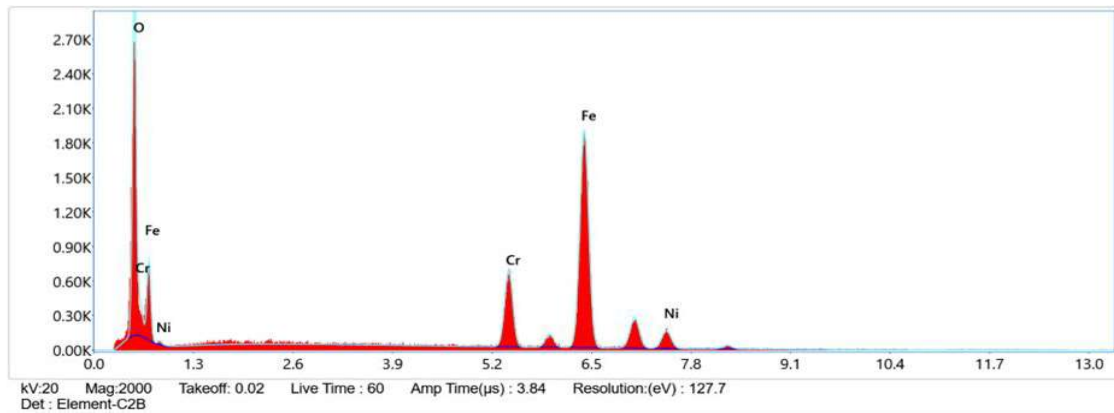


Fig. 3.46 EDX analysis of triangle marked laser surface as shown in Fig. 3.44 (c) site no.2

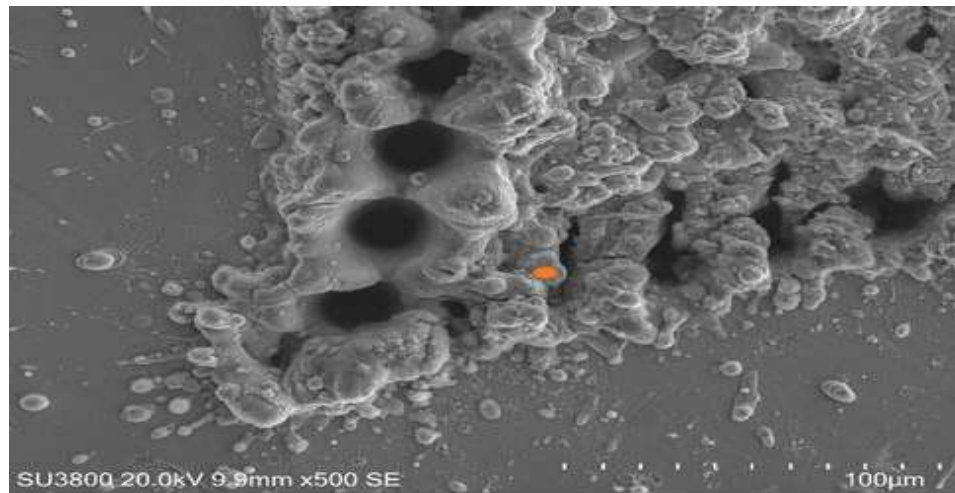


Fig. 3.47 SEM images of the surface at defocused position

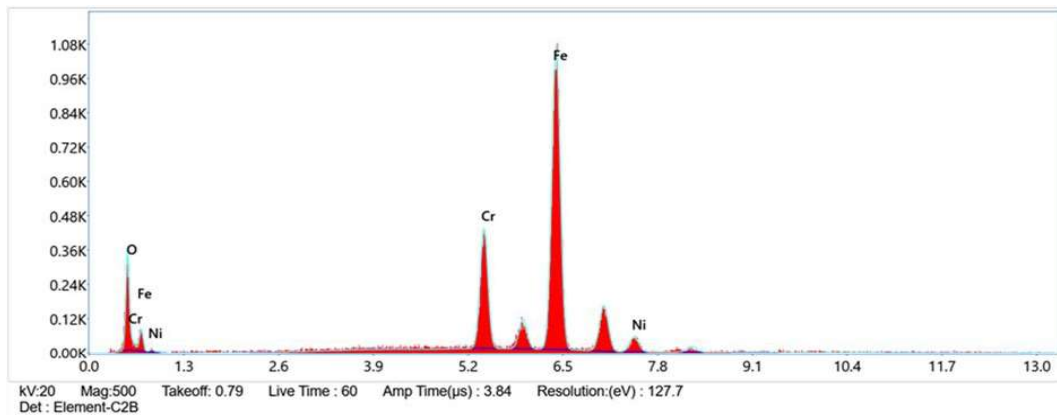


Fig. 3.48 EDX analysis of the spot as shown in Fig. 3.47

Fig. 3.45. (a) and (b) represents the SEM images of internal geometric laser marked surface at scan rate of 7 mm/s and 35 mm/s . The surface structure at lower scan rate provides higher oxidation as compared to scan rate of 35 mm/s. The Fig.3.45 also reveals the direction of laser travel and oxidation of materials at all sides.

Fig. 3.46 shows the EDX analysis of marked surface which provides illustration that the oxidation phenomena is responsible for the change of marking contrast. The surfaces were analyzed at a magnification of 250 X with the working voltage of 20 kV. The spot size used was 50 micron for EDX analysis. The spectrum analysis revealed that oxide layer were present inside the laser marked surface along with elements iron (Fe), nickel (Ni) and chromium (Cr).

The surface structure of the work piece also changes if marking were carried out at a defocused condition. The surface marked at the defocused condition resulted in spot material removal from the periphery of the laser-stained surface as revealed by SEM analysis. In fact, the EDX analysis also revealed that the oxidation value gets decreased as compared to the surface marked at the focused condition. The SEM images along with EDX analysis of the sample marked at the defocused condition are shown in Fig.3.47 and 3.48 respectively.

The studies carried out on marking surfaces reveals the fact that the sample should be set at the focused condition in order to have high marking contrast. However, marking at the defocused condition ensures the least oxidation with less material removal from the periphery of the marked portion.

The paper also showed the amount of time required to mark the different triangular sized surfaces ranging from 0.5 to 4 mm equilateral triangle-shaped marked laser surface. The surfaces were marked at 12.5 W laser irradiation, 50 kHz pulse rate, 99 % duty cycle, and 35 mm/s scan rate in order to observe the change of image quality on the surface of stainless steel 304 during laser marking operation as shown in Fig. 3.49.



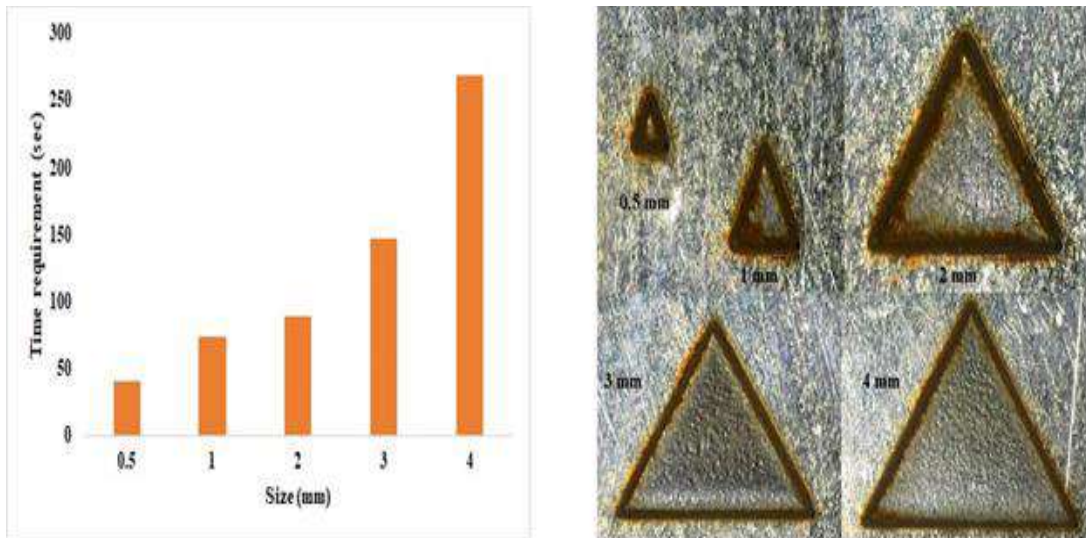


Fig. 3.49 Requirement of time to mark the different triangular sized surface

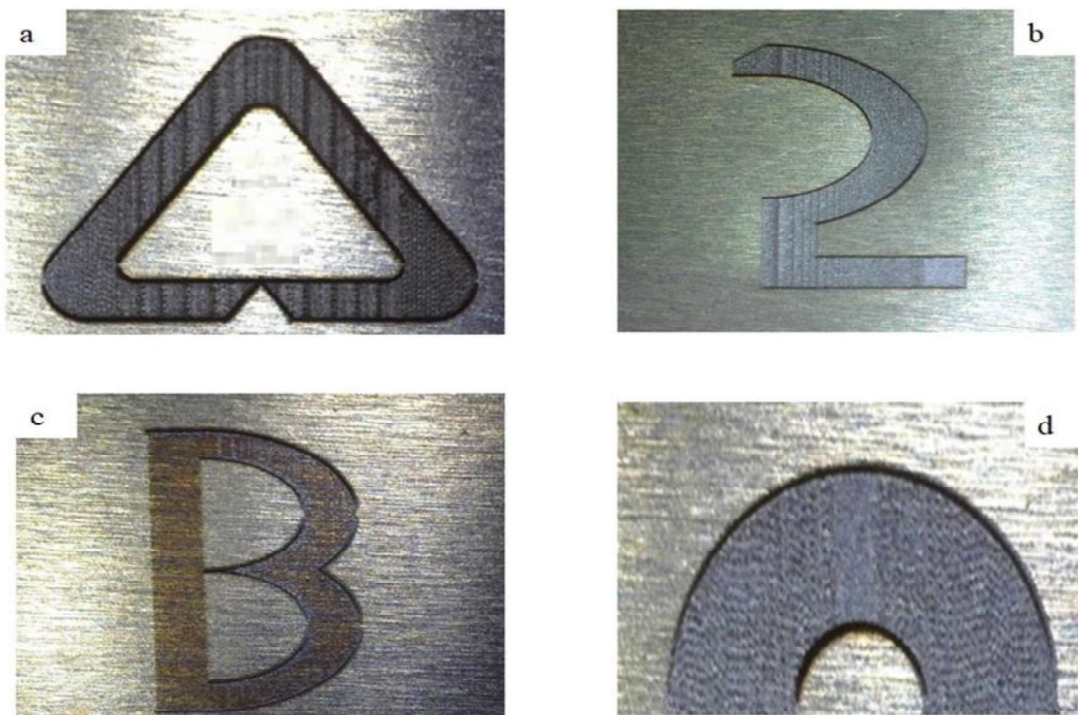


Fig. 3.50 Different geometric marked laser surface for setting the scan rate (a) at 7 mm/s (b) at 21 mm/s (c) at 35 mm/s (d) at 7mm/s

It was observed that the smaller the size of laser marked surface, the oxidation at the periphery of the marked portion gets dominant to the internal analyzed surface which in turn yields a higher mark quality value as compared to the surface which was marked at a

higher side length i.e. 4 mm. Apart from that, the visibility of heat-affected in the surrounding areas was much more significant in smaller sized triangular laser-stained surfaces as compared to surfaces marked at a higher side range. The studies presented in the thesis is not only confined to mark triangular shaped image but also can be used to any other geometric shaped as shown in Fig. 3.50.

Fig. 3.50 exhibit the different geometric laser-stained surface which can be used for other practical applications using laser irradiation of 12.5 W, pulse rate of 50 kHz, duty cycle of 99 % and variable scan rate varying from 7mm/s to 35 mm/s. Apart from that, other forms of geometric laser marked surface can also be produced using the same process variables settings. Attempt has also been made to make other geometrical shapes such as pentagon and hexagon using the process variables settings obtained by one factor at a time (OFAT) method as discussed below:

Fig.3.51 and 3.52 are the microscopic images of regular pentagon of sides and regular hexagon marked at laser irradiation of 12.5 W, pulse rate of 50 kHz, duty cycle of 99 % and variable scan rate varying from 35 mm/s respectively. Initially the average length of pentagon and hexagon were given as 2259.02  $\mu\text{m}$  and 2079.4  $\mu\text{m}$  respectively whereas average angle of pentagon and hexagon were 108° and 120° respectively. After carrying out the laser marking operation on pentagon and hexagon as shown in Fig.3.51 and Fig.3.52, they were used to analyses the variation in area deviation using Eq.3.1 and angle deviation using Eq.3.6.

$$\text{Angle deviation} = | \text{Standard angle} - \text{Measured average angle} | \quad \dots\text{Eq.3.6}$$

$$\text{Area of regular pentagon} = \frac{1}{4} \times \sqrt{5(5 + 2\sqrt{5})} \times a \times a \quad \dots\dots\text{Eq.3.7}$$

$$\text{Area of regular hexagon} = \frac{3\sqrt{3}}{2} \times a \times a \quad \dots\dots\text{Eq.3.8}$$

Where ‘a’ represent the sides of polygon

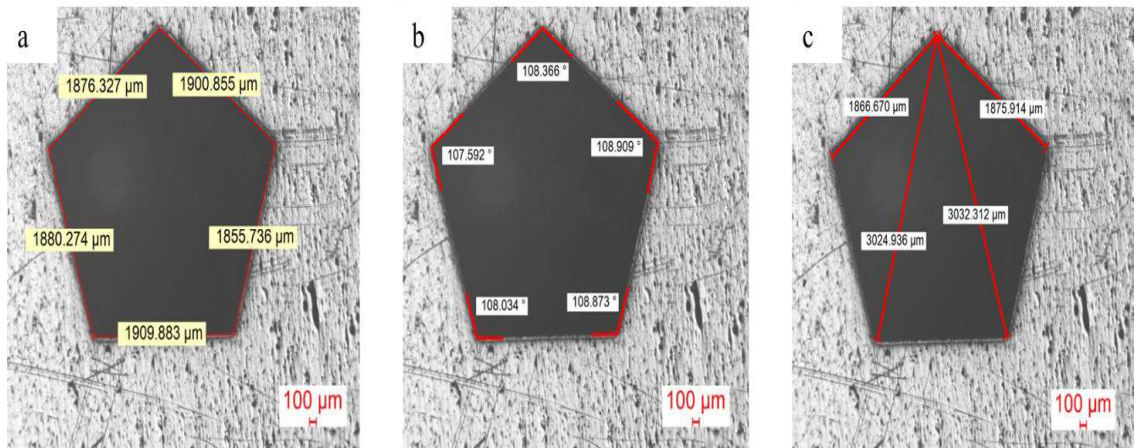


Fig.3.51 Laser marked surface of pentagon at better obtained process variables

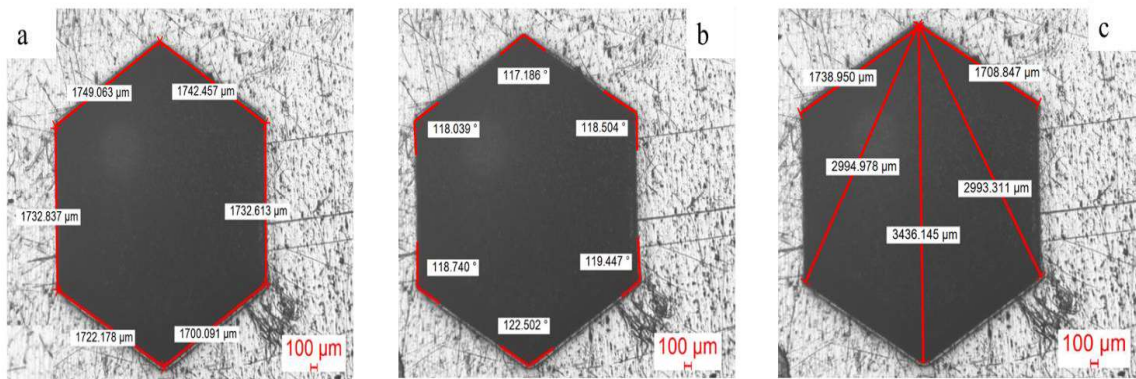


Fig.3.52 Laser marked surface of hexagon at better obtained process variables

Upon analysis the area deviation of regular pentagon and hexagon using equation 3.1, it was observed that area deviation of pentagon was  $2.6689 \times 10^6 \mu\text{m}^2$  and that of hexagon was  $3.47705 \times 10^6 \mu\text{m}^2$  whereas angular deviation of pentagon was  $0.354^\circ$  and that of hexagon was  $0.931^\circ$  respectively.

The error percentage has also been analyzed for laser marked surface of equilateral triangle, regular pentagon and regular hexagon after analyzing the average angle held by the sides of figures. After measuring through LEICA optical microscope, it was observed that the average angle for equilateral triangle was  $59.86^\circ$ ,  $108.346^\circ$  for regular hexagon,  $119.069^\circ$ . Upon analysis, it was observed that the error (%) for equilateral triangle was 0.233%, 0.32%, and 0.77% respectively.

### 3.6 Results and Discussion on Laser Marking of Circular Shaped Surface

Fig.3.53 shows the effects of transverse feed on mark intensity of circular shaped image when other process variables such as laser irradiation of 10 watt (W), pulse rate of 50 kHz, scan rate of 15 mm/s and duty cycle of 30% were held constant. Experiment results revealed that the lower value of transverse feed per laser stroke of laser beam, better value of mark intensity of circular shaped of marked region was obtained and vice versa. The transverse overlap factor is responsible for uniformity and higher value of mark contrast. Among the used transverse feed value of 4-14  $\mu\text{m}/\text{laser stroke}$  value, the transverse feed of 4  $\mu\text{m}$  per laser stroke provides uniformity and higher value of mark intensity. The use of transverse feed value below 4 $\mu\text{m}$  resulted in the non-uniformity of circular marked image, marked it unsuitable for further processed.

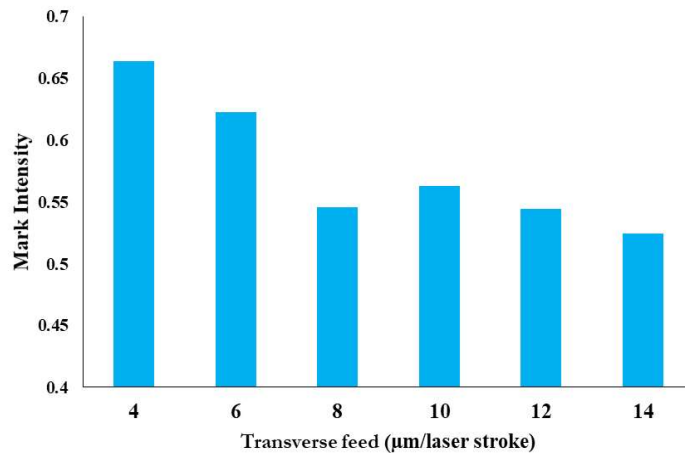


Fig.3.53 Deviation of Mark intensity with Transverse feed

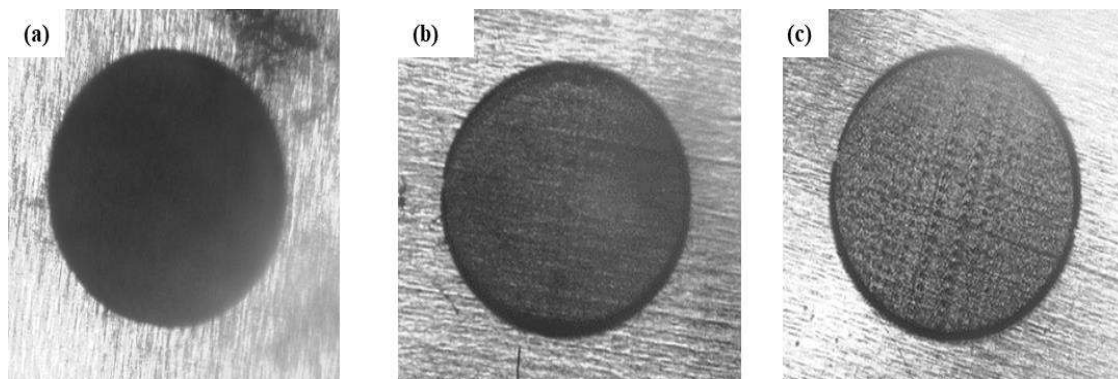


Fig.3.54 Microscopic view of laser marked surface at variable transverse feed per laser stroke (a) 4  $\mu\text{m}/\text{laser stroke}$  (b) 8  $\mu\text{m}/\text{laser stroke}$  (c) 12  $\mu\text{m}/\text{laser stroke}$ .

Fig.3.54.(a-c) shows the photographic view of marked surface at transverse feed value of 4  $\mu\text{m}/\text{laser stroke}$ , 8  $\mu\text{m}/\text{laser stroke}$  and 12  $\mu\text{m}/\text{laser stroke}$  on surface of stainless steel 304 which were captured by Leica Application Suite software of 1.25X magnification factor lens. The images clearly shows the change of marked surface from less oxidation to high oxidation upon decrease of transverse feed from 12  $\mu\text{m}/\text{laser stroke}$  to 4  $\mu\text{m}/\text{laser stroke}$ . Fig.3.54. (a), was uniformly and deeply marked with mark intensity value of 0.70. Since the laser marked surface was uniformly marked at a transverse feed value was set at 4  $\mu\text{m}$  per laser stroke so to observe the variation of marking color upon change of process variables transverse feed of 4  $\mu\text{m}/\text{laser stroke}$  was held constant while generating circular shaped laser marked surfaces. The variation of marking characteristics with change of other process variables were discussed in the subsequent subsection.

### **3.6.1 Influences of Laser irradiation on Marking Characteristics of Circular Shaped Laser Marked Surface**

Fig.3.55 shows the effects of laser irradiation on marking characteristics such as mark intensity, circularity and surface roughness value ( $R_a$ ) when process variables such as pulse rate, duty cycle, and scan rate were fixed at 50 kHz, 30%, 15 mm/s respectively. It was observed from Fig.3.55.(a) that the increase in laser irradiation between 10 -15 watt (W) resulted in the increase of mark intensity with change of color from light yellow to deep black. Higher energy laser pulse caused material removal with surface oxidation of laser irradiated zone. The average value of laser irradiation i.e. at 12.5 W provided us with higher intensity value of 0.70. Furthermore, increase of laser power beyond 17.5 W resulted in the formation of non-uniform heat affected zone (HAZ) around the periphery of the marked portion of the work piece.

Fig.3.55.(b) shows the variation of circularity of circular marked surface with respect to laser power. It was observed that the increase in laser beam power increases the pulse energy which in turn increases the length of marked area. The circularity is the ratio of minimum to maximum diameter of marked surface. The maximum marked length was minimum when laser power varies from 10-15 W but increase in laser irradiation beyond 15 W resulted in the formation of heat affected zone and increased the marked length which resulted in the decrease of circularity value.

Fig.3.55.(c) shows that increased laser power resulted in the increase of surface roughness



value (Ra) upto 12.5 W beyond which it decreases. Increased laser power resulted in the increase of rough surface area which occurred due to lower transverse overlap of laser spot. Higher transverse overlap results in the uniformity of surface area and thus surface roughness value decreased.

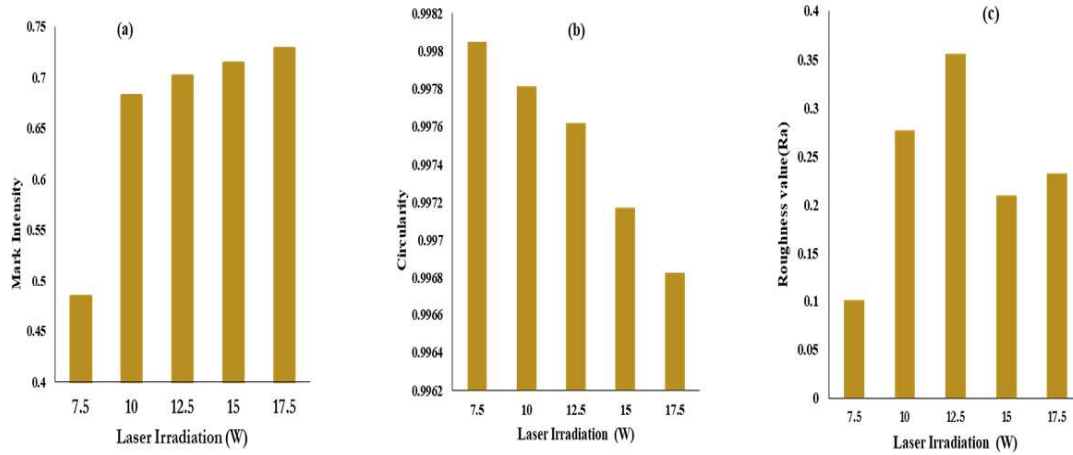


Fig.3.55 Variation of marking characteristics with change of laser irradiation

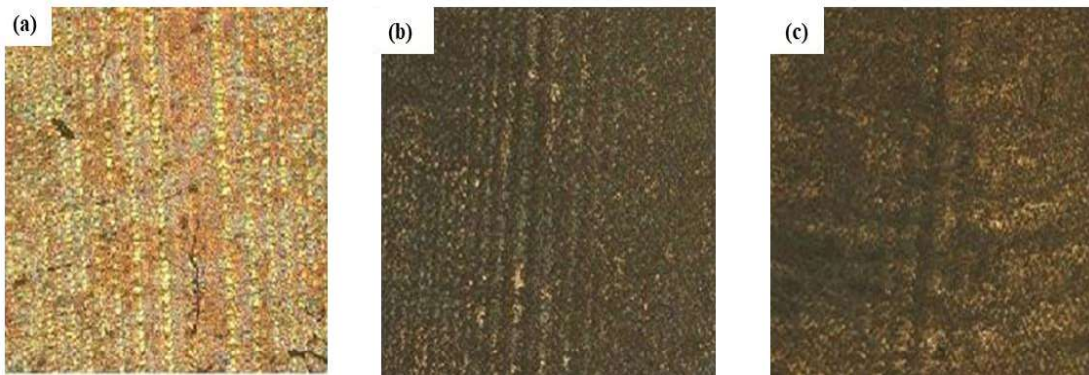


Fig.3.56 Microscopic view of laser marked surface at variant laser irradiation (a) 7.5 W, (b) 12.5 W, (c) 17.5 W

Fig.3.56 shows the surface topography of the laser marked surfaces which were captured using OLYMPUS STM 6 with 5X magnification optical lens in order to look after the variation of image quality under changing laser irradiation. Fig.3.56. (a-c) are the images of marked surface at laser power of 7.5 W, 12.5 W and 17.5 W respectively. The surface quality of inner marked surface changes from light yellow to black upon change of laser irradiation which is due to higher oxidation prevailed at high laser irradiation. Keeping

lower value of laser irradiation of 10 W constant, other process variables were varied in order to observe the change in marking characteristics as discussed in following subsection.

### 3.6.2. Influences of Pulse rate on Marking Characteristics of Circular Shaped Laser Marked Surface

Fig.3.57 shows the effects of pulse rate on marking characteristics of laser marked surface when other process variables such as laser irradiation of 10 W, duty cycle of 30%, scan rate of 15 mm/s were kept constant. Fig.3.57.(a) shows that higher value of mark intensity was achieved at minimum value of pulse frequency and vice-versa. Lower value of pulse frequency increased the peak power of pulsed laser beam when other variables such as laser power and pulse duration were kept constant. The peak power of laser beam possess the high energy and temperature at focused surface of work piece, penetrated deeply and higher oxidation phenomena led to the increase the mark intensity value of marked image.

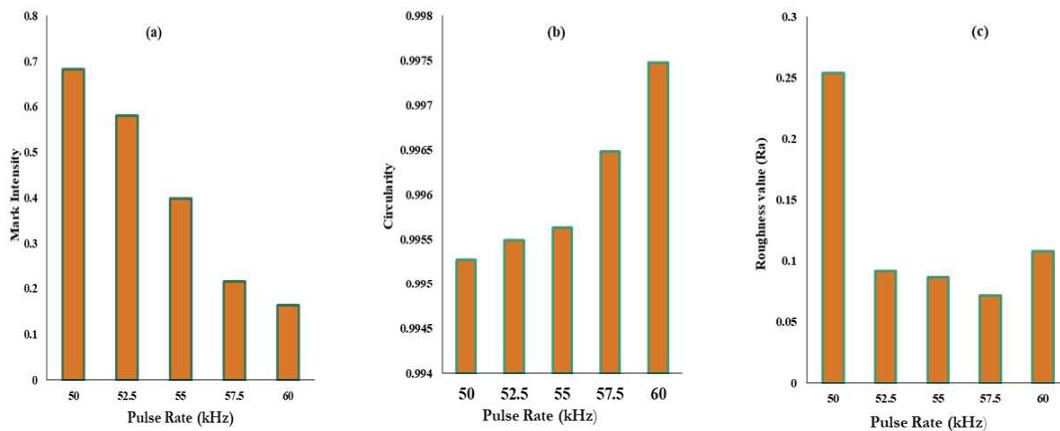


Fig.3.57 Variation of marking characteristics with change of pulse rate

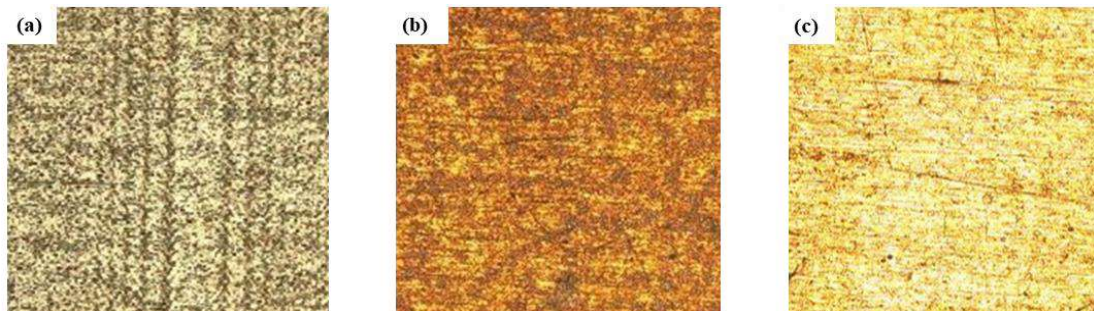


Fig.3.58 Microscopic view of laser marked surface at variant pulse rate (a) 50 kHz (b) 55 kHz (c) 60 kHz

Fig.3.58.(a-c) shows the microscopic view of laser marked surface at pulse rate of 50 kHz, 55 kHz, and 60 kHz respectively. The modification of laser marked surface from light black to orange to yellow upon change of pulse rate symbolizes the higher influences in surface modification. But since pulse rate of 50 kHz provides high value of mark intensity so it was held constant and further study was made upon change of other process variables.

Fig.3.57.(b) shows the variation of pulse rate on circularity of laser marked image. Increased pulse frequency resulted in lower peak power of laser beam. Due to which, the maximum marked length per laser stroke decreases and it resulted in the increase of circularity value. It was observed that high value of circularity of 0.9974 was achieved at pulse rate of 60 kHz.

Fig.3.57.(c) shows the variation of surface roughness value with change of pulse rate. Increased pulse rate has lower peak power of laser pulse. The low peak power resulted in the decrease of material removal from work piece and lower impact at workpiece surface which resulted in the decreases of surface roughness value. Thus based on above study laser irradiation of 10 W, and pulse rate of 50 kHz provides better results and it were held constant and further studies were made in the following subsection.

### **3.6.3 Influences of duty cycle on Mark intensity, Circularity and Surface roughness value (Ra)**

Fig.3.59 shows the variation of marking characteristics with duty cycle when other process variables such as laser irradiation, pulse rate and scan rate were fixed at 10 W, 50 kHz and 15 mm/s respectively. Fig.3.59.(a) shows that the increase of duty cycle increase the mark intensity approximately linearly from 20% to 30 %. Further, increase of duty cycle beyond 30% does not shows much increase of mark intensity. Increased duty cycle increases the laser beam operating condition due to which laser gets more time to interact with the workpiece surface which provides better oxidation and resulted in good value of marking intensity of circular shaped image.

Fig.3.59. (b) represents the variation of circularity with change of duty cycle. It was observed that the higher value circularity of 0.993 was achieved at duty cycle of 20 % and



increase of duty cycle beyond 20 % resulted in decrease of circularity value. It occurs due to increases of on time heat interaction which is responsible for the increase of length of marked circular image.

Fig.3.59.(c) shows the increase of duty cycle resulted in the increase of surface roughness value. Higher value of duty cycle increased the surface area roughness (Ra) due to increase of oxidation at workpiece surface. The surface roughness value rises rapidly from 20 % to 30% of duty cycle above which shows a gradual increase in surface roughness value (Ra).

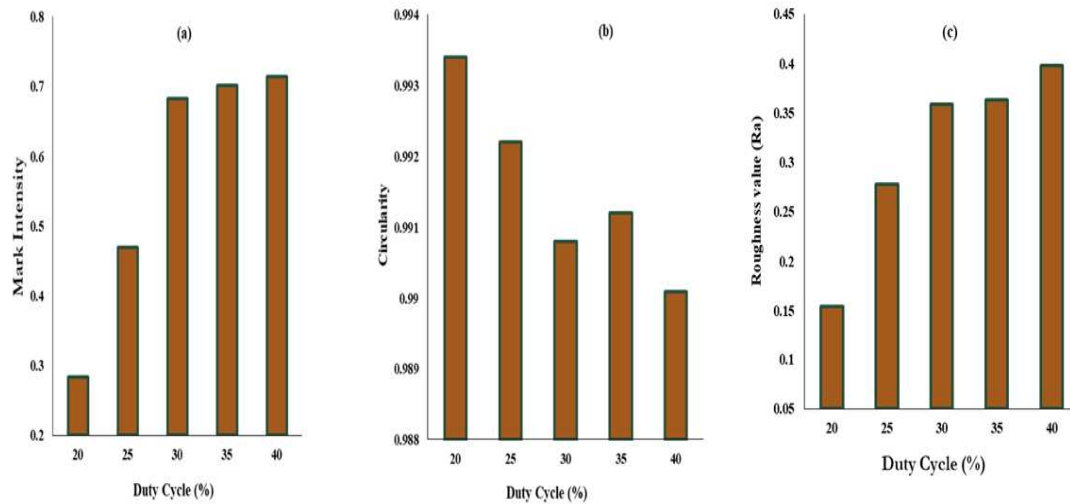


Fig.3.59 Deviation of mark intensity with duty cycle

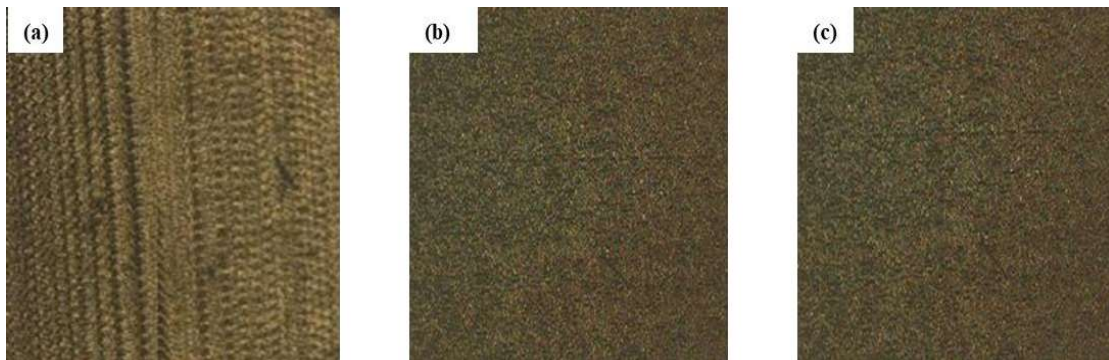


Fig.3.60 Microscopic view of laser marked surface at variant duty cycle (a) 20% (b) 30% (c) 40%

Fig.3.60. (a-c) are the microscopic image of laser marked surface at a duty cycle of 20%, 30% and 40% respectively. Microscopic view show the modification of laser marked surface with change of duty cycle. Marked surfaces of Fig.3.60.(a) was non uniform with

lower intensity value is less as compared to Fig.3.60.(b) and Fig.3.60.(c). Furthermore, higher value of duty cycle above 40% adds value to the mark intensity but it also cause side areas of circular marked surface to be heat affected.

#### **3.6.4. Influences of Scan rate on Marking Characteristics of Circular Shaped Laser Marked Surface**

Fig.3.61 shows the variation of scan rate on marking characteristics when the process variables such as laser irradiation, pulse rate, duty cycle were fixed at 10 W, 50 kHz, 30% respectively. Fig.3.61.(a) shows that higher value of scan rate provides less time of heat interaction with the work piece surface which resulted in the decrease of surface oxidation, penetration depth and vice versa. It was observed that higher value of mark intensity of 0.71 was achieved at scan rate of 5 mm/s and lower value of mark intensity at scan rate of 25 mm/s.

Fig.3.61. (b) shows the variation of circularity of circular shaped laser marked surface with change of scan rate. Increase of scan rate has less heat interaction with the work piece and as such heat produced to mark the surface becomes less. Due to which, increased scan rate has less contribution towards the increment of maximum length per laser stroke of circular image, which resulted in the increase of circularity value.

Fig.3.61.(c) shows variation of surface roughness (Ra) with change of scan rate. It was observed that the increase of scan rate from 5 mm/s to 25 mm/s resulted in the increase of surface roughness value from 0.2  $\mu\text{m}$  to 0.58  $\mu\text{m}$ . The roughness value (Ra) increases gradually between 10 mm/s to 20 mm/s of scan rate beyond which it increases drastically. Increased scan rate resulted in the formation of non-uniform oxidation on marked surface which were responsible for the increment of surface roughness value (Ra).

Thus based on studies using one factor at a time on circular laser marked surface, it was observed that limited colors were produced at the surface of stainless steel 304 upon varying process variables within the desired range. Thus appropriate method needs to be followed to produce variety of colors on laser marked surface so that the produced logos or part marking becomes much more attractive.

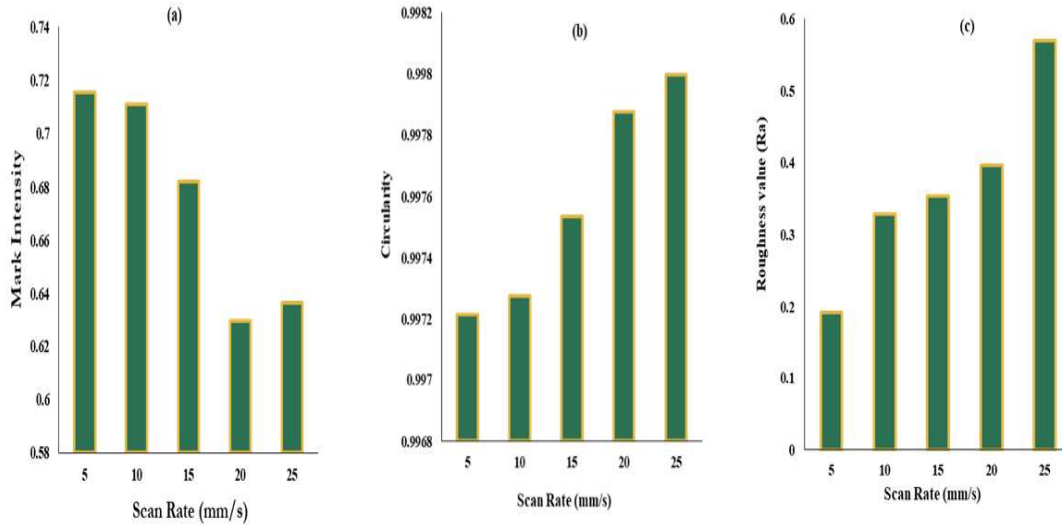


Fig.3.61 Variation of marking characteristics with change of scan rate

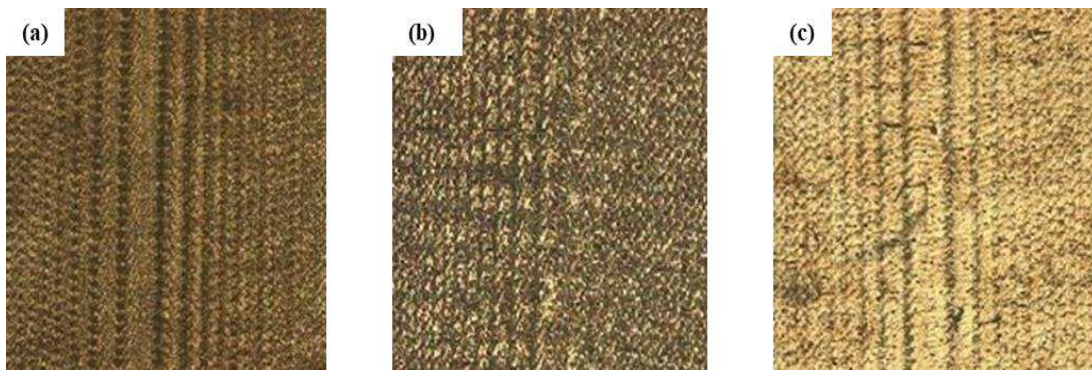


Fig.3.62 Microscopic view of laser marked surface at variant scan rate (a) 5 mm/s (b) 15 mm/s (c) 25 mm/s

Fig.3.62. (a-c) represents the microscopic view of the modification of laser marked surface with change of scan rate. The laser marked surface of Fig.3.62.(a) was deep marked with better mark intensity at lower value of scanning speed of 5mm/s. Scanning speed above 5mm/s shows the decrease in mark intensity value of image due to decrease of oxidation phenomena.

### 3.7 Outcomes of the Present Research Work

The laser marked surface produced through multi diode pumped fiber laser is much helpful in developing the logo of any organisation for making distinction of their products in a present day competitive market. The study content provides the possible combination of

process variables for the generation of laser marked surface in a less time. Apart from that, certain observations were encountered which may be summed up as follows:

- i. Surface Oxidation plays a crucial role in the generation of marking contrast when process were carried out at normal atmospheric condition.
- ii. Decrease in transverse feed from 8  $\mu\text{m}$ /laser stroke to 2  $\mu\text{m}$ /laser stroke resulted in higher laser spot overlap region in both horizontal and vertical directions which contributes to the higher oxidation and deep marks at the surface of workpiece whereas increase of transverse feed from 8  $\mu\text{m}$ /laser stroke to 14  $\mu\text{m}$ /laser stroke resulted in light marking. The surface resulted in line marking if transverse feed exceeds beyond 21  $\mu\text{m}$ /laser stroke.
- iii. The use of assist gas resulted in the dissipation of heat from the focussed zone making the surface quality poor with increase of width of laser marked surface.
- iv. Laser irradiation is more dominating than pulse rate, scan rate and duty cycle in providing the marking contrast. Higher laser irradiation not only increase oxidation but also increase width and HAZ thickness.
- v. Increased pulse rate led to the development of low peak power at laser spot region when other variables were kept constant. It contributes lower to the increase in width and depth of marked surface with fine surface finish.
- vi. Increased scan rate resulted in reduction of time requirement with lean marking at surface of stainless steel 304. Studies revealed that scan rate lower than 21 mm/s provides better results in case of mark intensity and scan rate above 21 mm/s provides minimum increase in width
- vii. Increase of laser pass beyond one resulted in the increase of time requirement to mark the surface of workpiece. It also resulted in the considerable increase in width and depth. Apart from that, adjoining areas also get heat affected due to more time of heat interaction with the surface.
- viii. Defocusing distance by 2 mm in negative z direction provides uniform oxidation throughout the laser marked surface but it increases the area deviation whereas movement of z axis by 2 mm in positive direction produces light marking and does not able to mark the surface above it.
- ix. The extremities of geometrical surfaces on SS304 were confined to high material removal with oxidation as compared to interior laser marked surface as revealed by SEM images with EDX analysis.

- x. To produce better marking characteristics of any geometric shapes using low power and minimum time, laser irradiation of 12.5 W, pulse rate of 50 kHz, duty cycle of 99 % and scan rate of 35 mm/s at focussed condition of workpiece provides better results.
- xi. The variation of process variables within the suitable range resulted in the production of limited colours at the surface of SS 304. But in order to produce desired prominent colours, appropriate method should be developed to accomplish the task.

### **4. MODELLING AND ANALYSIS OF FIBER LASER MARKING OF STAINLESS STEEL 304 BASED ON RESPONSE SURFACE METHODOLOGY**

A statistical technique called response surface methodology (RSM) examines the connections between a number of explanatory variables and one or more response variables. In 1951, George E. P. Box and K. B. Wilson presented the methodology. RSM is an empirical model that uses statistical and mathematical methods to establish a relationship between the response and the input variables. Because alternative approaches, like the theoretical model, might be highly difficult to apply, time-consuming, ineffective, prone to errors, and unreliable, RSM proved quite helpful. RSM's primary goal is to find the best response through a series of planned tests. To do this, Box and Wilson recommend utilising a second-degree polynomial model. They employ this model even though they are aware that it is merely an approximation since it is simple to estimate and apply, especially in situations when little is known about the process. Response surface methodology (RSM) uses desirability function analysis to optimise factorial variable settings so that the response meets a desired maximum or minimum value. RSM is a sort of augmentation where additional treatments are added to focus the effects and increase the prediction power of the model. It is based on the findings of a factorial research (screening, followed by a three-level factorial). A central composite design is a structure in which the additional treatments are positioned both outside and inside the factorial space (star points and centre point, respectively). Plotting the response surface can be done using the equation that results from the upgraded model analysis using multiple regression. Contour plots indicate locations where a reaction exhibits the same magnitude in addition to optimal levels for other variables.

#### **4.1 Modeling and Analysis of Fiber Laser marking of SS 304**

A program of equilateral triangle of 3 mm sides were fed into the I-Mark software of version 8.4.1 of CNC controlled diode pumped fiber laser for performing marking

operation on the surface of stainless steel 304. The marked surface and its schematic view is shown in Fig. 4.1

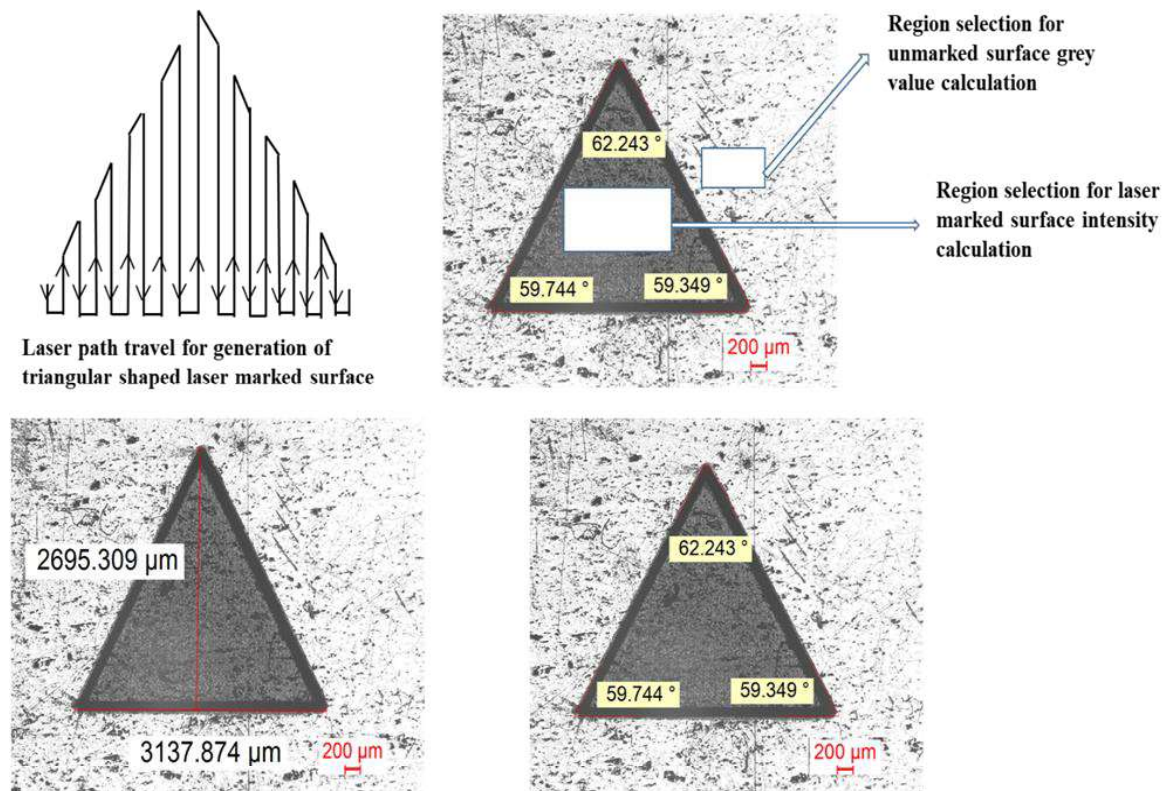


Fig.4.1 Schematic view of laser travel for the generation of equilateral shaped laser marked surface along with measurement of responses.

Fig. 4.1 were the triangular marked surface with measurement of responses obtained by Leica optical microscope (DM 2500 M; Leica Microsystem Limited) using 1.25 X magnification lens for the measurement of height, width, and angle in order to have angle and area deviation of the respective marked surface. The equipment has the resolution of 1 micron. The marked surface quality i.e. mark intensity was analyzed using grey value obtained through MATLAB software. Mark intensity is the visual distinction between the apparent brightness of a marked and unmarked section which was calculated by generating the grey level of region of marked and unmarked surface, and then computing the value in Eq. 2.1.

### 4.1.1 Experimental Planning

In this laser marking operation there is no supply of assist gas and the number of pass is fixed to one. Based on the pulsed diode pumped fiber laser specification, trial experiments were conducted for having an appropriate range of process variables for having better quality laser marked surface.

**Table 4.1** Process Parameter and their levels

Variables	unit	symbol	Levels				
			-2	-1	0	1	2
Laser irradiation ( $X_1$ )	W	LP	7.5	10	12.5	15	17.5
Pulse rate ( $X_2$ )	kHz	PF	50	52.5	55	57.5	60
Duty Cycle ( $X_3$ )	%	DC	10	30	50	70	90
Scan rate ( $X_4$ )	mm/s	SS	7	14	21	28	35

Table 4.1 list the process variables and their range which was obtained based on one factor at a time method which is then further utilized for developing the mathematical model using response surface methodologies and then analyzed the optimum results using the desirability function analysis. The analysis carried out using the above range of process variables based on one factor at a time (OFAT) revealed the fact that the laser irradiation of 12.5 W, pulse rate of 50 kHz, duty cycle of 90 % and scan rate of 35 mm/s yields mark intensity of 0.54, angle deviation of  $1.8^\circ$  and area deviation of  $120000 \mu\text{m}^2$ . But there is great certainty that better marking characteristics lies at some point which cannot be revealed by OFAT method. Thus it require a proper design methodology such as RSM or Taguchi for proper analyzation of better marking characteristics. Table 4.2 shows the experimental plan developed using RSM model and responses value obtained at different parametric setting of laser marking. In order to analyze the effects of process variables on marking characteristics, the measured responses were further utilized to develop empirical model and subsequently F and p test of developed ANOVA table for the suitability of the developed model. After surface and contour plot were developed based on the assigned value of process variables in order to analyze the range of process variables for better value of marking characteristics. Furthermore, efforts were also given to optimize the results of responses using desirability function analysis.



**Table 4.2** Response values based on experimental plan using CCRD

Sl.No.	Process variables				Output Responses		
	LP (W)	PF (kHz)	DC (%)	SS (mm/s)	Mark Intensity	Angle Deviation (°)	Area Deviation *10000 (µm <sup>2</sup> )
1	10	52.5	30	14	0.55	1.41	0.31
2	15	52.5	30	14	0.62	2.35	0.59
3	10	57.5	30	14	0.51	0.14	0.35
4	15	57.5	30	14	0.59	0.84	0.59
5	10	52.5	70	14	0.58	0.23	0.39
6	15	52.5	70	14	0.68	3.12	0.57
7	10	57.5	70	14	0.53	0.16	0.35
8	15	57.5	70	14	0.72	1.65	0.58
9	10	52.5	30	28	0.53	0.25	0.30
10	15	52.5	30	28	0.65	3.81	0.56
11	10	57.5	30	28	0.46	0.16	0.33
12	15	57.5	30	28	0.63	1.92	0.56
13	10	52.5	70	28	0.51	0.45	0.48
14	15	52.5	70	28	0.63	1.94	0.59
15	10	57.5	70	28	0.48	1.25	0.39
16	15	57.5	70	28	0.61	1.66	0.66
17	7.5	55	50	21	0.42	0.57	0.21
18	17.5	55	50	21	0.63	2.84	0.86
19	12.5	50	50	21	0.64	0.79	0.44
20	12.5	60	50	21	0.59	0.62	0.48
21	12.5	55	10	21	0.62	1.65	0.54
22	12.5	55	90	21	0.68	1.10	0.55
23	12.5	55	50	7	0.65	0.42	0.48
24	12.5	55	50	35	0.59	1.32	0.46
25	12.5	55	50	21	0.64	0.43	0.43
26	12.5	55	50	21	0.63	0.01	0.55
27	12.5	55	50	21	0.65	0.50	0.54
28	12.5	55	50	21	0.62	0.61	0.53
29	12.5	55	50	21	0.66	0.02	0.55
30	12.5	55	50	21	0.61	0.35	0.56
31	12.5	55	50	21	0.6	0.56	0.55

#### 4.1.2 Development of Empirical Modeling based on RSM

The output response obtained after conducting experiments and measured responses were utilized for the development of empirical models of responses such as mark intensity, angle deviation and area deviation which are marked as subsequent equation.

**Mark Intensity:**  $0.63 + 0.05833 \times \text{Laser Irradiation} - 0.01333 \times \text{Pulse Rate} + 0.01333 \times \text{Duty Cycle} - 0.01667 \times \text{Scan Rate} - 0.03000 \times \text{Laser Irradiation} \times \text{Laser Irradiation} -$

$0.00750 \times \text{Pulse Rate} \times \text{Pulse Rate} + 0.00125 \times \text{Duty Cycle} \times \text{Duty Cycle} - 0.00625 \times \text{Scan Rate} \times \text{Scan Rate} + 0.01000 \times \text{Laser Irradiation} \times \text{Pulse Rate} + 0.00625 \times \text{Laser Irradiation} \times \text{Duty Cycle} + 0.00625 \times \text{Laser Irradiation} \times \text{Scan Rate} + 0.00625 \times \text{Pulse Rate} \times \text{Duty Cycle} - 0.00375 \times \text{Pulse Rate} \times \text{Scan Rate} - 0.01750 \times \text{Duty Cycle} \times \text{Scan Rate} \dots$ 
**Eq.4.1**

**Angle Deviation:**  $0.4543 + 0.5962 \times \text{Laser Irradiation} - 0.3163 \times \text{Pulse Rate} - 0.1321 \times \text{Duty Cycle} + 0.2338 \times \text{Scan Rate} + 0.3374 \times \text{Laser Irradiation} \times \text{Laser Irradiation} + 0.1624 \times \text{Pulse Rate} \times \text{Pulse Rate} + 0.2561 \times \text{Duty Cycle} \times \text{Duty Cycle} + 0.1411 \times \text{Scan Rate} \times \text{Scan Rate} - 0.1656 \times \text{Laser Irradiation} \times \text{Pulse Rate} + 0.0119 \times \text{Laser Irradiation} \times \text{Duty Cycle} - 0.0044 \times \text{Laser Irradiation} \times \text{Scan Rate} + 0.3131 \times \text{Pulse Rate} \times \text{Duty Cycle} + 0.0744 \times \text{Pulse Rate} \times \text{Scan Rate} - 0.1456 \times \text{Duty Cycle} \times \text{Scan Rate} \dots$ 
**Eq.4.2**

**Area Deviation:**  $0.5300 + 0.1292 \times \text{Laser Irradiation} + 0.0042 \times \text{Pulse Rate} + 0.0183 \times \text{Duty Cycle} + 0.0042 \times \text{Scan Rate} - 0.00333 \times \text{Laser Irradiation} \times \text{Laser Irradiation} - 0.02208 \times \text{Pulse Rate} \times \text{Pulse Rate} - 0.00083 \times \text{Duty Cycle} \times \text{Duty Cycle} - 0.01958 \times \text{Scan Rate} \times \text{Scan Rate} + 0.0088 \times \text{Laser Irradiation} \times \text{Pulse Rate} - 0.0138 \times \text{Laser Irradiation} \times \text{Duty Cycle} - 0.0037 \times \text{Laser Irradiation} \times \text{Scan Rate} - 0.0075 \times \text{Pulse Rate} \times \text{Duty Cycle} + 0.0000 \times \text{Pulse Rate} \times \text{Scan Rate} + 0.0200 \times \text{Duty Cycle} \times \text{Scan Rate} \dots$ 
**Eq.4.3**

#### 4.1.3 ANOVA Test Results of the Developed Models

The above empirical relations thus obtained using MINITAB software were further checked based on F-ratio and p value for the accuracy of the developed mathematical models for mark intensity, angle deviation and area deviation of equilateral triangular shaped laser marked surface obtained by using pulsed diode pumped fiber laser on stainless steel 304. The ANOVA results for the corresponding responses are highlighted in Table 4.3-4.5.

As per Table 4.3, it is seen that p-value for Linear, and Square of the process variables of regression model are lower than 0.05 which means they are significant whereas 2 way interaction of the process variables is higher than 0.05 signifying statistically insignificant. The computed F value of lack of fit for mark intensity were found to be 1.36 and its p value is 0.368 which is higher than 0.05. Thus the effects of lack of fit is negligible and can be considered insignificant. The calculated value of R-Sq is 93.56%, R-sq (adj) value is

87.93% and R-sq (pred) value is 71.59% which are sufficiently high. As a result, the created models fit the observed data well.

**Table 4.3** ANOVA for Mark Intensity

Source	DF	Adj SS	Adj MS	F-Value	P-Value
Model	14	0.132705	0.009479	16.61	0.000
<b>Linear</b>	4	0.096867	0.024217	42.42	0.000
Laser Irradiation	1	0.081667	0.081667	143.07	0.000
Pulse Rate	1	0.004267	0.004267	7.47	0.015
Duty Cycle	1	0.004267	0.004267	7.47	0.015
Scan Rate	1	0.006667	0.006667	11.68	0.004
<b>Square</b>	4	0.027239	0.006810	11.93	0.000
Laser Irradiation x Laser Irradiation	1	0.025736	0.025736	45.09	0.000
Pulse Rate x Pulse Rate	1	0.001609	0.001609	2.82	0.113
Duty Cycle x Duty Cycle	1	0.000045	0.000045	0.08	0.783
Scan Rate x Scan Rate	1	0.001117	0.001117	1.96	0.181
<b>2-Way Interaction</b>	6	0.008600	0.001433	2.51	0.066
Laser Irradiation x Pulse Rate	1	0.001600	0.001600	2.80	0.114
Laser Irradiation x Duty Cycle	1	0.000625	0.000625	1.09	0.311
Laser Irradiation x Scan Rate	1	0.000625	0.000625	1.09	0.311
Pulse Rate x Duty Cycle	1	0.000625	0.000625	1.09	0.311
Pulse Rate x Scan Rate	1	0.000225	0.000225	0.39	0.539
Duty Cycle x Scan Rate	1	0.004900	0.004900	8.58	0.010
<b>Error</b>	16	0.009133	0.000571		
<b>Lack-of-Fit</b>	10	0.006333	0.000633	1.36	0.368
Pure Error	6	0.002800	0.000467		
Total	30	0.141839			

In the Table 4.4, it is seen that p-value for Linear, Square and 2 Way interaction of the process variables of regression model are lower than 0.05. The Lack of Fit computed F value for angle deviation were found to be 2.31 and p value is 0.159 which is higher than 0.05. Thus lack of fit is statistically insignificant. The calculated value obtained for R-Sq is 97.64%, R-sq(adj) value is 95.57% and R-sq(pred) value is 88.54% which are sufficiently high. As a result, the created models fit the observed data well

In the Table 4.5, it is seen that p-value of source of regression model for Linear is less than 0.05 whereas p values of Square and 2 Way interaction of the process variables was found to be higher than 0.05 which means they were statistically insignificant. The computed F value of Lack of Fit for area deviation were found to be 1.39 and its p value is 0.357 which is higher than 0.05. Thus lack of fit is statistically insignificant The calculated value

obtained for R-Sq is 91.65%, R-sq(adj) value is 84.34% and R-sq (pred) value is 62.99% which are sufficiently high. As a result, the created models fit the observed data well.

**Table 4.4** ANOVA for Angle Deviation

Source	DF	Adj SS	Adj MS	F-Value	P-Value
Model	14	20.2465	1.44618	47.24	0.000
<b>Linear</b>	4	12.6627	3.16568	103.41	0.000
Laser Irradiation (W)	1	8.5323	8.53234	278.70	0.000
Pulse Rate (kHz)	1	2.4003	2.40034	78.41	0.000
Duty Cycle (%)	1	0.4187	0.41870	13.68	0.002
Scan Rate ( mm/s)	1	1.3113	1.31134	42.83	0.000
<b>Square</b>	4	5.1458	1.28644	42.02	0.000
Laser Irradiation (W)*Laser Irradiation (W)	1	3.2546	3.25465	106.31	0.000
Pulse Rate (kHz)*Pulse Rate (kHz)	1	0.7539	0.75386	24.62	0.000
Duty Cycle (%)*Duty Cycle (%)	1	1.8758	1.87575	61.27	0.000
Scan Rate ( mm/s)*Scan Rate ( mm/s)	1	0.5694	0.56945	18.60	0.001
<b>2-Way Interaction</b>	6	2.4380	0.40634	13.27	0.000
Laser Irradiation (W)*Pulse Rate (kHz)	1	0.4389	0.43891	14.34	0.002
Laser Irradiation (W)*Duty Cycle (%)	1	0.0023	0.00226	0.07	0.789
Laser Irradiation (W)*Scan Rate ( mm/s)	1	0.0003	0.00031	0.01	0.922
Pulse Rate (kHz)*Duty Cycle (%)	1	1.5688	1.56876	51.24	0.000
Pulse Rate (kHz)*Scan Rate ( mm/s)	1	0.0885	0.08851	2.89	0.108
Duty Cycle (%)*Scan Rate ( mm/s)	1	0.3393	0.33931	11.08	0.004
<b>Error</b>	16	0.4898	0.03061		
<b>Lack-of-Fit</b>	10	0.3889	0.03889	2.31	0.159
Pure Error	6	0.1010	0.01683		
Total	30	20.7363			

**Table 4.5** ANOVA for Area Deviation

Source	DF	Adj SS	Adj MS	F-Value	P-Value
Model	14	0.443926	0.031709	12.55	0.000
<b>Linear</b>	4	0.409317	0.102329	40.48	0.000
Laser Irradiation	1	0.400417	0.400417	158.42	0.000
Pulse Rate	1	0.000417	0.000417	0.16	0.690
Duty Cycle	1	0.008067	0.008067	3.19	0.093
Scan Rate	1	0.000417	0.000417	0.16	0.690
<b>Square</b>	4	0.022834	0.005709	2.26	0.108
Laser Irradiation x Laser Irradiation	1	0.000318	0.000318	0.13	0.728
Pulse Rate x Pulse Rate	1	0.013945	0.013945	5.52	0.032
Duty Cycle x Duty Cycle	1	0.000020	0.000020	0.01	0.930
Scan Rate x Scan Rate	1	0.010967	0.010967	4.34	0.054
<b>2-Way Interaction</b>	6	0.011775	0.001962	0.78	0.600
Laser Irradiation x Pulse Rate	1	0.001225	0.001225	0.48	0.496
Laser Irradiation x Duty Cycle	1	0.003025	0.003025	1.20	0.290
Laser Irradiation x Scan Rate	1	0.000225	0.000225	0.09	0.769
Pulse Rate x Duty Cycle	1	0.000900	0.000900	0.36	0.559
Pulse Rate x Scan Rate	1	0.000000	0.000000	0.00	1.000
Duty Cycle x Scan Rate	1	0.006400	0.006400	2.53	0.131
<b>Error</b>	16	0.040442	0.002528		
<b>Lack-of-Fit</b>	10	0.028242	0.002824	1.39	0.357
<b>Pure Error</b>	6	0.012200	0.002033		
Total	30	0.484368			

Based on the above observation, it can be said that the developed model for the responses such as mark intensity, area deviation and angle deviation were valid and can be used to predict the value of responses using particular set of process variables employed for carrying out laser marking operations.

#### 4.1.4 Analysis of Fiber Laser Process variables on Marking Quality Characteristics of Stainless Steel 304

The section deals with analysis of process variables on marking quality characteristics when other process variables were held constant. Apart from that it also provides region for selection of better process variables for attaining better marking characteristics. The detailed analysis were shown in the subsequent section

#### 4.1.4.1 Parametric Influences on Mark Intensity of SS 304

Fig. 4.2 and 4.3 shows the contour plot and surface plot of mark intensity with respect to pulse rate and laser irradiation when other process variables such as duty cycle and scan rate were held constant. It has been found that laser irradiation and pulse rate affects the marking characteristics with former found to be a more dominating factor than latter when other process variables were held constant.

It was observed that from Fig. 4.3 that with the increase of laser irradiation, mark intensity value increases and reaches to a maximum value of 0.65 at a laser irradiation of 12.5 W and pulse rate of 55 kHz when other process variables such as duty cycle and scan rate were held constant at 50% and 21 mm/s respectively. High laser irradiation accelerates surface oxidation due to high energy content of laser beam which when interacts with the workpiece at ambient condition increases the mark intensity value. But increase of laser irradiation beyond 12.5 W resulted in laser spattering with non-uniform laser spot overlap which decreases mark intensity with corresponding increase of width and heat affected zone.

Higher pulse rate lowers the peak power of a pulsed laser beam. As a result, there is less surface oxidation present on the surface which resulted in the decrease of mark intensity value. It resulted in the generation of smooth surface with decrease in width. Analysis revealed that pulse rate of 55 kHz in the range of 50 kHz to 60 kHz provides better results in mark intensity value. Based on the contour plot as seen in Fig. 4.2 it can be said that pulse rate in the range of 50 to 60 kHz and laser irradiation greater than 13 W should be employed for achieving higher value of mark intensity.

Fig. 4.4 and 4.5 show the contour plot and surface plot of mark intensity for analysing the influences of duty cycle and scan rate when other process variables such as laser irradiation and pulse rate were held constant at 12.5 W and 55 kHz respectively. It was observed from Fig. 4.5 that with the decrease of scan rate from 35 to 7 mm/s resulted in the increase of mark intensity value to 0.73 whereas changes in duty cycle from 10 to 70 % had a minimum effects beyond which it increases the mark intensity value. Lower scan rate increases the duration of heat interaction with the surface of the workpiece which in turn causes high oxidation and thereby increases mark intensity value whereas increase in duty cycle increases the on time of laser pulsed duration which had a significant contribution in the

mark intensity value when it is set above 70 % which also increases the surface's laser-marked grey value. From contour plot of Fig. 4.4, it becomes evident that duty cycle of above 75 %, and scan rate in the range of 7 to 14 mm/s yields better value of mark intensity.

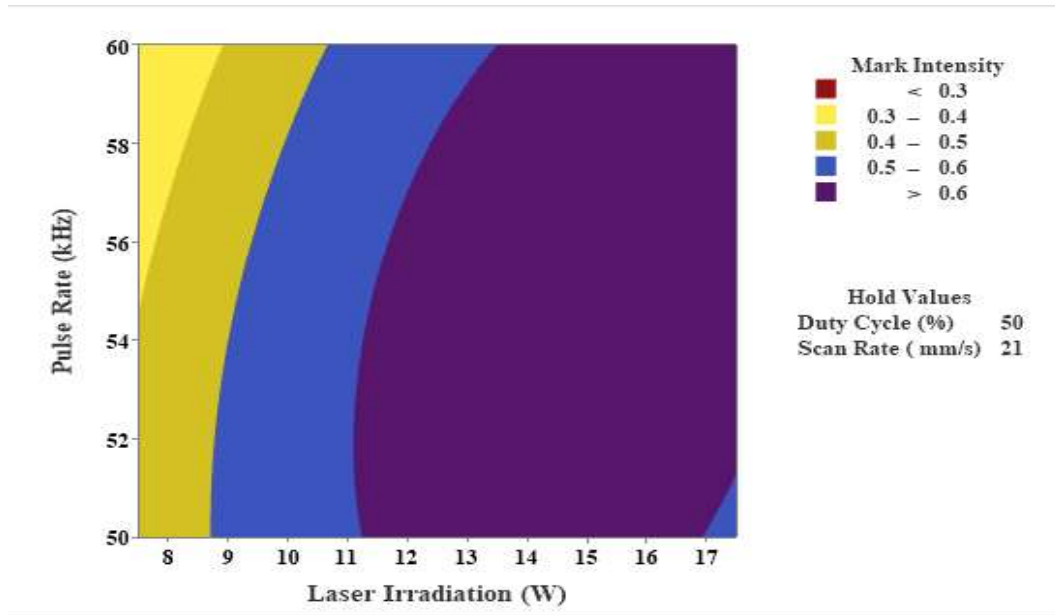


Fig. 4.2 Contour plot of Mark Intensity with respect to Pulse rate and Laser irradiation

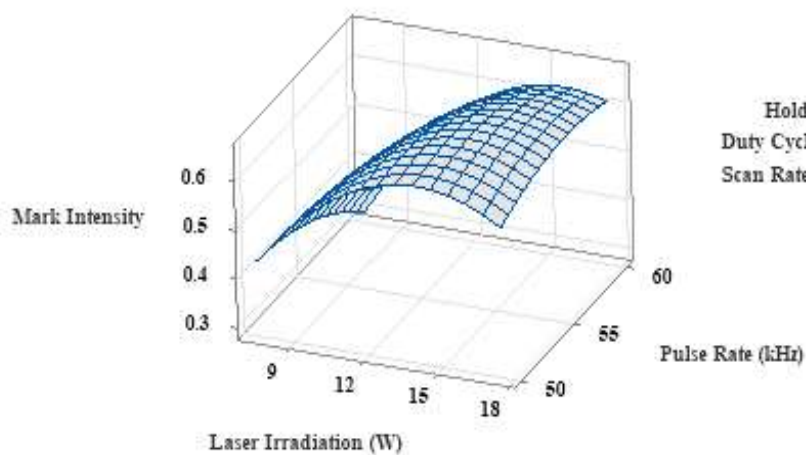


Fig. 4.3 Surface plot of Mark Intensity with respect to Pulse rate and Laser irradiation

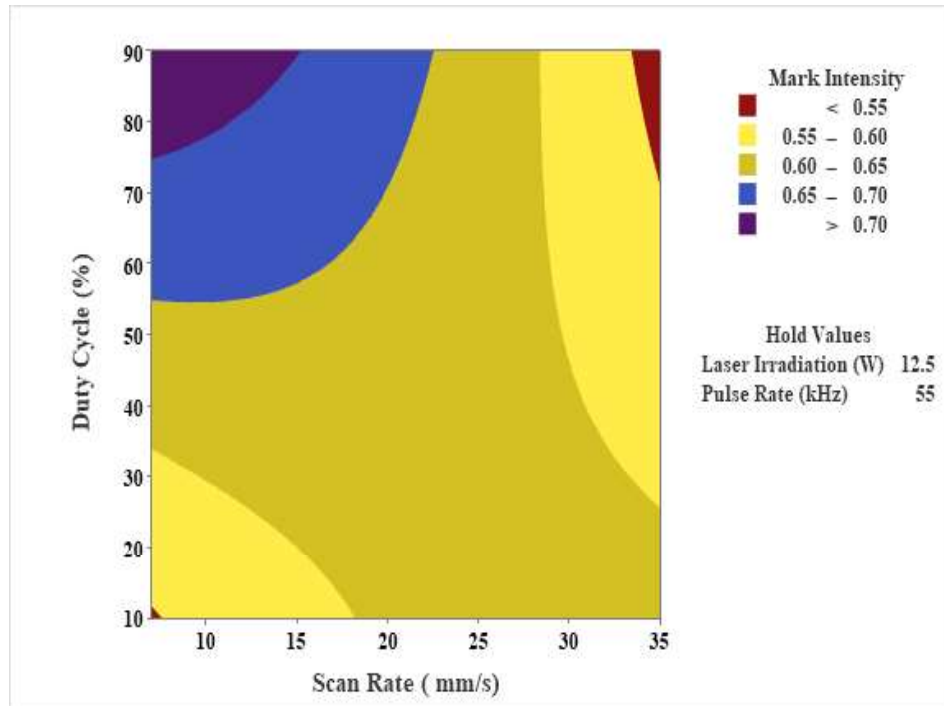


Fig. 4.4 Contour plot of Mark Intensity with respect to Duty cycle and Scan rate

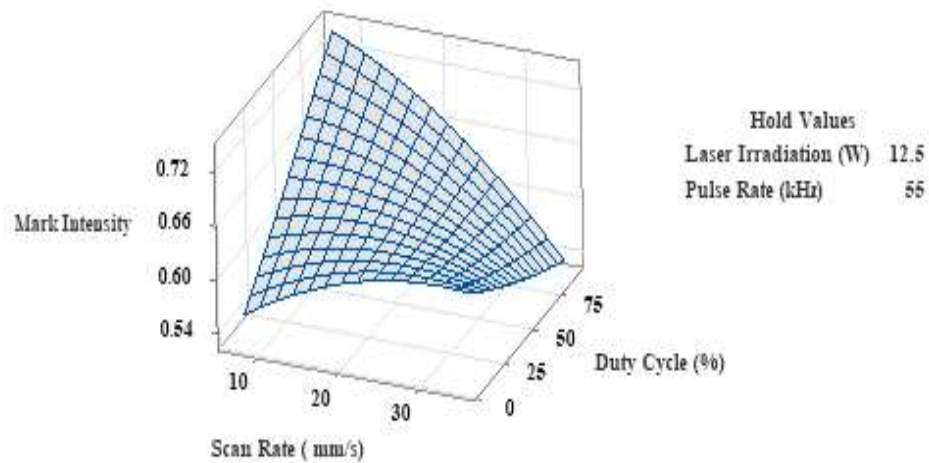


Fig. 4.5 Surface plot of Mark Intensity with respect to Duty cycle and Scan rate



#### 4.1.4.2 Parametric Influences on Angle deviation of SS 304

Fig. 4.6 and 4.7 show the contour plot and surface plot of angle deviation with respect to pulse rate and laser irradiation when other process variables such as duty cycle and scan rate were held constant at 50 % and 21 mm/s respectively. It was observed from Fig. 4.7 that for minimum value of angle deviation, laser irradiation should be set below 12.5 W and pulse rate of 50 kHz provides better results. High laser irradiation increases the deviation of angle due to greater heat interaction at the periphery which causes increment in angle above 60°. Apart from that, laser spattering was also observed at a laser irradiation above 15 W which also plays a role in the increase of angle deviation. Higher pulse rate possess minimum peak power which decreases the angle deviation close to 60° with decrease in width. Fig. 4.6 reveals the fact that in order to have minimum angle deviation, laser irradiation in the range of 8 to 12 W and pulse rate in the range of 51 kHz to 59 kHz should be employed.

Fig. 4.8 and 4.9 show the contour plot and surface plot of angle deviation with respect to duty cycle and scan rate when other process variables such as laser irradiation and pulse rate were held constant at 12.5 W and 55 kHz respectively. It was observed from Fig. 4.9 that with the decrease of scan rate from 35 mm/s increases the angle deviation and it reaches to a maximum value at a scan rate of 7 mm/s whereas duty cycle had a minimum impact on angle deviation and pointed to the decrease of angle deviation upon changing from 90 % to 10 %. Decrease of scan rate increases the heat interaction with the workpiece and increases the non-uniformity at the edges of marked surface which resulted in the increase of angle deviation whereas high duty cycle also results in the deviation of angle greater than 60° due to increase of on time heat interaction with the workpiece surface. It becomes evident from Fig. 4.8, that duty cycle in the range of 40 % to 60% and scan rate in the range of 10 mm/s to 21 mm/s should be selected for having minimum value of angle deviation.

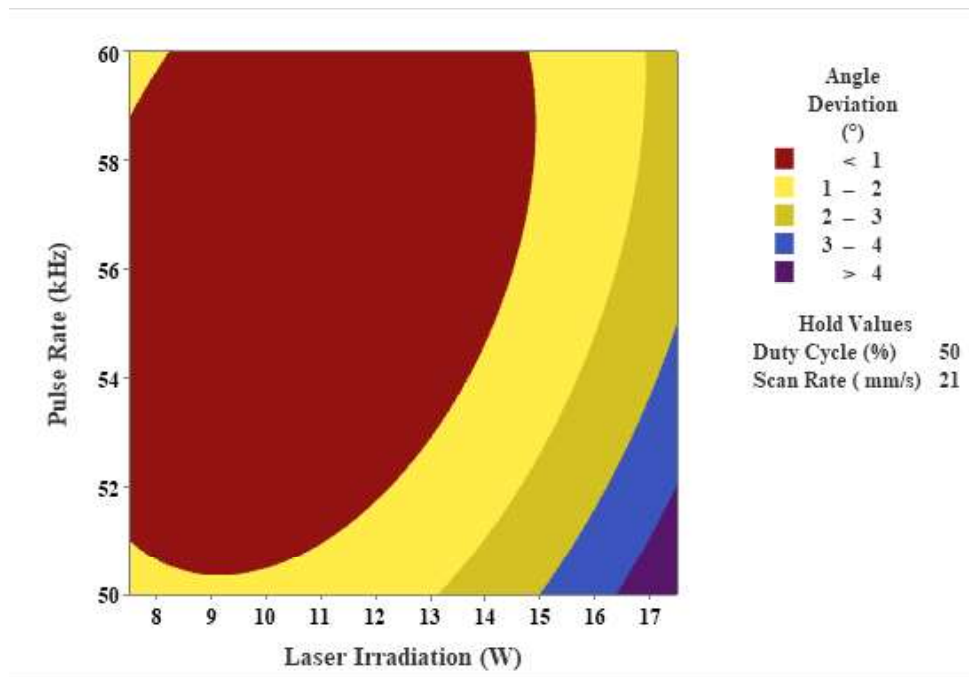


Fig. 4.6 Contour plot of Angle deviation with respect to Pulse rate and Laser irradiation

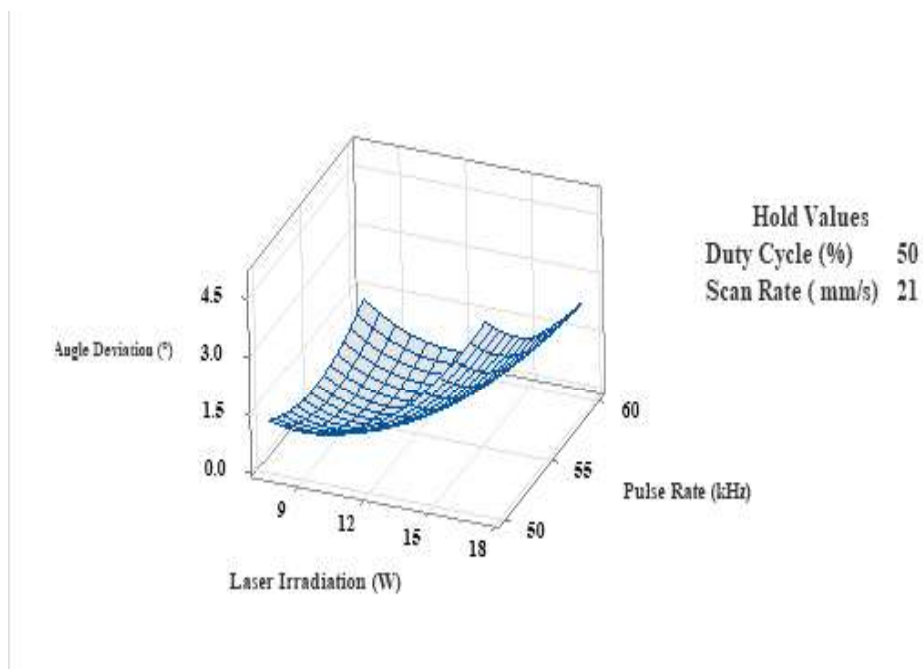


Fig. 4.7 Surface plot of Angle deviation with respect to Pulse rate and Laser irradiation

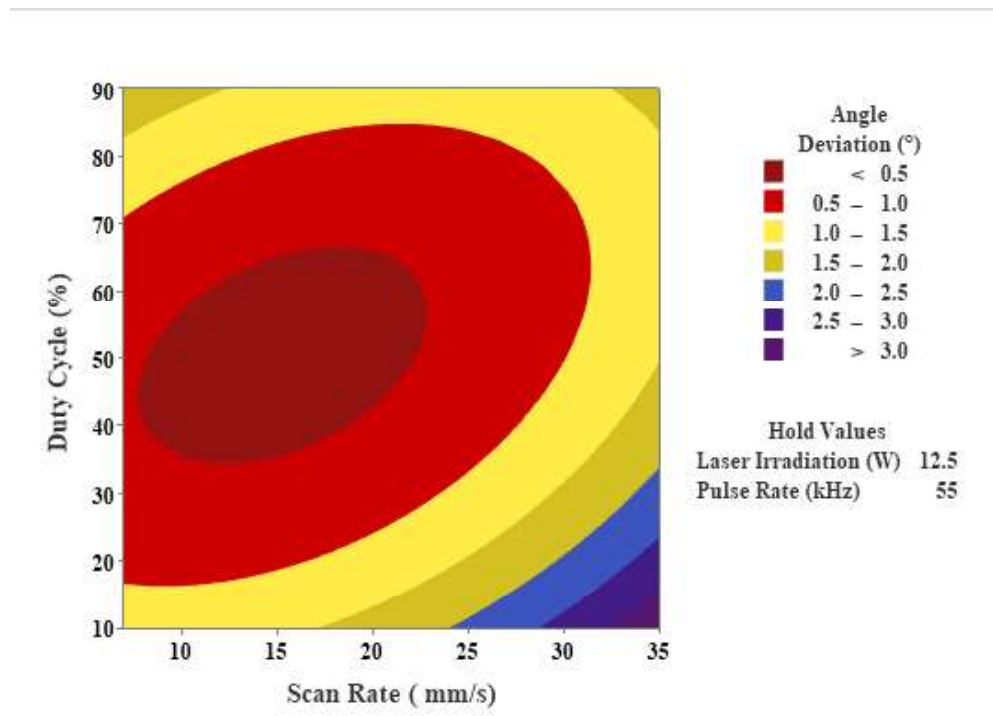


Fig. 4.8 Contour plot of Angle deviation with respect to Duty cycle and Scan rate

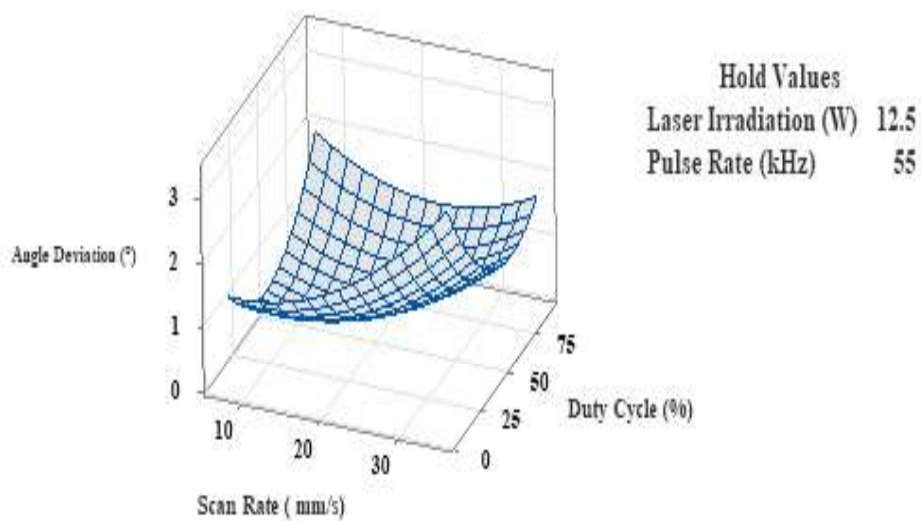


Fig. 4.9 Surface plot of Angle deviation with respect to Duty cycle and Scan rate

#### 4.1.4.3 Parametric Influences on Area Deviation of SS 304

Fig. 4.10 and 4.11 show the contour plot and surface plot of area deviation with respect to pulse rate and laser irradiation when other process variables such as duty cycle and scan rate were held constant at 50 % and 21 mm/s respectively. It was observed from Fig. 4.11 that with the increase of laser irradiation from 7.5 W resulted in the increase of area deviation and reaches to a maximum value of  $8000 \mu\text{m}^2$  at a laser irradiation of 17.5 W whereas increase of pulse rate from 50 kHz also resulted in the increase of area deviation and reaches to maximum value at pulse rate of 60 kHz. High laser irradiation causes laser spattering which is accountable for the increase in surface area. The deviation of area is lower at laser irradiation below 12.5 W which increases rapidly on further increase of laser irradiation. High pulse rate had low peak power of pulsed laser when other process variables are held constant. Due to which, the increase in area is low on employing higher pulse rate. From Fig. 4.10, it becomes evident that laser irradiation below 9 W and pulse rate in the range of 58 kHz to 60 kHz should be selected for lower value of marked area deviation.

Fig. 4.12 and 4.13 show the contour plot and surface plot of area deviation with respect to duty cycle and scan rate when other process variables such as laser irradiation and pulse rate were held constant at 12.5 W and 55 kHz respectively. It was observed from Fig. 4.13 that with the decrease of scan rate from 35 mm/s resulted in the increase of area deviation and reaches to a higher value of  $5000 \mu\text{m}^2$  at a scan rate of 14 mm/s whereas decrease of duty cycle from 90% to 10 % also resulted in the decrease of area deviation and reaches to lower value at a duty cycle of 10 %. Lower scan rate had more influence in increasing the area deviation as compared to duty cycle when they were varied within the suitable range. Decrease in scan rate increase the time of heat interaction and more prominent mark at the workpiece surface which resulted in the increase of area deviation whereas duty cycle has minimum effects on marking characteristics until it was allowed to vary by a larger difference. From contour plot of Fig. 4.12, it becomes evident that for lower value of area deviation, duty cycle in the range of 10% to 30% and scan rate in the range of 30 mm/s to 35 mm/s provides better results.

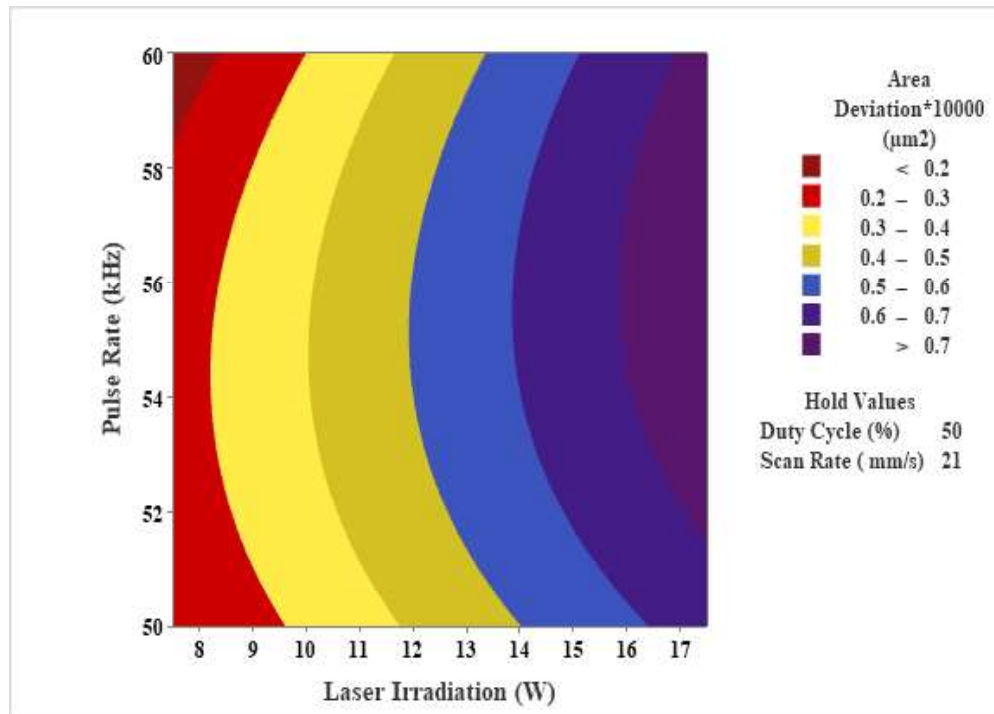


Fig. 4.10 Contour plot of Area Deviation with respect to Pulse rate and Laser irradiation

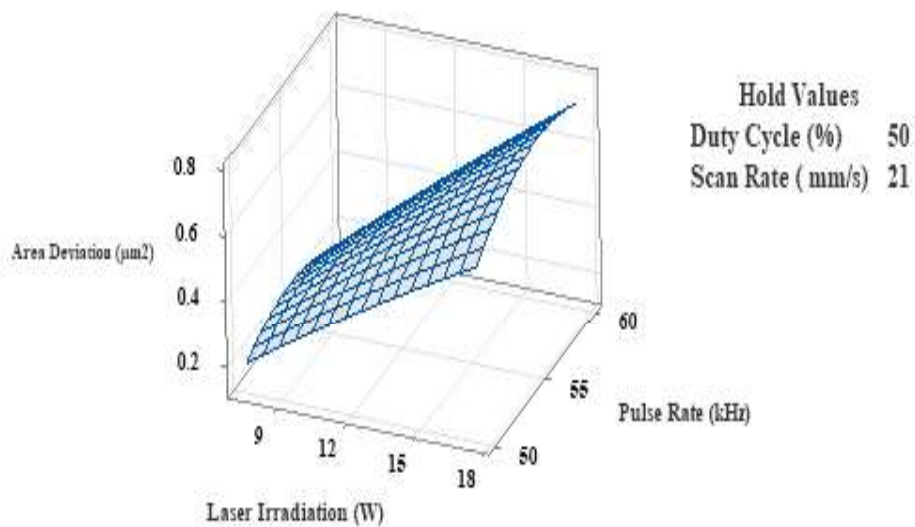


Fig. 4.11 Surface plot of Area Deviation with respect to Pulse rate and Laser irradiation

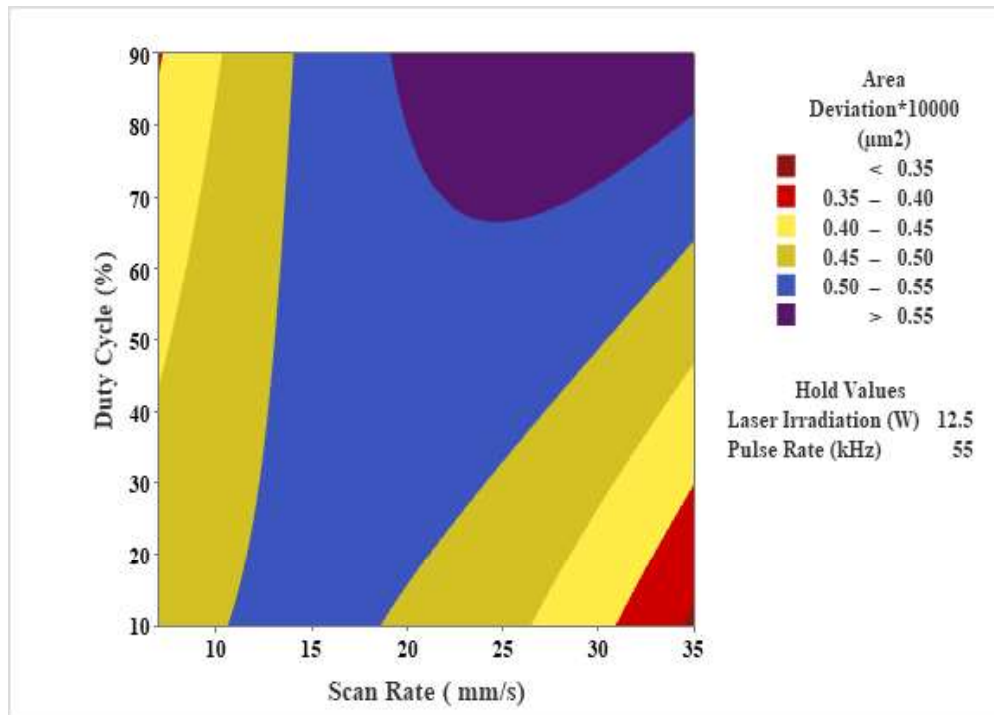


Fig. 4.12 Contour plot of Area Deviation with respect to Duty cycle and Scan rate

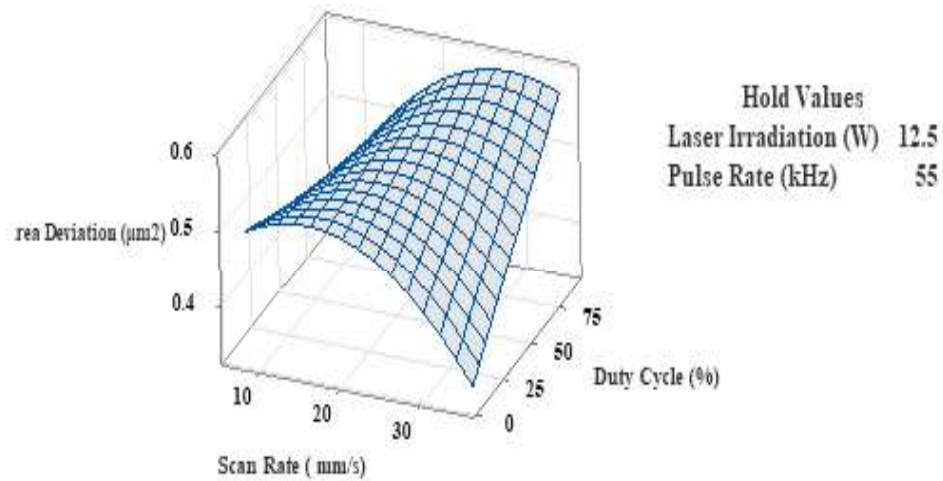


Fig. 4.13 Surface plot of Area Deviation with respect to Duty cycle and Scan rate

## 4.2 Parametric Optimization of Fiber Laser Marking on SS 304

The section deals with the optimization of the responses using desirability function analysis. It provides the ideal settings of process variables for optimum response output.

### 4.2.1 Single Objective Optimization of the Responses

Based on the proposed mathematical models, the analysis of every individual response has been done to achieve the maximum marking intensity, minimum angle and area deviation of the equilateral triangular shaped laser marked surface. The upper limit of desirability function (D) is supposed to have a weight value of 1 for optimum value of the responses. For laser marking on stainless steel 304, the software MINITAB was used to optimize the responses using desirability function analysis. Each column of the optimization graph that is subsequently obtained corresponds to a factor. The graph's rows each represent a response. While all other variables are fixed, each graph cell illustrates how one response varies as a function of one of the process variables. The experimental design's high and low settings are shown by numbers at the top of each column, while the row colored in red denotes the present values of the process variables that should be used to achieve the goals. Response goal, desired value, current y factor, and desirability value are provided to the left of each row.

Fig. 4.14 and 4.16 show the findings of single-objective optimization of the responses undertaken for laser marking operation. It was observed from Fig. 4.14 that the optimal process variables settings required for achieving maximum value of mark intensity are 15 W of laser irradiation, 50 kHz of pulse rate, 10 % of duty cycle, 28 mm /s of scan rate. From the Fig. 4.15 it was observed that minimum value of angle deviation could be achieved when the process variables settings are 11 W of laser irradiation, 60 kHz of pulse rate, 20 % of duty cycle, and 19 mm/s of scan rate. It was observed from Fig. 4.16 that the optimal process variables settings required for achieving minimum value of area deviation are 7.50 W of laser irradiation, 50 kHz of pulse rate, 50 % of duty cycle, 21 mm /s of scan rate.



Fig. 4.14 Optimization plot for mark intensity

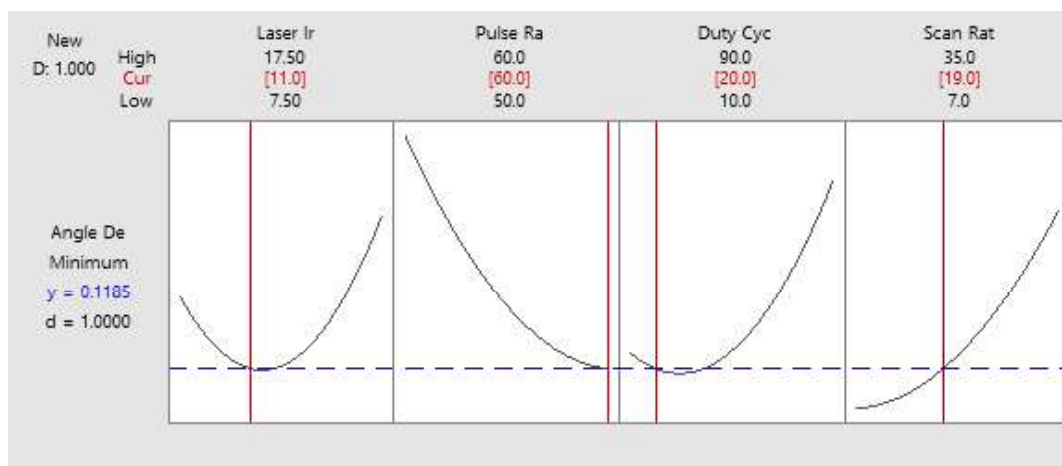


Fig. 4.15 Optimization plot for Angle Deviation

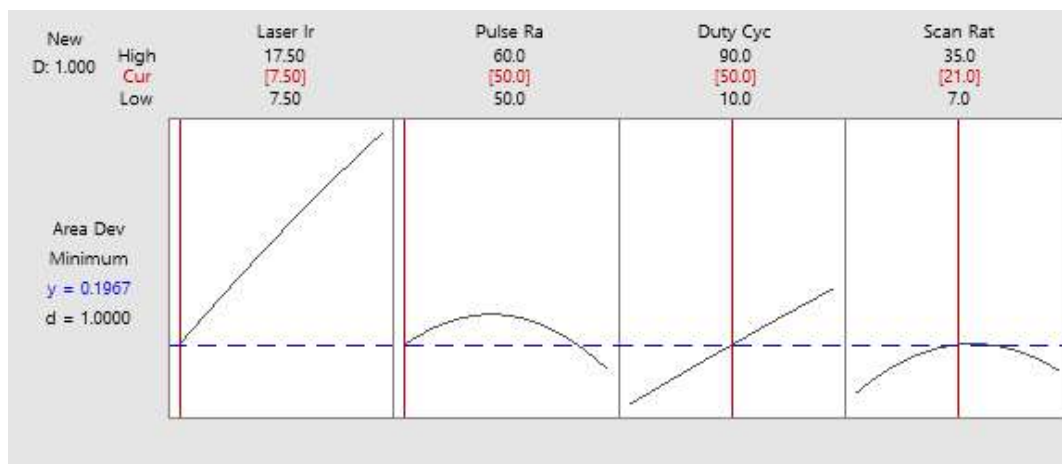


Fig. 4.16 Optimization plot for Area Deviation



## 4.2.2 Multi-Objective Optimization of the Responses

In order to carryout multi objective optimization of the responses using desirability function analysis, the goals of the responses should be assigned with the corresponding weightage value of the responses. From Fig. 4.17, it is observed that the current optimal process parameter settings obtained for maximum value of mark intensity, minimum angle and area deviation are 11 W of laser irradiation, 57 kHz of pulse rate, 63 % of duty cycle, and 7 mm/s of scan rate respectively. In the process the assigned weightage for mark intensity was 0.50, angle deviation was 0.25 and area deviation was 0.25 respectively.

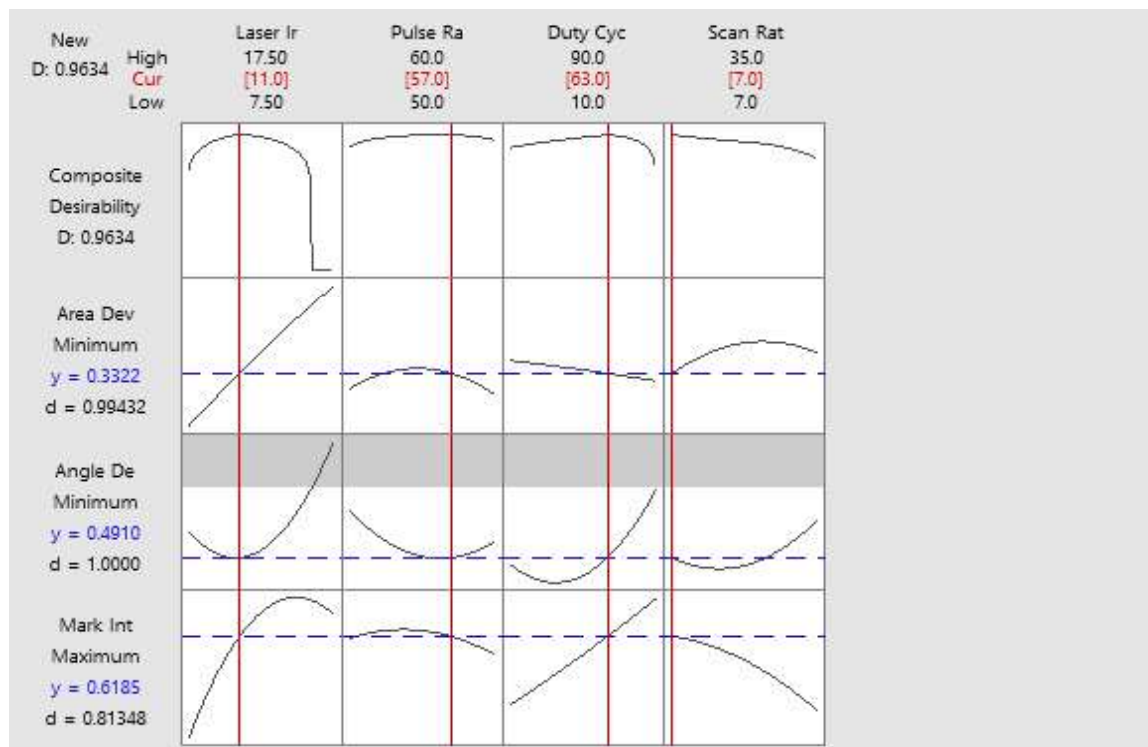


Fig. 4.17 Optimization plot for multi objective optimization

The sets of current process variables obtained from optimization plot for multi objective optimization are put forward to carry out experiment in order to ascertain the error of theoretical and predicted results using the formula as given in equation 4.4

$$\text{Error (\%)} = \left| \frac{\text{Predicted value} - \text{Actual value}}{\text{Actual value}} \right| * 100 \dots\dots \text{Eq. 4.4}$$

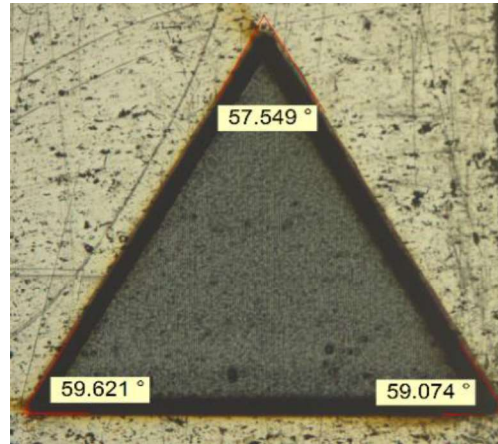


Fig. 4.18 Image of a laser-marked surface taken at its ideal parametric setting

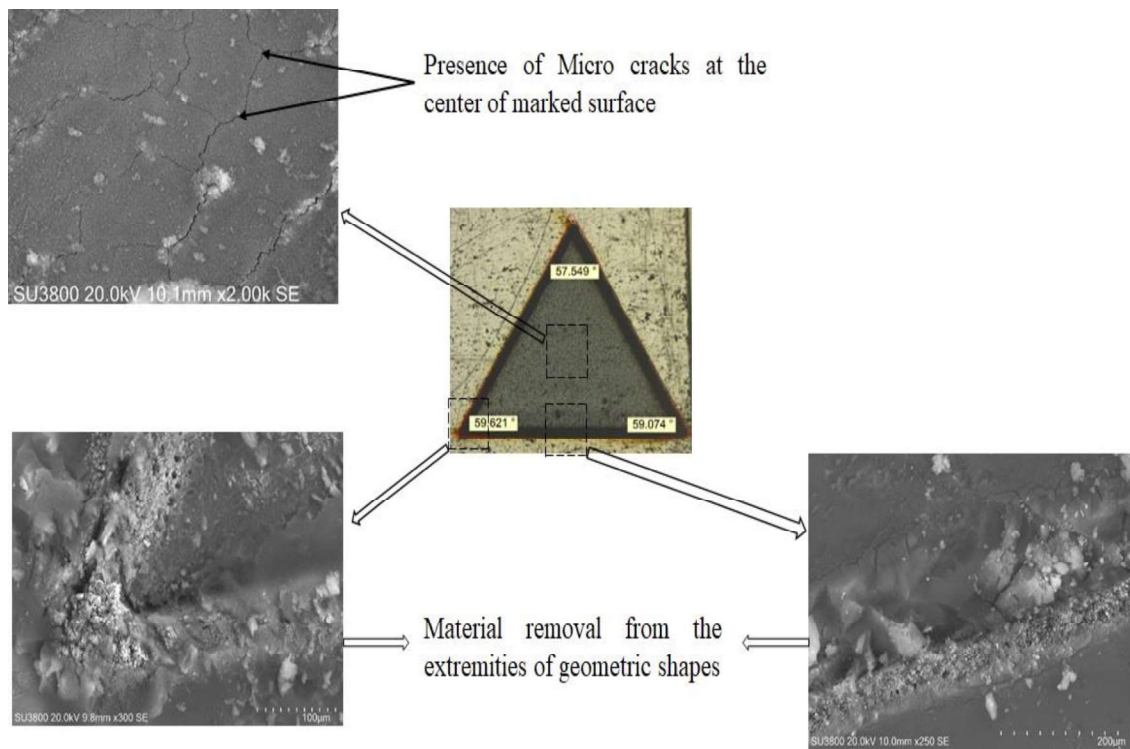


Fig. 4.19 SEM images of different sites of marked surface at optimal process variables settings

Fig. 4.18 shows an image of a laser-marked surface based on multi objective optimization plot. Upon analysis it is observed that the mark intensity value obtained from is 0.57, angle deviation is 1.25° and area deviation is  $(0.24 \times 10000) \mu\text{m}^2$ . The percentage of error obtained are 3.6 % for mark intensity, 2.08 % for angle deviation and 4.34 % for area deviation of

equilateral triangle laser marked surface. The time required to mark the surface at optimal parametric setting is 2.30 minutes. Thus it was observed that a significant improvement in marking characteristics were made possible using RSM methods. Furthermore it was also subjected to analysis using scanning electron microscope and CCI 3D non-contact type surface roughness tester as seen in Fig. 4.19 and 4.20 respectively.

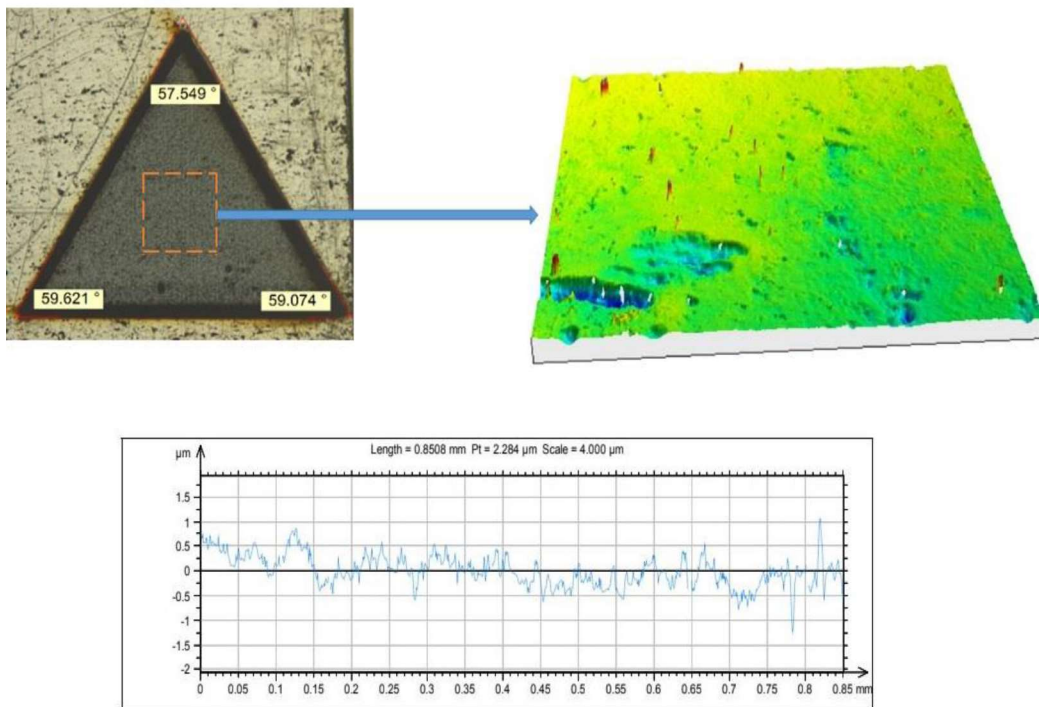


Fig. 4.20 3D and 2D Surface profile of laser marked surface at optimal parametric settings

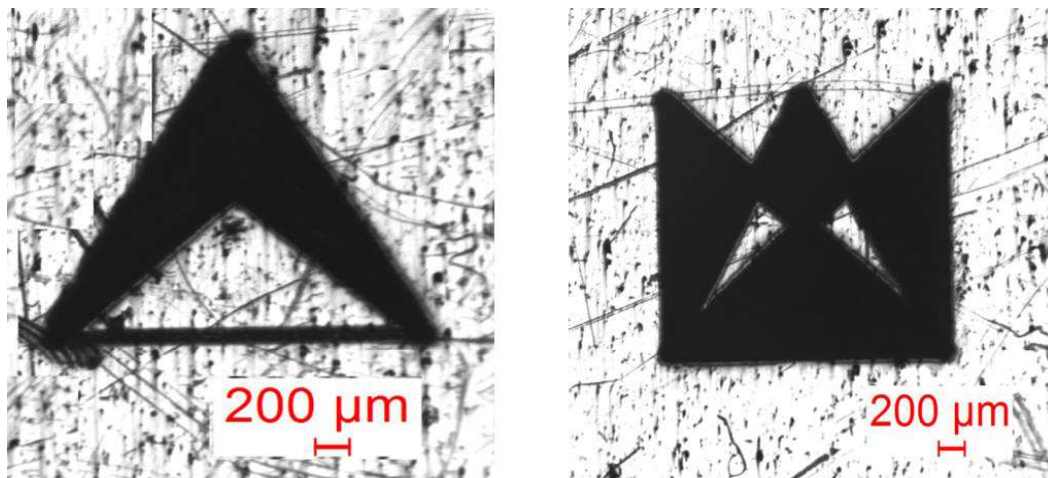


Fig. 4.21 Photographic view of other geometric shape marked at optimal parametric setting

Fig. 4.19 shows the SEM images (SU3800; Hitachi Corporation Ltd) of laser marked surface carried out at optimal process variables settings. Due to prolonged heat interaction with the workpiece, it has been observed that material is lost from the edge of laser-marked surfaces. The presence of micro cracks at the interior surface is less due to minimum time of heat interaction as compared to exterior surface.

Fig. 4.20 represents the 2D and 3D surface profile of laser marked surface at optimal parametric settings which are captured using CCI 3D Surface Profiler (CCI SunStar; Taylor and Hobson Ltd). It is non-contact automatic range setting for surface detection for the generation of curve. It has a resolution of 1nanometre (nm). The average roughness value obtained for interior marked surface is 0.1699  $\mu\text{m}$ , Root mean square roughness ( $R_q$ ) value is 0.2128  $\mu\text{m}$ , average maximum height of the profile ( $R_z$ ) is 1.115  $\mu\text{m}$ . The surface roughness obtained through laser marking operation at optimal parametric setting has minimum impact at the workpiece surface with better marking characteristics value. Therefore the optimal process variables obtained through multi objective optimization can be employed for the generation of geometric shaped marked surface as a part of product identification and traceability.

Fig. 4.21 represent some other geometric shape marked surface carried out at optimal parametric settings. The setting can also be used for the generation of any other combination of triangular or any other geometric laser marked surface as a part of product branding.

### **4.3 Outcomes of the Present Research Work**

The experimental results allow us to draw the following conclusions based on the creation of an empirical model, and simultaneous optimization of responses during laser marking operation which can be summed up as follows:

- a. The increase of laser irradiation increases the responses of the laser marking operation in terms of mark intensity, angle and area deviation. Its acts as the most dominating factor among all the responses providing significant removing material from the workpiece's surface.

- b. Higher duty cycle of 90 % has a significant contribution towards the increase of mark intensity value whereas for minimum area and angle deviation duty cycle in the range of 20 to 50 % are significant.
- c. Higher scan rate results in decrease of the mark intensity and area deviation but increases the angle deviation of marked surface. However for improved marking attributes, scan rate of 21 mm/s yields better value.
- d. The relationship between pulse rate and the marking characteristic is inversely related. Increased marking qualities are brought on by lower pulse rate, and vice versa.
- e. The optimal parametric settings obtained based on multi objective optimization are 10.63 W of laser irradiation, 60 kHz of pulse rate, 56.86 % of duty cycle, and 7 mm/s of scan rate respectively.
- f. The percentage of error obtained upon experimentation of equilateral triangle shaped laser marked surface using multi objective optimisation set of process variables are 3.6 % for mark intensity, 2.08 % for angle deviation and 4.34 % for area deviation of equilateral triangle laser marked surface.



### 5. EXPERIMENTAL INVESTIGATION INTO FIBER LASER MARKING ON Ti6Al4V

Ti6Al4V is the most used material among the other titanium alloys, and its total production is almost half of all titanium alloys. Titanium alloy of grade 5 is often used in the different bio-medical field of applications such as artificial hip joints, knee joint replacements, dental implants, etc. due to its capability to bond firmly with a bone for optimal function and durability. Therefore, enhanced bioactivity and improved implant-host interactions are essential to reduce biologically related implant failure. But if the quality of material is poor and specification is not upto the mark it may lead to premature failure. This essence the necessity to obtain the products related to Ti6Al4V from the organisation which follows international standard rules and regulations. The section deals with the influences of process variables on line and surface marking for the purpose of generation of any geometric characteristics as a part of product identification on Ti6Al4V alloys. The present study also on focus on the generation better image quality characteristics with use of lower laser and minimum possible time so that the work can be employed in organisation.

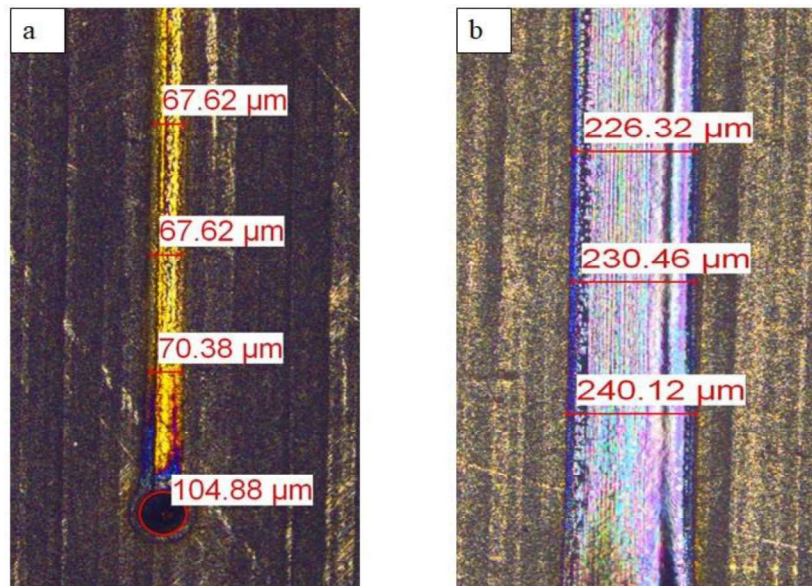


Fig.5.1 Microscopic view of (a) line and (b) surface laser marking on Ti6Al4V

Fig.5.1.(a &b) shows the microscopic view of line marking and surface marking respectively on Ti6Al4V along with the measurement of width captured with the help of OLYMPUS STM 6. The quality analysis has been done on the line marking and surface marking using MATLAB software. Apart from mark intensity analysis, the studies also provide the exposure to the generation of variety of colours on the surface of Ti6Al4V with change of process variables. The details of selection of the process variables and responses are discussed in subsequent subsection.

### **5.1 Selection of the Process variables and Responses**

The process variables taken for the research work are transverse feed, laser irradiation, pulse rate, duty cycle, and scan rate and the output responses considered are mark intensity, marked width and time. The mark intensity of line and surface marking is culmination of grey value of various colours obtained due to the change of process variables and laser heat interaction with the workpiece surface. The marked width was measured using OLYMPUS STM 6 microscope and time study is provided in laser marking system. The detail study regarding the effects of process variables on mark intensity is discussed in section 5.2.

### **5.2 Results and Discussion based on Line and Surface Marking Characteristics of Ti6Al4V**

The experiments were carried out in order to determine the impact of transverse feed, pulse rate, laser irradiation, scan rate, and the duty cycle on line marking of length 5 mm along vertical axis and surface marking of target length and width of 5 mm and 140  $\mu\text{m}$  with transverse feed of 8  $\mu\text{m}$ /laser stroke on Ti6Al4V under normal ambient conditions. The process variables were changed one at a time (OFAT) in order to ascertain the detailed analysis which are discussed below:

#### **5.2.1 Influences of Transverse feed on Marking Characteristics of Ti6Al4V**

Fig.5.2 shows the variation of marking characteristics with change of transverse feed when other process variables such as laser irradiation of 10 W, pulse rate of 50 kHz, scan rate of 35 mm/s and duty cycle of 99 % were held constant. It was observed better marking characteristic value was achieved at transverse feed of 8  $\mu\text{m}$ /laser stroke in comparison to the transverse feed in the range of 2 to 14  $\mu\text{m}$ /laser stroke. Moreover, application of lower transverse feed i.e. 2  $\mu\text{m}$ /laser stroke resulted in the formation of micro cracks throughout

the laser marked portion and at higher transverse feed above 8  $\mu\text{m}/\text{laser stroke}$  decrease the laser spot overlap which resulted in the fall of mark intensity value and further increase of transverse feed beyond 14  $\mu\text{m}/\text{laser stroke}$  provides an image with many significant vertical laser spot lines. Thus from point of better marking characteristics, transverse feed of 8  $\mu\text{m}/\text{laser stroke}$  yields better results with the time requirement of 2.14 minutes.

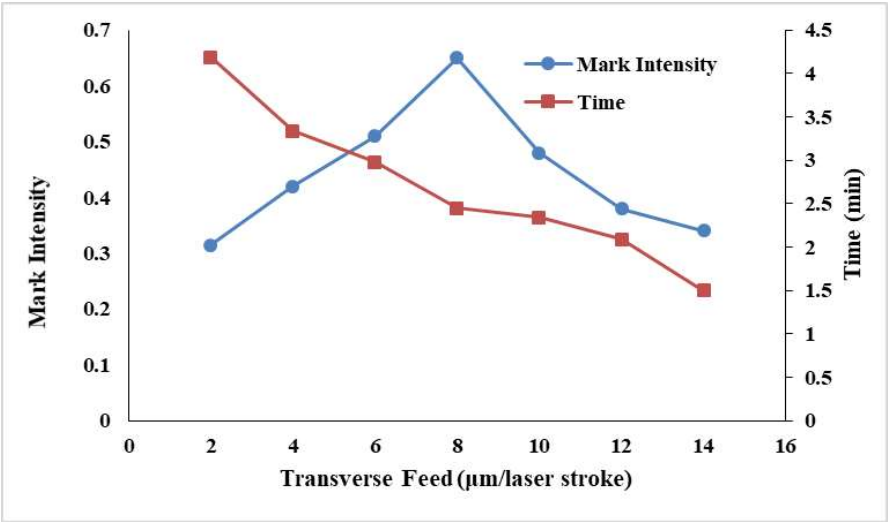


Fig.5.2 Variation of mark characteristics with change of transverse feed

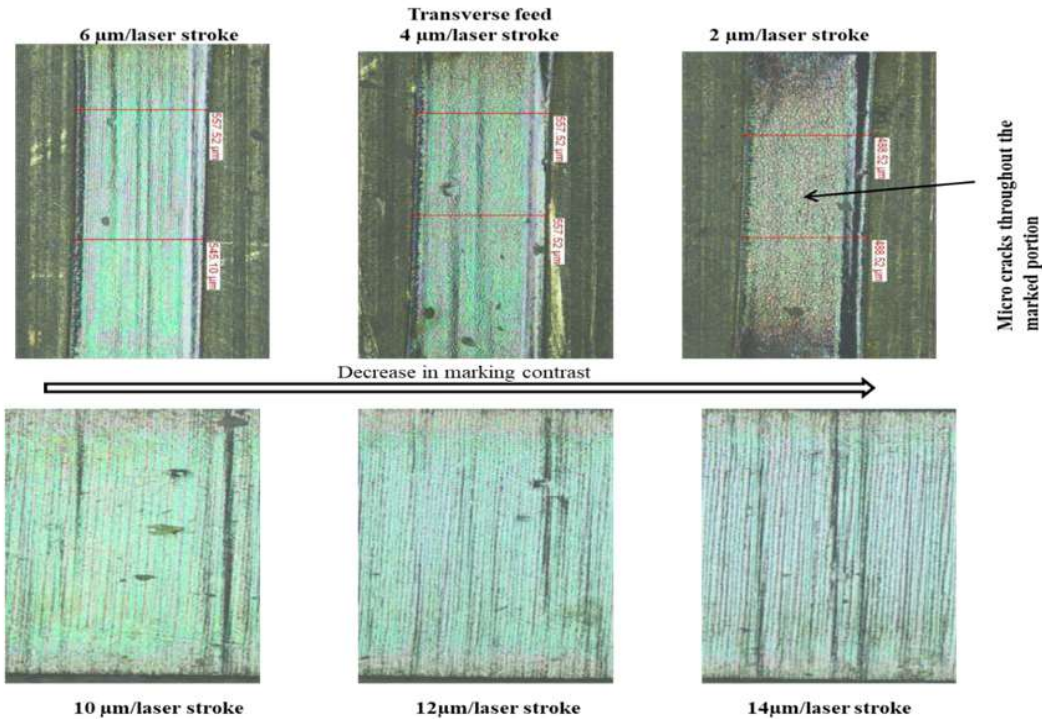


Fig.5.3 Microscopic images of laser marked surface at variant transverse feed



Fig.5.3 are the microscopic view of surface marking obtained as a result of change of transverse feed from 2  $\mu\text{m}/\text{laser stroke}$  to 14  $\mu\text{m}/\text{laser stroke}$ . The decrease of transverse feed below above 8  $\mu\text{m}/\text{laser stroke}$  resulted in the fall of gray value as per analysis. Lower value of transverse feed resulted in the formation of micro cracks throughout the marked portion whereas on the application of high transverse feed indicate the separation of laser spot apart which provides a fall in mark intensity value. Thus for the development of image on Ti6Al4V, transverse feed of 8  $\mu\text{m}/\text{laser stroke}$  yields better results.

### **5.2.2 Effects of Laser irradiation on Line and Surface Marking Characteristics of Ti6Al4V**

Fig.5.4 illustrates the influences of laser irradiation on marking characteristics when process variables like pulse rate of 50 kHz, scan rate of 35 mm/s, and duty cycle of 99 % were held constant. Decrease in laser irradiation from 25 W to 10 W resulted in the increase of mark intensity value of laser marked surface which happened due to luminous intensity of the colour which enhance the gray value of the marked surface in line and surface marking. The width of the marked laser surface at laser irradiation of 25 W is higher for surface marking due to high laser spattering across the marked portion which resulted in the increase of width and it decreases with the application of lower laser irradiation. Such phenomena is least observed in line marking due to which the increase of width is less. Experimental analysis revealed that better marking characteristics were obtained at a laser irradiation of 10 W as seen in Fig.5.4

Fig.5.5 are the microscopic view of line and surface marking obtained as a result of change of laser irradiation. The images were captured using OLYMPUS STM 6 microscope for analysis of marking characteristics. It was observed that laser irradiation of 25 W has high laser spattered on the surface which increases areas to be heat affected and thereby increases width. The different colours obtained also signifies the distribution of heat and its gray value analysis revealed its quality characteristics. The decrease of laser irradiation from 25 W not only minimises the effects of laser spattering on increase of width but also provides the combination of various colours which is responsible for the change of marking contrast as shown in Fig.5.5. Apart from laser irradiation, focus were also laid to investigate the influences of pulse rate on marking characteristics which is discussed in section 5.2.3

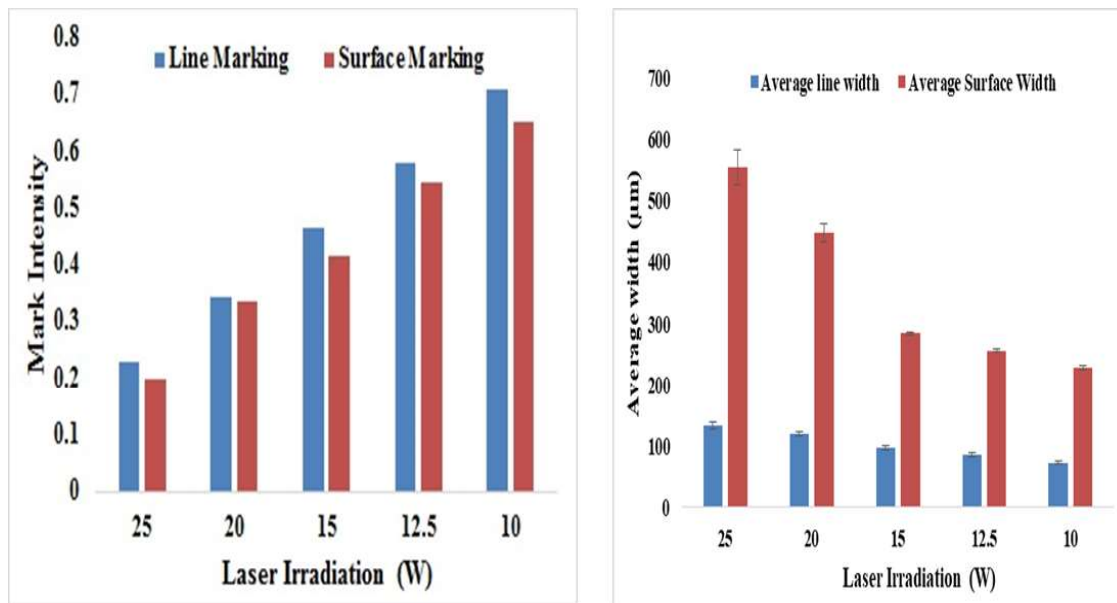


Fig.5.4 Influences of laser irradiation on line and surface marking

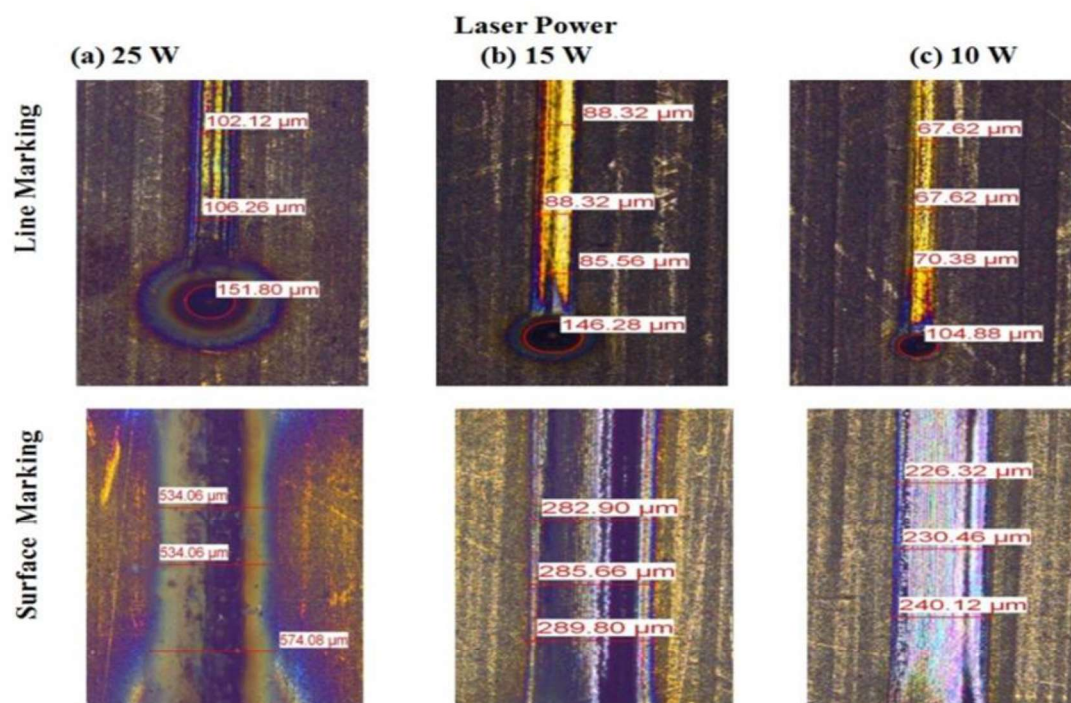


Fig.5.5 Microscopic view of line and surface marked surface with respect to laser irradiation

### 5.2.3 Effects of Pulse rate on Line and Surface Marking Characteristics of Ti6Al4V

Fig.5.6 illustrates the influences of pulse rate on marked properties when process variables like laser irradiation of 10 W, scan rate of 35 mm/s, and duty cycle of 99 % were held constant.

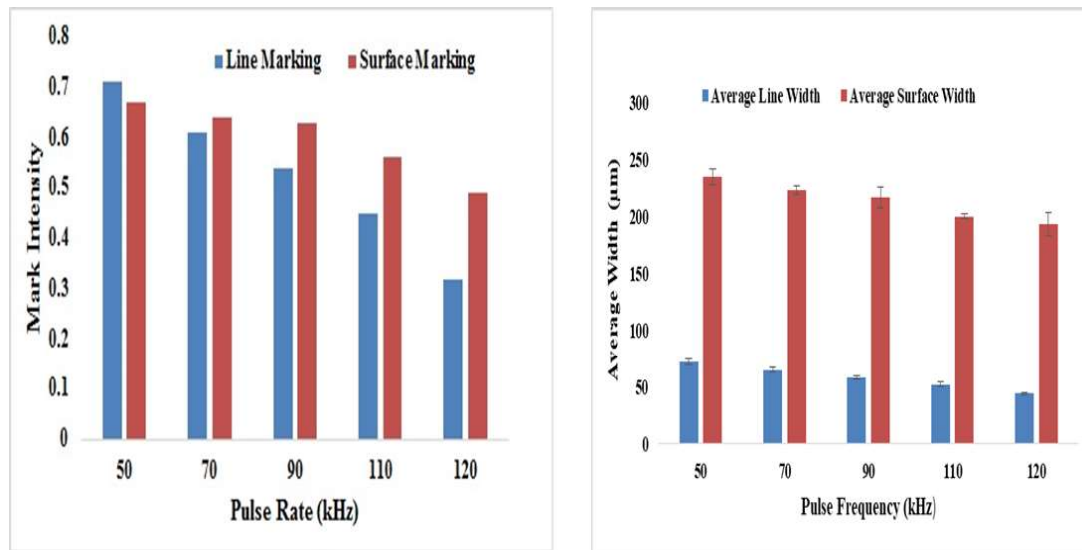


Fig.5.6 Influences of pulse rate on line and surface marking

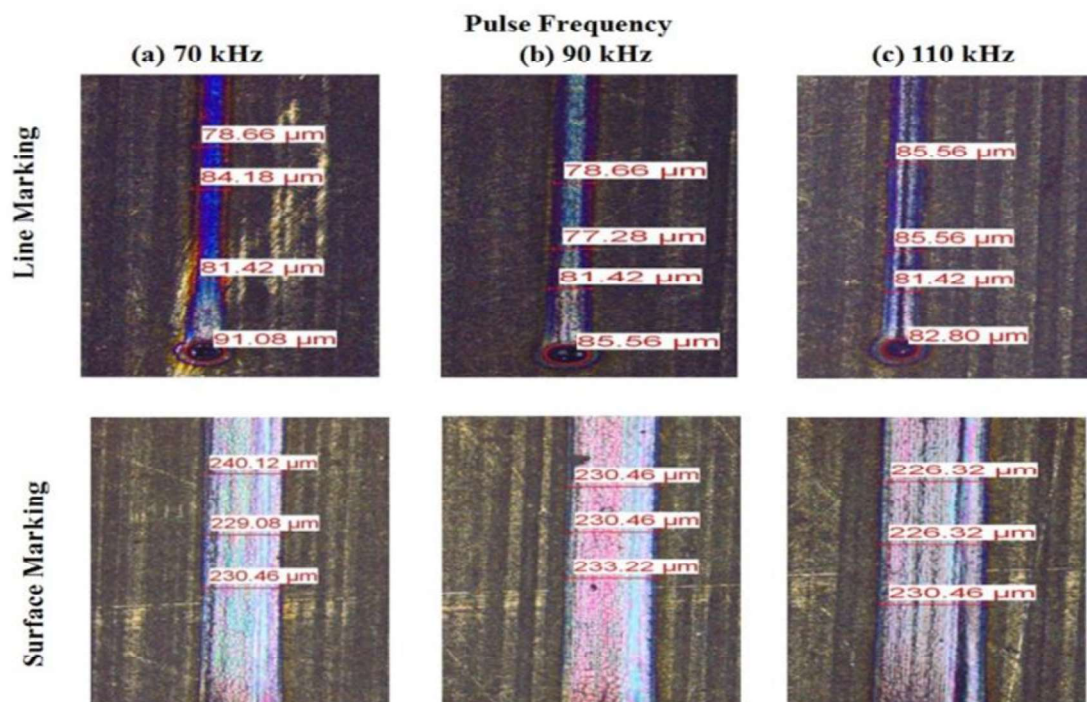


Fig.5.7 Microscopic view of line and surface marked surface with respect to pulse rate

It was observed that increase of pulse rate had less contribution in the change of surface marking characteristics as compared to the characteristics of line marking. The mark intensity value of line marking decreases with increase of pulse rate beyond 50 kHz whereas in surface marking the deviation of mark intensity was low due to the contribution of gray value of various colour obtained in surface marking. Lower pulse rate had high peak power which provides high oxidation with better luminous gray value in line marking and the value gets decreased on the application of higher value of pulse rate. It was observed from Fig.5.6 (b) that increase of pulse rate resulted in the decrease of width of both line and surface marking and reaches to a lower value at a pulse rate of 120 kHz.

Fig.5.7 are the microscopic view of line and surface marking obtained as a result of change of pulse rate. The increase of pulse rate decrease the width of marked surface with fall of mark intensity value. Such fall of marking characteristics is due to lower peak power of pulsed laser due to which the marking occurred on the surface is lighter which provide light intensity laser marked surface. Experimental analysis revealed that pulse rate of 50 kHz provides higher marking characteristics value as compared to other pulse rate laser marked surface.

Thus it was observed that lower value of pulse rate provides better marking characteristics as compared to the higher values of pulse rate. Therefore, laser irradiation of 10 W and pulse rate of 50 kHz were kept fixed and further efforts were laid to study the influences of scan rate on marking characteristics as shown in section 5.2.4

#### **5.2.4 Effects of Scan rate on Line and Surface Marking Characteristics of Ti6Al4V**

Fig.5.8 revealed the influences of scan rate on marking characteristics when other process variables such as laser irradiation of 10 W, pulse rate of 50 kHz, and duty cycle of 99 % were held constant. Lowered value of scan rate increases the heat interaction with the work piece which provides deeper marks on the surface of work piece which has lower gray value as compared to high value of scan rate. However there was a considerable increase of width in both line and surface marking on having lower value of scan rate. Thus from the point of view of less time and better marking characteristics, scan rate of 35 mm/s provides better results.

Fig.5.9 shows the microscopic view of laser marked surface at variant scan rate for line and surface marking. It was observed that on decreasing scan rate from 35 mm/s to 7 mm/s

resulted in the increase of width along with the change of colours which affects marking characteristics mainly mark intensity . Thus to minimise the width and maximum value of mark intensity higher scan rate of 35 mm/s should be used.

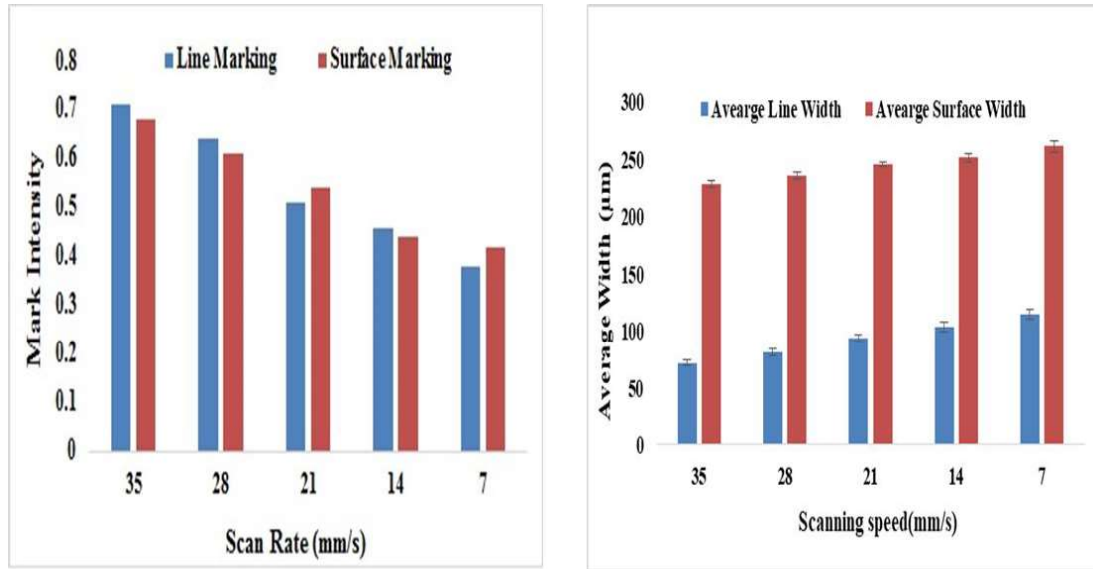


Fig.5.8 Influences of scan rate on line and surface marking

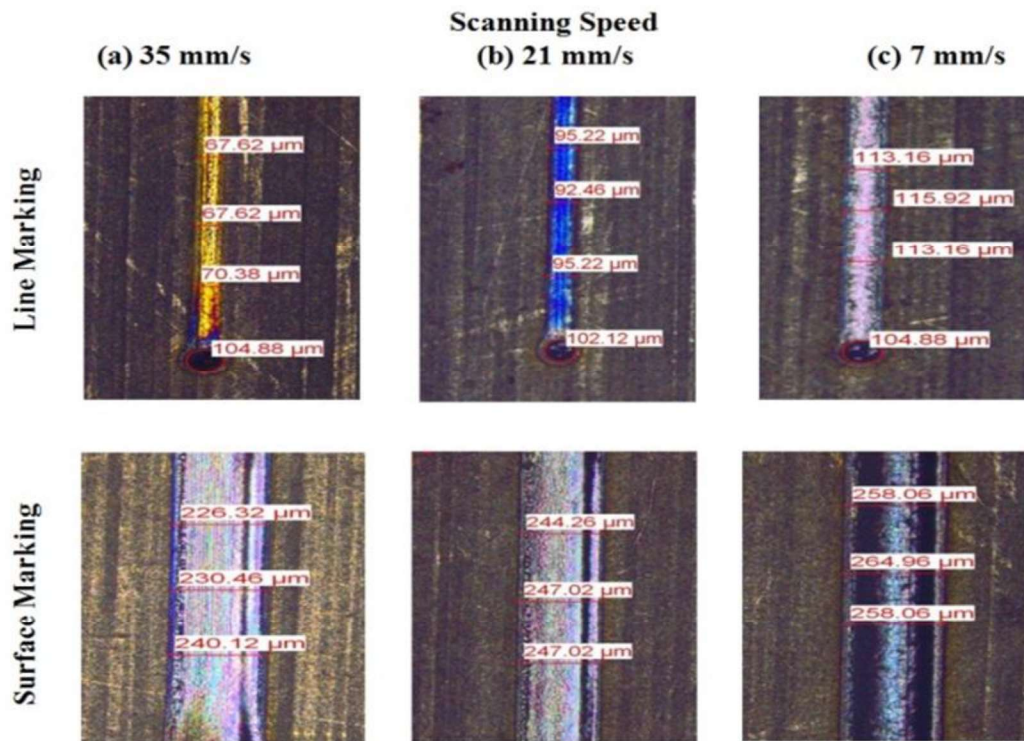


Fig.5.9 Microscopic view of line and surface marked surface with respect to scan rate

Efforts were also laid to study the effects of duty cycle on marking characteristics which are discussed in section 5.2.5.

#### **5.2.5 Effects of duty cycle on Line and Surface Marking Characteristics of Ti6Al4V**

Fig.5.10 illustrates the influences of duty cycle on marked characteristics when other process variables like laser irradiation of 10 W, pulse rate of 50 kHz and scan rate of 35 mm/s were held constant. Decrease of duty cycle decrease the on time of pulse rate which in turn resulted in less heat interaction with the work piece. As a result, marking characteristics such as mark intensity and average width decreases for both line and surface marking. Duty cycle had minimum effects on marking characteristics unless it was varied below 50%. It was observed that on decreasing duty cycle from 99% to 10 % resulted in the decrease of mark intensity for line and surface marking to about 0.35 and 0.42 respectively whereas width for line and surface marking 50  $\mu\text{m}$  and 245  $\mu\text{m}$  respectively.

Fig.5.11 are the microscopic view of line and surface marking obtained as a result of change of duty cycle from 99% to 10 %. Studies revealed that higher value of duty cycle provides high contrast value for both line and surface marking. Since duty cycle is less effective in the change of marking characteristics as compared to other process variables. Thus on analysis it can be revealed that process variables such as laser irradiation of 10 W, pulse rate of 50 kHz, scan rate of 35 mm/s and duty cycle of 99 % yields better value of marking characteristics.



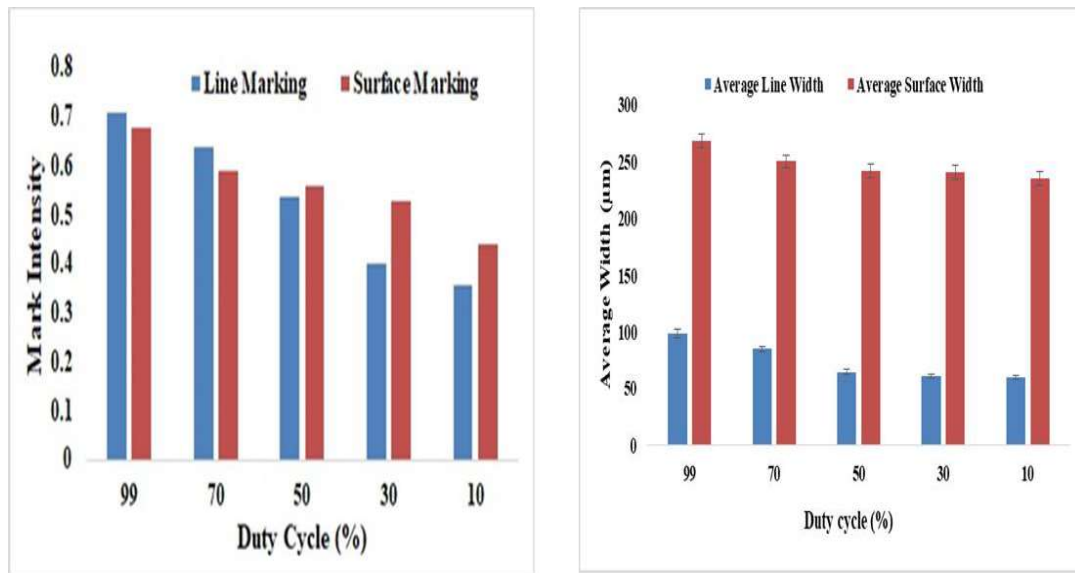


Fig.5.10 Influences of duty cycle on line and surface marking

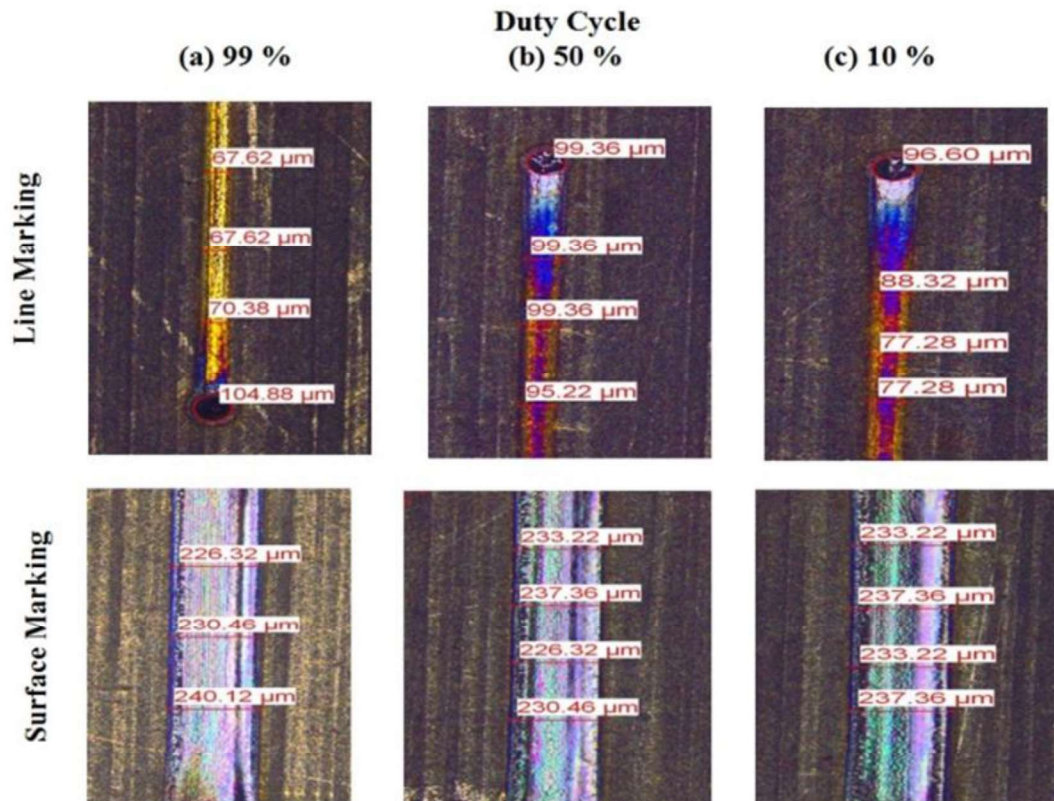














Fig.5.11 Microscopic view of line and surface marking with respect to duty cycle

Apart from the analysis of marking characteristics, some studies were also laid in the analysis of gray value of different colours obtained in the process of line and surface marking. It is then compared to the standard gray value of coloured images. The detailed of which is highlighted in table 5.3.

**Table 5.3: Comparison of Theoretical and Actual mark intensity of obtained colours on marked surface.**

Colour	Theoretical mark intensity	Obtained mark intensity
Purple	 0.15	 0.10
Deep Blue	 0.18	 0.13
Light Blue	 0.27	 0.15
Pink	 0.36	 0.19
Yellow	 0.48	 0.40
Pinkish	 0.80	 0.70

Among all the colours obtained by laser marking operation pinkish colour had highest gray value whereas least gray value was observed for purple colour. The analysis made in this section is also helpful in the generation of geometric shaped laser marked surface as a symbol of product identification and traceability.

Based on better value of process variables obtained through one factor at a time (OFAT) method, some geometric figures were also marked on Ti6Al4V as shown in Fig.5.12 to Fig.5.15



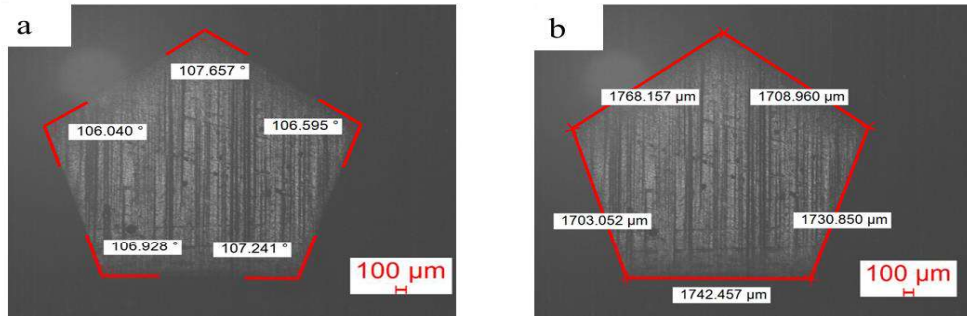


Fig.5.12 Laser marked surface of pentagon at better obtained process variables

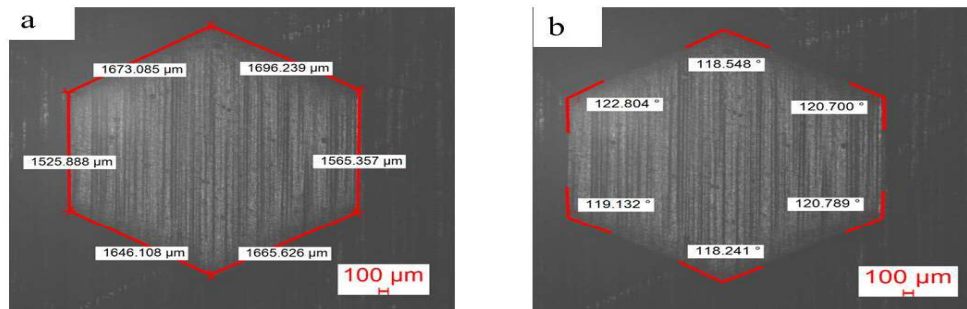


Fig.5.13 Laser marked surface of hexagon at better obtained process variables

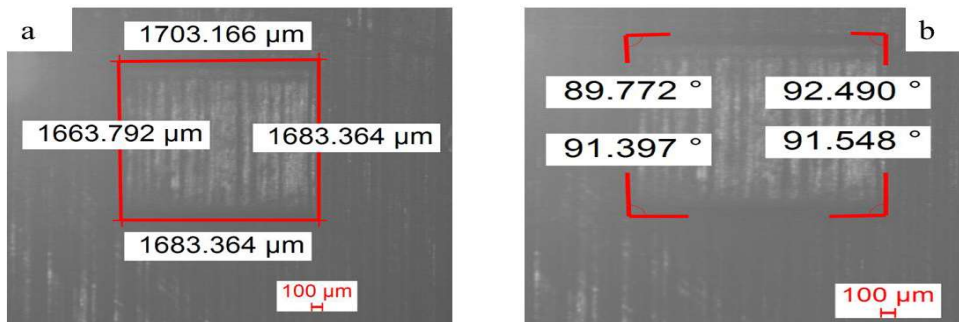


Fig.5.14 Laser marked surface of square at better obtained process variables

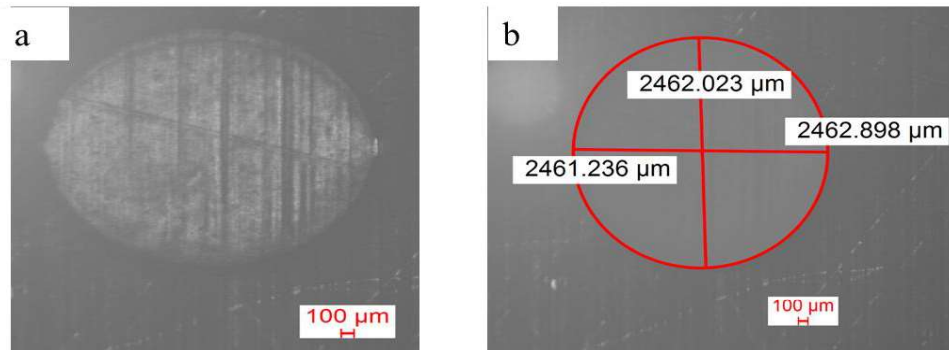


Fig.5.15 Laser marked surface of circle at better obtained process variables

The surfaces were marked based on better obtained process variables using OFAT method. The detailed of which are listed below.

- For **Regular Pentagon** (Fig.5.12): A program of 2259.02  $\mu\text{m}$  sides of pentagon and each interior angle measures  $108^\circ$  was fed to the laser marking machine. Upon analysis, it was observed from Eq.3.1 that the marked area deviation of regular pentagon is  $3.6289 \times 10^6 \mu\text{m}^2$ . The angle deviation as per Eq.3.6 is  $1.11^\circ$ .
- For **Regular Hexagon** (Fig.5.13): A program of 2079.4  $\mu\text{m}$  sides of hexagon and each interior angle measures  $120^\circ$ . Upon analysis, it was observed from Fig.3.1 that the marked area deviation of regular hexagon is  $4.20 \times 10^6 \mu\text{m}^2$ . The angle deviation as per Eq.3.6 is  $0.03^\circ$ .
- For **Square** (Fig.5.14): A program of 2000  $\mu\text{m}$  sides was fed to the laser marking machine. Upon analysis, it was observed from Eq.3.1 that the marked area deviation of square is  $1.1661 \times 10^6 \mu\text{m}^2$ . The angle deviation as per Eq.3.6 is  $1.3^\circ$ .
- For **Circle** (Fig.5.15): A program of 3000  $\mu\text{m}$  diameter of circle was fed to the laser marking machine. Upon analysis it was observed from Eq.3.1 that the marked area deviation of square is  $2.3066 \times 10^6 \mu\text{m}^2$ .

### 5.3 Outcomes of the Present Research

The laser marking operation on Ti6Al4V performed by diode pumped fiber laser provides a brief analysis regarding the process variables selection for better value of marking characteristics. The marking characteristics differ for line marking and surface marking upon using proper set of process variables which have been summed up as follows:

- Laser irradiation plays a major role in change of marking intensity. At higher power, laser spattering resulted in generation of various colours which had a different gray value and thus different mark intensity value.
- Higher pulse rate had lower peak power which aids in lesser surface oxidation and therefore there is a fall in mark intensity value.
- Higher scan rate not only lowers time but also increase the marking intensity which is an observation for Ti6Al4V biomedical material,
- Slight variation of duty cycle had less effects on Ti6Al4V until it is allowed to vary by a larger differences.

The present study focuses on laser marking characteristics of line and surface marking along with the analysis of gray value of different colours that aid in the process of laser marking. The colours obtained are limited but further research is possible regarding the generation of various colours of laser marked surface on Ti6Al4V and generation and enhancement of better laser marking quality of different geometrical shapes.

## **6. EXPERIMENTAL INVESTIGATION INTO FIBER LASER LINE MARKING ON PMMA**

### **6.1 Introduction to Fiber Laser Marking on PMMA**

Polymethyl methacrylate (PMMA) is one of the widely used amorphous thermoplastics material, utilized for various biomedical applications. PMMA  $[\text{CH}_2-\text{C}(\text{CH}_3)\text{COOCH}_3]$ , can also be used as a substitute for optically transparent glass. Processing of PMMA by the laser beam is widely needed, especially for different micro-machining applications. The literature survey of laser beam marking on PMMA signifies that mostly research works have been carried out on Black PMMA. Apart from that, laser marking on red and white PMMA has also been conducted in order to analyse the proper settings of process variables for the generation of better quality laser marked surface.

The present research work, the experimental observations and studies which have been conducted will be fruitful to imprint distinctive logos or any information on black, red and white PMMA materials. The analysis have been conducted based on one factor at a time (OFAT) method. The detailed discussions are listed below:

### **6.2 Results and Discussion on Laser Marking of Black PMMA**

The section deals with the influences of process variables on marking characteristics on line marked surface on black, red and white PMMA carried with the help of diode pumped fiber laser. The experiments were carried out in normal ambient condition in order to determine the impact of process variables such as pulse rate, laser irradiation, and scan rate on line marking. The process variables were changed one factor at a time (OFAT) in order to ascertain the detailed analysis which are discussed below:

#### **6.2.1 Impact of Laser Irradiation on Characteristics of Line Marking of Black PMMA**

When process variables including pulse rate of 50 kHz, and scan rate of 35 mm/s were held constant, Fig.6.1 shows the effects of laser irradiation on output responses of black PMMA.

Decrease in laser irradiation from 25 % to 15 % of 50 W caused an increase in the mark intensity value to 0.60 with corresponding decrease in deviation of length, width and HAZ thickness respectively. High power resulted in high material removal from the surface with corresponding increase in side affected areas which cause decrease in marking quality, increase in average width, length deviation and HAZ thickness. Infact, utilization of high power above 25 % resulted in charring of workpiece surface which restricts its further use. Efforts were also made to investigate the influences of laser irradiation below 10 % of 50 W but invisible marking was observed at such setting of process variables.

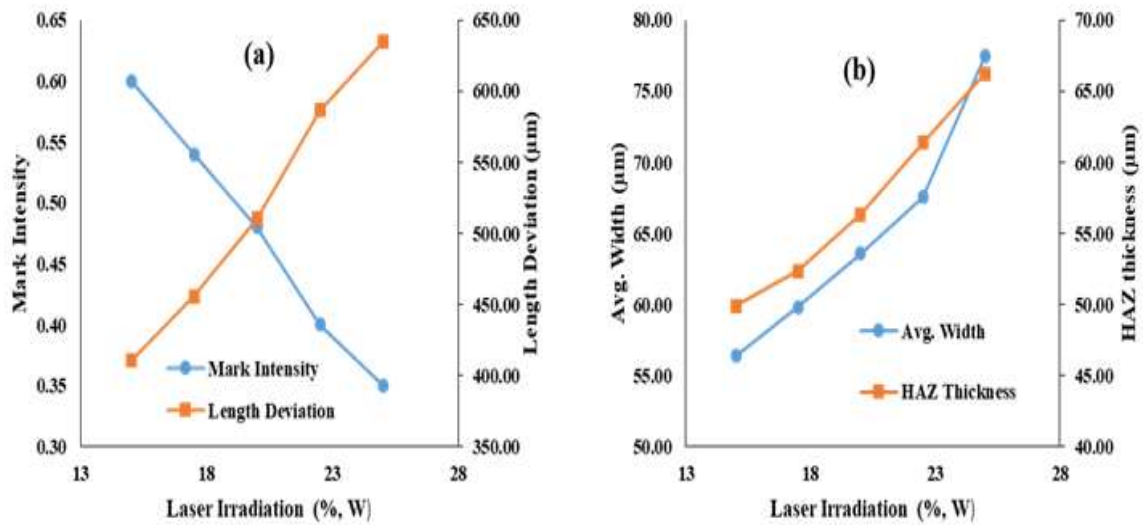


Fig.6.1 Influences of laser irradiation on marking characteristics of PMMA

Fig.6.1 (a) shows that higher value of mark intensity was achieved at laser irradiation of 25% of 50 W and lower value of length deviation was achieved at laser irradiation of 10% of 50 W. Fig.6.1 (b) shows that lower value of average width and HAZ thickness were achieved at laser irradiation of 10% of 50 W. Studies revealed that laser irradiation of 15 % of 50 W should be selected for average value of mark intensity, length deviation, average width, and HAZ thickness. Analysis were also done on other pro-cess variables in order to observe its effects on marking characteristics which were discussed in the following subsection.

## 6.2.2 Effects of Pulse Rate on Characteristics of Line Marking of Black PMMA

Fig.6.2 illustrates the influences of pulse rate on laser marking on black PMMA when other process variables like laser irradiation of 15 % of 50 W, and scan rate of 35 mm/s were held

constant. Upon varying the pulse rate in the range of 50 kHz to 120 kHz, it was observed that mark intensity increase up to 0.77, length deviation reduced to 40  $\mu\text{m}$ , Average width reduced to 33  $\mu\text{m}$ , and HAZ thickness reduced to 48  $\mu\text{m}$  at high pulse rate of 120 kHz. This is because high pulse rate decrease the peak power of laser beam which cause fine marking with minimal harm to the sample. Thus from point of view of better marking characteristics, pulse rate of 120 kHz is selected.

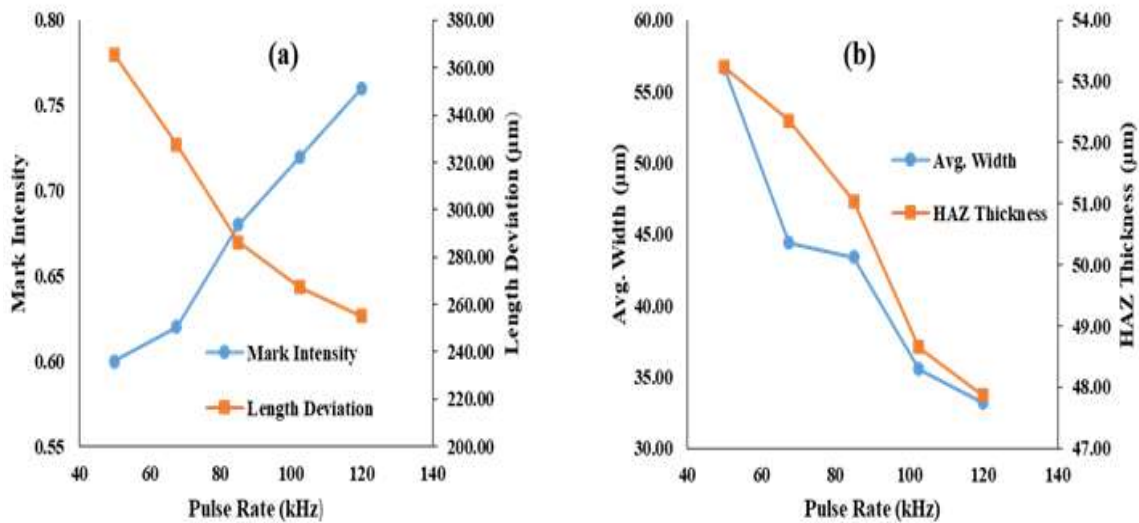


Fig.6.2 Influences of pulse rate on marking characteristics of PMMA

Thus holding pulse rate at 120 kHz, laser irradiation at 15 % of 50 W, process variables like scan rate were allowed to vary to investigate its further impact on marking characteristics as discussed in the subsequent subsection.

### 6.2.3 Effects of Scan Rate on Characteristics of Line Marking of Black PMMA

Fig.6.3 revealed the influences of scan rate on marking characteristics when other process variables such as laser irradiation of 15% of 50 W, and pulse rate of 120 kHz were held constant. Lowered value of scan rate increases the time of heat interaction with the work piece surface which causes deeper penetration and material removal of pulsed laser from the laser scanned area. The scan rate was allowed to vary in the range of 7 to 35 mm/s. It was observed from Fig.6.3.(a) that with the decrease of scan rate to 7 mm/s, mark intensity was reduced to 0.70, and length deviation was increased to 320  $\mu\text{m}$ . Fig.6.3. (b) shows that the average width was increased to 100  $\mu\text{m}$ , and average HAZ thickness was increased to 110  $\mu\text{m}$  on decrease of scan rate from 35 mm/s to 7 mm/s. Thus to decrease the undesired

marking characteristics and time, scan rate of 35 mm/s should be preferred. The application of scan rate below 7 mm/s resulted in the charring of material from the focused zone of laser beam which thus prevents its further use.

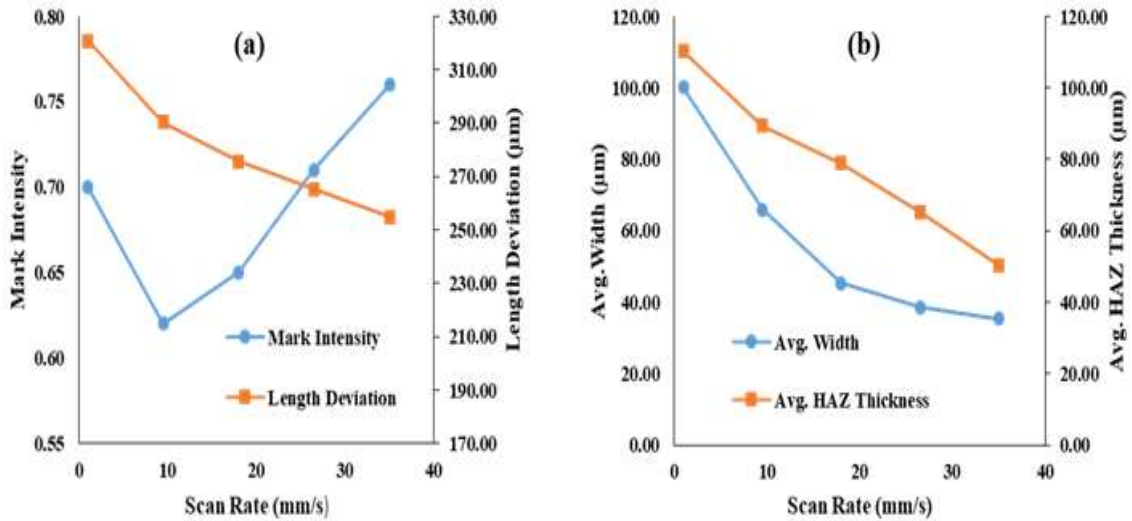


Fig.6.3 Influences of scan rate on marking characteristics of PMMA

Thus based on the studies using one factor at a time (OFAT) method, it was observed that laser irradiation of 15 % of 50 W , pulse rate of 120 kHz, and scan rate of 35 mm/s yields better marking characteristics in terms of mark intensity, length deviation , average width deviation , and average HAZ thickness.

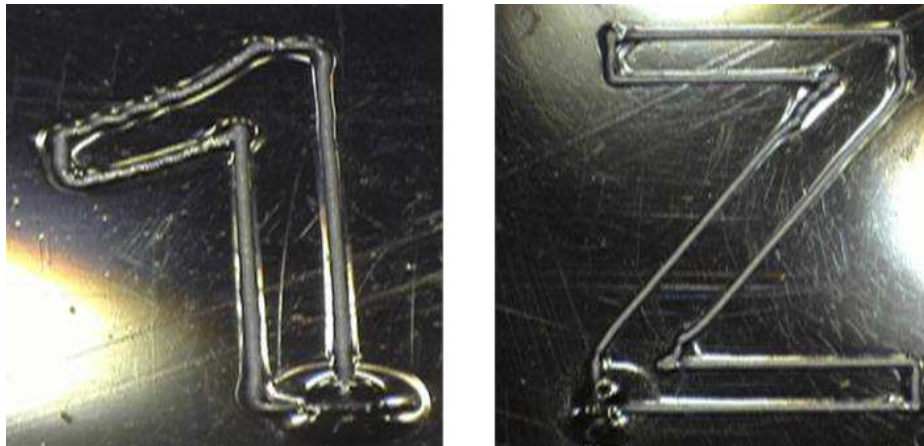


Fig.6.4 Character marked at better obtained process variables

The studies presented in the paper for the generation of better line marking characteristics provides the setting of process variables for the generation of better quality laser marked



surface on PMMA. Based on the studies some characters were marked on PMMA which is shown in Fig.6.4

### **6.3 Results and Discussion on Laser Marking of Red and White PMMA**

The experiments were carried out in order to determine the impact of pulse rate, laser irradiation, scan rate, and the duty cycle on line marking under normal ambient conditions. The process variables were changed one factor at a time (OFAT) in order to ascertain the detailed analysis which are discussed below:

#### **6.3.1 Spectrum analysis of black, red and white PMMA**

The spectrum analysis of red and white PMMA material was done at different wavelength with the use of Cary 5000 UV-VIS-NIR spectroscopy in order to analysis the absorbance, reflectance and transmittance of light by the PMMA material. They are all expressed in percentage. As compared to black PMMA, white and red PMMA has high absorbance rate due to which more energy is required to mark on the surface on white and red PMMA. A set of trial experiments were conducted by keeping process variables such as pulse rate at 50 kHz, scan rate of 35 mm/s and number of pass equal to one constant. It was observed that high laser irradiation such as 100 % of 50 W produces uniform line marking on the surface of W-PMMA material but such value seems insignificant in producing uniformity over the surface of red PMMA. The detailed of which is discussed in section 6.3.2. A brief analysis were also conducted on black PMMA where laser irradiation of 15% of 50 W, pulse rate of 120 kHz, and scan rate of 35 mm/s produces good quality marking on the surface of PMMA material. Fig. 6.5 shows some characters marked at laser irradiation of 15% of 50 W, pulse rate of 120 kHz, and scan rate of 35 mm/s.

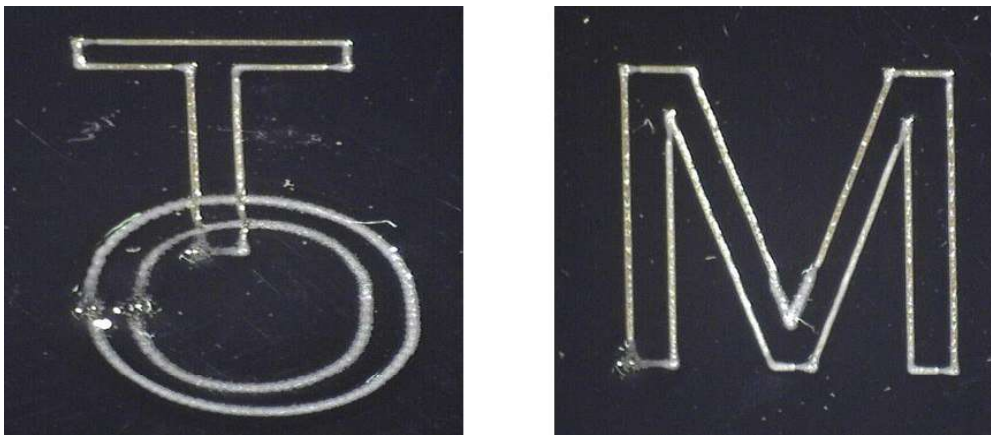


Fig.6.5 Symbol and Character marked at laser irradiation of 15% of 50 W, pulse rate of 120 kHz, and scan rate of 35 mm/s



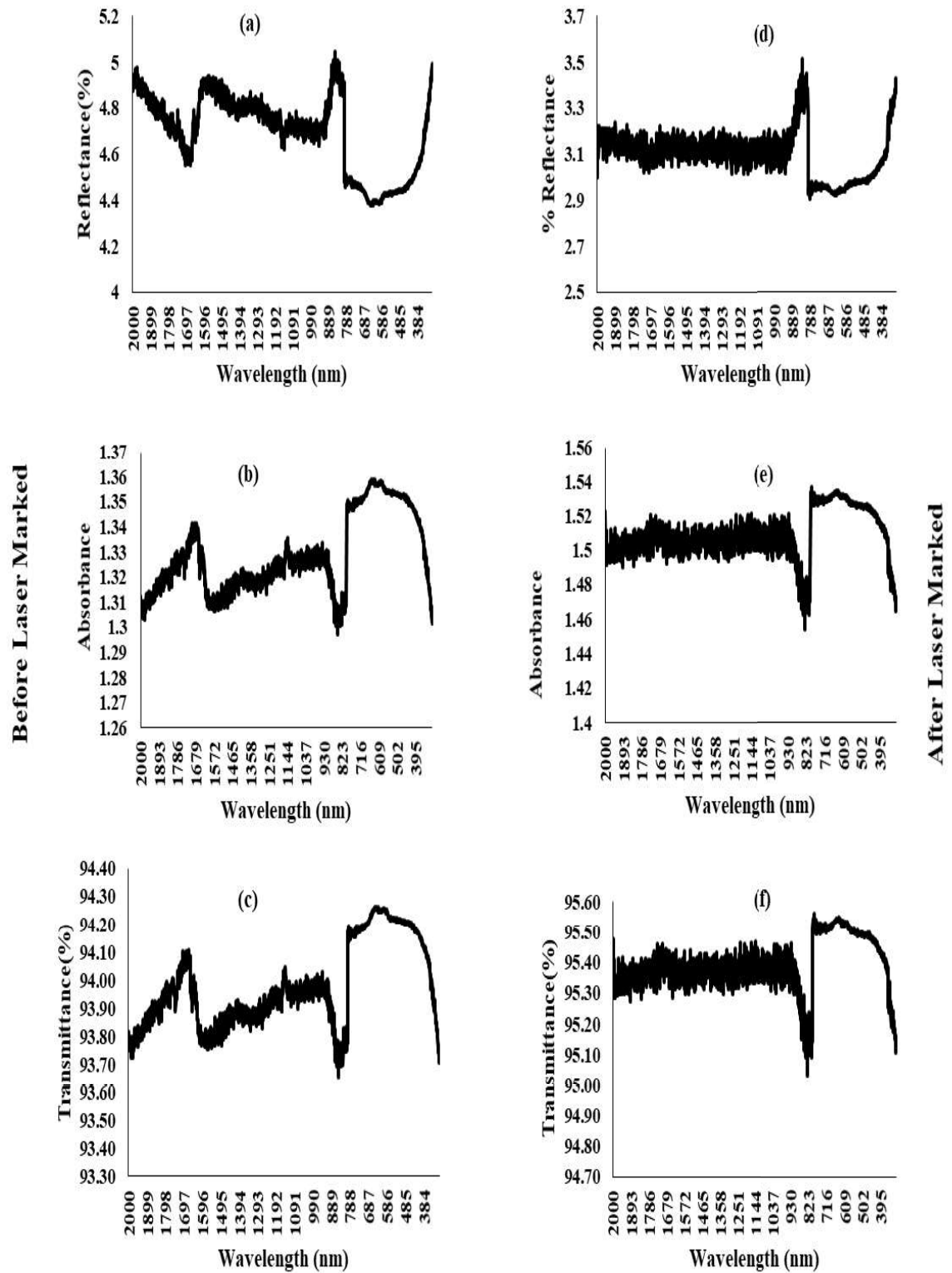


Fig.6.6 Spectroscopy test results of B-PMMA before and after laser marking operation (a, d) Reflectance, (b,e) Absorbance, (c,f) Transmittance

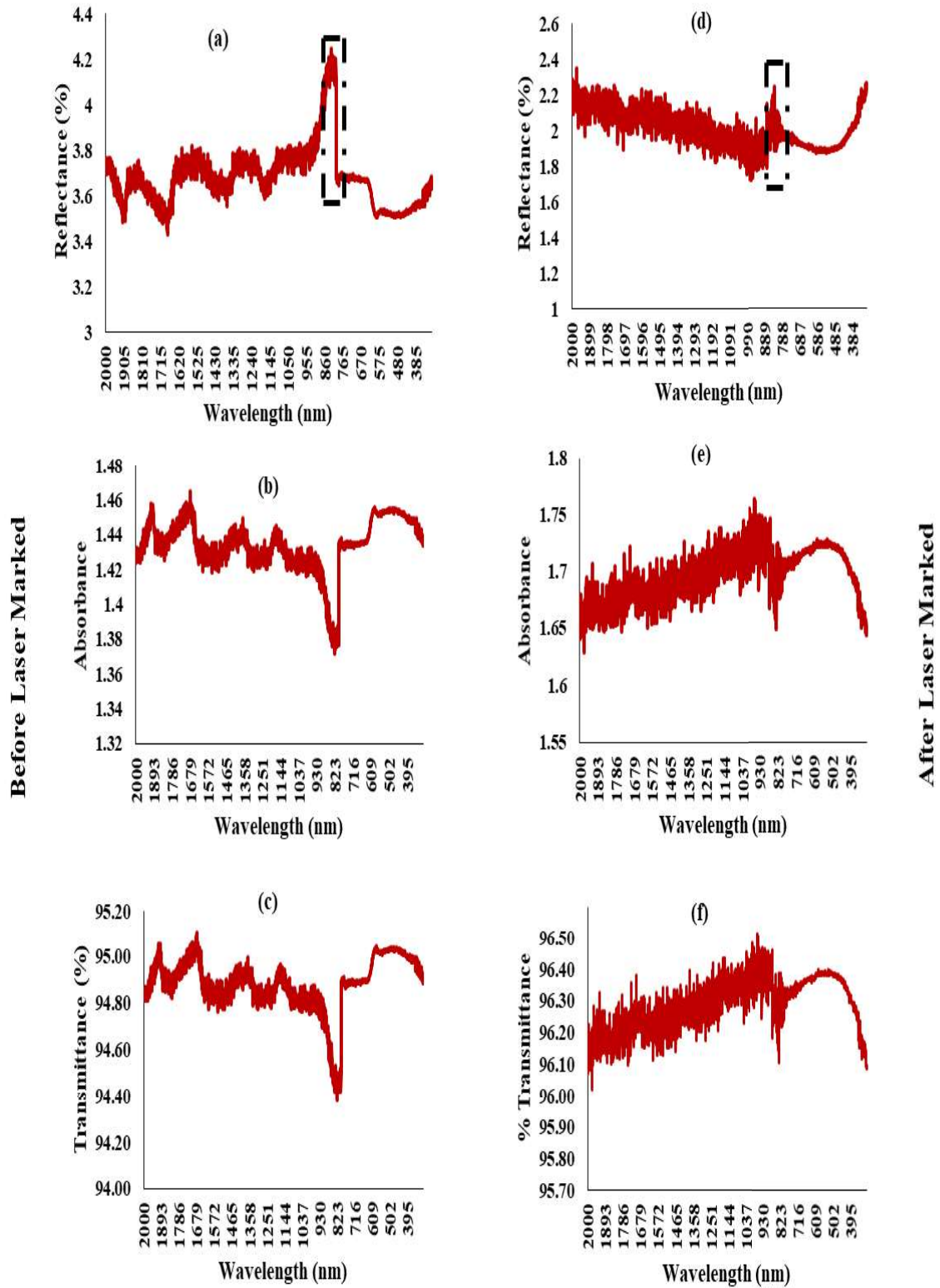


Fig.6.7 Spectroscopy test results of R-PMMA before and after laser marking operation (a, d) Reflectance, (b, e) Absorbance, (c, f) Transmittance

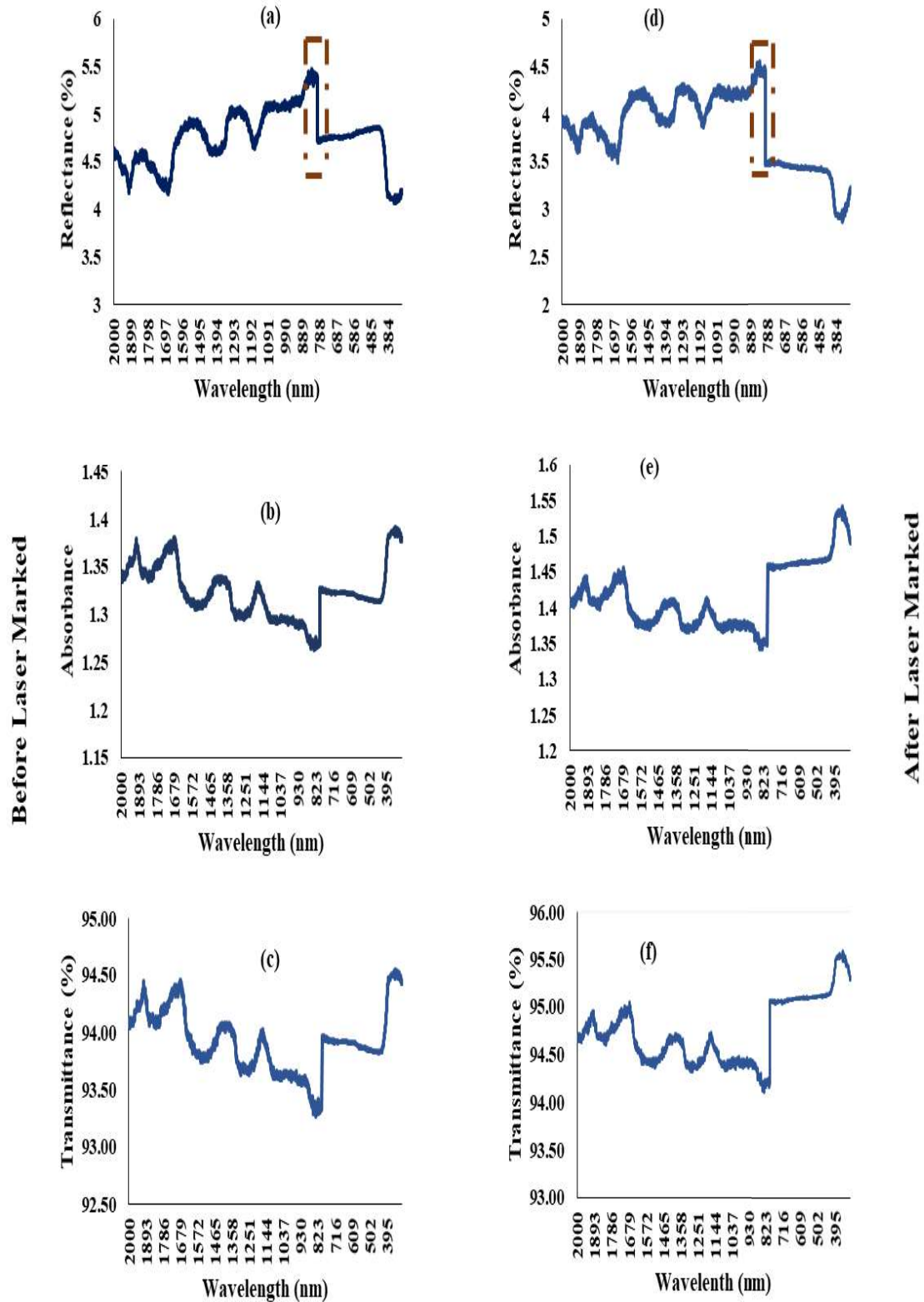


Fig.6.8 Spectroscopy test results of W-PMMA before and after laser marking operation (a, d) Reflectance, (b, e) Absorbance, (c, f) Transmittance

This necessitates to conduct spectrum analysis of B-PMMA, R-PMMA and W-PMMA materials. The detailed of which is highlighted in Fig. 6.6 and Fig. 6.8 respectively. Upon analysis it was observed that at a wavelength of 1064 nm

- For **B-PMMA**: The reflectance, absorbance and transmittance of material for B-PMMA before laser marking operation were 4.7 %, 1.33 and 4.8 % respectively and after laser marking operation were 3.15 %, 1.51, and 3.16 % respectively.
- For **R-PMMA**: The reflectance, absorbance and transmittance of material for B-PMMA before laser marking operation were 3.67 %, 1.43 and 3.75 % respectively and after laser marking operation were 2.09 %, 1.71, and 2.05 % respectively
- For **W-PMMA**: The reflectance, absorbance and transmittance of material for B-PMMA before laser marking operation were 5.10 %, 1.30 and 5.07 % respectively and after laser marking operation were 4.21 %, 1.38, and 4.30 % respectively.

Apart from that, sudden rise and fall of graph was noticed at a wavelength of 800 nm due to change of detector and filter and it is highlighted in dotted line in Fig. 6.6 to Fig.6.8.

### **6.3.2 Effects of Laser irradiation on Marking Characteristics of red and white PMMA**

Fig.6.9 shows the effects of laser irradiation on marking intensity of white and red PMMA when other process variables such as pulse rate of 50 kHz , and scan rate of 35 mm/s. Laser irradiation is equivalent to the average power that has been set in programmable software I -Mark. Upon verification using power meter, it was observed that the set value is equivalent to the observed value. Thus laser irradiation is allowed to vary at appropriate interval in order to observe its influences on marking characteristics. Unlike black PMMA, white and red PMMA possesses less transmittance and high absorptivity. Due to which, it requires high energy of laser to produce uniform marking on PMMA materials. In the process laser irradiation is allowed to vary in the range of 20% to 100% of 50W. It was 100% of 50W where a uniform marking was observed in W-PMMA but not in R-PMMA. Experimental results revealed that 100 % of 50 W laser irradiation produces mark intensity value of 0.70 whereas length deviation, average marked width and HAZ thickness were observed as 160  $\mu\text{m}$ , 115  $\mu\text{m}$ , and 105  $\mu\text{m}$  respectively. High increase in marking characteristics occurred due to maximum energy utilisation of laser beam which increases the mark intensity, average width and HAZ thickness, and length deviation. Apart from that the start and end point of laser is also responsible for the increase of length deviation. The application of

high power causes material vaporisation from the surface of W-PMMA with corresponding increase of side affected areas.

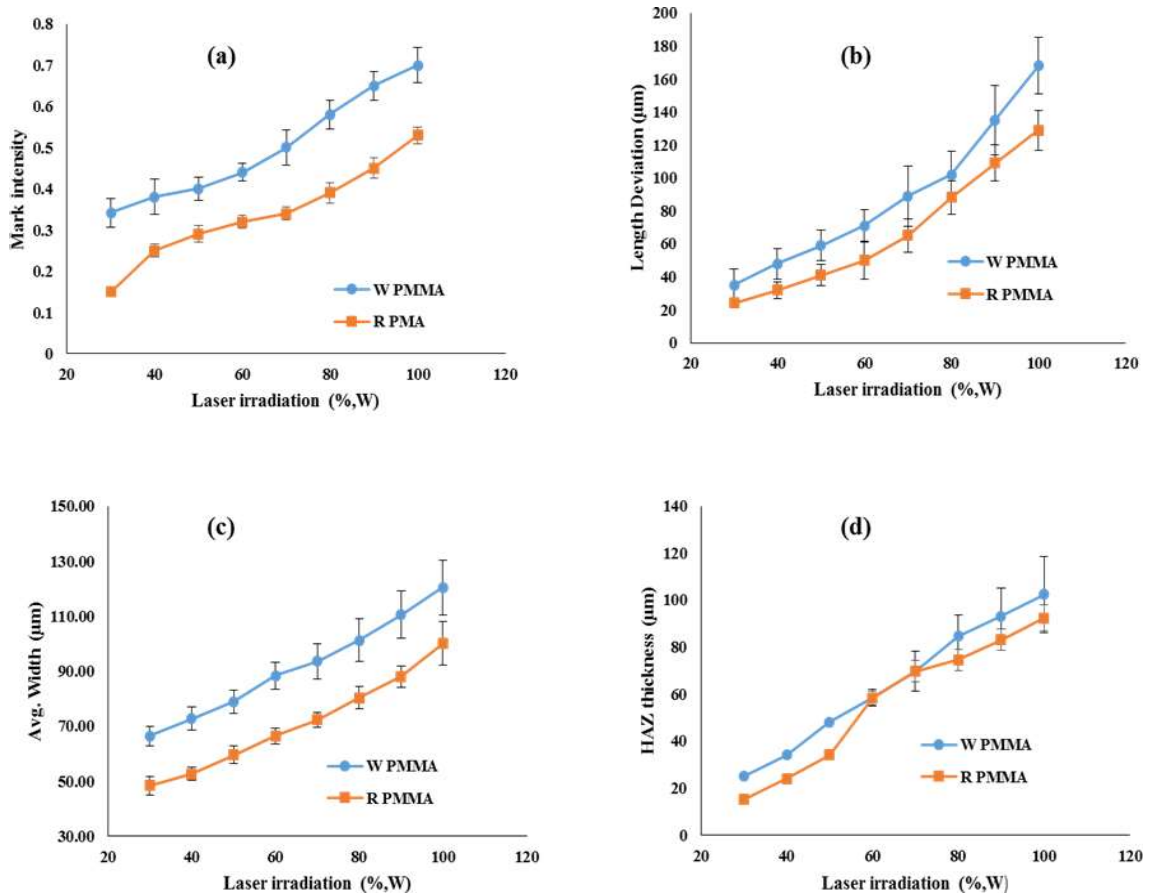


Fig.6.9 Influences of laser irradiation on marking characteristics of R-PMMA and W-PMMA

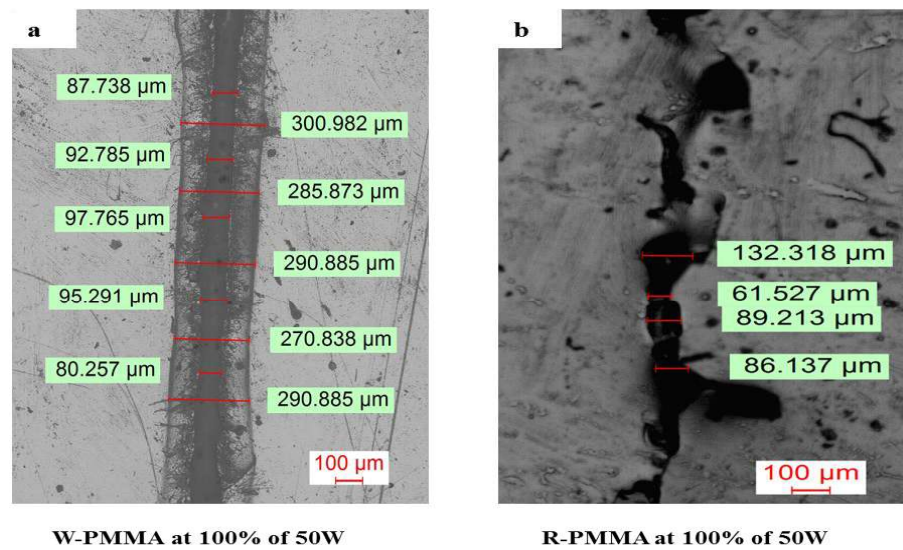


Fig. 6.10 Laser surface marked on W-PMMA and R-PMMA at 100 % laser irradiation

In case of R- PMMA, the higher value of mark intensity value achieved was 0.48 whereas length deviation, average marked width and HAZ thickness were observed as 129  $\mu\text{m}$ , 98  $\mu\text{m}$ , and 85  $\mu\text{m}$  respectively. But no uniformity was observed throughout the surface. In fact, uniformity over the surface of R-PMMA was not achieved at 100 % of 50 W. Thereafter further analysis were carried out by changing pulse rate and scan rate which were discussed in subsequent subsection.

Fig. 6.10.(a & b) are the view of laser surface marked on white and red PMMA at laser irradiation 100 % of 50 W when other process variables such as pulse rate of 50 kHz , and scan rate of 35 mm/s were held constant. It is evident that higher laser irradiation provides better marking at the surface of W-PMMA as compared to R-PMMA due to distinctive reflectance, absorbance and transmittance. Furthermore, no clear HAZ thickness was observed on R-PMMA as compared W-PMMA. It was computed based on difference between maximum and minimum value of width. Thus to further increase the marking characteristic of marked surface based on higher mark intensity, and minimum average width, length deviation and HAZ thickness, other process variables such as pulse rate and scan rate were allowed to vary keeping laser irradiation of 100% of 50 W fixed and their subsequent effects were seen in the following subsection.

### **6.3.3 Effects of Pulse rate on Marking Characteristics of red and white PMMA**

When process variables including laser irradiation of 100% of 50 W, and scan rate of 35 mm/s were held constant, Fig. 6.11 shows the impact of pulse rate on white and red PMMA laser marking. It was observed that with the increase of pulse rates from 50 kHz to 120 kHz, the mark intensity decreases to 0.43, length deviation reduced to 125  $\mu\text{m}$ , average width decreased to 60  $\mu\text{m}$ , and the HAZ thickness decreased to 68  $\mu\text{m}$  in case of W-PMMA whereas in case of R-PMMA, the mark intensity decreases to 0.34, length deviation reduced to 150  $\mu\text{m}$ , average width decreased to 70  $\mu\text{m}$ , and the HAZ thickness decreased to 55  $\mu\text{m}$ . It is due to fact that higher pulse decreases the peak power of laser beam when other process variables such as average power and pulse duration (i.e.120 ns) were held constant. Equation 3.3 provides the relation between peak power, pulse rate, average power and pulse duration of pulsed mode laser. In the present system pulse duration of 120 nanosecond (ns) was system constant and when a particular average power were held constant, peak power totally depends on pulse rate. So on increasing pulse rate, peak power of laser decrease and vice versa.

Thus by the application of high pulse rate resulted in the decrease of peak power of laser beam which resulted in the production of light marking. Due to which, marking characteristics such as mark intensity, length deviation, average width and HAZ thickness decreases and produces a minimum value at higher value of pulse rate which is quite desirable.

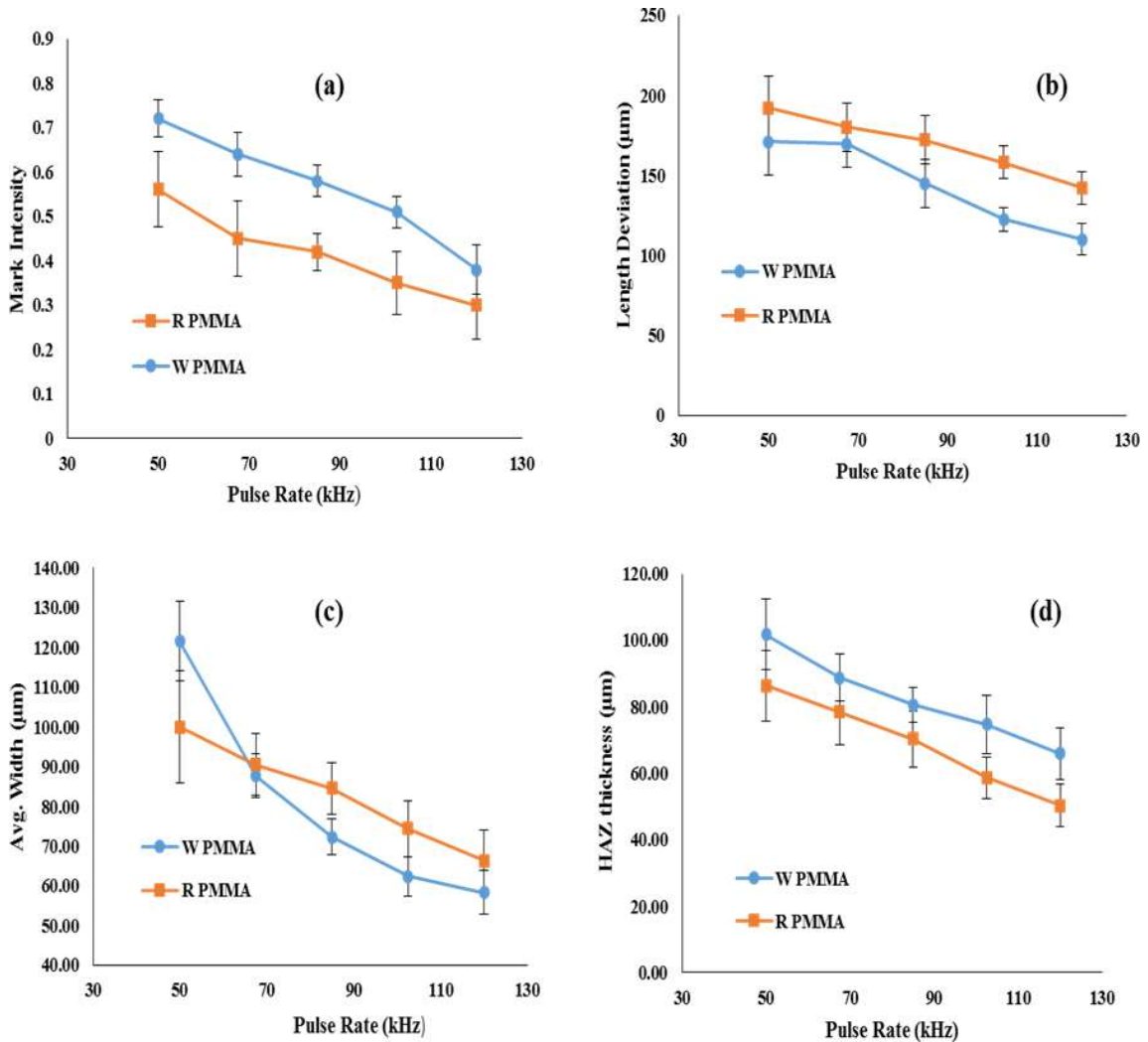


Fig.6.11. Influences of pulse rate on marking characteristics of R-PMMA and W-PMMA

Considering better value of marking characteristics in terms of higher value of mark intensity and minimum value of average width, HAZ thickness and length deviation, pulse rate of 85 kHz seems to be better in the pulse rate range of 50 to 120 kHz and therefore pulse rate of 85 kHz and laser irradiation of 100 % of 50 W is held constant and scan rate



is permitted to change in order to observe its influences on marking characteristics value which can be seen in subsequent sub section.

#### **6.3.4 Effects of Scan rate on Marking Characteristics of red and white PMMA**

Fig. 6.12 illustrates the effects of scan rate on laser marking on white and red PMMA when other process variables like laser irradiation of 100 % of 50 W, and pulse rate of 85 kHz were held constant. Reduction in scan rate resulted in raising of marking characteristics value because the work piece surface is exposed to heat for a longer period of time. It was seen that with the decrease of scan rate from 35 to 7 mm/s, mark intensity increases and reaches to a value of 0.88, length deviation increases to 512  $\mu\text{m}$ , average width increases to 256  $\mu\text{m}$ , HAZ thickness increases to 299  $\mu\text{m}$  respectively in case of W-PMMA whereas in case of R-PMMA, mark intensity reached up to 0.78, length deviation increases to 679  $\mu\text{m}$ , average width increases to 275  $\mu\text{m}$ , HAZ thickness increases to 262  $\mu\text{m}$  respectively. The marking characteristics was further increased on decrease of scan rate below 7 mm/s for W-PMMA but it catches fire in case of R-PMMA. On the other hand, it also increases the time required to mark the surface. Thus to mark the surface in a less time and also for better value of marking characteristics, higher scan rate of 35 mm/s should be set.

Fig. 6.13. (a-c) are the view of laser marked surface of red PMMA extracted from microscope at scan rate of 35 mm/s, 21 mm/s and 7 mm/s respectively when other process variables such as laser irradiation of 100 % of 50 W, and pulse rate of 85 kHz were held constant. It was noted that with decrease of scan rate value from 35 mm/s to 7 mm/s increases the unwanted marking characteristics such as average width and HAZ thickness and at scan rate of 7 mm/s with HAZ thickness superimposed the average width making it difficult to differentiate unlike W-PMMA.

Upon analysis through one factor at a time it was observed that better value of marking characteristics, process variables such as laser irradiation of 100 % of 50 W, pulse rate of 85 kHz, and scan rate of 35 mm/s yields better results for W-PMMA and R-PMMA materials



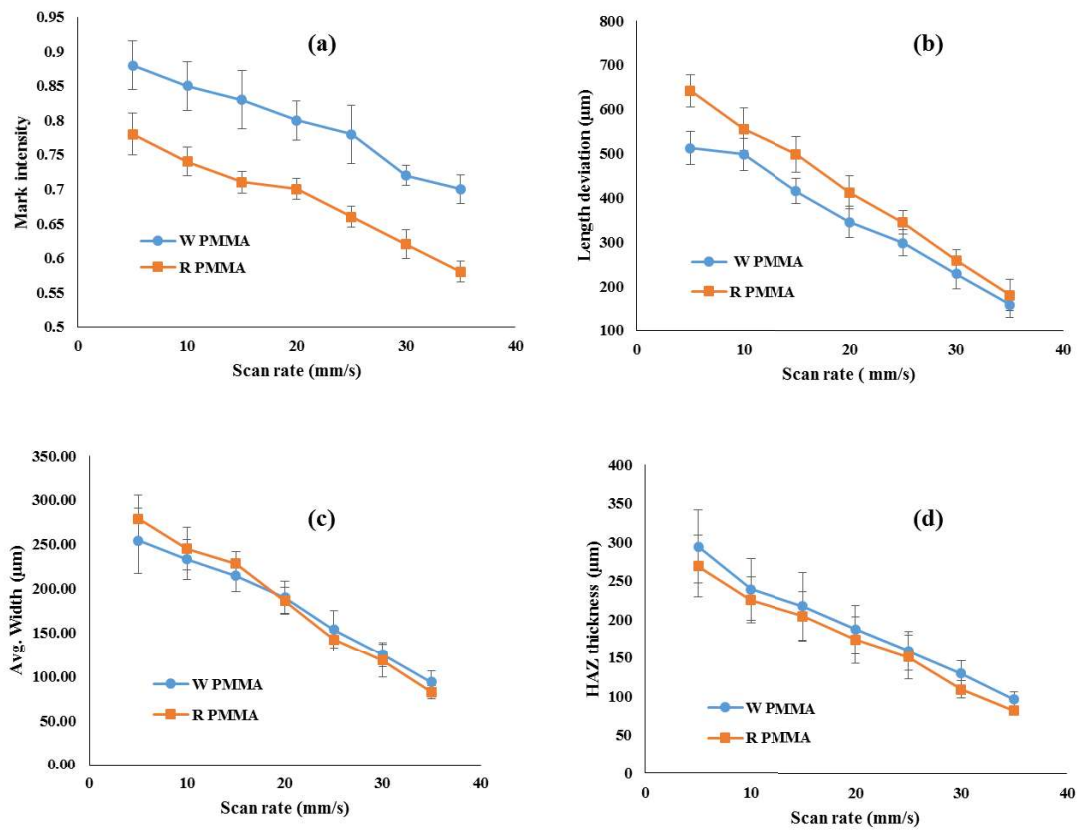


Fig. 6.12. Influences of scan rate on marking characteristics of R-PMMA and W-PMMA

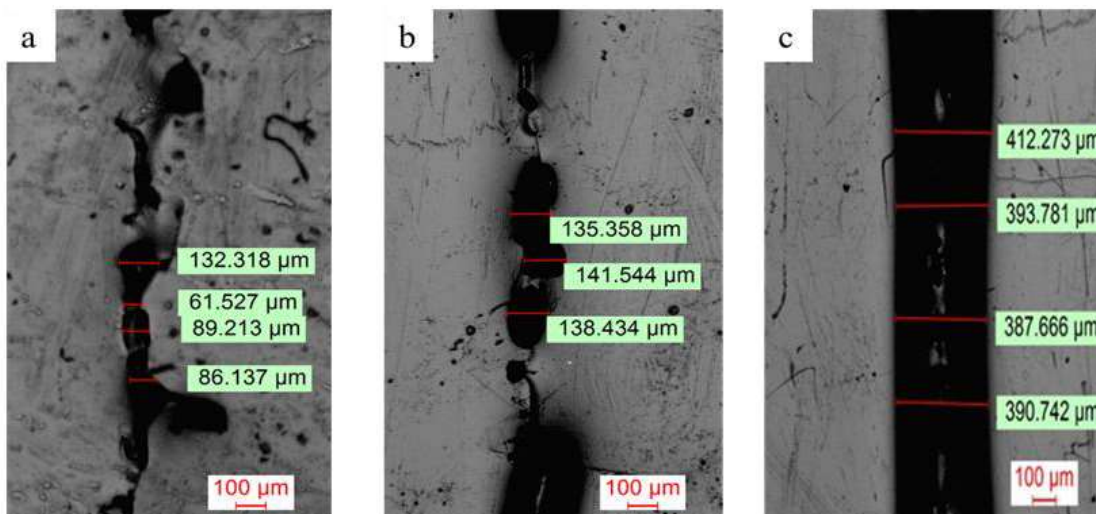


Fig. 6.13 Microscopic view of marked laser surface on red PMMA (a) 35 mm/s, (b) 21 mm/s and (c) 7 mm/s

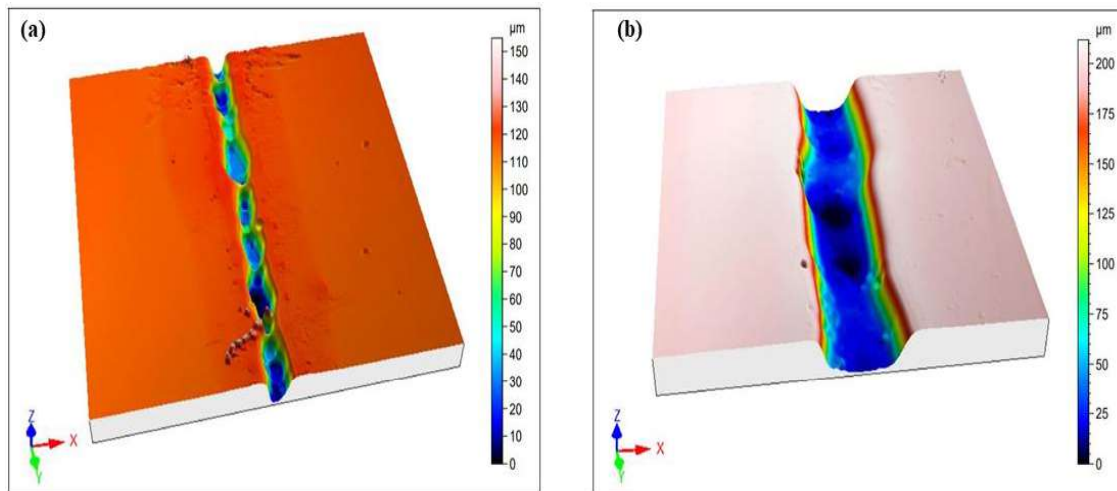


Fig.6.14. 3D Surface Profile of W-PMMA at variant scan rate (a) 35mm/s and (b) 7 mm/s

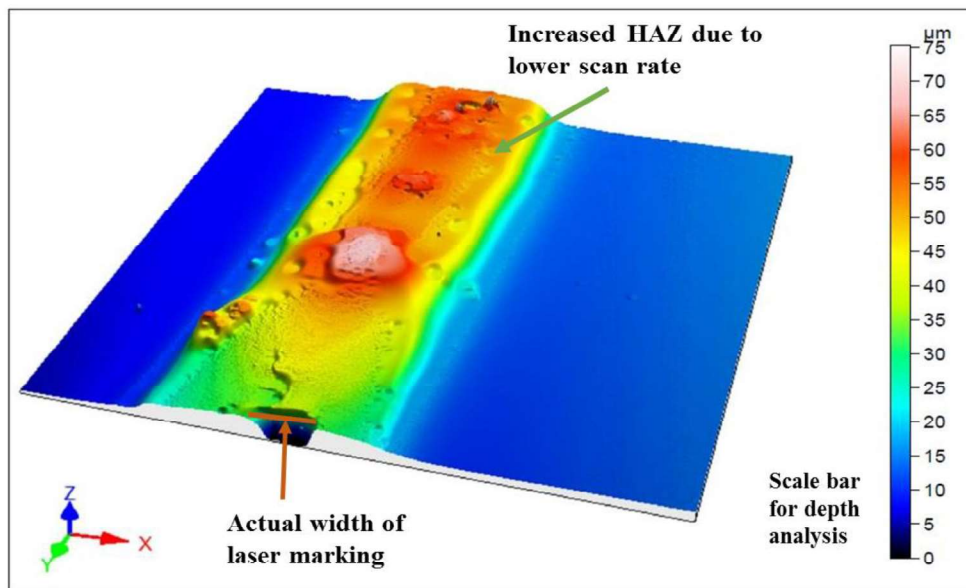


Fig. 6.15 3D surface view of laser surface marked at scan rate of 7 mm/s

Fig.6.14. (a-b) shows the 3-D view of W-PMMA surface marked by laser at scan rate of 35 mm/s and 7 mm/s respectively when other process variables such as laser irradiation of 100 % of 50 W, pulse rate of 85 kHz were held constant. The images were captured using CCI non-contact profilometer which has a resolution of 1 nm. It was also observed that depth of laser marked surface increased from 84.98 $\mu$ m to 185.3  $\mu$ m setting of scan rate from 35 mm/s to 7 mm/s. Since lower scan rate of 7 mm/s increases the more material removal from the focussed zone with corresponding increase in width so lower value of scan rate of 7

mm/s should not be used for better marking characteristics view on the surface of W-PMMA. Also based on shortest possible time to mark the surface of work piece, high scan rate of 35 mm/s yields better results as compared to scan rate of 7 mm/s. Efforts were also given to analyse the surface texture of R-PMMA which is shown in Fig.6.15.

Fig. 6.15 shows the 3-D microscopic view of R-PMMA of laser marked surface at laser irradiation of 100 % of 50 W, pulse rate of 85 kHz, and scan rate of 7 mm/s. It was observed that HAZ thickness increase a lot which is superimposing the actual width of laser marked surface on R-PMMA. The depth of marked surface achieved on the surface of R-PMMA was 45  $\mu\text{m}$ .

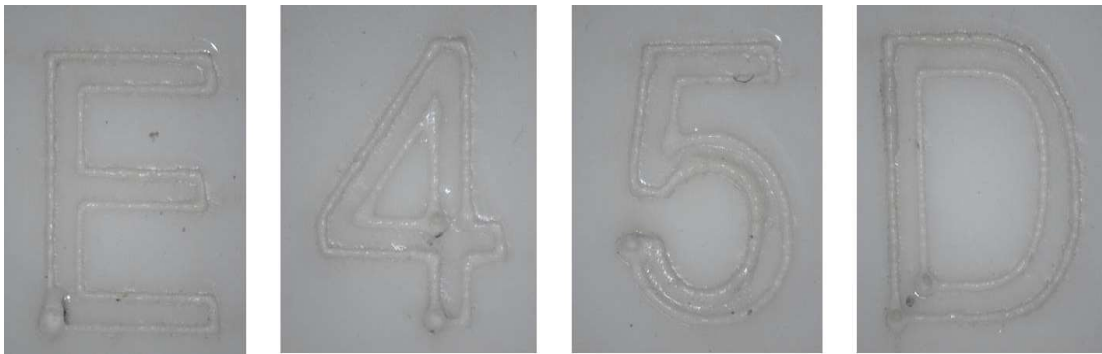


Fig.6.16. Photographic view of some character marked on W-PMMA at laser irradiation of 100 % of 50 W, pulse rate of 85 kHz, and scan rate of 35 mm/s.

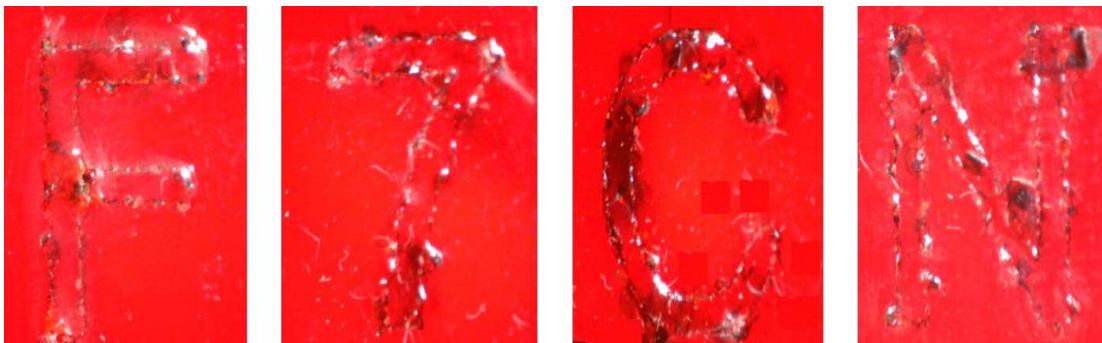


Fig.6.17. Photographic view of some character marked on R-PMMA at laser irradiation of 100 % of 50 W, pulse rate of 85 kHz, and scan rate of 35 mm/s.

Fig.6.16 and Fig.6.17 are the photographic views of characters marked on W-PMMA and R-PMMA marked at laser irradiation of 100 % of 50 W, pulse rate of 85 kHz, and scan rate of 7 mm/s. Apart from characters some simple logos can also be marked at the surface of the materials as a part of product branding.

#### 6.4 Outcomes of the Present Research

PMMA is an amorphous transparent thermoplastic polymer with low water absorption capability was successfully marked by fiber laser. Analysis revealed that PMMA materials are generally has high transmission of light but its acts as good insulation of heat which make it a prime choice of constructing green houses. Studies made in the paper may be modelled as follows:

- i. Laser marking on different PMMA material possess different absorbance, reflectance and transmittance. Due to which, laser irradiation required to produce good quality mark were different for different types of PMMA.
- ii. Laser irradiation and scan rate is more dominating factor in the change of marking characteristics as compared to pulse rate in case of W-PMMA and R-PMMA.
- iii. Laser irradiation of 100 % of 50 W through provides uniform marking on white PMMA but such value of laser is insignificant to produce uniform marking at the surface of red PMMA.
- iv. Decrease in scan rate from 35 mm/s to 7 mm/s resulted in the increase of unwanted marking characteristics such as width, HAZ thickness and length deviation. Lowering scan rate below 7 mm/s resulted in burning of R-PMMA materials.
- v. High pulse rate produces fine marking with corresponding decrease in mark intensity, width, length deviation and HAZ thickness.

Thus generation of good quality with uniform marking is the toughest work on R-PMMA material thus require proper methods to generate. The paper also projects another future work which needs to be focused for having better marking quality characteristics on white and red PMMA by applying suitable mathematical modelling and then optimization of process variables for having optimum value marking characteristics value.

## CHAPTER 7.

### 7.1 General Conclusions

Diode pumped pulsed fiber laser possesses the capability to mark on various engineering materials such as stainless steel 304, Ti6Al4V, PMMA materials and the process variables have much influences in the generation of various geometrical shaped marked surface for achieving high quality marking characteristics. The results of the investigation showed that the marking characteristics of the image were significantly influenced by process variables including laser irradiation, pulse rate, scan rate, defocussing distance, and assist gas. Based on the experimental investigations and modelling on laser marking for generating marked surfaces on various types of engineering materials, the following conclusions are drawn:

- i. Fiber Laser Marking has been performed successfully on SS 304, Ti6Al4V and PMMA materials for generating various regular geometrical shapes with better quality of marking characteristics and it has wide potential for marking complex geometrical shapes by controlling laser marking process variables.
- ii. Surface Oxidation plays a crucial role in the generation of marking contrast when process were carried out at normal atmospheric condition on SS 304, Ti6Al4V and PMMA materials.
- iii. Decrease in transverse feed from 8  $\mu\text{m}$ /laser stroke to 2  $\mu\text{m}$ /laser stroke on SS304 and Ti6Al4V resulted in higher laser spot overlap region in both horizontal and vertical directions which contributes to the higher oxidation and deep marks at the surface of workpiece whereas increase of transverse feed from 8  $\mu\text{m}$ /laser stroke to 14  $\mu\text{m}$ /laser stroke resulted in light marking. The surface resulted in line marking if transverse feed exceeds beyond 21  $\mu\text{m}$ /laser stroke.
- iv. The application of assist gas pressure on SS 304 provide less significant in achievement of goals of marking characteristics of SS 304. It partly caused distribution of heat away from focused surface which makes surface quality poor. However, the assist gas pressure of 1 bar seems to be good in terms of mark width but fall in mark intensity restrict its use.
- v. Laser irradiation is more dominating than pulse rate, scan rate and duty cycle in providing the marking contrast on SS304, Ti6AL4V and PMMA materials. Higher

laser irradiation not only increase oxidation but also increase width and HAZ thickness.

- vi. Increased pulse rate led to the development of low peak power at laser spot region when other variables were kept constant. It leads to a lower rate of increase in width and depth of marked surface with fine surface finish on SS 304, Ti6Al4V and PMMA materials.
- vii. Increased scan rate resulted in reduction of time requirement with lean marking at surface of stainless steel 304. Studies revealed that scan rate lower than 21 mm/s provides better results in case of mark intensity and scan rate above 21 mm/s provides minimum increase in width but in case of Ti6Al4V, scan rate greater than 21 mm/s yields better marking characteristics in terms of mark intensity and width.
- viii. In case of black PMMA, higher scan rate and pulse rate with lower laser irradiation and for both white PMMA and red PMMA, lower scan rate and pulse rate with high laser irradiation yields better marking characteristics.
- ix. Increase of pass beyond one resulted in the increase of time requirement to mark the surface of SS 304, Ti6Al4V, and PMMA materials. It also resulted in the considerable increase in width and depth which is undesirable for laser marking characteristics.
- x. In order to mark equilateral triangle shaped laser marked surface using one factor at a time (OFAT), laser irradiation of 12.5 W, pulse rate of 50 kHz, scan rate of 35 mm/s and duty cycle of 99 % yields better marking characteristics on SS 304. It produces mark intensity value of 0.58, average angle of 61.5°, and area deviation of 120000  $\mu\text{m}^2$ . This set of process variables can also be employed to mark any other geometric shapes as a part of its product authenticity.
- xi. The multi objective optimization using desirability function analysis on marking of equilateral triangle shaped laser marked surface at the surface of Stainless steel 304 (SS 304) shows that 11 W of laser irradiation, 57 kHz of pulse rate, 63 % of duty cycle, and 7 mm/s of scan rate produces mark intensity value of 0.57, angle deviation of 1.25° and area deviation of (0.24 x 10000)  $\mu\text{m}^2$ .
- xii. The percentage of error obtained on marking of equilateral triangle shaped laser marked surface at the surface of Stainless steel 304 using the set of process variables obtained through multi objective optimization using desirability function analysis are 3.6 % for mark intensity, 2.08 % for angle deviation and 4.34 % for area deviation of equilateral triangle laser marked surface.

- xiii. In order to produce good quality line and surface marking on Ti6Al4V using OFAT method, laser irradiation of 10 W, pulse rate of 50 kHz, scan rate of 35 mm/s and duty cycle of 99 % producing mark intensity of 0.70 and average width of 100µm for line marking whereas for surface marking, the mark intensity value is 0.67 and average width is 263 µm respectively.
- xiv. Slight variation of duty cycle had less effects on SS304, Ti6Al4V and PMMA materials until it is allowed to vary by a larger difference greater than 40%.
- xv. In order to produce good quality marking on B-PMMA, laser irradiation of 15 % of 50 W, pulse rate of 120 kHz, and scan rate of 35 mm/s and number of pass equal to one yield better result. It produces mark intensity value of 0.77, length deviation of 250 µm, average width of 38 µm, and average HAZ thickness of 50 µm.
- xvi. In order to produce good quality marking on R-PMMA and W-PMMA, laser irradiation of 100 % of 50 W, pulse rate of 85 kHz, and scan rate of 35 mm/s and number of pass equal to one yield better result. It produces mark intensity value of 0.70, length deviation of 150 µm, average width of 110 µm, and average HAZ thickness of 100 µm in case of W-PMMA whereas in R-PMMA, it produces mark intensity value of 0.58, length deviation of 210 µm, average width of 90 µm, and average HAZ thickness of 85 µm respectively.
- xvii. The spectroscopy analysis of B-PMMA, R-PMMA and W-PMMA revealed that optical properties of the materials such as reflectance, absorbance and transmittance get changed after laser marking operations. It resulted in the decrease of reflectance and transmittance with increase of absorbance which occurred due to oxidation after laser marking operation.

Though some work has been carried as per the objectives in the field of laser marking but there are also future scopes which should be carried for the enrichment of the work in the field of laser marking.

## **7.2 Future Scopes of the Present Work**

While laser marking, particularly CNC pulsed fiber laser systems, is recognized for its precision, efficiency, and eco-friendly characteristics, there are sustainability challenges and areas for improvement. These issues provide opportunities for future research to enhance the environmental impact and efficiency of laser marking processes.

**i. Toxicity of Materials:** Many laser marking systems are used on materials that may be toxic when subjected to high heat. For instance, marking metals or plastics with certain coatings (e.g., PVC) can release harmful gases, such as chlorine or phosgene, which require careful management. The rising demand for environmentally friendly and non-toxic materials across industries places pressure on the sustainability of fiber laser marking systems.

- **Future Research:** Developing safer and more environmentally benign materials to be used in laser marking processes, along with advanced laser systems that minimize toxic emissions, will be a key area of investigation. Sustainable material choices and low-toxicity alternatives could drive the future of the laser marking industry.

**ii. Resource Usage and Manufacturing:** Fiber lasers themselves require the use of rare earth materials, such as ytterbium, for the fiber medium, which can raise concerns regarding the sourcing and sustainability of these materials. These elements are often extracted in energy-intensive and environmentally disruptive mining operations.

- **Future Research:** Research into reducing reliance on rare earth metals by discovering alternative materials or processes for fiber laser manufacturing is crucial. Additionally, advancements in recycling fiber lasers at the end of their lifecycle could mitigate some of the environmental concerns related to resource extraction.

In addition to the above, the following can also be focussed for enhancement work in the areas of fiber laser marking which are modelled as follows:

- To study the influences of other types of lasers on marking characteristics of difficult to mark engineering materials.
- To study the performance of fiber laser marking process on curved surfaces of cylindrical object.
- To study on colour marking on engineering materials by fiber laser.
- To study and execute the process of laser marking of other complex shapes on difficult to mark materials.



### 7.2.1 Limitations in the Context of Industry 4.0

Industry 4.0 is defined by its integration of cyber-physical systems, IoT, and AI-driven automation. While fiber laser marking is an important enabler of Industry 4.0, there are several limitations that need addressing in the context of the emerging trends in smart manufacturing. Some of them are listed below:

1. **Lack of Integration with IoT Systems** Fiber laser systems are typically isolated in manufacturing environments and may lack seamless integration with IoT platforms for real-time data collection, process optimization, and predictive maintenance. This limits the potential for lasers to be used in fully automated and data-driven production lines.

- **Limitation:** The absence of standardized communication protocols and the complexity of integrating with existing enterprise systems.
- **Future Research:** Developing fiber laser systems with IoT connectivity, real-time monitoring capabilities, and compatibility with Industry 4.0 standards would allow for more intelligent, adaptive manufacturing environments.

2. **High Cost of Adoption** Although fiber lasers are cost-effective over time, their initial investment remains relatively high, which can be a barrier for small- and medium-sized enterprises (SMEs) looking to transition to Industry 4.0. Additionally, the cost of maintaining and upgrading these systems can be significant.

- **Limitation:** High capital expenditure and the need for specialized skills for operation and maintenance.
- **Future Research:** There is a need to develop cost-effective laser technologies, more efficient service models (e.g., as-a-service), and better training solutions for SMEs to adopt and integrate laser marking technology into their operations.

3. **Adaptability to Diverse Materials:** While fiber lasers work well on metals and some plastics, they are less effective on certain materials like ceramics, glass, or some composites, which are increasingly being used in advanced manufacturing due to their unique properties (e.g., lightweight, durability, heat resistance).

- **Limitation:** Difficulty in adapting fiber lasers to non-metallic or highly reflective materials.

- **Future Research:** Developing more versatile fiber laser systems capable of working with a wider range of materials, or hybrid systems that combine laser and other marking techniques, will be necessary to keep pace with the diverse materials in modern Industry 4.0 manufacturing.

4. **Automation and Scalability** The potential for fiber laser marking to be scaled in fully automated, flexible production lines is hindered by the need for high-precision handling and material positioning. In high-speed production environments, fiber lasers may face challenges in maintaining quality control and consistency across large batches of products.

- **Limitation:** Difficulty in integrating high-precision marking into high-throughput systems.

- **Future Research:** Advancements in robotic handling, AI-based adaptive marking strategies, and real-time quality monitoring systems will enable greater scalability and adaptability of fiber lasers within Industry 4.0 systems.

## BIBLIOGRAPHY

- [1] Haeffliger, D., Cahill, B. P., & Stemmer, A. (2003). Rapid prototyping of micro-electrodes on glass and polymers by laser-assisted corrosion of aluminum films in water. *Microelectronic Engineering*, 67, 473-478.
- [2] Sánchez-Amaya, J. M., Delgado, T., González-Rovira, L., & Botana, F. J. (2009). Laser welding of aluminium alloys 5083 and 6082 under conduction regime. *Applied Surface Science*, 255(23), 9512-9521.
- [3] Ion, J. (2005). *Laser processing of engineering materials: principles, procedure and industrial application*. Elsevier.
- [4] Jundt, H., & Junghans, J. (1987, January). Microscopic material interactions by laser engraving. In *Lasers in Motion for Industrial Applications* (Vol. 744, pp. 147-155). SPIE.
- [5] Luxon, J. T. (1992). Industrial lasers and their applications. In *Industrial lasers and their applications* (pp. 301-301)
- [6] Ready, J. F. (1997). *Industrial applications of lasers*. Elsevier.
- [7] Ready, J. F. (2001). *LIA handbook of laser materials processing*.
- [8] Houle, F. A. (1986). Basic mechanisms in laser etching and deposition. *Applied Physics A*, 41, 315-330.
- [9] Pham, D. T., Dimov, S. S., & Petkov, P. V. (2007). Laser milling of ceramic components. *International Journal of Machine Tools and Manufacture*, 47(3-4), 618-626.
- [10] Cabalin, L. M., & Laserna, J. J. (1998). Experimental determination of laser induced breakdown thresholds of metals under nanosecond Q-switched laser operation. *Spectrochimica Acta Part B: Atomic Spectroscopy*, 53(5), 723-730.
- [11] Sugioka, K., Meunier, M., & Piqué, A. (Eds.). (2010). *Laser precision microfabrication* (Vol. 135). Springer.
- [12] Rizvi, N. H., & Apte, P. (2002). Developments in laser micro-machining techniques. *Journal of Materials Processing Technology*, 127(2), 206-210.
- [13] Dahotre, N. B., & Harimkar, S. (2008). *Laser fabrication and machining of materials*. Springer Science & Business Media.
- [14] Nedialkov, N. N., Imamova, S. E., Atanasov, P. A., Berger, P., & Dausinger, F. (2005). Mechanism of ultrashort laser ablation of metals: molecular dynamics simulation. *Applied surface science*, 247(1-4), 243-248.
- [15] Lati thermoplastics laser marking- high performance thermoplastics- Manual.
- [16] Sabreen, S. R. *Advancements in Laser Marking of Plastics*.
- [17] Kranj, Remote Laboratory Exercise in LASER MARKING, 2007.
- [18] Han, A., & Gubencu, D. (2008). Analysis of the laser marking technologies. *Nonconventional Technologies Review*, 4, 17-22.

- [19] Ricciardi, G., Cantello, M., & Aira, G. S. (1996). Marking of computer keyboards by means of excimer lasers. *CIRP annals*, 45(1), 191-196.
- [20] Plinski, E. F., Witkowski, J. S., & Abramski, K. M. (2000). Diffractive scanning mechanism for laser marker. *Optics & Laser Technology*, 32(1), 33-37.
- [21] Valette, S., Steyer, P., Richard, L., Forest, B., Donnet, C., & Audouard, E. (2006). Influence of femtosecond laser marking on the corrosion resistance of stainless steels. *Applied Surface Science*, 252(13), 4696-4701.
- [22] Penide, J., Quintero, F., Riveiro, A., Fernández, A., Del Val, J., Comesaña, R., ... & Pou, J. (2015). High contrast laser marking of alumina. *Applied Surface Science*, 336, 118-128.
- [23] Peter, J., Doloi, B., & Bhattacharyya, B. (2013). Analysis of Nd: YAG laser marking characteristics on alumina ceramics. *Journal of The Institution of Engineers (India): Series C*, 94, 287-292.
- [24] Noor, Y. M., Tam, S. C., Lim, L. E. N., & Jana, S. (1994). A review of the Nd: YAG laser marking of plastic and ceramic IC packages. *Journal of materials processing technology*, 42(1), 95-133.
- [25] Qi, J., Wang, K. L., & Zhu, Y. M. (2003). A study on the laser marking process of stainless steel. *Journal of Materials Processing Technology*, 139(1-3), 273-276.
- [26] Stewart, R., Li, L., & Thomas, D. (2000). Laser ablation of multilayers of ink from a paper substrate for tactile printing. *Optics & Laser Technology*, 32(5), 301-305.
- [27] Zheng, H. Y., Lim, G. C., Wang, X. C., Tan, J. L., & Hilfiker, J. (2002). Process study for laser-induced surface coloration. *Journal of Laser Applications*, 14(4), 215-220.
- [28] Dumont, T., Lippert, T., Wokaun, A., & Leyvraz, P. (2004). Laser writing of 2D data matrices in glass. *Thin Solid Films*, 453, 42-45.
- [29] Gao, W., Xue, Y., Li, G., Chang, C., Li, B., Hou, Z., ... & Wang, J. (2019). Investigations on the laser color marking of TC4. *Optik*, 182, 11-18.
- [30] Ma, X., Nie, X., Zhao, J., Han, Y., Shrotriya, P., Wang, Y., & Guo, J. (2020). Coloring stability analysis of nanosecond pulsed laser induced surface coloring on stainless steel. *Optics & Laser Technology*, 123, 105936.
- [31] Chen, M. F., Chen, Y. P., Hsiao, W. T., & Gu, Z. P. (2007). Laser direct write patterning technique of indium tin oxide film. *Thin Solid Films*, 515(24), 8515-8518.
- [32] Kathuria, Y. P. (2007). Laser surface nitriding of yttria stabilized tetragonal zirconia. *Surface and Coatings Technology*, 201(12), 5865-5869.
- [33] Fernández-Pradas, J. M., Restrepo, J. W., Gómez, M. A., Serra, P., & Morenza, J. L. (2007). Laser printing of enamels on tiles. *Applied Surface Science*, 253(19), 7733-7737.
- [34] Chen, M. F., Chen, Y. P., Hsiao, W. T., Wu, S. Y., Hu, C. W., & Gu, Z. P. (2008). A scribing laser marking system using DSP controller. *Optics and Lasers in Engineering*, 46(5), 410-418.

- [35] O'Hana, S., Pinkerton, A. J., Shoba, K., Gale, A. W., & Li, L. (2008). Laser surface colouring of titanium for contemporary jewellery. *Surface engineering*, 24(2), 147-153.
- [36] Leone, C., Lopresto, V., & De Iorio, I. (2009). Wood engraving by Q-switched diode-pumped frequency-doubled Nd: YAG green laser. *Optics and Lasers in Engineering*, 47(1), 161-168.
- [37] Li, Z. L., Zheng, H. Y., Teh, K. M., Liu, Y. C., Lim, G. C., Seng, H. L., & Yakovlev, N. L. (2009). Analysis of oxide formation induced by UV laser coloration of stainless steel. *Applied Surface Science*, 256(5), 1582-1588.
- [38] Alexander, D. R., & Khlif, M. S. (1996). Laser marking using organo-metallic films. *Optics and lasers in Engineering*, 25(1), 55-70.
- [39] Dascalu, T., Acosta-Ortiz, S. E., Ortiz-Morales, M., & Compean, I. (2000). Removal of the indigo color by laser beam–denim interaction. *Optics and lasers in engineering*, 34(3), 179-189.
- [40] Feng, Y., Liu, Z. Q., & Yi, X. S. (2001). Marking carbon black/polypropylene compounds using a Nd: YAG laser. *Journal of materials science letters*, 20(6), 517-520.
- [41] Chitu, L., Cernat, R., Bucatica, I., Puiu, A., & Dumitras, D. C. (2003). Improved technologies for marking of different materials. *Laser physics*, 13(8), 1108-1111.
- [42] Kim, G. D., Kang, H. J., Ahn, S. H., Song, C. K., Back, C., & Lee, C. S. (2005). Laser-marking process for liquid-crystal display light guide panel. *Proceedings of the Institution of Mechanical Engineers, Part B: Journal of Engineering Manufacture*, 219(7), 565-569.
- [43] Dusser, B., Sagan, Z., Bruneel, D., Jourlin, M., & Audouard, E. (2007, July). Laser deep marking of metals and polymers: potential interest for information coding. In *Journal of Physics: Conference Series* (Vol. 77, No. 1, p. 012002). IOP Publishing.
- [44] Jangsombatsiri, W., & Porter, J. D. (2007). Laser direct-part marking of data matrix symbols on carbon steel substrates.
- [45] Chen, M. F., Hsiao, W. T., Huang, W. L., Hu, C. W., & Chen, Y. P. (2009). Laser coding on the eggshell using pulsed-laser marking system. *Journal of Materials Processing Technology*, 209(2), 737-744.
- [46] Leone, C., Genna, S., Caprino, G., & De Iorio, I. (2010). AISI 304 stainless steel marking by a Q-switched diode pumped Nd: YAG laser. *Journal of Materials Processing Technology*, 210(10), 1297-1303.
- [47] Leone, C., Bassoli, E., Genna, S., & Gatto, A. (2018). Experimental investigation and optimisation of laser direct part marking of Inconel 718. *Optics and Lasers in Engineering*, 111, 154-166.
- [48] Shivakoti, I., Kibria, G., & Pradhan, B. B. (2019). Predictive model and parametric analysis of laser marking process on gallium nitride material using diode pumped Nd: YAG laser. *Optics & Laser Technology*, 115, 58-70.

- [49] Sun, X., Wang, W., Mei, X., Pan, A., & Zhang, Y. (2020). Femtosecond laser-induced periodic oxidization of titanium film: Structural colors both in reflection and transmission mode. *Optical Materials*, 109, 110240.
- [50] Liu, H., Tang, Y., Xie, Y., Lu, L., Wan, Z., Tang, W., ... & Yang, D. (2019). Effect of pulsed Nd: YAG laser processing parameters on surface properties of polyimide films. *Surface and Coatings Technology*, 361, 102-111.
- [51] Łęcka, K. M., Gąsiorek, J., Mazur-Nowacka, A., Szczygieł, B., & Antończak, A. J. (2019). Adhesion and corrosion resistance of laser-oxidized titanium in potential biomedical application. *Surface and Coatings Technology*, 366, 179-189.
- [52] Odintsova, G., Andreeva, Y., Salminen, A., Roozbahani, H., Van Cuong, L., Yatsuk, R., ... & Veiko, V. (2019). Investigation of production related impact on the optical properties of color laser marking. *Journal of Materials Processing Technology*, 274, 116263.
- [53] Jwad, T., Walker, M., & Dimov, S. (2018). Erasing and rewriting of titanium oxide colour marks using laser-induced reduction/oxidation. *Applied Surface Science*, 458, 849-854.
- [54] Astarita, A., Genna, S., Leone, C., Minutolo, F. M. C., Squillace, A., & Velotti, C. (2016). Study of the laser marking process of cold sprayed titanium coatings on aluminium substrates. *Optics & Laser Technology*, 83, 168-176.
- [55] Penide, J., Quintero, F., Riveiro, A., Fernández, A., Del Val, J., Comesaña, R., ... & Pou, J. (2015). High contrast laser marking of alumina. *Applied Surface Science*, 336, 118-128.
- [56] Cheng, J., Zhou, J., Zhang, C., Cao, Z., Wu, D., Liu, C., & Zou, H. (2019). Enhanced laser marking of polypropylene induced by “core-shell” ATO@ PI laser-sensitive composite. *Polymer degradation and stability*, 167, 77-85.
- [57] Kibria, G., Chatterjee, S., Shivakoti, I., Doloi, B., & Bhattacharyya, B. (2018, June). RSM based experimental investigation and analysis into laser surface texturing on titanium using pulsed Nd: YAG laser. In *IOP conference series: materials science and engineering* (Vol. 377, No. 1, p. 012203). IOP Publishing.
- [58] Cui, C. Y., Cui, X. G., Ren, X. D., Qi, M. J., Hu, J. D., & Wang, Y. M. (2014). Surface oxidation phenomenon and mechanism of AISI 304 stainless steel induced by Nd: YAG pulsed laser. *Applied surface science*, 305, 817-824.
- [59] Adams, D. P., Hodges, V. C., Hirschfeld, D. A., Rodriguez, M. A., McDonald, J. P., & Kotula, P. G. (2013). Nanosecond pulsed laser irradiation of stainless steel 304L: Oxide growth and effects on underlying metal. *Surface and coatings technology*, 222, 1-8.
- [60] Lawrence, S. K., Adams, D. P., Bahr, D. F., & Moody, N. R. (2013). Mechanical and electromechanical behavior of oxide coatings grown on stainless steel 304L by nanosecond pulsed laser irradiation. *Surface and Coatings Technology*, 235, 860-866.

- [61] Adams, D. P., Murphy, R. D., Saiz, D. J., Hirschfeld, D. A., Rodriguez, M. A., Kotula, P. G., & Jared, B. H. (2014). Nanosecond pulsed laser irradiation of titanium: Oxide growth and effects on underlying metal. *Surface and Coatings Technology*, 248, 38-45.
- [62] Liu, H., Tang, Y., Xie, Y., Lu, L., Wan, Z., Tang, W., ... & Yang, D. (2019). Effect of pulsed Nd: YAG laser processing parameters on surface properties of polyimide films. *Surface and Coatings Technology*, 361, 102-111.
- [63] Raillard, B., Gouton, L., Ramos-Moore, E., Grandthyll, S., Müller, F., & Mücklich, F. (2012). Ablation effects of femtosecond laser functionalization on steel surfaces. *Surface and Coatings Technology*, 207, 102-109.
- [64] Senegačnik, M., Hočevár, M., & Gregorčič, P. (2019). Influence of processing parameters on characteristics of laser-induced periodic surface structures on steel and titanium. *Procedia CIRP*, 81, 99-103.
- [65] Moura, C. G., Carvalho, O., Gonçalves, L. M. V., Cerqueira, M. F., Nascimento, R., & Silva, F. (2019). Laser surface texturing of Ti-6Al-4V by nanosecond laser: Surface characterization, Ti-oxide layer analysis and its electrical insulation performance. *Materials Science and Engineering: C*, 104, 109901.
- [66] Lehr, J., De Marchi, F., Matus, L., MacLeod, J., Rosei, F., & Kietzig, A. M. (2014). The influence of the gas environment on morphology and chemical composition of surfaces micro-machined with a femtosecond laser. *Applied Surface Science*, 320, 455-465.
- [67] Amara, E. H., Haïd, F., & Noukaz, A. (2015). Experimental investigations on fiber laser color marking of steels. *Applied Surface Science*, 351, 1-12.
- [68] Flury, M., Clauss, E., Gérard, P., Fontaine, J., & Fogarasssy, E. (2007). Encoded complex reconstruction into diffractive optical elements for high power Nd: YAG laser marking system. *Optics communications*, 273(2), 575-580.
- [69] Chen, M. F., Chen, Y. P., & Hsiao, W. T. (2009). Correction of field distortion of laser marking systems using surface compensation function. *Optics and Lasers in Engineering*, 47(1), 84-89.
- [70] Diaci, J., Bračun, D., Gorkič, A., & Možina, J. (2011). Rapid and flexible laser marking and engraving of tilted and curved surfaces. *Optics and lasers in engineering*, 49(2), 195-199.
- [71] Lin, C. S., Huang, J. T., Wei, T. C., Yeh, M. S., & Chen, D. C. (2011). High speed and high accuracy inspection of in-tray laser IC marking using line scan CCD with a new calibration model. *Optics & Laser Technology*, 43(1), 218-225.
- [72] Wang, D., Yu, Q., & Ye, X. (2014). Correction of the field distortion in embedded laser marking system. *Optics & Laser Technology*, 57, 52-56.
- [73] Ng, T. W., & Yeo, S. C. (2000). Aesthetic laser marking assessment. *Optics & Laser Technology*, 32(3), 187-191.
- [74] Ng, T. W., & Yeo, S. C. (2000). Aesthetic laser marking assessment using spectrophotometers. *Journal of Materials Processing Technology*, 104(3), 280-283.

- [75] Velotti, C., Astarita, A., Leone, C., Genna, S., Minutolo, F. M. C., & Squillace, A. (2016). Laser marking of titanium coating for aerospace applications. *Procedia Cirp*, 41, 975-980.
- [76] Park, Y. W., & Rhee, S. (2007). Study of a line width estimation model for laser micro material processing using a photodiode. *Optics & Laser Technology*, 39(7), 1461-1471.
- [77] Antończak, A. J., Kocoń, D., Nowak, M., Koziol, P., & Abramski, K. M. (2013). Laser-induced colour marking—Sensitivity scaling for a stainless steel. *Applied Surface Science*, 264, 229-236.
- [78] Chen, Y. H., Tam, S. C., Chen, W. L., & Zheng, H. Y. (1996). Application of the Taguchi method in the optimization of laser micro-engraving of photomasks. *International Journal of Materials and Product Technology*, 11(3-4), 333-344.
- [79] Peligrad, A. A., Zhou, E., Morton, D., & Li, L. (2002). Dynamic models relating processing parameters and melt track width during laser marking of clay tiles. *Optics & Laser Technology*, 34(2), 115-123.
- [80] Peligrad, A. A., Zhou, E., Morton, D., & Li, L. (2002). A multi-input and multioutput dynamic model for laser marking of ceramic materials. *Journal of Laser Applications*, 14(1), 31-38.
- [81] Jangsombatsiri, W., & Porter, J. D. (2006). Artificial neural network approach to data matrix laser direct part marking. *Journal of Intelligent Manufacturing*, 17, 133-147.
- [82] Chen, M. F., Wang, Y. H., & Hsiao, W. T. (2009). Finite element analysis and verification of laser marking on eggshell. *Journal of materials processing technology*, 209(1), 470-476.
- [83] Lehmuskero, A., Kontturi, V., Hiltunen, J., & Kuittinen, M. (2010). Modeling of laser-colored stainless steel surfaces by color pixels. *Applied Physics B*, 98, 497-500.
- [84] Kang, H. J., Kim, H. J., Kim, J. S., Choi, W. Y., Chu, W. S., & Ahn, S. H. (2010). Laser marking system for light guide panel using design of experiment and web-based prototyping. *Robotics and Computer-Integrated Manufacturing*, 26(5), 535-540.

Mohit Pandey